Structural and Functional Characterisation of Dioxolane A3, a New Eicosanoid Generated by Cycooxygenase-1 in Platelets.

Christine Hinz

A thesis submitted to Cardiff University in accordance with the

requirements for the degree of

DOCTOR OF PHILOSOPHY

Institute of Infection and Immunity
School of Medicine
Cardiff University

September 2016

ACKNOWLEDGEMENTS

ABSTRACT

Platelet-derived eicosanoids play important signalling roles in haemostasis and innate immunity and have major medical implications in cardiovascular disease, inflammation and cancer. Therefore, identification and characterisation of novel platelet lipids is an important goal. Prior to my PhD, our group identified a novel cyclooxygenase-1 (COX-1) product generated by platelets upon agonist activation in an aspirin–sensitive manner. Preliminary structural data suggested this lipid to be 8-hydroxy-9,11-dioxolane eicosatrienoic acid (DXA_3) (Aldrovandi, unpublished). However, this required further investigation and its biology was unknown. In this study, I undertook a detailed structural characterisation of DXA_3. Using GC/MS, high resolution LC/MS^n and UV enabled structural characterisation of the lipid. Through pharmacological studies on isolated platelets and using mutant COX-2 enzymes, I revealed a distinct enzymatic mechanism of COX where the dioxolane forms within the COX catalytic site, then a radical escapes from the enzyme to form DXA_3 possibly via a peroxidase. I developed a quantitative assay and showed that DXA_3 is generated in ng amounts by thrombin-activated platelets (human and murine) with 77% of DXA_3 esterified to phosphatidylethanolamine (PE). In addition to platelets, I detected the lipid in human serum derived from whole blood following clot formation *in vitro* and the macrophage cell line RAW246.7 in response to calcium ionophore A23187 stimulation. Last, DXA_3 stimulated expression of the integrin Mac-1 on human neutrophils. In conclusion, DXA_3 represents a novel eicosanoid, generated by activated platelets that activates neutrophils and may play a role in early immune responses.

Maceler Aldrovandi, **Christine Hinz**, Helen Podmore, Martin Hornsha, David A Slatter, Victoria J Tyrrell, Stephen R Clark, Lawrence J Marnett, Peter W Collins, Robert C Murphy and Valerie B O'Donnell. Cyclooxygenase-1 generates procoagulant dioxolane A3-phospholipids in platelets and human clots. In preparation for publication

Christine Hinz, Maceler Aldrovandi, Charis Uhlson, Lawrence J Marnett, Hilary J Longhurst, Timothy D Warner, Saydul Alam, David A Slatter, Sarah N Lauder, Keith Allen-Redpath, Robert C Murphy, Christopher P Thomas and Valerie B O'Donnell, 2016. Human platelets utilize cyclooxygenase-1 to generate dioxolane A3, a neutrophil activating eicosanoid. JBC, 291, 13448-13464

Phillip M Freeman, Konstantinos E Moschonas, **Christine Hinz**, Valerie O'Donnell, Tim D Kinnaird, Philip E James, Richard A Anderson (2015). Changes in platelet function independent of pharmacotherapy following coronary intervention in non-ST-elevation myocardial infarction patients. *Atherosclerosis,* 243, 320-327

LIST OF FIGURES

LIST OF TABLES

LIST OF SCHEMES

ACD	Acid Citrate Dextrose
ACS	acute coronary syndrome
Bq	Becquerels
BSA	bovine serum albumin
BSTFA	N,O-bis(trimethylsilyl)trifluoroacetamide
Ca	calcium
COX	cyclooxygenase
$cPLA_2$	cyclic phospholipase A_2
cps	counts per second
Da	Dalton
d4 or *d8*	contains 4 or 8 deuterium atoms
DMEM	Dubecco's Modified Eagle Medium
DMPE	1,2-Bis(dimethylphosphino)ethane
DTPA	diethylene triamine pentaacetic acid
DXA_3	8-hydroxy, 9, 11 dioxolane eicosatrienoic acid
EDTA	Ethylenediaminetetraacetic acid
fMLP	N-Formylmethionyl-leucyl-phenylalanine
h	hour
HEPES	4-(2-hydroxyethyl)-1-piperazineethanesulfonic acid
HpETE	hydroperoxyeicosatetraenoic acid
HPLC	high performane liqid chromatography
hrs	hours
L	liter
LC	liquid chromatography
LOX	Lipoxygenase
LPS	Lipopolysaccharide
LTB_4	leukotriene B_4
M	molar
m/z	mass-to-charge ratio
min	minutes
ml	milliliter
mM	millimolar
MOX	Methyloxime
MS	mass spectrometry
mV	millivolt
ng	nanogram
nM	nanamolar
nm	nanometer
NMBHA	N-methyl benzohydroxamic acid
PAR 1/4	protease-activated receptors 1/4

PC	phosphatidylcholine
Pd-C	palladium on carbon
PE	phosphatidylethanolamine
PFB	2,3,4,5,6-Pentaflourobenzyl bromide
PGD_2	Prostaglandin D_2
PGE_2	Prostaglandin E_2
PGES	Prostaglandin E_2 synthase
PL	phospholipid
pM	picomolar
sec	seconds
$sPLA_2$	Soluble phospholipase A_2
TxB_2	thromboxane B_2
TxS	thromboxane synthase
UPLC	Ultra Performance Liquid Chromatography
UV	ultra violet
vs	versus
µl	microliter
µM	micromolar

CHAPTER ONE

GENERAL INTRODUCTION

1.1 EICOSANOIDS

Eicosanoids are oxidation products of 20 carbon polyunsaturated fatty acids such as arachidonate that play an important signalling role in haemostasis and innate immunity (Smith & Murphy 2002; Fahy 2005). They are generated via three enzymatic pathways, namely cyclooxygenases (COXs) (described in 1.3), lipoxygenases (LOXs) and epoxygenases (Scheme 1.1) (Smith 1989; O'Donnell & Murphy 2012; Wolfe 1982; Hammond & O'Donnell 2012; Smith & Murphy 2002).

COXs oxidise arachidonate to PGH_2, which subsequently form prostanoids, e.g. thromboxane (Tx) and Prostaglandin E2 (PGE_2) (Smith & Murphy 2002). The structures, signalling receptors and functions of the mayor prostanoids are shown in Table 1.1. In this thesis I will characterise a novel lipid generated by cyclooxygenase-1 (COX-1). Therefore, COX biology and prostanoid function will be described in more detail in 1.3.
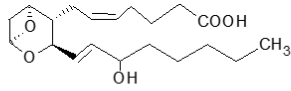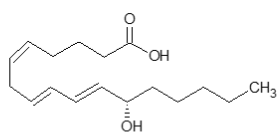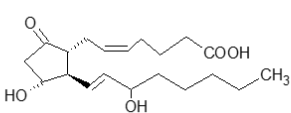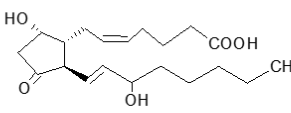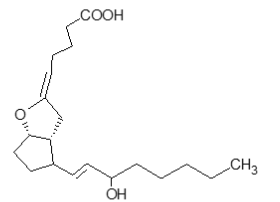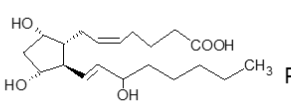
LOXs mediate synthesis of hydroperoxy eicosatetraenoic acids (HpETEs) from arachidonate. These unstable intermediates act as precursors for formation of hydroxy eicosatetraenoic acids (HETEs), dihydroxyeicosatetraenoic acids (DIHETEs), lipoxins and leukotrienes (Rådmark 2002; Borgeat et al. 1976; Serhan et al. 1986; Goetzl & Sun 1979; Lindgren 1981). LOX products are generated by several tissues and cell types such as platelets and leukocytes, and play an important role in

Phospholipids

Phospholipases (PLA_2s)

Arachidonate

Cyclooxygenases | 5-, 8-, 12-, or 15-Lipoxygenase | Epoxygenases Cytochrome P450

Prostaglandin H_2 (PGH_2) | Hydroperoxy eicosatetraenoic acids (HpETEs) | 5,6-, 8,9-, 11,12-, or 14,15- Epoxy eicosatrienoic acids (EpETrEs or EETs)

Prostanoids
Prostaglandins
and thromboxanes
(PGD_2, PGE_2, $PGF_2\alpha$, PGI_2, TxA_2)

Glutathione-peroxidase → Hydoxy eicosatetraenoic acids (HETEs)

Lipoxygenases → Dihydroxyeicosatetraenoic acids (DIHETEs)

Lipoxygenases → Lipoxines (Lx)

5-Lipoxygenase → Leukotriene A_4

Glutathione / H_2O

Peptidoleukotrienes (LTC_4, LTD_4, LTE_4) | Leukotriene B_4

Scheme 1.1. Eicosanoid generation via cyclooxygenases (COXs), Lipoxygenases (LOXs) and Epoxygenases. Modified from Smith & Murphy 2002; Hammond & O'Donnell 2012.

Table 1.1 Chemical structures, generating enzymes, signalling receptors, and mediated functions of the major COX products.

Chemical structures drawn using Chemsketch (ACD labs). Matsunobu et al. 2013; Okuno et al 2008,2015; Hirata and Narumiya 2011; Yuhki et al. 2011; Takahashi et al. 2002; Nagao et al. 2003; Zhou et al. 2007; Nakajima et al. 2010; Sugimoto et al. 1997; Alexander, et al. 2002; Liu et al. 2014

Prostanoid	Chemical Structure	Generating Enzyme	Signalling Receptor	Mediated Function
TxA_2		COX and TxS	TP	Platelet activation and aggregation, vasoconstriction
12-HHT		COX and unknown	BLT-2	Acceleration of wound healing in mice.
PGE_2		COX and PGES	EP1-4	Pro- or anti-inflammatory effects that are receptor and cell type dependent. PGE_2 is involved in regulation of pain perception, systolic blood pressure, fever generation, and spinal inflammatory hyperalgesia. It inhibits platelet activation.
PGD_2		COX and PGDS	DP1 and 2	Vasodilation, bronchodilation, inhibition of platelet aggregation (via DP1). Mediation of chemotaxis of Th2 cells, basophils, and eosinophils; leads to IL-4, IL-5 and IL-13 release by Th2 cells (via DP2)
PGI_2		COX and PGIS	IP	Vasodilation; inhibition of platelet activation; celltype-dependent pro- and anti-inflammatory effetcts
PGF2α		Reduction of PGH_2, PGE_2 or PGD_2	FP and EP1 and 3	Plays a role in mammalian reproduction, renal function, cardiac hypertrophy, and regulation of intraocular pressure

inflammation, for example by acting as chemoattractants (Goetzl et al. 1980; Bryant et al. 1982; Rabinovitch et al. 1981; Hamberg & Samuelsson 1974; Jakschik et al. 1980; Samuelsson 1983; Kühn & O'Donnell 2006; Smith & Murphy 2002; Bray et al. 1981).

Epoxygenases synthesise 5,6-, 8,9-, 11,12- and 14,15-epoxy eicosatrienoic acids (EETs) from arachidonate (Capdevila et al. 2000; Zeldin 2001; Daikh et al. 1994). EETs are generated by several tissues and cells including liver, heart or endothelial cells (Rosolowsky & Campbell 1996; Zeldin et al. 1996). They mediate a wide range of biological functions including vasodilation, inhibiting calcium mobilization, and decreasing ischemic and/or reperfusion injury (Pratt et al. 2002; Node et al. 1999; Rosolowsky & Campbell 1993; Chen et al. 1999; Gross et al. 2005).

In addition to their physiological roles, eicosanoids are associated with a range of diseases including cancer, artherosclerosis and Alzheimer's disease suggesting that they mediate important roles in both health and disease (Manev et al. 2011; McGeer & McGeer 1999; Greene et al. 2011; Sheng et al. 1997; Levy 1997; Theken et al. 2012; Smith et al. 1984; Willis et al. 1986). Consequently, studies characterising eicosanoid signalling and function and moreover, the identification of novel eicosanoids are essential for furthering our understanding of the biological significance of this lipid family.

1.2 PLATELETS

Platelets are anucleate circulating cells that play important roles in haemostasis, inflammation, wound healing and immune responses (Machlus & Italiano 2013).

After erythrocytes, platelets are the most abundant blood cell. In an adult human the normal platelet count is 150-350 x 10^9 L^{-1} and approximately 100 billion are generated per day (Thon et al. 2012; George 2000).

1.2.1 PLATELET LIFECYCLE: FROM PRODUCTION TO DESTRUCTION

The progenitors for platelets, megakaryocytes (MKs), are large (50-100 μm) bone marrow resident cells (Wright 1906, Pease 1956; Nakeff & Floeh 1976). During the first stage of platelet formation, MKs undergo maturation and become polyploid in shape with an enlarged cytoplasm. Simultaneously, they become filled with cytoskeletal proteins and platelet-specific granules (Bartley et al. 1994; de Sauvage et al. 1994; Kaushansky et al. 1994). During the second stage of platelet formation, residual cell bodies and nuclear material are degraded and 10-20 proplatelets are packed within each MK (Richardson et al. 2005). MKs migrate to the vascular niche and release the proplatelets into sinusoidal blood vessels (Zhang et al. 2012) During the final stage proplatelets elongate, thin and branch, forming platelets at their tips, that subsequently fragment into individual cells (Richardson et al. 2005; Thon et al. 2010).

Human platelets circulate in the bloodstream with a typical life span of 7 - 10 days (Mustard et al. 1966; Murphy & Francis 1971). After this time, they are selectively removed by the reticuloendothelial system. This is regulated by anti- and pro-apoptotic BcL-2 family proteins (Bcl-XL, Bak, and Bax) and a proteasome, multiprotein complex (Nayak et al. 2013; Mason et al. 2007; Nussbaum et al. 1998). A fine balance between platelet synthesis and destruction maintains the number of mature platelets in the circulation (Kaushansky 2005; Mason et al. 2007).

1.2.2 PLATELET STRUCTURE

Resting platelets are discoid with a smooth, undulating surface (Feder et al. 1985). As the smallest component of the blood, they range between 1 - 2 µm in diameter (Nayak et al. 2013; Kamath 2001). They contain a large surface area due to an open canalicular system that connects the surface with the cytoplasm along with α-granules, dense granules and lysosomes. Upon activation granules fuse with the membrane and release their contents into the extracellular space. Platelets also contain a dense tubular system, which is a derivative of the smooth endoplasmic reticulum derived from the megakaryocyte. This sequesters calcium and is important during platelet activation (Ebbeling et al. 1992; White 1972).

The well-defined cytoskeleton maintains the platelet's disc shape and integrity when they are exposed to shear forces in the circulation (Semple et al. 2011). Following activation, calcium is mobilized leading to the formation of filopodia and pseusopods, and enabling the disc shaped platelet to change into spiny spheres (Hartwig 1992).

1.2.3 PLATELETS IN HAEMOSTASIS AND IMMUNE RESPONSES

Platelets play a central role in haemostasis and immune responses through direct interaction with other cells or *via* the mediators they release. They store bioactive mediators in their granules that are released on activation, including small molecules such as adenosine diphosphate (ADP) and calcium, and proteins, e.g. growth factors, cytokines and haemostatic factors (Marcus et al. 1966; Martin et al. 1974; Whiteheart 2011; Coppinger et al. 2004). Furthermore, platelets contain mRNA and all the translational machinery to generate proteins (Denis et al. 2005; Lindemann & Gawaz 2007; Shashkin et al. 2008). Proteomic analysis revealed that thrombin-

activated platelets release approxmately 300 proteins that are involved in both haemostasis and immune responses (Coppinger et al. 2004). A major early event during platelet activation is the generation of eicosanoids. During this, phospholipases are activated that cleave fatty acids from the sn2 position of phospholipids (further description see 1.3.3.1). Arachidonate is the most abundant fatty acid released and is oxidised by LOX and COX enzymes as a substrate to generate eicosanoids such as thromboxane A_2 (TxA$_2$) and 12-HETE (O'Donnell et al. 2014). The proaggregatory TxA$_2$ represents a major product generated by COX and thromboxane synthase (TxS). Following generation in ng amounts, this is quickly converted to TxB$_2$. TxA$_2$ binds to G-protein coupled receptors (TPα and β), mainly expressed by platelets and smooth muscle cells (Raychowdhury et al. 1994). Activation of TP receptors results in intracellular activation of phospholipase C and calcium release from intracellular stores (Dorn & Becker 1993). This induces platelet aggregation and smooth muscle contraction, highlighting a key role for TxA$_2$ during haemostasis (Chiyotani et al. 1992; Spurney et al. 1993).

1.2.3.1   PLATELETS IN HAEMOSTASIS

Following injury to the blood vessel, circulating platelets bind to matrix proteins such as the collagen substratum that becomes exposed on the endothelium. This enables platelet activation, and shape change, with release of granule contents and newly synthesised mediators such as TxA$_2$. Consequently, as more platelets become recruited and activated, the cycle continues with binding to fibrinogen and formation of a clot that seals the damaged vessel (Scheme 1.2)

A   **Platelets adhere to the site of injury**

Neutrophil

Red blood cell

Platelets

Endothelial cells

Collagen and proteins

B   **Platelets aggregation and activation**

TxA_2

ADP

C   **Heamostatic plaque formation**

Fibrin
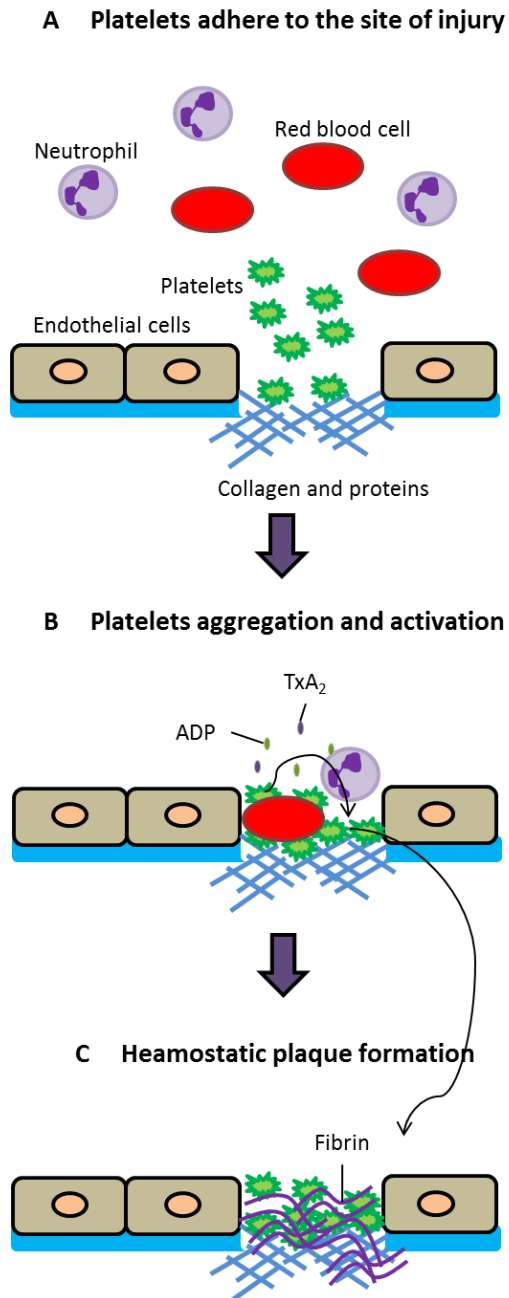
Scheme 1.2. Platelets in haemostasis. In the event of vascular injury, collagen and other membrane proteins become exposed at the vessel lumen. This leads to adhesion and activation of circulating platelets (A). Consequently, activated platelets release mediators such as ADP and TxA_2 resulting in further platelet activation (B). Simultaneously, the coagulation cascade is activated leading to the formation of thrombin, which causes the further activation of platelets and the enhanced formation of fibrin. Fibrin forms stands, which stabilize the platelet plaque to prevent bleeding (C). Modified from Semple et al. 2011.

(Richardson et al. 2005; Semple et al. 2011). Platelet activation by TxA_2 is counteracted by prostacyclin (PGI_2) and PGE_2, which are synthesised by endothelial cells and inhibit platelet aggregation and induce vasodilatation (Van Hinsbergh 2012; Shankarraman et al. 2012). The regulation of clot formation by pro- and anti-aggregatory stimuli maintains a balance between coagulation and bleeding in healthy individuals. An imbalance can either lead to elongated bleeding or thrombosis, which is often a consequence of cardiovascular diseases (CVD). For example, atherosclerosis and its thrombotic complications are the largest cause of morbidity and mortality in the industrialized world. Atherosclerosis is an inflammatory multi-factorial disease characterised by thickening and hardening of arteries (Zaman et al. 2000). This disease is further characterised by accumulation of primarily leukocytes, endothelial cells, lipids and smooth muscle cells forming an atherosclerotic lesion within the intima of arteries (Swirski & Nahrendorf 2013; Elneihoum 1997; de Korte 2002; Jonasson et al. 1985). Most atherosclerotic lesions remain asymptomatic until the lesion ruptures resulting in exposure of collagen that can interact with circulating platelets causing their adhesion and activation (Penz 2005). Simultaneously, tissue factor is released by smooth muscle cells and monocytes resulting in further recruitment and activation of platelets and subsequently formation of a thrombotic clot on the lesion surface (Libby 2005). Rupture of these clots leads to acute myocardial infarction and/or stroke. To prevent thrombus formation, CVD patients are administered antithrombotic therapies that can include the inhibition of the proaggregatory TxA_2 by either aspirin that targets COX-1 (1.3.7) or by thromboxane receptor antagonists

such as terutroban (S18886) that targets TxA$_2$ signalling (Viles-Gonzalez et al. 2005; Lesault et al. 2011).

1.2.3.2   PLATELETS IN IMMUNE RESPONSES AND THE INTERACTION WITH LEUKOCYTES

In addition to their essential role in haemostasis, platelets also participate in immune responses through their interactions with leukocytes via receptor cross-talk or the secretion of eicosanoids. At the site of injury platelets induce both haemostasis and leukocyte recruitment. The circulating platelets adhere to exposed subendothelial matrix through interaction with matrix proteins and then become activated.

Following activation, several platelet receptors become externalised, including P-selectin, which interacts with the P-selectin glycoprotein ligand-1 (PSGL-1) present on the surface of polymorphonuclear leukocytes (PMNs) and Mac-1 on dendritic cells (DCs) and neutrophils. This induces rolling and adhesion of the PMNs and activation (Weyrich & Zimmerman 2004; V Sreeramkumar et al. 2014; Langer et al. 2007). Secretion of platelet-activating factor (PAF) and platelet derived cytokines such as platelet factor 4 (CXCL4), leads to the expression of β2 integrins on the PMN surface, which are essential for their adhesion and migration (Weyrich & Zimmerman 2004; Gleissner et al. 2008; Brandt et al. 2000). Platelet-neutrophil interactions aid neutrophil adhesion to the endothelium and induce neutrophil extracellular trap (NET) release that results in increased bacterial clearance *in vivo*. These interactions are not only mediated by P-selectin but also toll like receptor 4 (TLR4) (Sreeramkumar et al. 2014; Clark et al. 2007; Andonegui et al. 2005). Platelets also express TLRs 1, 2, 6 and 9 on their surface following activation suggesting an active role in immune

reactions (Shiraki et al. 2004; Andonegui et al. 2005; Cognasse et al. 2005; Aslam et al. 2006). Furthermore, they express CD40 ligand (CD40L), a transmembrane protein structurally related to the cytokine TNF-α, in response to activation (Henn et al. 1998). Platelet CD40L enables interaction with T-cells and endothelial cells, resulting in increased T-cell recruitment, chemokine and adhesion molecule secretion, and inhibiting endothelial cell migration (Danese et al. 2004; Henn et al. 1998; Henn et al. 2001).

Circulating platelets can also interact with leukocytes to form aggregates. Platelet-leukocyte aggregates are detected in patients with inflammatory or thrombotic conditions (Schrottmaier et al. 2015). P-selectin mediated platelet-leukocyte interactions are greatest for monocytes and neutrophils (Rinder et al. 1991). Platelet-monocyte and -neutrophil interactions can result in either pro- or anti-inflammatory responses. For example, platelet-neutrophil clusters generate lipoxin A4 (LXA$_4$), which regulates downstream vascular inflammatory responses. Platelet-monocyte interactions enhance the number of activated monocytes in the circulation suggesting pro-inflammatory properties (Passacquale et al. 2011; Gudbrandsdottir et al. 2013; Corken et al. 2014; Zarbock et al. 2007; Schrottmaier et al. 2015; Brancaleone et al. 2013). Of relevance, increased levels of platelet-leukocyte aggregates have been detected in patients with acute thrombotic events, such as myocardial infarction or stroke suggesting an involvement of these aggregates in disease (Mickelson et al. 1996; Michelson et al. 2001; Htun et al. 2006). Although several signalling molecules that trigger platelet-leukocyte interaction have been identified, the roles of platelet-derived lipid mediators in immune responses remain unclear. A notable example of a platelet derived lipid that leads to neutrophil

recruitment is platelet-activating factor (PAF), which is a pro-inflammatory phosphoglyceride (Kulkarni et al. 2007; Hanahan 1986; Prescott et al. 2000). However, the role of platelet-derived eicosanoids in immune responses remains poorly understood. Inhibition of COX-1 by aspirin reduces the formation of platelet-leukocyte aggregates, inhibits the release of platelet derived CD40L, and reduces platelet-induced formation of reactive oxygen species (ROS) by monocytes (Miedzobrodzki et al. 2010; Santilli et al. 2006; Nannizzi-Alaimo et al. 2003). These studies indicate that platelet COX-1 products affect platelet-leukocyte interactions and platelet mediated leukocyte function. However, it is unknown whether these effects occur because of reduced platelet activation as a consequence of reduced TxA_2 levels or whether COX-1-derived lipids mediate these interaction and functions. Therefore, the identification and characterisation of platelet derived mediators and their effects upon haemostasis and immunity warrant detailed study.

1.3 CYCLOOXYGENASES

Cyclooxygenases-1 and -2 (COX-1 and -2) are the generic names for prostaglandin endoperoxide H synthases-1 and 2 and so the term COX will be used from here on. COXs catalyse the first committed step in prostanoid synthesis, namely the conversion of arachidonate and oxygen to prostaglandin H_2 (PGH_2). PGH_2 is the precursor for PGs and Tx. COX-1 and COX-2 are homodimeric, membrane-bound, glycosylated proteins that contain a heme group and two catalytic sites (1.3.2). Pharmacologically, they are important targets of NSAIDs such as aspirin and ibuprofen (1.3.7).

Prior to my PhD, our group discovered a new lipid generated by COX-1 in activated platelets. Preliminary structural analysis suggested that the lipid is a novel COX product. Based on this data, this lipid was proposed to be 8-hydroxyl, 9,11-dioxolane eicosatrienoic acid (DXA$_3$). However, its structure was not fully established, and its cellular biology, including synthetic pathway of generation and biological actions were unknown. Therefore, in this thesis I undertook a detailed structural and functional analysis of this novel lipid. A full description of the discovery of DXA$_3$ will be shown in 1.5.

1.3.1   HISTORY AND CLASSIFICATION OF COX AND ITS PRODUCTS

Goldblatt and Euler independently discovered prostaglandins in the 1930s. The purified "substances" from prostate gland extracts and seminal vesicles lowered blood pressure and caused contraction of smooth muscle cells. In reference to the tissue in which these substances were first discovered, Euler named them prostaglandins (Goldblatt 1935; Euler 1935; Euler 1936). In the 1960s, several researchers attempted to purify prostaglandins and reveal their structure, and these later were identified and named as PGE 1, 2, 3, PGF 1α, and 2α (Structures of PGE$_2$ and PGF2α shown in Table 1.1) (Bergstroem et al. 1963; Samuelsson 1963; Bergstroem & Sjoevall 1960). Bergstroem & Sjoevall were the first to propose a chemical formula of $C_{20}H_{34}O_5$ for prostaglandins and in 1964, the 20-carbon long chain fatty acid arachidonate was identified as the substrate for prostaglandin synthesis (Bergstroem et al. 1964; van Dorp et al. 1964). In 1967, the enzymatic pathway responsible for the conversion of arachidonate to prostaglandins was discovered (Hamberg & Samuelsson 1967). Subsequently, Smith and Willis (1969,

1973) demonstrated that platelets generate prostaglandins during clotting. Aspirin had already been marketed for 74 years but its biological function remained unknown until 1971, when Sir John Vane discovered that aspirin blocked prostaglandin synthesis. This Nobel prize winning discovery led to an enormous increase in prostaglandin research. In 1973, an endoperoxide product (PGG_2) was postulated as an intermediate in the prostaglandin synthesis pathway (Hamberg & Samuelsson 1973; Mats Hamberg & Samuelsson 1974). Soon after, the enzyme responsible for prostaglandin synthesis was purified from bovine seminal vesicles and termed prostaglandin H synthase or prostaglandin endoperoxide synthase (E.C. 1.14.99.1), typically referred to as COX (Hemler et al. 1976; van der Ouderaa et al. 1977; Miyamoto et al. 1976). The identification of the gene encoding COX-1 then led to the cloning of the COX-1 enzyme in the 1980s (DeWitt & Smith 1988; Merlie et al. 1988). Functionally, researchers had already proposed in the 1970s that COX elicited both cyclooxygenase and peroxidase activity, but only 12 years later, in 1988, was it demonstrated that the enzyme has two distinct enzymatic sites (O'Brian &Rahimtula 1976; Marshall & Kulmacz 1988).

In the 1970s, researchers began to speculate whether there was more than one COX isoform. In 1972, Smith and Lands (1972) proposed two distinct prostaglandin synthase activities in acetone powder extracts of sheep vesicular glands. During the 1980s, studies investigating NSAID inhibition and time course profiles of PGE_2 and $PGF_{2\alpha}$ synthesis provided further evidence that more than one COX enzyme existed (Lysz 1982, 1988). These findings were supported by a study conducted by Habenicht et al. who showed that the human platelet-derived growth factor induces early (within minutes) and late (after 2-4 hrs) prostaglandin generation in Swiss 3T3 cells,

suggesting a constitutive (COX-1) and inducible (COX-2) isoform of COX enzymes (Habenicht *et al*. 1985). Four years later, in 1989, Rosen et al. further demonstrated that there are two mRNAs for COX present within seminal vesicles, and LPS stimulation of monocytes resulted in prostaglandin and Tx synthesis in a time- and dose-dependent manner. These findings led to the proposal that these cells contain two pools of COX enzymes (Fu et al 1990). Indeed, this was confirmed in the 1990s when the gene encoding for COX-2 was found and overexpression of this gene resulted in increased COX activity, which was inhibited by NSAIDs (O'Banion et al. 1991; Meade et al. 1993; Hla & Neilson 1992). In 2002, a third cyclooxygenase, COX-3, was discovered which is encoded by the same gene as COX-1 but is retaining an intron that is not retained COX-1 during translation. COX-3 is inhibited by *N*-(4-hydroxyphenyl) ethanamide *N*-(4-hydroxyphenyl) acetamide (paracetamol), however, its biological function warrants further investigation (Chandrasekharan et al. 2002; Botting 2003).

To date, COX and prostanoids have been of significant pharmacological interest and consequently, targeted NSAIDs (1.3.7) or drugs targeting prostanoid synthesis downstream of COX have been developed, as well as selective COX-2 inhibitors, used for inflammatory disease.

1.3.2 STRUCTURE OF COX

The genes encoding COX-1 and COX-2 consist of about 600 base pairs and both isomers have a similar primary structure (Michael Garavito et al. 2002). The x-ray crystal membrane structure of ovine COX-1 was first shown in 1994 by Picot et al. (1994). COX-1 is a homodimer with the two monomers connected by a non-

crystallographic two-fold symmetry axis (Figure 1.1). The polypeptide chain has a high content of α-helices (40%) and almost no β-pleated sheets. The tertiary structure of COX reveals three units. The first is an epidermal growth factor (EGF) module at the C-terminal end (amino terminal residues 34-72), followed by a series of four amphipathic helices forming the membrane binding motif (residues 73-116), which represents the second unit, allowing insertion of the enzyme into the lipid bilayer. The third unit is a catalytic domain, which contains the cyclooxygenase (COX) and the peroxide (POX) active sites. The first catalytic domain, POX, is located at the interface between the large and small lobes of this catalytic domain, furthest from the membrane. This site is solvent accessible and contains the Fe(III)-protoporphyrin IX prosthetic group (heme group). POX is structurally homologous to other mammalian peroxidase sequences (MPO, 70% sequence homolog), as well as cytochrome c peroxidase (CCP) and fungal lignin peroxidase (LiP) (18 % sequence homolog each). However, the EGF module and membrane binding motif are not seen in other MPOs (Picot et al. 1994). The second catalytic domain, COX, is a narrow tunnel (8 Å wide and 25 Å long) that is highly hydrophobic and opens to the membrane binding domain. This enables arachidonate to enter the COX site after the lipid is cleaved from intracellular membranes (Picot et al. 1994).

In 2000, Malkowski et al. determined the x-ray crystal structure of apo-COX-1 with Co^{3+} bound to the endogenous substrate arachidonate at the catalytic site (Figure 1.2). A resolution of 3Å allowed the identification of 49 amino acid residues of COX that interact with arachidonate (Malkowski et al. 2000). Subsequently, Thuresson et al. (2001) identified five functional categories of these residues that mediate the arachidonate-COX interaction:
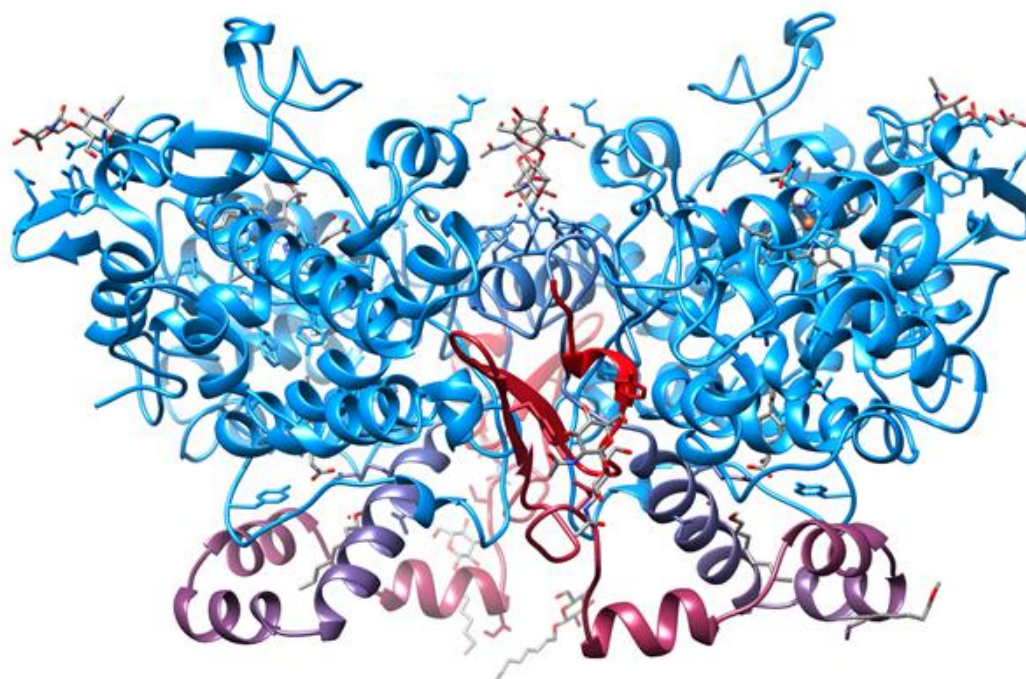
Figure 1.1. X-ray crystal structure of COX-1 complex with fluriprofen. The homodimer COX-1 shown along the dimer interface with the molecular two-fold axis vertical. Protein data bank (PDB), identification number 1CQE, Picot et al. 1994.
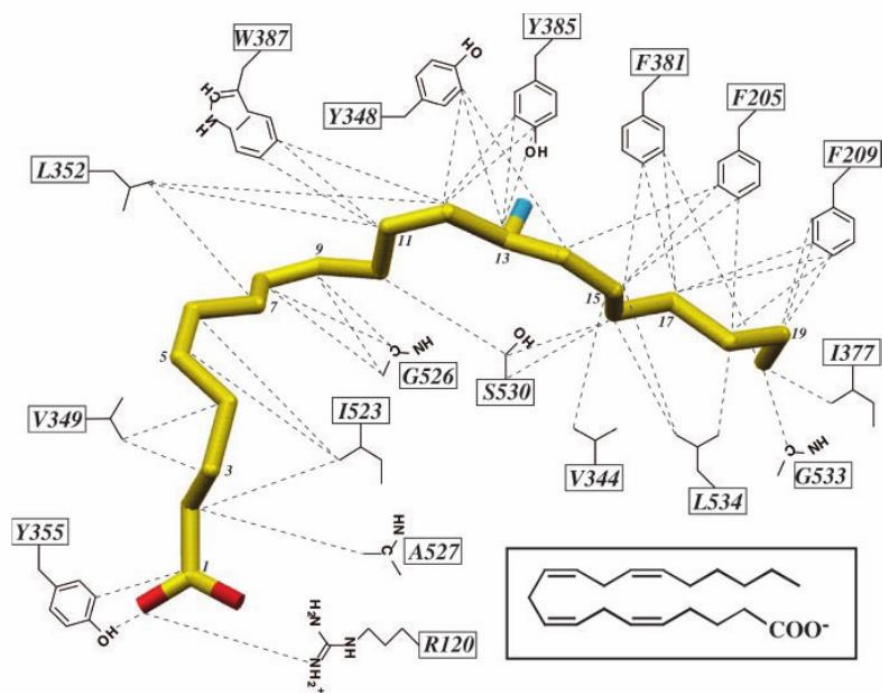
Figure 1.2. Schematic interaction between arachidonate and COX channel residues. The carbon backbone of arachidonate is shown in yellow and oxygen atoms in red. The 13 pro (S) hydrogen is depicted in blue. The 49 interactions are shown as dashed lines indicating a distance within 4.0Å between the side chain atom of COX and arachidonate (Malkowski et al. 2000).

- Tyr-385 that mediates hydrogen abstraction from carbon 13 (C13) of arachidonate

- Gly-533 and Tyr-348 are critical to position C13 of arachidonate for hydrogen abstraction

- Arg-120 is essential for high affinity binding of arachidonate to COX

- Val-349, Trp-387, and Leu- 534 position arachidonate following hydrogen abstraction within the active site in order to yield PGG_2 rather than mono-hydroperoxy acid products (11(R)-HETE and 15(S,R)-HETE)

- Other residues contribute to an optimal catalytic efficiency

Arachidonate is positioned in a L-shaped conformation in the active site of COX-1 or COX-2 (Malkowski et al. 2000; Rowlinson et al. 1999). The active sites in both isoforms are identical apart from minor amino acid changes (Gierse et al. 1996). These increase the size of the COX-2 channel and explain the isoform specific substrate tolerance (Laneuville et al. 1995). The increased size also accounts for COX-2 specific inhibitors and clarifies why aspirin fully inhibits COX-1 but allows turnover of arachidonate by COX-2 to 15-HETE (Lecomte et al. 1994; Gierse et al. 1996).

1.3.3 PROSTANOID GENERATION

Prostanoids are generated *de novo* in response to extracellular hormonal stimuli, e.g. in platelets in response to thrombin. Their generation requires three steps: First, arachidonate is mobilised from membrane phospholipids by phospholipases (described in 1.3.3.1). Second, COX enzymes oxidise arachidonate to PGH_2 (described in 1.3.3.2), which is then converted to prostanoids via cell specific synthases

downstream of COXs (described in 1.3.3.5) (Smith et al. 2000). Finally, they are either released from the cell as free fatty acids or in the case of PGE_2 esterified to phospholipids (Aldrovandi et al. 2013). Aside from the enzymatic oxidation of arachidonate, prostanoid-like structures are produced *in vivo* independently of COX, primarily by free radical-induced peroxidation of arachidonic acid. These so called isoprostanes are measured to assess the oxidative stress status *in vivo* (Montuschi et al. 2004).

1.3.3.1 MOBILISATION OF ARACHIDONATE

Engagement of cell surface receptors including PAR1/PAR4 causes the activation of phospholipases and subsequently the hydrolysis of arachidonate (Holinstat 2006; RM et al. 1995; Henriksen & Hanks 2002). Five main groups of phospholipases including 30 different enzymes have been identified (Burke & Dennis 2009; Six & Dennis 2000; M. Murakami et al. 2011). However, cytosolic phospholipase A_2 ($cPLA_2$) is the key player in eicosanoid generation since cells lacking this are unable to generate these lipids (Tramposch et al. 1994; Brooke et al. 2014; Riendeau et al. 1994; Bartoli et al. 1994). During prostanoid generation, two phases are described: the immediate phase and the delayed phase. In the immediate phase, receptor activation, e.g. PAR1/4 receptor stimulation by thrombin in platelets, leads to intracellular calcium mobilisation (Coughlin 2000). The calcium-dependent $cPLA_2$, which is located in the cytoplasm in resting cells, translocates to the endoplasmic reticulum and the nuclear envelope. Calcium binds to the N-terminal CalB domain of $cPLA_2$. This interaction enables the $cPLA_2$ to bind to intracellular membranes and to hydrolyse the sn2 ester

bond of phospholipids yielding arachidonate. Arachidonate is released within seconds of receptor activation. Therefore, the constitutively expressed COX-1, and not the inducible COX-2, is believed to be responsible for prostanoid generation during the immediate phase (Clark et al. 1991; Evans et al. 2001).

The delayed phase is characterised by long term cell stimulation (2-3 hrs), e.g. cytokine or growth factor stimulation of macrophages or mast cells, and results in increased activity of calcium-dependent secretory PLA$_2$s (sPLA$_2$) and expression of COX-2 (Reddy & Herschman 1997; Balsinde & Dennis 1996). sPLA$_2$s can be subdivided into five isoforms and are secreted by cells such as mast cells (Fonteh et al. 1994; M. Murakami et al. 2011). sPLA$_2$s show less substrate specificity than cPLA$_2$ and interact with heparin sulphate containing proteoglycans present on the cell surfaces, where they hydrolyse phospholipids at the sn2 position (Murakami et al. 2001; Murakami et al. 2010). Several transgenic or knockout studies have demonstrated that sPLA$_2$s mediate an array of homeostatic roles, including those involved in coagulation and cellular proliferation and have been implicated in diseases including asthma, atherosclerosis and cancer (Murakami et al. 2011; Murakami et al. 2010; Shridas et al. 2014).

In vitro studies have demonstrated that sPLA$_2$ expression in the macrophage cell line P33D$_1$ depends on previous activation of cPLA$_2$. Therefore, cPLA$_2$ also acts as a regulator of PG generation in the delayed phase (Shinohara et al. 1999; Balsinde et al. 1998).

1.3.3.2 GENERATION OF PGH₂ BY COX

Once arachidonate is hydrolysed from phospholipids, COXs catalyse its oxidation to PGH$_2$. In contrast to COX-1, which exclusively utilises arachidonate as its substrate, COX-2 can also oxidise 2-arachidonylglycerol, dihomo-gamma-linolenic acid (DGLA), eicosapentaenoic acid (EPA) and docosahexaenoic acid (DHA), (Kozak et al. 2000; Chen 2010; Levin et al. 2002). Both enzymes perform two semi-independent reactions: the oxygenation of arachidonate using two oxygen molecules at the COX active site and the two electron reduction of the product PGG$_2$ to PGH$_2$ at the POX active site. As shown in 1.3.2, the two reactions occur at different sites within the enzyme, but these are structurally and functionally connected.

The COX enzymatic cycle is based on a co-ordinated series of radical reactions summarised in Scheme 1.3 (Hamberg & Samulsson 1967; Mason et al. 1980; Hecker et al. 1987; Elizabeth D Thuresson et al. 2001; Wu et al. 2011). COX turnover is initiated by a two-electron oxidation of the heme group to an oxo-ferryl porphyrin cation radical at the POX active site (A). This radical then oxidises a tyrosine (Tyr-385) to a tyrosyl radical at the COX active site (D). When arachidonate enters the active site of the enzyme, Tyr-385. mediates the abstraction of the 13-pro(S)-hydrogen from arachidonate, representing the rate limiting step of the COX reaction, then isomerisation leads to a carbon-centred radical at C11 (E). Oxygen traps this radical as the 11-hydroperoxyl radical (F). This then attacks the double bond at C9 forming an endoperoxide. The carbon-centred radical relocates to C8, which attacks at C12 forming the prostanoid ring, with the radical migrating to C15. At this position the radical is trapped by a second oxygen forming a 15 -(S)-hydroperoxyl radical (G). In the last step this is reduced to a hydroperoxide at C15 forming PGG$_2$ (H). PGG$_2$ moves
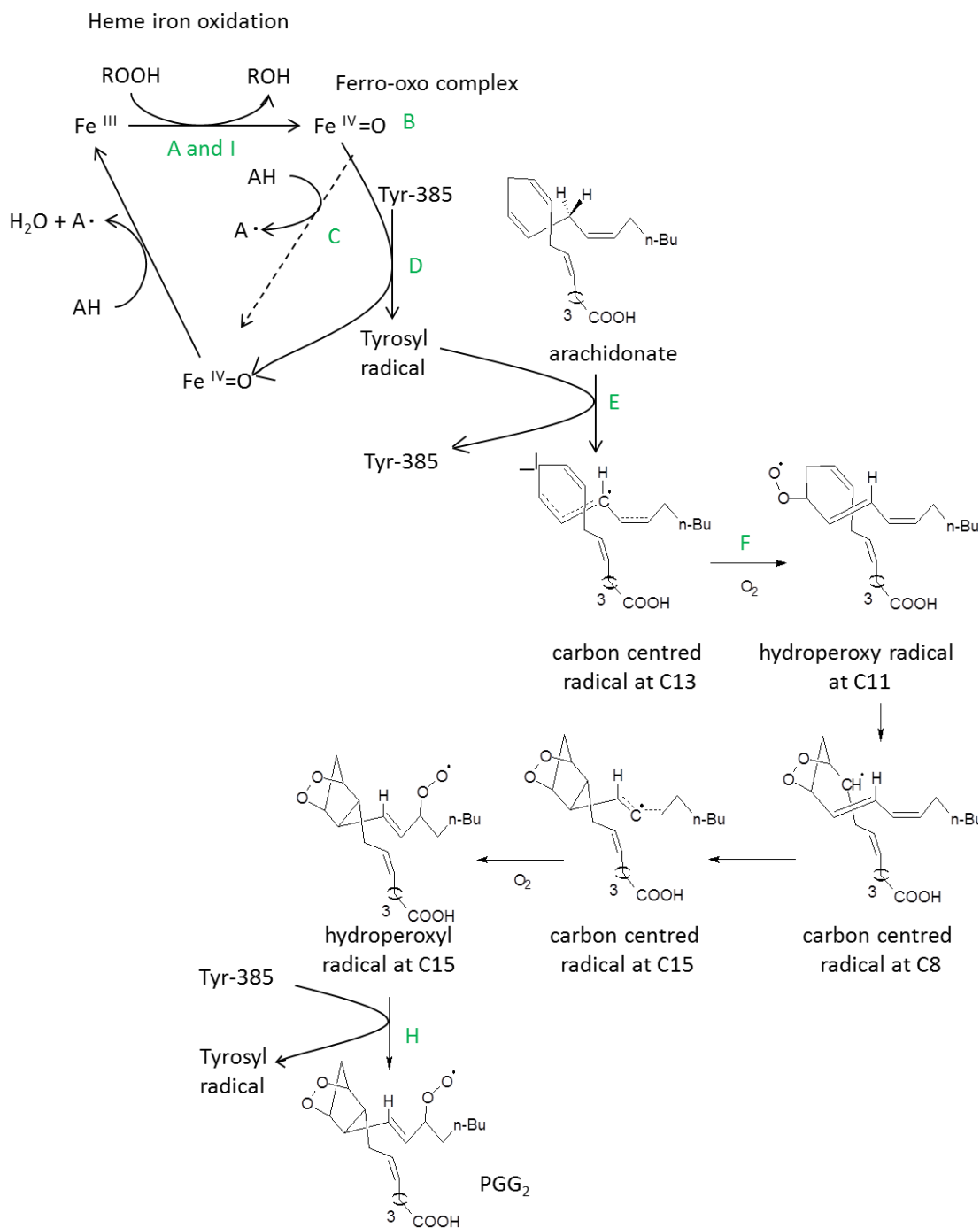
Scheme 1.3. Oxidation of arachidonate to PGH₂ by COX. Redox reactions at the POX active site (A-C) lead to radical formation of Tyr-385 at the COX active site (D). This radical attacks arachidonate forming a carbon centred radical at C13 (E). Subsequently, the C13 radical is oxidised resulting in PGG₂ (F-H). At the POX active site PGG₂ is reduced to PGH₂, then the cycle continues (I). A detailed description of this pathway is shown in 1.3.3.2. Modified from Marnett 2000.

to the POX active site of the enzymes where the hydroperoxide at C15 is reduced to a hydroxide to form PGH_2 by 2-electron oxidation of the heme group (Scheme 1.3) (Marnett 2000; Elizabeth D. Thuresson et al. 2001; Smith & Murphy 2002; Rouzer & Marnett 2003; Lassmann et al. 1991). The POX site acts independently of COX function and can also reduce long chain fatty acids other than PGG_2 (Lambeir et al. 1985; Koshkin & Dunford 1999). COX activity is initiated at 10-fold lower concentrations of hydroperoxides for COX-2 than for COX-1 suggesting that COX-1 and COX-2 can act independently when expressed in the same cell (Kulmacz 1998; Kulmacz & Wang 1995).

1.3.3.3   SUICIDE INACTIVATION OF COXS

Arachidonate oxidation by COXs is an enzymatic reaction initiated by the generation of radicals at the POX catalytic site which activates COX function. This perpetuates further POX and COX activation in a continual amplification cycle, which is terminated when the amplifying radicals cause damage to the catalytic sites. This leads to a suicide inactivation of the enzyme that irreversibly terminates COX turnover within 1-2 min even if sufficient substrate is available (Wu et al. 1999; Tsai & Kulmacz 2010). Inactivation of POX can be studied independently of COX function and is thought to originate from oxidative damage due to increasing hydroperoxide levels and the high oxidation state of the oxoferryl heme (Rouzer & Marnett 2003). POX-derived oxidants then cause distinct types of damage at the COX active site, however, their identity remains unknown (Wu et al. 2003). In addition, the Tyr radical itself causes COX inactivation (Song et al. 2001; Tsai & Kulmacz 2010). Whether there are

differences between inactivation mechanisms of COX-1 vs. COX-2 also remains undetermined.

1.3.3.4 COXs GENERATE 11-AND 15-HETE IN ADDITION TO PGH_2

COX oxidises arachidonate to generate PGH_2, the precursor for PGE_2, PGD_2, $PGF2\alpha$, TxA_2 and PGI_2 (Smith et al. 2000). However, COX also exhibits "lipoxygenase activity" generating small amounts of 11 (S)- and 15 (S) and (R)-HETEs (Xiao et al. 1997). These products form when the 11- and 15-hydroperoxyl radicals escape from the COX active site, instead of finishing the catalytic cycle. Indeed, mutations in the COX domain of COX-1 lead to enhanced formation of PGG_2 and both 15(S)– and 15(R)-HETE (mutant V349L) or 11(R)-HETE (mutant V349A/W387F) (Thuresson et al. 2000; Harman et al. 2004a). The latter forms after the 11-hydroperoxyl radical escapes from the COX site and is subsequently reduced twice, first to 11-HpETE and then to 11(R)-HETE independently of COX (Harman et al. 2004a).

1.3.3.5 CELL SPECIFIC PROSTANOID GENERATION VIA SPECIFIC SYNTHASES

COX-derived PGH_2 is the precursor for prostanoids that are generated via specific synthases PGE synthase (PGES), PGD synthase (PGDS), $PGF_{2\alpha}$ synthase, PGI synthase (PGIS), and TxA synthase (TxS), which catalyse the conversion of PGH_2 to PGE_2, PGD_2, $PGF_{2\alpha}$, PGI_2 and TxA_2, respectively. All these reactions involve isomerisation of PGH_2, except $PGF_{2\alpha}$ formation, which is a two-electron reduction of PGH_2 or reduction of PGE_2 or PGD_2 (Moriuchi et al. 2008). Prostanoid synthesis is regulated at different levels including expression, activation and tissue distribution of the enzymes

involved. Constitutively COX-1 plays a role in several physiological processes including platelet aggregation and renal function. The inducible form, COX-2, is expressed in cells in response to stimuli such as cytokines and growth factors (Chandrasekharan & Simmons 2004). Consequently, COX-2 is associated with inflammatory events. However, the co-ordinated action of COXs along with prostanoid synthases downstream of COX leads to a cell specific generation of prostanoids. For example, TxS is highly abundant in platelets whilst PGIS is present in endothelial cells (Bos et al. 2004; Caughey et al. 2001). Such cell specific generation indicates that prostanoid generation is tightly controlled within each cell type. In addition, several studies suggest that these synthases are selectively coupled to the upstream enzymes, COX-1 and COX-2 (Ueno et al. 2001). For example, COX-2 couples preferentially to either PGE synthase or PGI synthase depending on the cell type and stimulus used. For example, IL-1α and TNF stimulation of human lung carcinoma cells (A549 cells) or bone marrow-derived mast cells (BMMC) results in PGE synthase coupling, whereas LPS stimulation of peritoneal macrophages results in PGI synthase coupling (Chen et al. 1997; Matsumoto et al. 1997; Smith et al. 2000). These coupling mechanisms promote specific biological activities and differential signalling of COX-1 and COX-2 leading to a diverse range of important biological functions mediated by prostanoids (Bos et al. 2004; Naraba et al. 1998).

1.3.4 PROSTANOID RECEPTORS AND FUNCTIONS

Prostanoids represent a large group of bioactive oxidised lipids. Following their generation and release, they interact with seven-transmembrane receptors that belong to the G-protein-coupled, rhodopsin-type family (Bos et al. 2004). The

nomenclature of these receptors follows the name of the binding ligand. PGD_2 binds

to the DP receptors (DP1 and DP2), TxA_2 to TP (TPα and TPβ), PGI_2 to IP, $PGF_{2α}$ to FP

and PGE_2 to the EP receptor (EP1-4) (Kennedy et al. 1982; Bos et al. 2004; Hirata &

Narumiya 2011). In 1989, the first prostanoid receptor was structurally identified as

the TP receptor (Ushikubi et al. 1989). This was followed by homology based

screening, which enabled structural identification of the other prostanoid receptors

(Nakagawa et al. 1994; Hirata et al. 1994; Regan et al. 1994; Abramovitz et al. 1994).

Since then subtypes of these receptors have been identified.

Receptor signalling induces several functions, including platelet aggregation and

smooth muscle contraction via TxA_2, platelet inhibition and smooth muscle

contraction via PGI_2 and generation of fever and suppression of type I allergic

reactions via PGE_2 (Ushikubi et al. 1998; Kunikata et al. 2005; Spurney et al. 1993;

Hamberg et al. 1975; Dorn & Becker 1993). Therapeutically, prostanoids are targeted

by inhibition of either COX through NSAIDs (described in 1.3.7) or the prostanoid

receptor. For example, the inhibition of the TP receptor by terutroban (S18886) is

used in atherosclerotic therapy and causes a regression of advanced atherosclerotic

lesions (Viles-Gonzalez et al. 2005; Lesault et al. 2011).

1.3.5 CLASSIFICATION OF PROSTANOIDS

Prostanoids can be subdivided into PGs, which contain a five-membered ring

encompassing carbons 8 to 12 and TXs, which contain a heterocyclic six-membered

ring. Prostanoids contain a trans double bond between C13 and C14 and a hydroxyl

group at C15 (Simmons et al. 2004; Smith & Murphy 2002). The nomenclature of

prostaglandins contains the abbreviation PG plus letters A-I that indicate the nature

and location of oxygen substituent present in the ring. Likewise, thromboxanes are classified in TxA and TxB (Samuelsson & Hamberg 1978). Numerical subscripts indicate the number of carbon-carbon double bonds such as PGE_2, which has two double bonds (Nelson 1974). Based on the number of double bonds prostanoids can be further classified into series 1, 2 and 3, where class 2 is the most abundant in mammals (Bos et al. 2004). Greek subscripts, e.g. PGF2α, symbolise the orientation of hydroxyl groups attached to the cyclopentane ring.

1.3.6   PHOSPHOLIPID-ESTERIFIED PROSTANOIDS

During 1980-90s, exogenously-added eicosanoids were shown to be incorporated into phospholipids in cultured cells. For example, 15-HETE was esterified to phosphatidylinositol (PI) in human airway epithelial cells (Alpert & Walenga 1993). More recent studies demonstrated that esterified eicosanoids are acutely generated in human and murine platelets, neutrophils and monocytes/macrophages using endogenous substrate and that they can play a role in inflammation and coagulation (Thomas et al. 2010; Maskrey et al. 2007; Morgan et al. 2009; Clark et al. 2011; Aldrovandi et al. 2013).

Whereas esterified eicosanoids such as HETE-PLs are well studied regarding their generation and biological activity, little is known about prostanoids that attach to PLs. In 2013, Androvandi et al. revealed that thrombin activated platelets generate PGE_2 esterified to PE. Mechanistically, PGE_2, synthesised by COX, is immediately incorporated into PE by esterification enzymes including CoA-synthetases and lysophospholipid acyltransferases. In contrast to free PGE_2, esterified PGE_2 remains

cell associated following its generation suggesting a role in membrane-associated functions (Aldrovandi et al. 2013).

Recent studies from our group demonstrated that the novel COX-product, DXA$_3$, which is characterised as a free fatty acid in this study, is esterified to PE and PC upon thrombin activation of platelets and both the pathway of generation and localisation are identical to PGE$_2$-PEs (Aldrovandi et al, unpublished). However, as for PGE$_2$-PE, the function of DXA$_3$-PE remains unknown and warrants further study.

1.3.7 INHIBITION OF COXS BY ASPIRIN

NSAIDs such as acetylsalicylic acid (aspirin) or 2-(4-Isobutylphenyl) propanoic acid (ibuprofen) inhibit COX functions and therefore prostanoid generation. There are two families that include the classical NSAIDs and COX-2 inhibitors. Classical NSAIDs such as aspirin inhibit both COX-1 and COX-2. In contrast, COX-2 inhibitors such as 4-[5-(4-Methylphenyl)-3-(trifluoromethyl) pyrazol-1-yl] benzenesulfonamide (celecoxib) or 4-(4-methylsulfonylphenyl)-3-phenyl-5H-furan-2-one (rofecoxib) block COX-2 due to the structural difference of the active sites of COXs. All NSAIDs except aspirin compete with arachidonate for binding to the COX active site. However, there are three classes of NSAIDs differing in their kinetic inhibitory properties (Smith et al. 2000; Marnett et al. 1999). The first group that includes ibuprofen exhibits rapid, reversible binding. The second type binds to the enzyme in two stages, first the drug binds rapidly but reversibly with low affinity, then the affinity is increased reducing the reversibility. A drug belonging to this second class is (*RS*)-2-(2-fluorobiphenyl-4-yl) propanoic acid (fluriprofen). The third group that includes aspirin, binds rapidly and reversibly in the first instance but time-dependently acetylates the Ser-530

residue at the COX site and irreversibly inhibits the enzyme (Smith et al. 2000; Marnett et al. 1999). NSAIDs are commonly used as anti-platelet therapy in cardiovascular disease, in cancer therapy, and to target inflammation, pain and fever (Cook et al. 2013; Chan et al. 2012; Cuzick et al. 2009; Seibert et al. 1994; DeWitt 1999; Cao et al. 1997; Gladding et al. 2008; May et al. 1982).

Aspirin was first discovered in 1935 by Felix Hoffman and represents the most popular classic NSAID with a worldwide consumption of 100 billion tablets per year (Vane & Botting 2003). It mediates broad pharmacological actions that include anti-inflammatory, anti-pyretic and analgesic effects.

Aspirin is 170-fold more potent in its inhibition of COX-1 than COX-2 (Vane et al. 1998). Thus, COX-2 can still oxidise arachidonate to 15-HETE following aspirinisation, whereas COX-1 function is completely abolished (O'Neill et al. 1994; Mancini et al. 1994). This is due to the larger active site present in COX-2 which allows arachidonate to enter even if aspirin is already bound (Vane et al. 1998). Mechanistically, aspirin enters the COX active site and interacts with Arg-120, which is located close to the opening of the catalytic channel, through a weak iconic bond. Aspirin then covalently modifies COX via acetylation of Ser-530 in COX-1 and Ser-516 in COX-2 (Lecomte et al. 1994; Loll et al. 1995). This causes inactivation of COX and prevents arachidonate from accessing the active site. In contrast, aspirin does not inhibit POX (Shimokawa & Smith 1992; DeWitt et al. 1990).

1.3.8   INHIBITION OF PLATELETS BY ASPIRIN

Aspirin has been used for many years to combat a broad range of pathophysiological processes due to its anti-inflammatory and pain relieving properties. A major

pharmacological target of aspirin is platelet COX-1. This leads to inhibition of TxA_2 formation and subsequently prevents blood clotting (Hata & Breyer 2004). Therefore, low dose aspirin (<75 mg per day) is used as an antithrombotic therapy in acute or secondary prevention of myocardial infarction, atherosclerosis or cerebrovascular disease such as ischemic stroke (Patrono & Baigent 2009; Antithrombotic Trialists' (ATT) Collaboration 2009; Patrono 2004; Warner et al. 2011).

When administered orally, aspirin is rapidly absorbed in the upper gastrointestinal (GI) tract and inhibits platelet function within 60 min (Jimenez et al. 1992). As platelets circulate in the portal system, they are exposed to aspirin. Thus, inhibition occurs pre-systemically before the drug is metabolised by the liver. Consequently, low dose aspirin is sufficient to inhibit COX-1 in platelets *in vivo*. A repeated daily aspirin intake lower than 100 mg causes a dose-dependent and cumulative inhibition of platelet TxA_2 production explaining the drugs clinical efficiency as an antithrombotic agent at low doses (Patrignani et al. 1982; Tohgi et al. 1992). Despite its rapid clearance, aspirin inhibits TxA_2 production for the lifetime of the platelet. This is due to irreversible COX-1 inhibition by aspirin and the inability of platelets to induce COX-1. Therefore, TxA_2 generation is suppressed for 7-10 days post aspirin consumption (Patrono & Baigent 2009; Warner et al. 2011).

Higher single doses of aspirin (> 100 mg) can lead to inhibition of COX-2, which is upregulated during inflammation. Therefore, aspirin can be used at higher doses for analgesia and during inflammation (Patrono 2004).

Aspirin also inhibits COX-1 expressed by the gastric mucosa, where PGE_2 and PGI_2 are cytoprotective (Jackson et al. 2000). Consequently, the inhibition of PGE_2/PGI_2

mediated gastric cytoprotection can result in dose dependent GI bleeding (Patrignani & Patrono 2015; Rodriguez et al. 2001). Long-term, this can lead to GI complications, including gastric ulcers, but also renal failure and an increased risk of hemorrhagic stroke (Awtry & Loscalzo 2000). However, low-dose aspirin therapy remains the drug regime of choice for anti-platelet therapy in the prevention of cardiovascular events. Recent studies have examined the use of aspirin in the treatment of other diseases, such as cancer, and suggest that low-doses can reduce metastasis and overall mortality (Algra & Rothwell 2012; Peter M. Rothwell et al. 2012). However, the effect of aspirin upon different cancer types and its long term effects still warrants further study.

1.4   DISCOVERY OF DXA$_3$

Recent studies from our group aiming to identify PL-esterified prostaglandins demonstrated that platelets generate a novel lipid (Hinz and Aldrovandi, unpublished). This is formed during platelet activation and corresponds to an arachidonate-based structure containing three additional oxygen atoms. With a parent ion mass of *m/z* 351.2175, this fatty acid is the same molecular mass as prostaglandins with an elemental composition of $C_{20}O_5H_{32}$. The LC/MS/MS spectrum (Figure 1.3, Panel B) of this lipid did not match any known eicosanoid spectrum listed on LipidMaps or other databases.

Based on preliminary structural work using GC/MS in collaboration with Dr. Robert Murphy (University of Colorado, Denver) prior to my PhD, this lipid was initially proposed to contain a dioxolane ring. Dioxolanes are heterocyclic acetals formed

during oxidation of alkanes. They can form as oxidation products of arachidonate-cholesteryl esters *in vitro* with 11-HpETE as an intermediate (Havrilla et al. 2000). The proposed lipid products generated during this reaction are depicted in Scheme 1.. Furthermore, arachidonate-derived dioxolanes were recently shown to be generated enzymatically by LOX isoforms *in vitro* (Teder et al. 2014). However, to date dioxolanes have not been described in any cell type and are not known to be biologically active. Therefore, DXA$_3$ represents the first dioxolane generated in platelets in response to a physiological agonist. A detailed description of the proposed structure and further structural characterisation will be shown in Chapter 3.

Prior to my PhD, DXA$_3$ was shown to be generated by platelets as both a free acid eicosanoid and esterified to PE (Figure 1.3, Panels A-D) (Aldrovandi et al., unpublished). Moreover, the lipid was found to be generated by recombinant COX-1 (Figure 1.3, Panels E and F) and COX-2 *in vitro* (Aldrovandi, unpublished). DXA$_3$ and DXA$_3$-PE generation was also found to be coordinated by the same signalling pathway as COX-1-derived prostanoids. Specifically, PAR1/PAR4 receptors activated a signalling cascade that involves the activation of Src tyrosine kinases, p38 MAPK, PLC and cPLA$_2$. COX-1 then formed free DXA$_3$, which was subsequently re-esterified to DXA$_3$-PE via LPAT enzymes (Aldrovandi et al., unpublished). However, up to now the enzymatic mechanism of formation of DXA$_3$ by COX, amounts of the lipid generated by platelets and its biological functions have not been characterised.
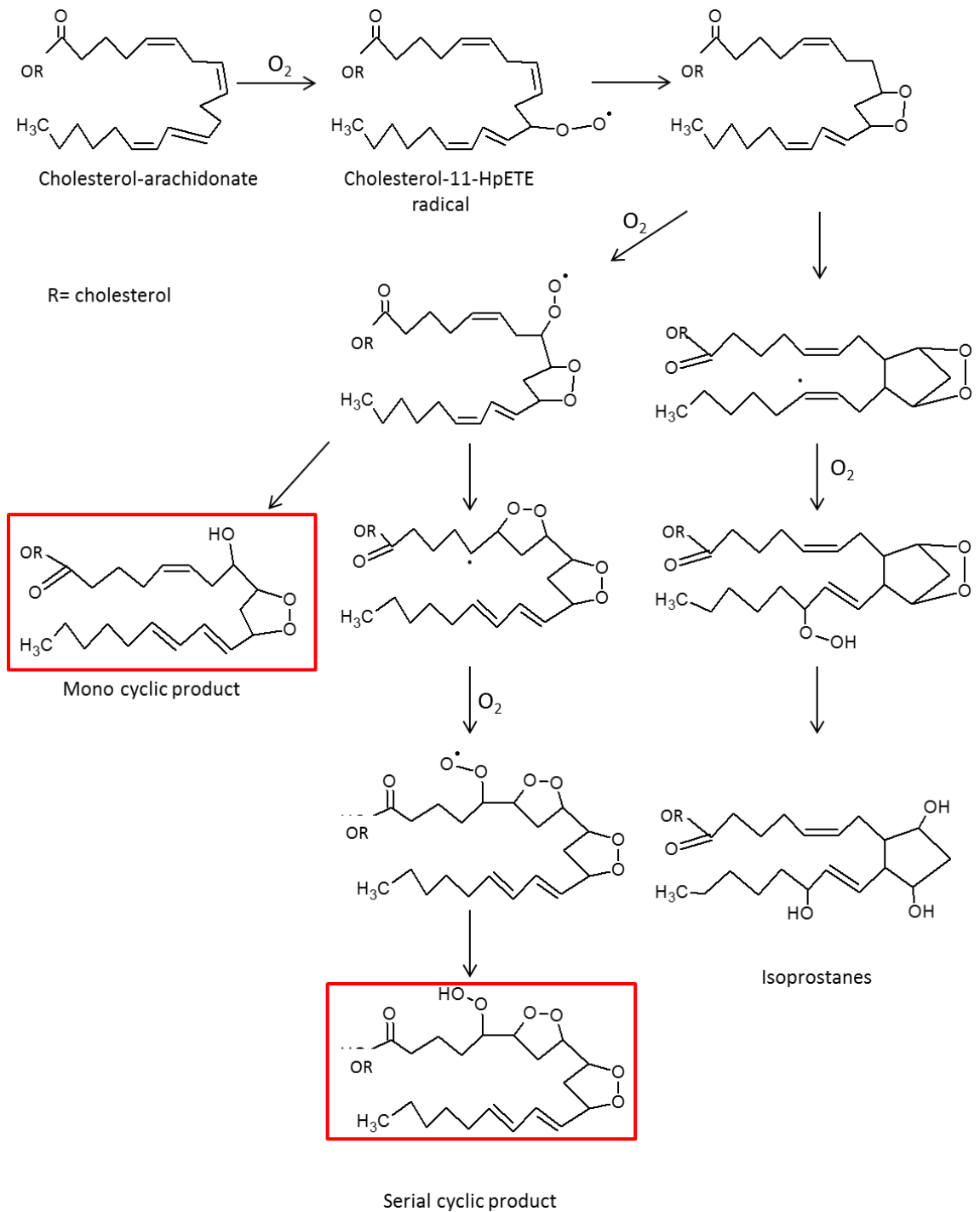
Scheme 1.4. Structures of lipid products derived from a two-step oxidation of arachidonate-cholesterol ester *in vitro* via cholesterol-11-HpETE. Oxidation of cholesterol-arachidonate and subsequently cholesterol-11-HpETE results in the formation of isoprostanes, monocyclic and serial cyclic products. Dioxolanes are marked in red. R = cholesteryl. Modified from Havrilla et al. (2000).
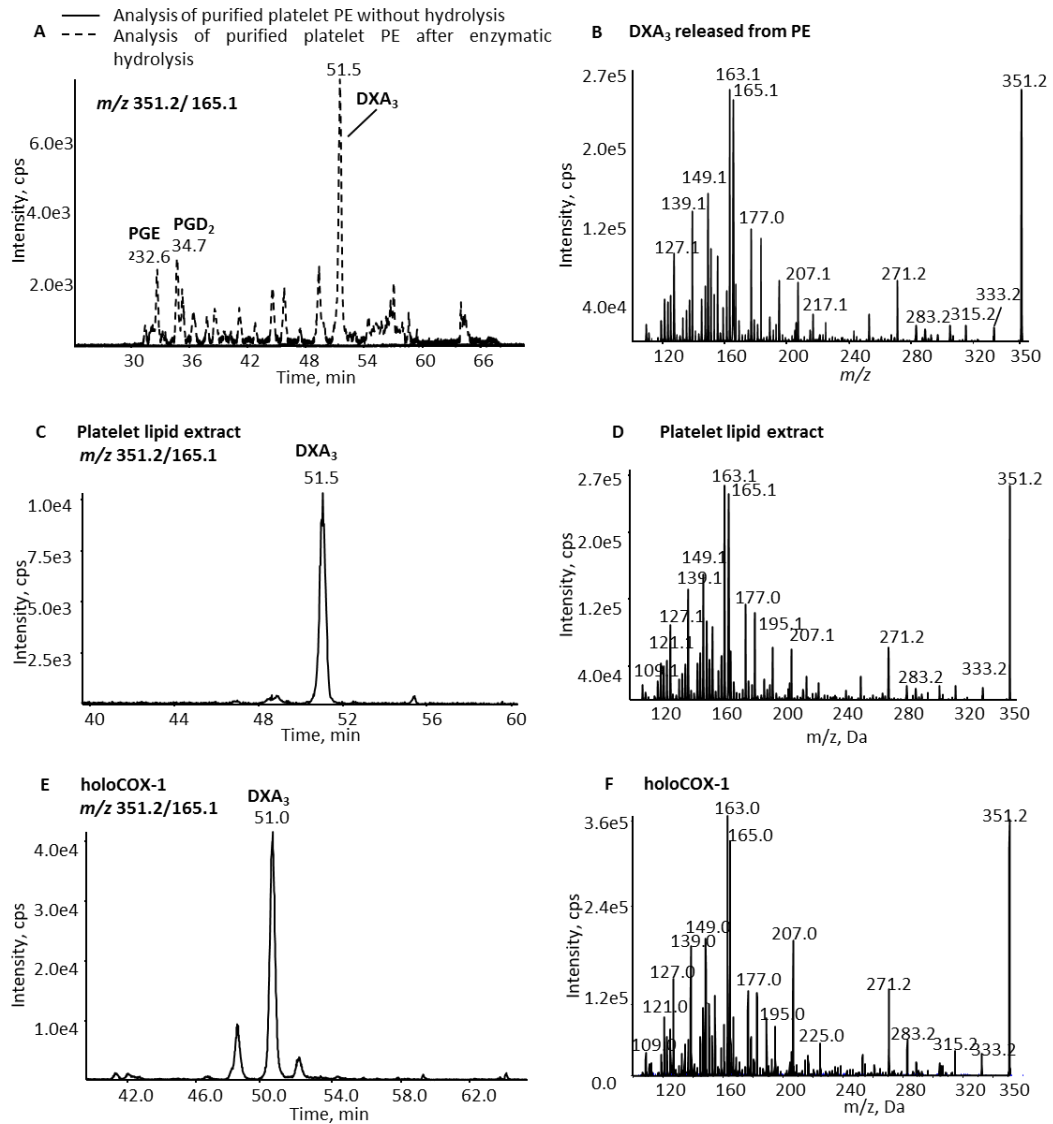
Figure 1.3. DXA₃ is esterified at *sn2* position in DXA₃-PE and is generated as free acid by thrombin activated platelets and recombinant COX-1 *in vitro*. LC/MS/MS chromatograms monitoring DXA₃ *m/z* 351.2 to 165.1 derived from (A) purified platelet PE, (C) thrombin activated platelets and (E) *in vitro* COX-1 reaction utilizing arachidonate. The product ion spectra of all three approaches are identical (Panel B, D and F). Modified from Aldrovandi et al., unpublished.

1.5   CHROMATOGRAPHY COUPLED MASS SPECTROMETRY OF LIPIDS

Mass spectrometry (MS) is an important and powerful analytical technique that has enabled quantification and structural characterisation of eicosanoids since the 1960s (Bergström & Samuelsson 1962). MS analysis requires lipids to be ionised. Historically, electron ionisation in combination with gas chromatography (GC) was used for eicosanoid characterisation. For GC the lipids are derivatised to convert them into a volatile state in order to pass into the gas chromatograph. However, not all lipids are suitable for GC/MS. Leukotriene C_4 (LTC_4) cannot be made volatile for GC and therefore, a different approach was necessary for structural characterisation (Murphy et al. 1979). In contrast, electrospray ionisation (ESI) represents a more recent and rapid technique that generates gas-phase ions and allows analysis of negatively ($[M-H]^-$) and positively ($[M-H]^+$) charged lipids (Yamashita & Fenn 1984). These molecular ions (parent ions) of the eicosanoid reveal important structural information, for example about the number of oxygen atoms within the oxidised arachidonate, when analysed using high resolution instruments. Full structural characterisation and identification of eicosanoids requires collision induced dissociation (CID) of the parent ion with an inert gas such as N_2. This enables the formation of unique fragments (fragment ions) to give a specific fragmentation pattern (MS/MS spectrum) (Murphy et al. 2005). In general, there are two principles of lipid analysis using ESI-MS that include shotgun MS and liquid-chromatography (LC)-MS.

1.   "Shotgun" lipidomics analyses lipid extracts without on-line chromatography. Separation of lipids is achieved "in source" according to the lipid's specific

ionisation and adduct formation properties. Shotgun lipidomics allows detection of the most abundant lipids. This approach is high throughput and large amounts of lipidomic data can be generated within a relatively short time frame. However, it is not generally quantitative and can miss low abundant lipids (O'Donnell et al. 2014). Ion suppression is one of the major challenges during shotgun analysis. For example, when classes of lipids are present at high abundance, they dominate the spectrum. Consequently, lipids that are present at a much lower abundance can be missed (Yang & Han 2011).

2. LC/MS is a robust and reliable quantitative and qualitative analytical tool that is routinely used in lipid research (O'Donnell et al. 2014). Coupling LC to MS allows analysis of single lipids within a lipid mixture, for example in biological samples (Bylund et al. 1998; Nithipatikom et al. 2001; Kita et al. 2005; Kempen et al. 2001). In addition, lipids are kept in solution during LC and are not exposed to atmospheric oxygen. This prevents lipid oxidation and subsequently formation and detection of artefacts (Pulfer & Murphy 2003).

1.5.1 TRIPLE QUADRUPOLE MASS SPECTROMETRY FOR LIPID ANALYSIS

Mass spectrometric analysis consists of three general steps: ionisation, mass analysis and detection. The direct coupling of high performance liquid chromatography (HPLC) to MS yielded a breakthrough in analysis of biological samples. However, lipids need to be in the gas phase for MS analysis, and this is commonly achieved by ESI (Murphy et al. 2005). Briefly, lipids elute from the LC column and reach the MS source in solution through a thin stainless steel or quartz silica capillary, which is maintained at a high voltage. This results in formation of an aerosol of highly charged droplets,

57

which have the same polarity as the capillary voltage. Within a nebulising gas (N_2), which shears around the droplets and increases the sample flow rate, they pass down a pressure and potential gradient towards the MS. High source temperatures (heated ESI, hESI) lead to solvent evaporation and subsequently result in a decreased droplet size. Simultaneously, the same amount of charge remains on their surface leading to an increased surface charge density. Then, the electric field strength reaches a critical point causing a coulombic repulsion and explosion and consequently, the ejection of ions from these highly charged droplets. The ions are collected in a sampling skimmer before they enter the MS (illustrated in Scheme 1.4) (Ho et al. 2003; Bruins 1998). The ions travel through an oscillating electric field applied between quadrupoles, which consist of four cyclindrical rods that are allocated parallel to each other (e.g. Q1, Scheme 1.). The principle of separating these ions within the MS is based on their mass to charge (*m/z*) ratio, which affects their movement through the quadrupoles towards the detector. For example, when a specific *m/z* is selected, ions with a different *m/z* are not stable in their flight path, and will be discharged and consequently, fail to reach the detector. For lipid identification and quantification, CID is applied using a triple quadrupole instrument, which consists of three linear assembled quadrupoles (Q1, Q2 and Q3), thus, this system is also known as a "tandem-MS". Whereas Q1 and Q3 represent mass analysers, Q2 is the collision cell. When the ion of interest (parent ion) enters the MS it is mass-selected by its *m/z* ratio in Q1 and travels towards Q2. In Q2, the parent ion is fragmented into fragment ions through CID with an inert gas such as N_2. The fragment ions generated in Q2 are monitored in Q3. The MS can be set for a static parent *m/z* (in Q1) and static fragment *m/z* (in Q3). For example, PGE$_2$ is monitored using the transition *m/z* 351.2 (parent
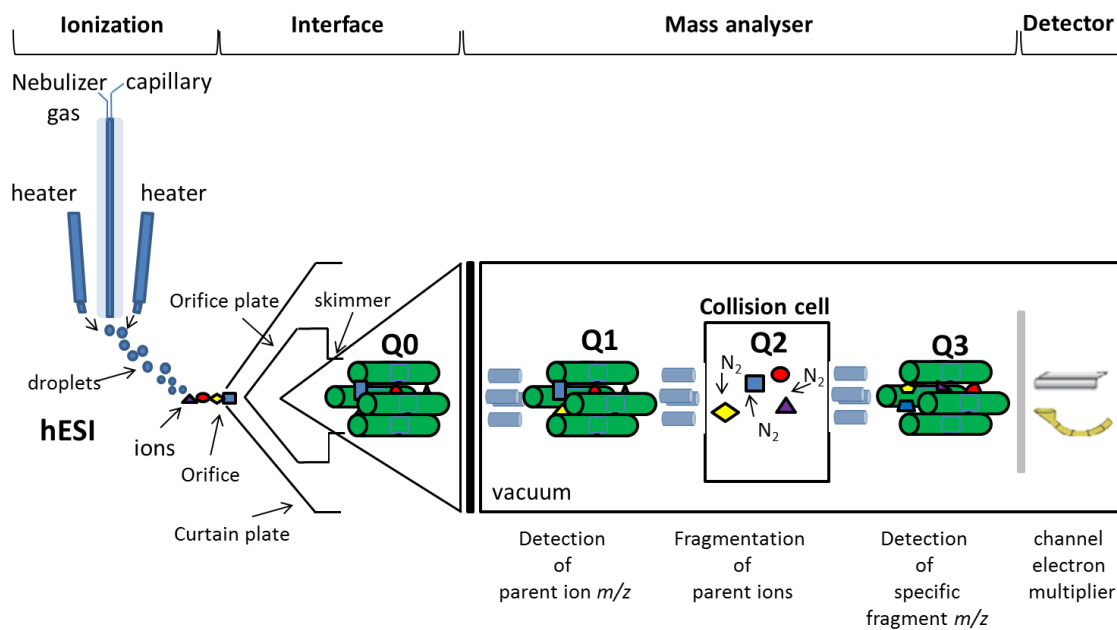
Scheme 1.5. Principle of Triple Quadrupole mass spectrometry. Parent ions are introduced to the mass spectrometer either through direct injection or chromatography. The parent ion *m/z* is detected in Q1 and parent ions fragmented in the collision cell, e.g. through collision with N_2. Specific fragment ions are detected in Q3. Modified from O'Donnell et al. 2014.

ion) to 271.1 (fragment ion) (LipidMaps.org). Ions with different *m/z* ratios will be filtered out and will not reach the detector. This mode of data acquisition is called *multiple reaction monitoring* (MRM), allows a high degree of specificity and sensitivity, and is commonly used for quantification (O'Donnell et al. 2014; Ho et al. 2003). For identification, the MRM is coupled to an *enhanced product ion* (EPI) analysis that generates a spectrum of the MRM for the selected transition. Parent and fragment ions reaching the detector generate signals that are transmitted by a computer system and displayed graphically as chromatograms (intensity of signals over time) and spectra (relative abundance of parent and fragment signals according to their *m/z* ratio) (Ho et al. 2003).

1.5.2   DISCOVERY OF NOVEL LIPIDS USING LC/MS/MS

Eicosanoids were first discovered in the 1960s and research in this area dramatically increased in the 1970s following the discovery of the biological function of aspirin (as described in 1.3.1). GC/MS, HPLC-UV and thin layer chromatography (TLC) were employed for quantitative and qualitative lipid analyses whilst NMR and UV techniques were used for structural characterisation. Data from these analytical methods were combined to yield the structure of unknown lipids. Although GC/MS was applied for structural elucidation of novel lipids such as the PGs, very few lipids could be characterised in detail using these approaches. This is due to the requirement of the lipid to be volatile to enter as a gas into the MS as well as the relative insensitivity of NMR (Granström & Samuelsson 1669; Murphy & Gaskell 2011). Structural lipid analysis using MS significantly increased with the development of fast atom bombardment ionization and ESI (Barber et al. 1982; Murphy et al. 1982;

Fenn et al. 1989, Wheelan et al. 1993). Combined with CID and MS/MS this enabled the structural elucidation of several lipids including arachidonate-derived oxidation products (Murphy 1993; Fruteau de Laclos et al. 1993, Zirrolli & Murphy 1993). Due to the continuing evolution of LC/MS/MS, increased precision, sensitivity, selectivity and accuracy now allow the study of femtomole quantities of non-volatile and thermally labile molecules (Murphy et al. 2005; Ho et al. 2003). Furthermore, high resolution instruments such as the Orbitrap platform allow accurate mass analysis of parent and product ions to be determined (O'Donnell et al. 2014; Perry et al. 2008). These advantages allowed the identification and structural analysis of novel lipid classes such as protectins and resolvins, which are generated in picomolar concentrations (Hong et al. 2007; Masoodi et al. 2008; Serhan et al. 2002; Schwab et al. 2007). In our laboratory many phospholipid-esterified eicosanoids were structurally identified (Thomas et al. 2010; Maskrey et al. 2007; Morgan et al. 2009; Clark et al. 2011; Aldrovandi et al. 2013). This work utilised precursor scanning tandem-MS, where a particular fragment ion is selected in Q3 and the precursor masses are scanned in Q1. For example, Aldrovandi et al. (2013) identified PGE_2 attached to four species of PE generated by activated platelets when scanning for PGE_2 ([M-H]$^-$ 351.2) in Q3. Alongside PGE_2-PE another lipid with an identical parent mass was discovered and later identified as DXA_3-PE. This will be further discribed in 1.5.

LC/MS/MS has fast become an essential analytical tool in lipid research that enables detailed analyses of platelet-derived lipids to be undertaken, leading to significantly improved understanding of their role in platelet biology (O'Donnell et al. 2014).

1.6   GENERAL AIM

Prior to this study, DXA_3 as novel COX product was discovered using LC/MS/MS. To classify a novel lipid as a physiological mediator, it is crucial to undertake a detailed structural and functional characterisation of the lipid. Specifically, for any new lipid mediator, this should include studies on the following:

- Tissue/cell distribution

- The lipid amount generated by cells and tissues

- Lipid generation in response to a physiological agonist

- Bioactivity of the lipid

Therefore, in this thesis I will obtain further structural characterisation, examine the generation of DXA_3 at a cellular and enzymatic level, then I will quantify DXA_3 in biological samples and determine its biological activity towards neutrophils.

CHAPTER TWO

MATERIALS AND METHODS

2.1 MATERIALS

2.1.1 ANTIBODIES

IgG1 mouse anti-human isotype control Alexa Fluor 647 and anti-human CD11b Alexa Fluor 647 were supplied from eBioscience (CA, USA).

2.1.2 CHEMICALS

All chemicals were from Sigma Aldrich (MO, USA) unless otherwise stated.

2.1.3 DERIVATISATION AND HYDROGENATION CHEMICALS

2,3,4,5,6-pentaflourobenzyl bromide (PFB) and palladium on carbon (Pd-C) were from Sigma Aldrich (MO, USA), Methyloxime (MOX) from biomedicals (France) and BSTFA from Supleco (PA USA).

2.1.4 ENZYMES

Purified ovine or human recombinant COX-1 and COX-2 as well as the COX-2 mutants were a kind gift from Prof. Larry Marnett (Vanderbilt University, TE, USA) or from Cayman Chemicals (MI, USA). Snake venom $cPLA_2$ was from Calbiochem (UK). Thrombin was supplied by Sigma Aldrich (MO, USA).

2.1.5 LIPID STANDARDS

[^{14}C]-Arachidonate was from Perkin Elmer (MA, USA) and 1,2-Dimyristoyl-sn-glycero-3-phosphoethanolamine (DMPE) from Avanti Polar Lipids (AL, USA), all other lipid standards were from Cayman Chemicals (MI, USA)

All solvents were HPLC-grade and from Thermo Fisher (MA, USA).

2.1.7 BUFFERS AND SOLUTIONS

Acid Citrate Dextrose (ACD) buffer

85 mmol/L trisodium citrate, 65 mmol/L citric acid and 100 mmol/L glucose.

Flow Cytometry buffer

0.5 % BSA, 5 mM EDTA, 2 mM sodium azide in phosphate buffer saline (PBS) pH 7.4
(Gibco, Thermo Fisher Scientific).

HEPES buffer

100 mM NaCl, 5 mM KCl, 1 mM NaH_2PO_4 x 2 H_2O, 2 mM glucose at pH 7.4.

Kreb's buffer

50 mM HEPES, 100 mM NaCl, 5 mM KCl, 1 mM $NaH_2PO4*2H_2O$, 2 mM Glucose. After
adjusting the pH to 7.4, 2.5 mM $CaCl_2$ was added.

Phosphate buffer

100 mM potassium phosphate, pH 7.4

Tyrode's buffer

134 mmol/L NaCl, 12 mmol/L $NaHCO_3$, 2.9 mmol/L KCl, 0.34 mmol/L Na_2HPO_4, 1.0
mmol/L $MgCl_2$, 10 mmol/L HEPES and 5 mmol/L glucose at pH 7.4

2.1.8 SOFTWARE

Analyst 1.6 (Applied Biosystems, CA, USA), ChemSketch (ACD labs, MO, USA), FlowJo (FlowJo, LLC, OR, USA), Microsoft Office (Microsoft corporation, WA, USA), and XCalibur (Thermo Scientific, MA, USA).

2.2 METHODS

2.2.1 CELL BIOLOGY

2.2.1.1 ISOLATION OF HUMAN PLATELETS FROM BLOOD

Whole blood was collected from healthy donors with informed consent (SMREC 12/37, SMREC 12/10). This study was approved by the Cardiff University School of Medicine Ethics Committee and conducted in accordance with the Declaration of Helsinki. For blood samples relating to cPLA$_2$-deficient studies, blood was collected as follows: healthy volunteer samples; approved by St Thomas's Hospital Research Ethics Committee, reference 07/Q0702/24: cPLA2-deficient patient samples; approved by South East NHS Research Ethics Committee.

For platelet purification, 50 ml of fresh human blood was obtained and mixed with ACD buffer at a ratio 8.1:1.9 (v/v blood: ACD) and slowly transferred into two 50 ml falcon tubes. The blood:ACD was centrifuged at 250 g (1500 rpm, 12 cm rotor) for 10 min at room temperature (RT) with no brake. The platelet rich plasma (PRP) was collected and transferred into a fresh tube, then centrifuged at 900 g (2900 rpm, 12 cm rotor) for 10 min at RT with the brake switched off. The supernatant was discarded and the pellet resuspended in 10 ml of calcium free Tyrode's buffer containing ACD (9:1, v/v Tyrodes:ACD) and centrifuged at 800 g (2800 rpm, 12 cm rotor) for 10 min at RT with no brake. The pellet was resuspended in 2 ml of calcium free Tyrode's, before diluting the platelets 1:100 using Tyrode's and trypan blue. Platelets were counted using a haemocytometer and the count adjusted using Tyrode's to the required concentration and the platelets used within 2 h.

2.2.1.2 PURIFICATION OF MURINE PLATELETS

All animal experiments were performed in accordance with the United Kingdom Home Office Animals (Scientific Procedures) Act of 1986. 12/15-LOX knockout mice generated as described previously (Cyrus et al. 1999) and wild-type male C57BL/6 mice (25–30 g) from Charles River, UK, were kept in constant temperature cages (20–22 °C) and given access to water and standard chow ad libitum.

For studies on isolated murine platelets whole blood was collected via cardiac puncture (all mice were 28 weeks old) into 150 µl ACD buffer. 150 µl 3.8 % sodium citrate and 300 µl Tyrode's buffer were added and the blood centrifuged at 150 g for 5 min at RT. PRP was collected and 400 µl Tyrode's buffer added to the red cells and centrifuged again at 150 g for 5 min at RT. PRPs were combined and centrifuged at 530 g for 5 min at room temperature. Platelets were resuspended in Tyrode's buffer at 2×10^8 ml^{-1}.

2.2.1.3 ACTIVATION OF WASHED PLATELETS

1 mM $CaCl_2$ was added 5 min prior to activation and platelets incubated at 37 °C. 0.2 units ml^{-1} thrombin was added and platelets incubated at 37 °C for 0 min to 2 h. In some experiments, platelets were treated with 50 µM picotamide or 1-10 mM iodoacetate for 10 min at 37 °C prior to $CaCl_2$ and thrombin. Lipids were extracted as described in 2.2.5.1.

2.2.1.4   cPLA₂ HYDROLYSIS OF ESTERIFIED LIPIDS

Lipids were extracted (2.2.5.1) and dried under N_2, then were resuspended in 1 ml Tris buffer (150 mmol/l NaCl, 5 mmol/l $CaCl_2$, 10 mmol/l Trizma base at pH 8.9) and hydrolysed using 100 µg snake venom $cPLA_2$ for 60 min at 37 °C. Lipids were extracted as described in 2.2.5.1.

2.2.1.5   SERUM AND CLOT ISOLATION

5 ml whole blood was collected without anti-coagulant and allowed to clot for 15 min at 37 °C. Clots and serum were separated by centrifugation at 1,730 g for 10 min at RT. Lipids were extracted from serum as described in 2.2.5.1. 500 mg (wet weight) clot was placed in a pre-frozen mortar and pestle on dry ice and further cooled with liquid N_2. The clot was ground up and added to 3 ml PBS pH 7.4 containing 10 mM diethylene triamine pentaacetic acid (DTPA). Lipids were extracted from 1 ml samples as described in 2.2.5.1.

2.2.1.6   ISOLATION OF HUMAN NEUTROPHILS FROM WHOLE BLOOD

For neutrophil isolation, human blood was drawn into a 20 ml syringe and mixed with HetaSep: 2 % sodium citrate (1:2) at a ratio of 3.3:1. The syringe was placed upright on its base to allow erythrocytes to sediment at room temperature for 45 – 60 min. The plasma layer was removed by slowly ejecting the layer into a fresh, chilled centrifugation tube using a butterfly needle tube with the needle removed. The plasma layer was slowly underlayered with Lymphoprep at a ratio 1:3 (v:v) by ejecting Lymphoprep into the bottom of the tube using a 3 ml plastic pasteur pipette. This

was centrifuged at 800 g (2000 rpm, 12 cm rotor) for 20 min at 4 °C with no brake. The supernatant was removed using a pasteur pipette drawing the supernatant up from the Lymphoprep interface. The pellet was resuspended into 10 ml of 0.4 % (w/v) Na-tricitrate/PBS and decanted into a new chilled tube. Neutrophils were centrifuged at 4 °C, 400 g (1400 rpm, 12 cm rotor) for 5 min and the supernatant discarded.

To remove contaminating erythrocytes a hypertonic shock was performed by adding 3 ml of ice cold 0.2 % (w/v) NaCl, then 3 ml of ice cold 1.6 % (w/v) NaCl and slowly mixing using a pasteur pipette for 35 – 50 s. 6ml of PBS was added and the neutrophils centrifuged at 4 °C, 400 g (1400 rpm, 12 cm rotor) for 5 min. The supernatant was discarded and the hypertonic shock repeated once or twice again as required. The pellet was resuspended in 1 ml of Kreb's buffer. Neutrophil numbers were adjusted to the required cell number using Kreb's buffer and kept on ice till used.

2.2.1.7 NEUTROPHIL ACTIVATION AND ANTIBODY STAINING

For flow cytometry experiments, purified neutrophils (2.2.1.6) were diluted to a concentration of 2×10^6 ml^{-1}. Cells were activated using 1 µM fMLP or 10 µM DXA$_3$ and incubated at 37 °C for 20 min. In some experiments, neutrophils were incubated with 10 nM- 10 µM DXA$_3$ for 10 min at 37 °C prior to fMLP treatment. Cells were centrifuged at 1330 rpm for 5 min at 4 °C, the supernatant was removed and 50 µl flow cytometry buffer containing 5 % mouse serum added. Neutrophils were incubated for 1 h on ice, then centrifuged again and the supernatant removed. 0.0625 µg anti-human CD11b Alexa Flour647 antibody or isotype control was added

to each sample and incubated for 30 min on ice. Neutrophils were washed twice with flow cytometry buffer and cells resuspended in 700 µl flow cytometry buffer prior to analysis.

2.2.1.8 CULTURING AND ACTIVATION OF RAW246 CELLS

RAW246 cells were cultured in DMEM (10 % FBS, 1 x Pen/Strep) at 37 $^{\circ}$C and 5 % CO_2. Cells were defrosted, added to 9 ml of media and centrifuged at 400 g (1200 rpm) for 5 min at RT with no brake. The supernatant was discarded and the cells resuspended in 1 ml of medium. The cells were added to 50 ml of media into a T175 cell culture flask.

Upon reaching a confluency of 80 - 90 % the medium was removed and the cells washed twice using PBS. 10 ml trypsin was added and the cells incubated at 37 $^{\circ}$C for 3 - 5 min. In order to stop the reaction, medium was added and the cell suspension transferred into a 50 ml falcon tube and centrifuged at 400 g (1200 rpm) for 5 min at RT without brake. The supernatant was discarded and the cells resuspended in 10 ml. Cells were diluted into a new flask at required ratios and incubated at 37 $^{\circ}$C and 5 % CO_2.

2.2.1.9 ACTIVATION OF RAW246 CELLS

Upon reaching a confluency of 80 - 90 % the medium was removed and cells washed twice using PBS. Serum free DMEM (1 x Pen/Strep) was added and the cells incubated for 1 h at 37 $^{\circ}$C and 5 % CO_2. For some experiments, 200 ng/ml LPS was added and cells incubated for 24 hrs at 37 $^{\circ}$C and 5 % CO_2. The cells were counted using a

disposable haemocytometer (Immune Systems). The cell concentration was adjusted to 8 x 10^6 ml^{-1}. In some experiments cells were incubated for 30 min with 10 µM calcium ionophore A23187 at 37 °C. Lipids were extracted according to 2.2.5.1 following addition of PGE$_2$-d$_4$ as internal standard (IS).

2.2.2 GENERATION OF DXA$_3$ USING RECOMBINANT OR PURIFIED CYCLOOXYGENASES

For enzyme reconstitution, COX-1 purified from sheep seminal vesicles, recombinant ovine COX-1, COX-2 or the COX-2 mutants V349A or W387F were incubated with two molar equivalents of hematin in 100 mM phosphate buffer for 20 min on ice. A final amount of 3.4 µg COX-1 was incubated with 150 µM arachidonate or deuterated arachidonate (arachidonate-*d8*) and 500 µM phenol in 100 mM phosphate buffer for 3 min at 37 °C under oxygen atmosphere. For COX-2, V349A or W387F 30 µM arachidonate was oxidised using 10.2 µg enzyme and 500 µM phenol in 100 mM phosphate buffer for 5 min at 37 °C under O$_2$ atmosphere. Lipids were extracted using the hexane-isopropanol-extraction method (2.2.5.1).

2.2.3 *IN VITRO* OXIDATION OF ARACHIDONATE

3.5 eq. N-methyl benzohydroxamic acid (NMBHA) and 0.1 eq. 2,2'-azobis(4-methoxy-2,4,dimethyl valeronitrile) (MeOAMVN) were added to a 6.5 mM arachidonate solution in chlorobenzene and the mixture was stirred at 37 °C for 5 h under O$_2$ atmosphere. Both NMBHA and MeOAMVN were a gift from Prof. Ned A. Porter (Vanderbilt University, TN,USA). The sample was dried under N$_2$ and dissolved in methanol. Purification of the free hydroperoxide positional isomers was accomplished using reverse phase HPLC using a Spherisorb ODS2 column (5 µm, 150

mm x 4.6 mm; Waters) with a solvent gradient of 50 - 90 % solvent B (acetonitrile, 0.1 % formic acid) in solvent A (water, 0.1 % formic acid) over 60 min, 90 % solvent B 60 - 64.5 min, 50 % solvent B 65.5 - 75 min and a flow rate of 1 ml min^{-1}. Lipids were monitored at 205 nm (unoxidized lipid) and 235 nm (HpETE) and fractions were collected at 30 second intervals. HpETEs were identified in these fractions using MS/MS: m/z 317.2 to 115.1 (5-HpETE); m/z 317.2 to 155.1 (8-HpETE); m/z 317.2 to 151.1 (9-HpETE); m/z 317.2 to 167.1 (11-HpETE), m/z 317.2 to 179.1 (12-HpETE); m/z 317.2 to 219.1 (15-HpETE). The fraction containing 11-HpETE was purified using Sep Pak purification as described in 2.2.5.2.

2.2.4   GENERATION OF DXA$_3$ VIA OXIDATION OF ISOLATED 11-HPETE

The purified 11-HpETE was oxidised using 0.1 eq. MeOAMVN in 5 ml chlorobenzene stirring at 37 °C for 5 h under O$_2$ atmosphere. Hydroperoxides generated via oxidation of 11-HpETE were reduced using 95 µg SnCl$_2$ in water for 10 min at RT. Lipids were extracted using hexane-isopropanol-extraction (2.2.5.1) and analysed by LC/MS/MS (2.2.7.3).

2.2.5   LIPID PURIFICATION

2.2.5.1   ISOPROPANOL-HEXANE LIPID EXTRACTION

For all experiments 5 - 10 ng deuterated standards PGE$_2$-d$_4$, 12-HETE-d_8, TxB$_2$-d$_4$, DMPE (IS) were added to samples prior to extraction. Lipids were extracted using a solvent mixture (1 mol/L acetic acid, isopropyl alcohol, hexane (2:20:30, v/v/v)) at a ratio of 2.5 ml to 1 ml sample. The sample was vortexed, and 2.5 ml of hexane added.

Following vortexing and centrifugation at 1500 rpm for 5 min at 4 $^{\circ}$C, lipids were recovered from the upper hexane layer. The samples were then re-extracted by addition of an equal volume of hexane. The combined hexane layers were dried under vacuum and analysed using LC-MS/MS (2.2.7).

2.2.5.2 LIPID PURIFICATION USING SOLID PHASE EXTRACTION COLUMNS

Silica-based solid phase extraction columns (Sep Pak, Waters, MA, USA) were equilibrated with 5 ml of water pH 3.0 followed by 5 ml of methanol. Samples for purification were diluted with water to an organic content of 15 % and purified over the column. The column was washed with 20 ml water at pH 3.0 and lipids extracted using 5 ml of methanol. The mixture was dried using nitrogen flow and the lipids dissolved in 100 - 200 µL of methanol.

2.2.6 LIPID DERIVATISATION AND HYDROGENATION

2.2.6.1 METHYLOXIME (MOX) DERIVATISATION OF CARBONYL GROUPS.

Lipids were dried under nitrogen flow in a glass vial. In a second vial, 1 mL of 1 N NaOH was combined with a few grains of MOX. The tubes were connected with the dry lipid uppermost to prevent solvation, and incubated for 2 h at 60 °C.

2.2.6.2 2,3,4,5,6-Pentaflourobenzyl bromide (PFB)-derivatisation of carboxyls.

Lipid was dried under N_2 and 25 μl of 1 % PFB and 25 μl of n,n-diisopropylethylamine (DIEA), both in acetonitrile, added. The mixture was vortexed and incubated for 30 min at 20 °C. The sample was dried under N_2.

2.2.6.3 Trimethylsilane (TMS)-derivatisation of hydroxyl groups.

Lipid was dissolved in 50 μl of N,O-bis(trimethylsilyl)trifluoroacetamide (BSTFA) and 50 μl of acetonitrile, vortexed and incubated for 1 h at 60 °C. The lipid was dried under N_2 and 2 mL of ethylacetate and 1 mL of H_2O added. The sample was vortexed and the ethylacetate layer recovered, dried, then dissolved in acetonitrile for GC/MS (2.2.9).

2.2.6.4 Catalytic hydrogenation using palladium on carbon (Pd-C).

Purified DXA_3 was incubated with 731 μM Pd-C (10 wt. % loading) in methanol for 2.5 h at 20 °C in a C18 solid phase extraction cartridge under hydrogen flow. The solution was centrifuged through the column and used for derivatisation according to 2.2.6.1, 2.2.6.2, 2.2.6.3 and analysed using GC/MS (2.2.9).

2.2.7 Analytical Methods

2.2.7.1 HPLC-purification of DXA_3 from lipid extract

Lipid extracts were separated using reverse-phase HPLC (Agilent) employing a Spherisorb ODS2 column (5 μm, 150 mm x 4.6 mm; Waters) with a gradient of 20-

42.5 % solvent B (100 % acetonitrile, 0.1 % formic acid) in solvent A (100 % water, 0.1 % formic acid) over 50 min, 42.5 - 90 % solvent B 50 - 60 min, 90 % solvent B 60 - 64.5 min, 90 - 20 % 64.5 - 65.5 min and 20 % solvent B 65.5 - 75 min with a flow rate of 1 ml min^{-1}. 30 sec fractions were collected and analysed using MS/MS monitoring m/z 351.2 to 165.1. Water was removed from DXA$_3$ containing fractions using Sep-Pak C18 cartridge purification as described in 2.2.5.2. Simultaneously, absorbance was monitored at 210, 235 and 270 nm.

In some experiments, [14C]-labelled lipids were monitored using a radioflow detector (Berthold Technologies).

2.2.7.2 Q1 SCAN

Lipid extracts were injected directly without LC separation at a flow rate of 10 µl/min and analysed in full scan mode (Q1) in a mass range of m/z 100 - 400 on the 4000 Q-Trap (AB Sciex, Canada).

2.2.7.3 REVERSE-PHASE LC/MS/MS OF FREE FATTY ACIDS (75 MIN)

Lipid extracts were separated using reverse-phase HPLC as described in 2.2.7.1. LC/MS/MS was performed using a HPLC (Shimadzu, Japan) and 4000 Q-Trap (AB Sciex, Canada). Analysis was performed in negative MRM mode monitoring the parent to fragment m/z listed in Table 2.. Lipid spectra were monitored in *Enhanced Product Ion* (EPI) mode. For further explanations please see 1.5.1.

2.2.7.4 REVERSE PHASE LC/MS/MS OF FREE FATTY ACIDS (30 MIN)

Lipid extracts were separated using a Spherisorb ODS2 column (5 μm, 150 mm x 4.6 mm; Waters) with a gradient of 50 - 90 % solvent B (60 % methanol, 40 % acetonitrile, 0.1 % glacial acetic acid) in solvent A (75 % water, 25 % acetonitrile, 0.1 % glacial acetic acid) over 20 min, 90 % solvent B over 5 min, 90 - 50 % solvent B from 25 – 25.1 min and 50 % solvent B from 25.1 - 30 min with a flow rate of 1 ml.min^{-1}. LC/MS/MS was performed with a HPLC (Shimadzu, Japan) and 4000 Q-Trap (AB Sciex, Canada), using negative MRM or EPI mode monitoring the lipids listed in Table 2..

2.2.7.5 REVERSE PHASE LC/MS/MS OF PHOSPHOLIPIDS

Lipid extracts were analysed using a Luna column (3 μm, 150 x 2.0 mm) with a gradient of 50 - 100% solvent B (100 % methanol, 1 mM ammonium acetate) in solvent A (60 % methanol, 20 % water, 20 % acetonitrile, 1 mM ammonium acetate) over 10 min, 100 % solvent B from 10 - 40 min, 100 - 50 % solvent B from 40.0-42.0 min and 42.1 to 50 min 50 % solvent B with a flow rate of 0.2 ml min^{-1}. DXA$_3$-PE was identified using LC/MS/MS on the HPLC (Shimadzu, Japan) coupled 4000 Qtrap (AB

Table 2.1. MS/MS parameters monitoring eicosanoids.
DP: declustering potential [mV], CE: collision energy [mV]

Lipid	Q1 [m/z]	Q3 [m/z]	DP [mV]	CE [mV]
DXA_3	351.2	165.1	-55	-26
[^{14}C] DXA_3	353.2	165.1	-55	-26
PGE_2	351.2	271.1	-55	-26
TxB_2	396.2	169.1	-50	-22
12-HETE	319.2	179.1	-85	-20
PGE_2-d_4	355.2	271.1	-55	-26
TxB_2-d_4	373.2	173.1	-95	-36
12-HETE-d_8	327.2	184.1	-85	-20

Sciex, Canada) employing negative MRM mode monitoring the transitions shown in Table 2..

2.2.8   Reverse phase LC/MS^3

To determine the accurate mass of lipids of interest and their MS^3 fragmentation spectra, a reverse phase HLPC approach was employed on an Orbitrap Elite instrument (Thermo Fisher, MA, USA) with a Spherisorb ODS2 column (5 μm, 150 mm x 4.6 mm, Waters) and a solvent gradient described in 2.2.7.1. Analysis was performed using h-ESI in negative ion mode at sheet, auxillary and sweep gas flows of 70, 20, and 0. Capillary and source heater temperatures were set to 300 and 350 °C, respectively. MS/MS analysis of DXA$_3$ (*m/z* 351.2177) or DXA$_3$-*d8* (*m/z* 359.2679) was undertaken in negative FTMS mode using CIDwith a resolving power of 30,000. Data dependent MS^3 monitoring DXA$_3$ or DXA$_3$-*d8* was carried out in negative FTMS mode with resolving power of 15,000.

2.2.9   GC-MS

GC/MS was carried out on a DSQ Finnigan (Thermo Fisher, MA, USA) at the laboratory of Dr. Robert Murphy (University of Denver, USA). Samples were analysed using a Phenomenex 30M ZB-1 column in negative polarity mode with a source temperature of 200 °C and methane as reagent gas applying a gas flow of 1.8 ml min^{-1}.

Table 2.2. MS/MS parameters monitoring DXA$_3$-PEs.
DP: declustering potential [mV], CE: collision energy [mV]

Lipid	Q1 m/z	Q3 m/z	DP [mV]	CE [mV]
DXA$_3$-PE 18:0a	814.7	351.1	-140	-45
DXA$_3$-PE 18:0p	798.6	351.1	-140	-45
DXA$_3$-PE 18:1p	796.6	351.2	-140	-45
DXA$_3$-PE 16:0p	770.6	351.2	-140	-45
DMPE	634.4	227.2	-140	-45

2.2.10 FLOW CYTOMETRY ANALYSIS OF NEUTROPHILS

Flow cytometric analysis was performed using a Cyan ADP analyser (Beckman Counter, CA, USA). The forward scatter (FSC), side scatter (SSC) and Alexa Fluor 647 voltage parameters were determined using unstained purified neutrophils prior to acquisition of the experimental samples. Data was analysed using *flowjo* software (FlowJo, LLC, OR, USA).

2.2.11 STATISTICS

Statistical significance was assessed using one way ANOVA followed by Bonferroni multiple comparisons test, as indicated on legends. * $p \leq 0.05$ was considered statistically significant and *** indicated $p \leq 0.005$.

CHAPTER THREE

STRUCTURAL CHARACTERISATION OF A NOVEL PLATELET

LIPID

3.1 INTRODUCTION

Preliminary structural studies performed by members of the O'Donnell group in collaboration with Prof. Robert Murphy (University of Colorado, Denver) revealed that DXA$_3$ contains three double bonds and five oxygen atoms in total. Three of those form a carboxyl and one hydroxyl group. These studies also demonstrated that DXA$_3$ contains no carbonyl group and is acid stable, effectively excluding epoxides (unpublished). DXA$_3$ elutes later than PGE$_2$ on reverse phase chromatography indicating it to be less polar than PGE$_2$. Hence, for the two remaining oxygen atoms a dioxolane ring structure and three double bonds were proposed yielding m/z 351.2175 and a elemental composition of C$_{20}$O$_5$H$_{32}$.

As described in Chapter 1 (1.4), arachidonate - derived dioxolanes have been demonstrated previously to form in chemical reactions. Havrilla et al. proposed a structure for the mono-cyclic product (Scheme 1.) that contains a dioxolane ring and three double bonds and calculation of its ion mass as a free fatty acid form reveals m/z 351.2177, which is identical to that of DXA$_3$. Therefore, the free fatty acid structure of the monocyclic product we found in platelets was initially proposed to be 8-hydroxy-9,11-dioxolane eicosatrienoic acid (DXA$_3$) (Scheme 3.1).

m/z 351.2177
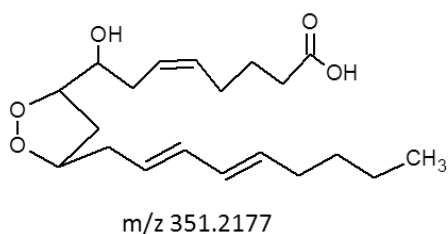
Scheme 3.1.Proposed structure of DXA$_3$.

However, Havrilla et al. (2000) analysed dioxolanes that were esterified to cholesterol using positive ion mode. Thus, their data cannot be compared with our MS/MS of DXA$_3$ obtained in negative ion mode. Therefore, in this chapter I will structurally characterise HPLC -purified DXA$_3$ generated by COX-1 *in vitro.* In order to open the chemically-stable dioxolane ring and to determine the number of double bonds, I will hydrogenate DXA$_3$ using palladium on carbon (Pd-C) as catalyst (as shown by Yin et al. 2004), then derivatise and analyse using GC/MS. In addition, high resolution LC/MS^n of DXA$_3$ and its deuterated analogue DXA$_3$-d$_8$ derived from oxidation of arachidonate and arachidonate-d$_8$ by COX-1 *in vitro* will be undertaken. The proposed structure for DXA$_3$ contains a conjugated diene (Scheme 3.1). Structurally similar dioxolanes derived from LOX *in vitro* were shown to be UV active with an absorbance max of λ 238 nm (Teder et al. 2014). Therefore, DXA$_3$ should absorb at similar wavelength. To provide further evidence for our proposed structure, I will determine whether COX-derived DXA$_3$ is UV-active.

3.1.1 AIMS

- Elucidate the functional groups of the two remaining oxygen atoms in DXA$_3$ through hydrogenation using Pd-C.

- Determine the fragmentation pathway of DXA$_3$ by employing high resolution MS^n analysis using lipid generated from either arachidonate or arachidonate-*d8*, to further support the proposed structure of DXA$_3$.

- Investigate whether DXA$_3$ contains a conjugated diene by using LC/UV.

3.2 RESULTS

To confirm the proposed structure of DXA$_3$ derived from COX-1 *in vitro* (2.2.2), I utilised GC/MS at the University of Denver (3.2.1), high resolution MS (3.2.2) and LC/UV (3.2.5). These studies were carried out in collaboration with Prof. Robert Murphy (University of Colorado, USA).

3.2.1 HYDROGENATION OF HPLC-PURIFIED DXA$_3$ REVEALS A DIOXOLANE RING AND THREE DOUBLE BONDS

Yin et al (2004) demonstrated that dioxolanes can be hydrogenated using Pd-C as catalyst leading to ring opening and hydrogenation of double bonds. Therefore, in this study, HPLC-purified DXA$_3$ generated by purified COX-1 *in vitro* was hydrogenated using the same catalyst.

Following hydrogenation, DXA$_3$ was derivatised using methoxyamine hydrochloride (MOX), N,O-Bis (trimethylsilyl) trifluoroacetamide (BSTFA) and /or pentafluorbenzyl bromide (PFB) as described in 2.2.6. MOX derivatises carbonyl groups leading to a mass increase of +29 amu. Derivatisation with BSTFA results in addition of trimethylsilyl (TMS) to hydroxyl groups and a mass increase of +72 amu. The carboxyl group, common to all eicosanoids, is derivatised using PFB. This enables lipids to become sufficiently volatile for GC/MS. During ionisation, electrons generated are captured by the electrophilic PFB leading to cleavage of this group from the lipid, and resulting in regeneration of the carboxylate anion, which is detected in negative ion mode (termed negative chemical ionisation, NICI).

The proposed lipid structures were drawn in *ChemSketch* (ACD Labs), allowing calculation of masses of DXA$_3$, its hydrogenated analogue, and following derivatisation using BSTFA (Scheme 3.2).
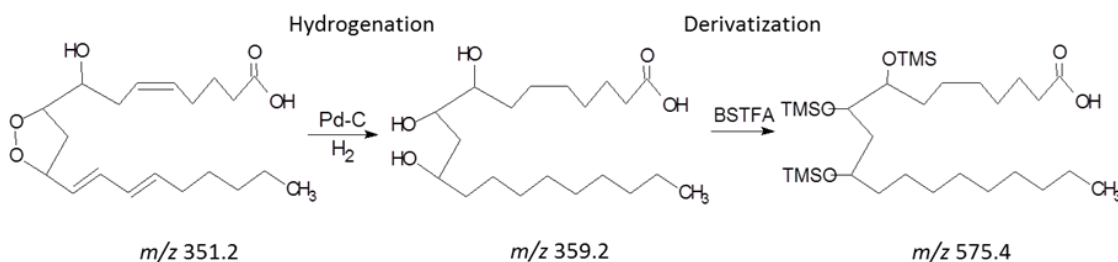
Scheme 3.2. Hydrogenation and derivatisation of DXA$_3$.
Hydrogenation of DXA$_3$ with *m/z* 351.2 should result in ring opening and hydrolysis of double bonds to *m/z* 359.2. Thus, derivatisation using BSTFA reagent should lead to the addition of three TMS groups resulting in *m/z* 575.4.

Hydrogenation of DXA$_3$ is expected to open the dioxolane ring, forming two hydroxyl groups. Along with reduction of the three double bonds this would lead to *m/z* 359.2. The hydroxyl groups can then be derivatised using BSTFA resulting in *m/z* 575.4. Indeed, when extracting this mass from a GC/MS full scan, four peaks (1-4) elute (Figure 3.1). As expected, the mass spectra for all four peaks show *m/z* 575.4 (Figure 3.2). This data is consistent with the presence of three hydroxyl groups and three double bonds. Alongside DXA$_3$, several unknown ions appear in the spectra including *m/z* 427.3, 501.3 and 517.4. However, when extracting them from the TIC, it was seen that none of those coeluted with DXA$_3$. Therefore, these ions remain unidentified but do not originate from DXA$_3$ itself (data not shown).

A TIC

B TIC, extracted *m/z* 575.4
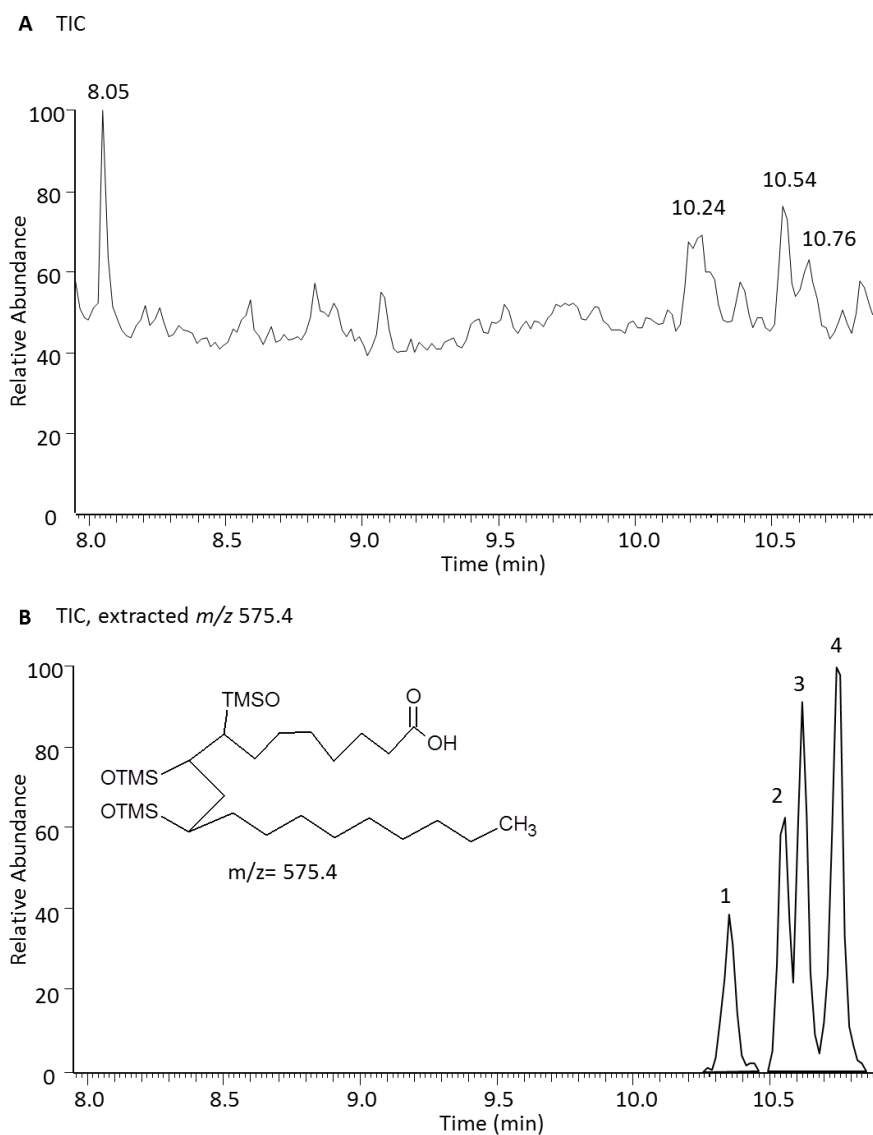
m/z= 575.4

Figure 3.1. Four products are detected when monitoring *m/z* 575.4 in HPLC-purified DXA$_3$ generated by COX-1 *in vitro* following hydrogenation. DXA$_3$ was generated by COX-1 *in vitro,* then purified as described in 2.2.2 and 2.2.7.1. HPLC-purified DXA$_3$ was hydrogenated and derivatised using TMS (2.2.6) and analysed using GC/MS (2.2.6, 2.2.9). (A) Total ion current (TIC). (B) The extracted ion *m/z* 575-576 shows four peaks eluting at 10.35 min (Peak 1), 10.54 min (Peak 2), 10.62 min (Peak 3) and 10.74 min (Peak 4).
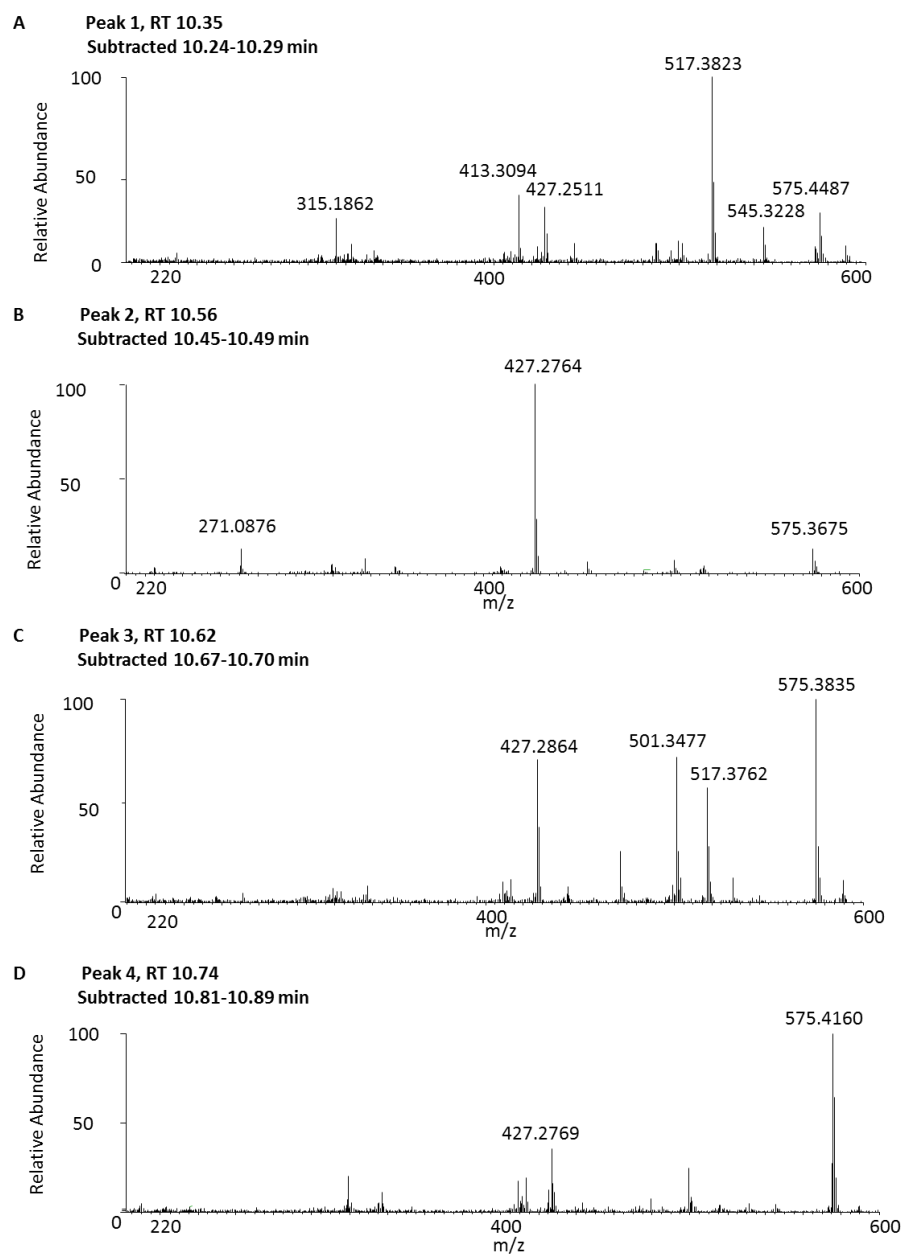
Figure 3.2. GC/MS of DXA₃ is consistent with three double bonds and a dioxolane ring. DXA₃ was generated by COX-1 *in vitro*, purified, then hydrogenated and derivatised using BSTFA as described in 2.2.2, 2.2.7.1 and 2.2.6. GC/MS spectrum of (A) Peak 1, (B) Peak 2, (C) Peak 3 and (D) Peak 4 eluting in 3.1. For all peaks a background spectrum was subtracted. *m/z* 575.4 represents the *m/z* for hydrogenated DXA₃ + 3x TMS groups.

3.2.2 The fragmentation pathway for DXA₃ supports the previous proposed structure

To determine the CID fragmentation pattern of DXA$_3$, I generated data dependent MS^n utilizing high resolution Orbitrap MS, which allows a mass accuracy down to 1 ppm.

In this approach, MS^n data are used to generate a fragmentation pathway, as illustrated in Scheme 3.3: A parent ion is detected in an MS experiment and fragmented in MS/MS mode generating several product ions (Scheme 3.3, 1-3). These can then be fragmented again in a data dependent MS^3 experiment to determine which ion originates from which parent. Utilizing high resolution MS allows calculation of the chemical composition of parent and fragment ions, thus enabling the structural elucidation of both.

In this study I analysed DXA$_3$ and its deuterated analogue (DXA$_3$ -*d8*) generated by COX-1 *in vitro* as described in 2.2.2. Both were analysed using LC/MS/MS to generate a fragmentation spectrum of the parent ions (3.2.2.1). This was followed by MS^n of the most abundant fragment ions (3.2.2.2, 3.2.2.3). Based on the data obtained, I propose two fragmentation pathways including structures for the parent and fragment ions (3.2.3, 3.2.4).

3.2.2.1 Generation of a MS/MS spectrum of both DXA₃ and DXA₃-D₈ using high resolution Orbitrap mass spectrometry

Due to the different pump system on the Orbitrap platform, DXA$_3$ and DXA$_3$-d$_8$ elute slightly later than on the 4000 QTrap system, at 47.61 min (Figure 3.3, Panel A) and 47.18 min (Figure 3.4, Panel A) respectively. DXA$_3$ was identified based on its MS/MS

89
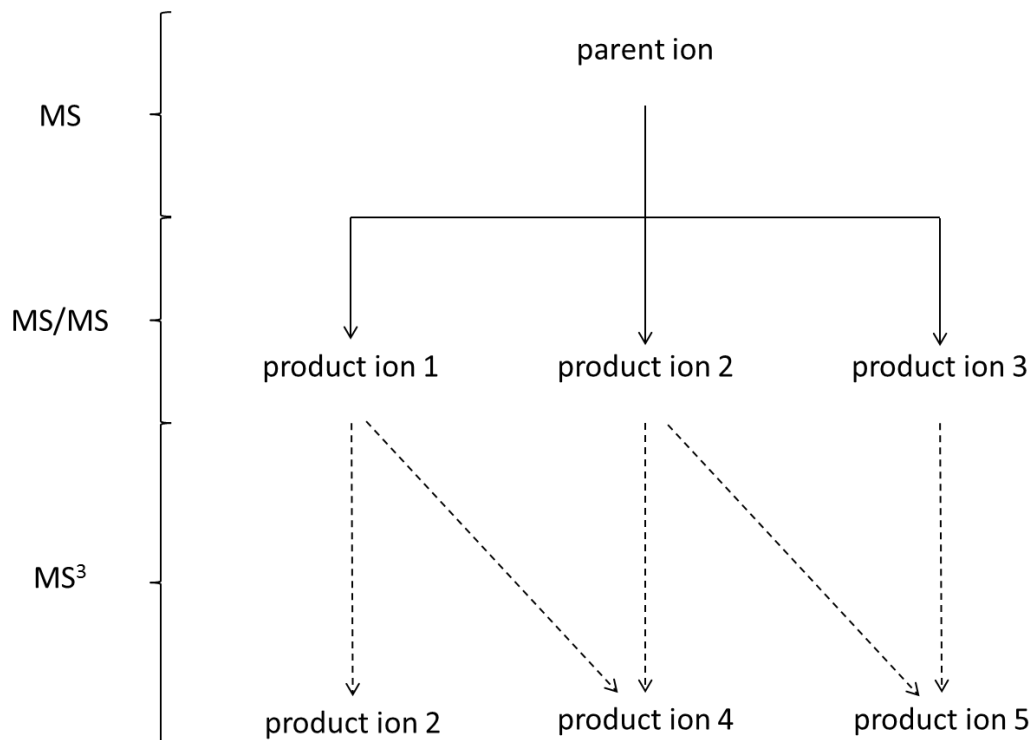
Scheme 3.3. Building a pathway of fragmentation based on MS^n experiments. A parent ion, which is observed in an MS spectrum, is fragmented in a MS/MS experiment generating fragment ions 1-3. These ions can be fragmented again in a MS^3 experiment to determine the relationship between fragment ions and consequently develop a fragmentation pathway.

A MS chromatogram of m/z 351.2177
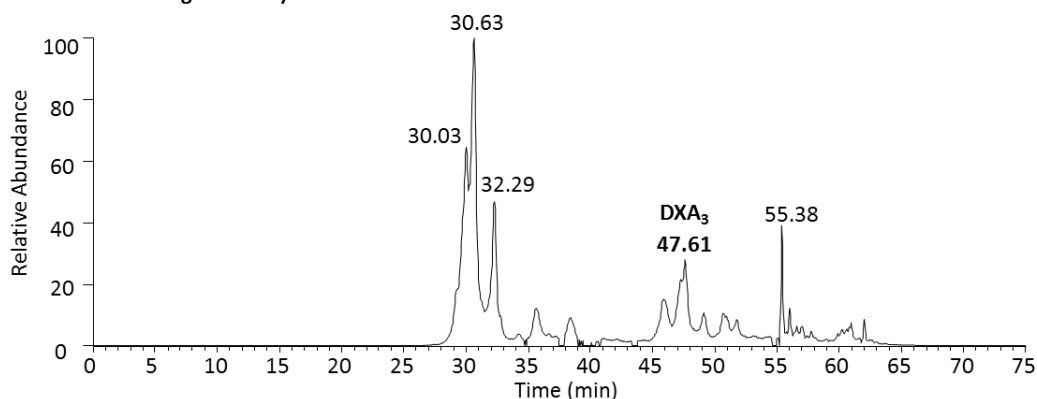
B MS spectrum, peak 47.61 min
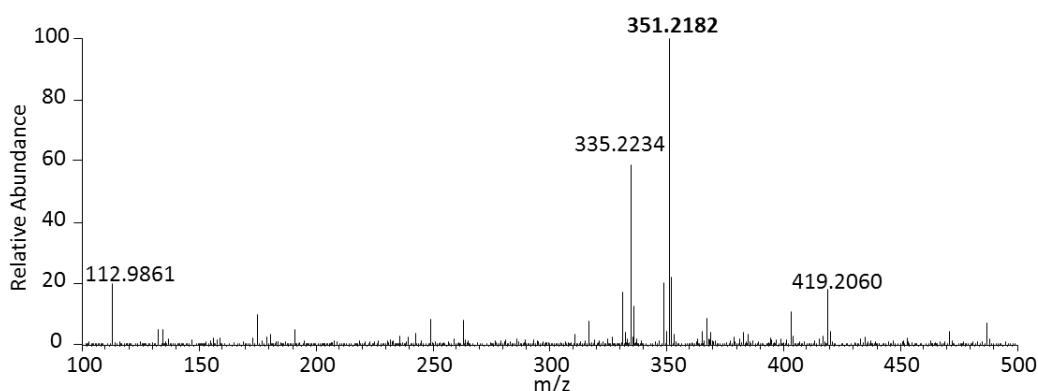
C MS/MS spectrum, peak 47.61 min
m/z 351.22
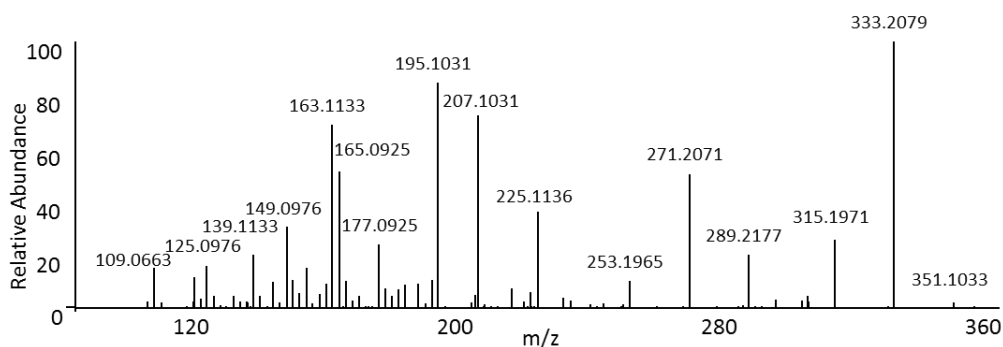
Figure 3.3. DXA$_3$ generated by COX-1 *in vitro* elutes at 47.61 min on the Orbitrap Elite platform. DXA$_3$ was generated by COX-1 *in vitro* and analysed using high resolution LC/MS as described in 2.2.2 and 2.2.7.3. (A) DXA$_3$ elutes at 47.61 min in the MS chromatogram monitoring the parent ion m/z 351.2175. (B) MS spectrum of DXA$_3$ eluting at 47.61 min in (A). m/z 351.2182 is the most abundant ion. (C) MS/MS spectrum of DXA$_3$.

A m/z= 359.2675

B MS spectrum

C MS/MS of *m/z* 359.27
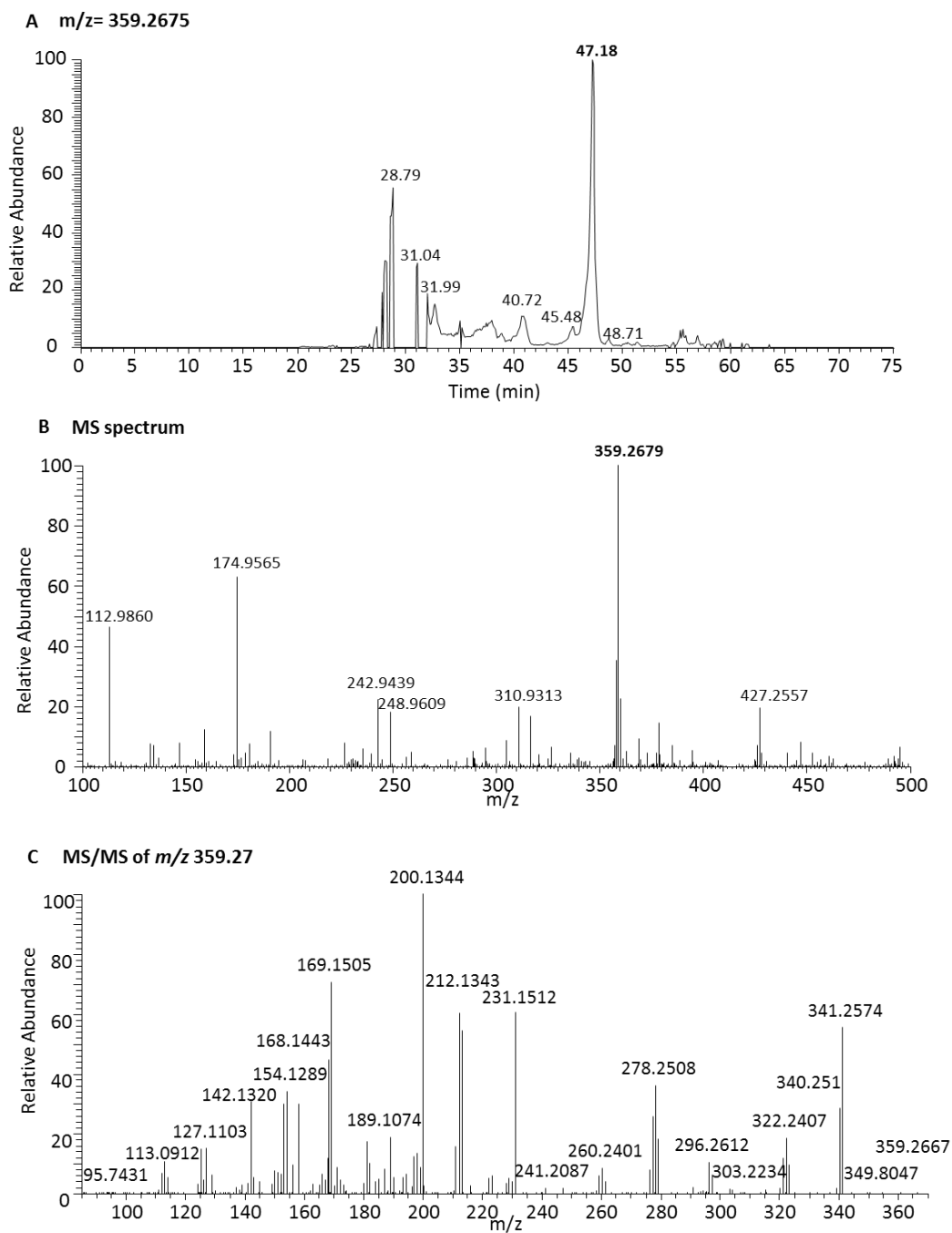
Figure 3.4. DXA₃-*d8* derived from COX-1 *in vitro* elutes at 47.18 min on the Orbitrap platform. LC/MS analysis of DXA₃ generated by oxidation of arachidonate-*d8* using COX-1 *in vitro* as described in 2.2.2 and 2.2.7.3. (A) LC/MS chromatogram monitoring *m/z* 359.2675 for DXA₃-*d8* reveals one major peak eluting at 47.18 min. (B) MS spectrum of this peak shows *m/z* 359.2679 as the most abundant ion. (C) MS/MS spectrum of ion *m/z* 359.27.

spectrum and retention time in regard to that of PGE$_2$, which elutes at 30.03 min on the Orbitrap system. Therefore, shifts in retention time of both lipids would be identical. DXA$_3$ with *m/z* 351.2182 (Figure 3.3, Panel B) is within the acceptable 5 ppm range for ion identification compared to a theoretical ion mass of DXA$_3$ *m/z* 351.2177, which I calculated using *ChemSketch*. LC/MS/MS analysis of this ion (Figure 3.3, Panel C) shows an identical fragment spectrum as detected prior to this study for DXA$_3$ attached to PE (Aldrovandi et al, unpublished). The MS spectrum of DXA$_3$-d$_8$ reveals *m/z* 359.2679 as the most abundant ion (Figure 3.4, Panel B), which is only 1.1 ppm different from the theoretical calculated ion mass for DXA$_3$-*d8*. As a consequence of deuteration, the MS/MS spectrum of this lipid is expected to reveal fragment ions differing by up to 8 Da from those of the undeuterated lipid (Figure 3.4, Panel C).

3.2.2.2   MS^N DATA OF DXA$_3$

The ten most abundant fragment ions generated during DXA$_3$ MS/MS fragmentation (Figure 3.3, Panel C) were selected for further LC/MS^3 analysis (Figure 3.5). The fragmentation spectrum of *m/z* 333.2078 shows the ions *m/z* 315.1968, *m/z* 289.2166 and *m/z* 271.2077 (Figure 3.5, Panel A). As described in 3.2.2.1, this indicates that *m/z* 315.1968 and *m/z* 271.2077 originate from *m/z* 333.2078. Following fragmentation of *m/z* 315.1971 the ion *m/z* 271.2068 is detected (Figure 3.5, Panel B). Hence, this ion originates from *m/z* 315.1971. MS^3 of *m/z* 271.2171 reveals minor ions (Figure 3.5, Panel C), which are not detected in MS/MS spectra (Figure 3.3, Panel C). Therefore these will not be considered in
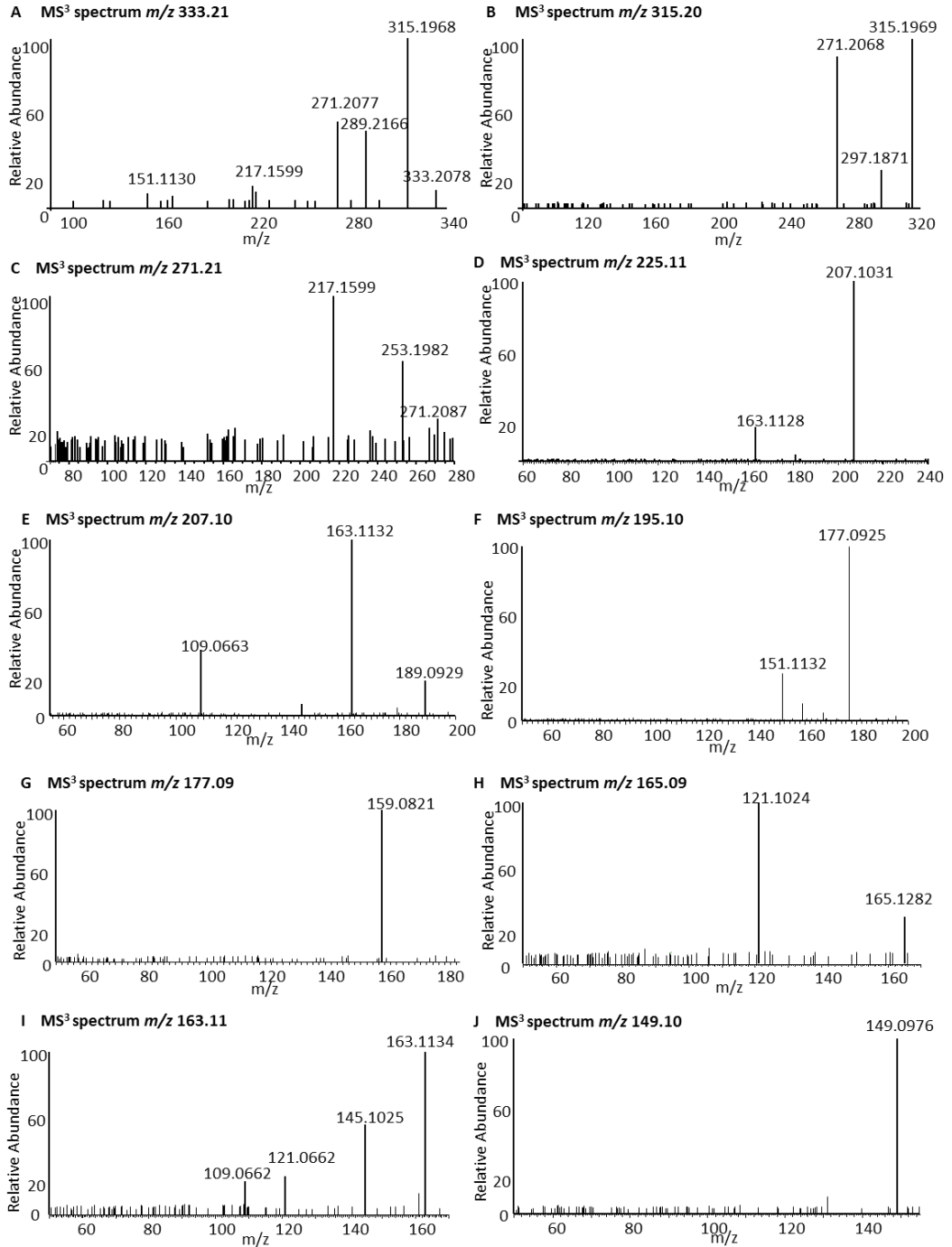
Figure 3.5. Data dependent MS³spectra of DXA₃. LC/MSⁿ of DXA₃ derived from COX-1 *in vitro* as described in 2.2.2 and 2.2.8. MS³spectra of (A) *m/z* 333.21, (B) *m/z* 315.20, (C) *m/z* 271.21, (D) *m/z* 225.11, (E) *m/z* 207.10, (F) *m/z* 195.10, (G) *m/z* 177.09, (H) *m/z* 165.09, (I) *m/z* 163.11 and (J) *m/z* 149.10. Data obtained on high resolution Orbitrap MS.

this fragmentation pathway. The spectra indicate that m/z 271.2077 originates from m/z 315.1968, which itself originates from m/z 333.2078. The ions m/z 225.1136, m/z 207.1031 and m/z 163.1133 belong to an additional fragmentation pathway. The ion m/z 163.1133 originates from m/z 207.1031 (Figure 3.5, Panel I), which itself is a result of fragmentation of m/z 225.1136 (Figure 3.5, Panel D). Fragmentation of m/z 163.1133 results in minor ions not considered in this pathway.

MS^3 spectra for the remaining ions m/z 195.1031 (Figure 3.5, Panel F), m/z 177.0925 (Figure 3.5, Panel G), m/z 165.0915 (Figure 3.5, Panel H), and m/z 149.0976 (Figure 3.5, Panel J) suggest that m/z 177.0925 is a product ion of m/z 195.1031. The mass difference of 18 Da between these ions indicates the loss of a water molecule. However, the ions m/z 195.1031, m/z 165.0915 and m/z 149.0976 show no relation to each other or other ions investigated. This suggests that these ions are fragments of either the parent ion m/z 351.2177 or ions not chosen for MS^3 experiments. Therefore, these ions were neither structurally identified nor considered in the fragmentation pathway presented herein.

3.2.2.3 MS^N DATA OF DXA$_3$-$D8$

To determine the fragmentation pathway of DXA$_3$-$d8$, the same analytical process was employed as described for DXA$_3$ (3.2.2.2). The MS/MS spectrum of the parent ion m/z 359.2667 is depicted in Figure 3.4, Panel C. From this spectrum the ten most abundant fragment ions were selected for data

dependent MS^3 analysis (Figure 3.6). The parent ion m/z 359.2667 is fragmented into m/z 341.2574 and m/z 340.251 (Figure 3.4, Panel C). MS^3 spectra of both ions show the product ion m/z 322.2405 (Figure 3.6, Panels A and B) and fragmentation of this results in m/z 278.2522 (Figure 3.6, Panel C), which could not be further fragmented (Figure 3.6, Panel D). Therefore, m/z 278.2522 is considered to be the end of the fragmentation pathway.

As for DXA$_3$, also MS^3 for DXA$_3$-*d8* indicates a second pathway of fragmentation in which m/z 168.14 is a fragment of m/z 212.13 (Figure 3.6, Panel F). The latter originates from m/z 231.15 (Figure 3.6, Panel E). The fragment ions of DXA$_3$-*d8* are consistent with deuterium atoms on the carbon backbone of DXA$_3$.

MS^3 spectra of the remaining ions m/z 200.13 (Figure 3.6, Panel G), m/z 181.12 (Figure 3.6, Panel H) and m/z 169.15 (Figure 3.6, Panel I) do not indicate a relationship to each other or the other ions investigated. Thus, these ions were not considered further.

3.2.3   FRAGMENTATION PATHWAY OF DXA$_3$ M/Z 351.2177 TO M/Z 271.2067

All MS^n results are summarised in Table .1 for DXA$_3$ and Table 3.2 for DXA$_3$-*d8*. Both demonstrate that all MS/MS and MS^3 fragment ions are generated through fragmentation of the parent ion m/z 351.2182 or m/z 359.2667. Additional MS^3 fragment ions generated from their corresponding MS/MS fragments, formed as a result of m/z 351.2182 or m/z 359.2667 parent ion fragmentation are also described.
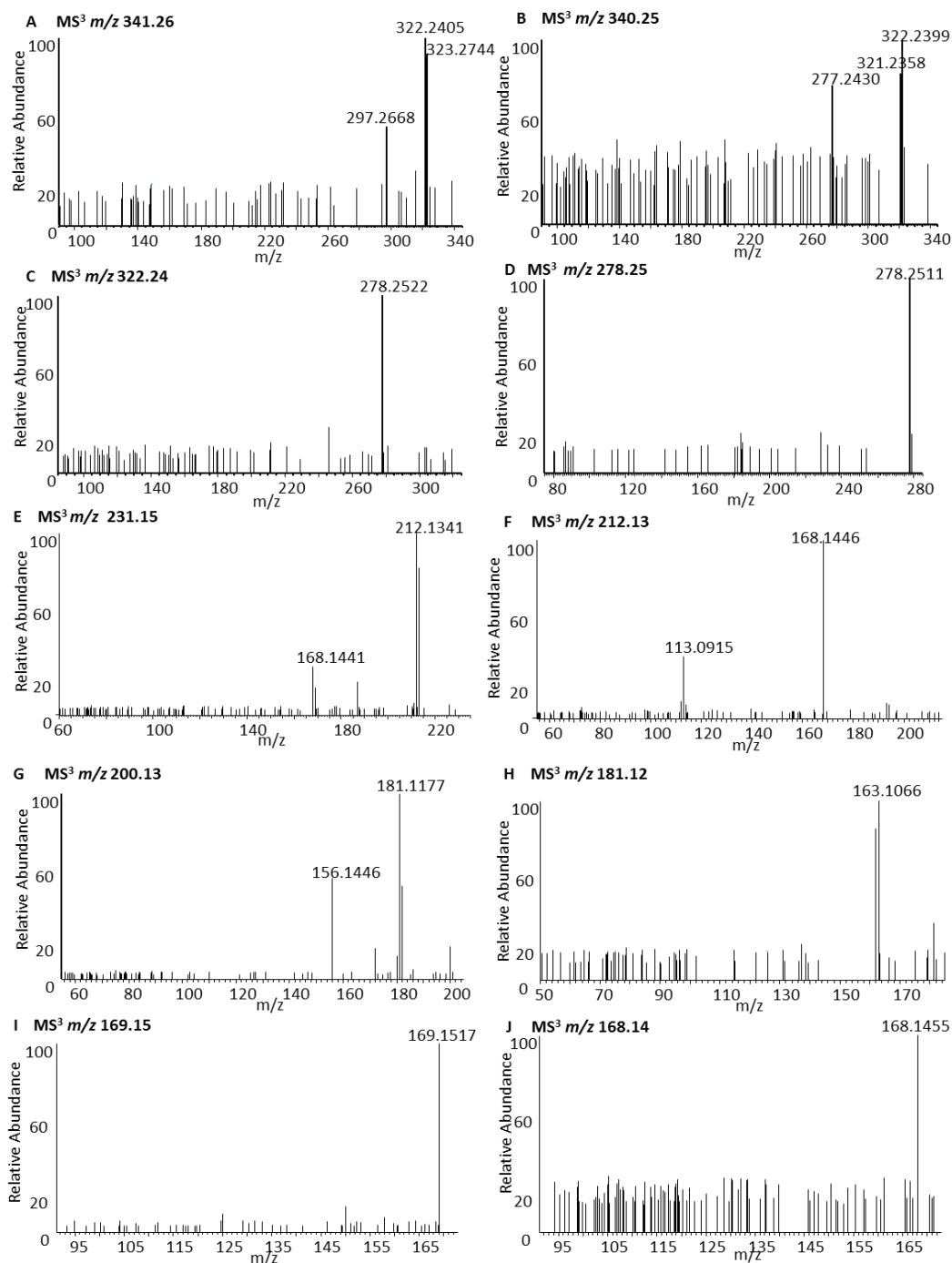
Figure 3.6. Data dependent MS^3 spectra of DXA$_3$-*d8*. LC/MS^n of DXA$_3$-*d8* generated by COX-1 *in vitro* as described in 2.2.2 and 2.2.8. MS^3 spectra of (A) *m/z* 341.26, (B) *m/z* 340.25, (C) *m/z* 322.24, (D) *m/z* 278.25, (E) *m/z* 231.15, (F) *m/z* 212.13, (G) *m/z* 200.13, (H) *m/z* 181.12, (I) *m/z* 169.15 and (J) *m/z* 168.14. Data obtained on high resolution Orbitrap MS.

Table 3.1 Fragmentation of DXA$_3$ *m/z* 351.2182 using MS/MS and MS^{3}performed using the Orbitrap Elite.

DXA$_3$ parent mass m/z	MS/MS fragments m/z	MS^3 fragments m/z			
351.2182	333.2078	315.1969	289.2173	271.2072	219.1664
351.2182	315.1971	297.1971	271.2069		
351.2182	271.2071	253.1983	217.1599		
351.2182	225.1136	207.1031	163.1128		
351.2182	207.1031	189.0924	163.1132	109.0662	
351.2182	195.1031	177.0925	151.1132		
351.2182	177.0925	159.0821			
351.2182	165.0915	121.1023			
351.2182	163.1133	145.1023	121.0662	109.0662	
351.2182	149.0976				

Table 3.2 Fragmentation of DXA$_3$-*d8* m/z 359.2667 using MS/MS and MS^{3}experiments using the Orbitrap Elite.

DXA$_3$-*d8* parent mass m/z	MS/MS fragments m/z	MS^3 fragments m/z				
359.2667	341.2573	323.2483	322.2409	297.2668		
359.2667	340.251	321.2348	322.2397	296.2589	277.243	
359.2667	322.2406	278.2511				
359.2667	278.2508					
359.2667	231.1511	213.1405	212.1344	211.1283	168.1441	165.1505
359.2667	212.1342	168.1451	113.0907			
359.2667	200.1343	181.1177	156.1445	182.1235		
359.2667	181.1174	163.1066	162.1067			
359.2667	169.1175	150.1343	125.1281			
359.2667	168.1443					

Notably, in addition to a parent mass of m/z 359.2681, m/z 358.2621 was detected in the LC/MS spectrum of DXA$_3$-*d8*. This mass corresponds to an open ring structure as shown in Figure 3.7, Panel B. In contrast, ring opening of undeuterated DXA$_3$ does not result in a mass change and remains at m/z 351.2177 (Figure 3.7, Panel A). Consequently, this cannot be detected in the spectrum. However, as ring opening is detected for DXA$_3$-*d8*, it will be considered in the fragmentation pathway.

Some MS^n spectra of DXA$_3$-d$_8$ contain additional ions not found for DXA$_3$. As demonstrated on m/z 341.2575 and m/z 340.2513 (Figure 3.8, Panel A), these ions differ by approximately 1 Da from one another and appear with similar abundance in the MS/MS spectra. This is due to the deuterium atoms within DXA$_3$-*d8*, since the substrate for COX-1, arachidonate-d8, contains eight deuterium atoms at positions 5, 6, 8, 9, 11, 12, 14, and 15. Consequently, DXA$_3$-*d8* contains deuterium at the same positions:

m/z 359.2679
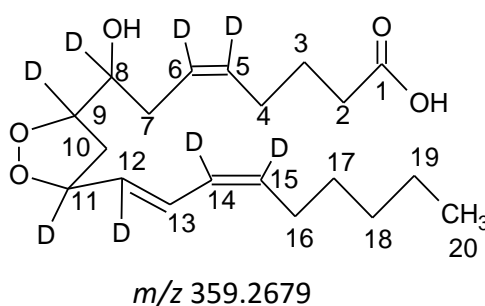
As a result of deuteration, fragmentation or the loss of a water molecule from DXA$_3$-*d8* leads to the abstraction of either hydrogen (H) or deuterium (D) atoms. Consequently, additional DXA$_3$-d$_8$ fragments are formed that are not seen for DXA$_3$. For example, the loss of a water molecule from DXA$_3$-*d8* will result in m/z 341.2 and m/z 340.2 (Figure 3.8, Panel B):
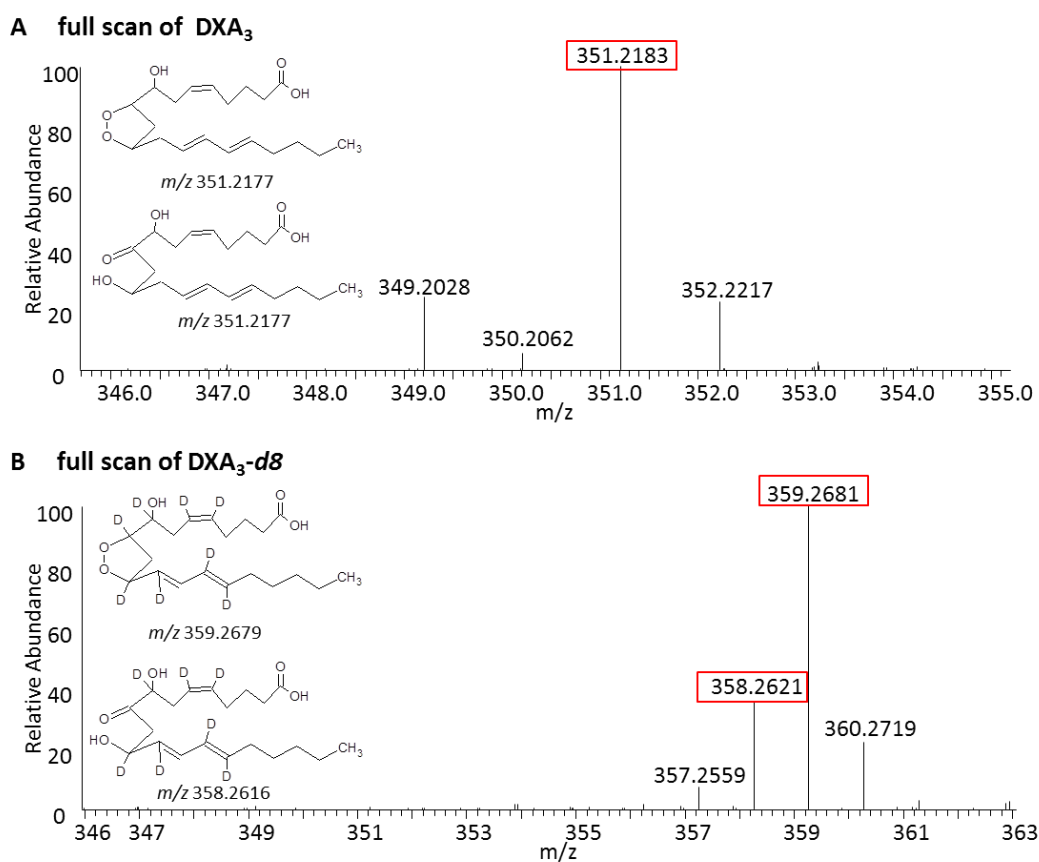
Figure 3.7. Ring opening is detected during DXA₃-*d8* fragmentation. MS spectra obtained on high resolution Orbitrap MS of DXA₃ and DXA₃-*d8* derived from COX-1 *in vitro* as described in 2.2.2 and 2.2.8. Extraction of the parent ion masses of (A) DXA₃ *m/z* 351.2177 and (B) DXA₃-*d8 m/z* 359.2979.

A MS/MS spectrum of *m/z* 359.27
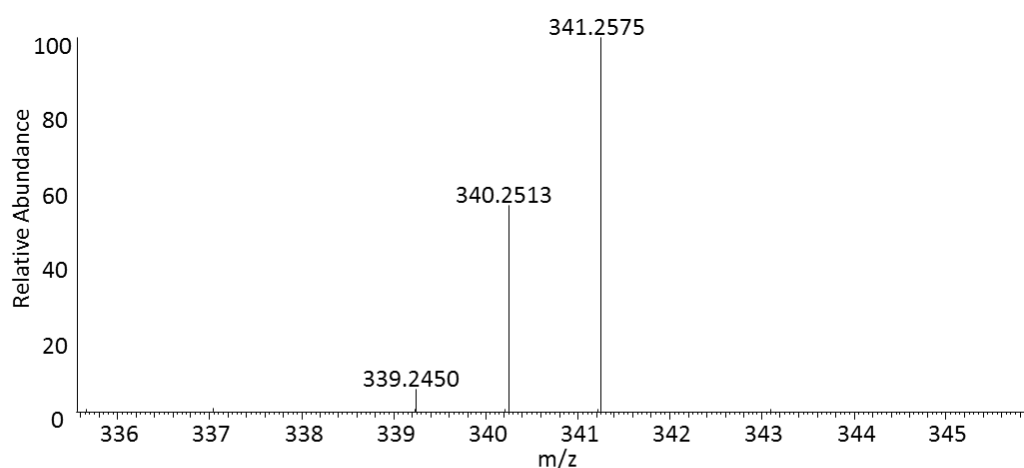
B Loss of water at position C8 without ring opening

m/z 341.2573   *m/z* 340.2511
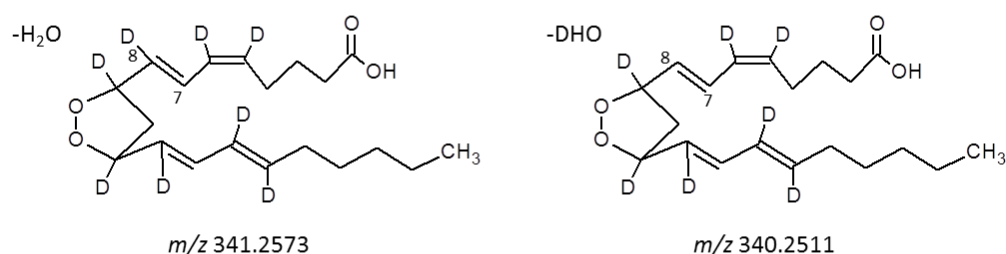
C Loss of water at position C8 following ring opening, carbonyl at C11

m/z 340.2511   *m/z* 339.2448
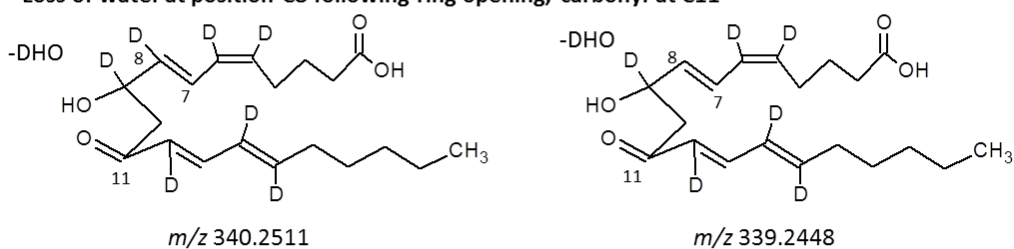
D Loss of water at position C11 following ring opening, carbonyl at C9

m/z 340.2511   *m/z* 339.2448
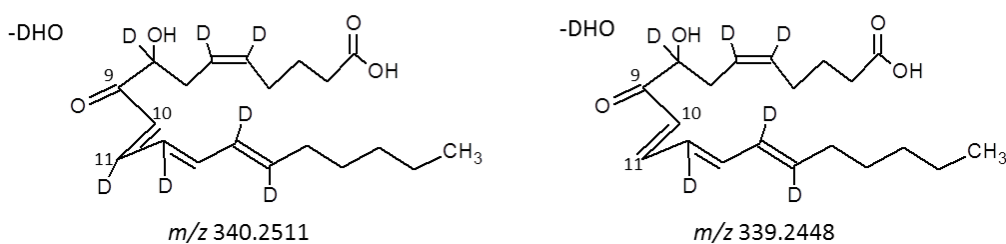
Figure 3.8. Loss of water from DXA$_3$-*d8* results in several product ions. DXA$_3$-*d8* derived from COX-1 *in vitro* was analysed using high resolution LC/MS/MS as described in 2.2.2 and 2.2.8. (A) MS/MS spectrum of DXA$_3$-d$_8$ shown within the range *m/z* 335-360. During fragmentation a water molecule can be abstracted either as H$_2$O or DHO from position C8 or C11. This results in (B) the ions *m/z* 341.2573 or *m/z* 340.2511, (C) *m/z 340.2511 or m/z 339*.2448 or (D) *m/z 340.2511 or m/z*339.2448. Structures were drawn using *Chemsketch*.

- 359.2 Da -18 Da (H_2O) = 341.2 Da, resulting from loss of H at position C7 and a hydroxyl group (OH) at position C8

- 359.2 Da -19 Da (DHO) = 340.2 Da, resulting from loss of D at C8 and OH at C8.

If ring opening occurs first (resulting in *m/z* 358.2), a carbonyl group is either formed at C9 or C11 and loss of a water molecule leads to *m/z* 340.2 and *m/z* 339.2 (Figure 3.8, Panels C and D):

- 358.2 Da -18 Da= 340.2 Da, resulting from loss of H at C7 and OH at C8 or H at C10 and OH at C11.

- 358.2 Da – 19 Da (DHO) = 339.2 Da, resulting from loss of D at C8 and OH at C8 or D at C11 and OH at C11.

To compare the MS^n data for DXA$_3$-*d8* and DXA$_3$, the ion mass differences of both lipids were calculated shown as Δ *m/z* in Table 3.3. These differences correlate with the number of remaining deuterium atoms in the ion following fragmentation. This provides information regarding deuterium or hydrogen abstraction during fragmentation.

Based on the data shown in Table 3.2 and Table 3.3 and opening of the dioxolane ring (Figure 3.7), I propose two fragmentation pathways for DXA$_3$ (*m/z* 351.2177) leading to *m/z* 271.2067 and *m/z* 163.1132. This is supported by data obtained on DXA$_3$-*d8* fragmentation.

The fragmentation pattern of DXA$_3$ to *m/z* 271.2067 is shown in the MS/MS spectrum (Figure 3.9). Parent and fragment ion structures for this pathway are depicted in Figure 3.10 and Figure 3.11. I propose that fragmentation commences with the loss of a water molecule from the parent ion

Table 3.3 DXA$_3$ and DXA$_3$-*d8* parent and product ion masses differ by up to 8 Da.

Ion masses of DXA$_3$ and DXA$_3$ d-8 were subtracted giving *Δm/z*. This value correlates with the number of deuterium atoms in the ion.

	DXA$_3$ m/z	DXA$_3$-*d8* m/z	*Δm/z* (DXA$_3$/ DXA$_3$ d-8)
Parent ion mass	351.2177	359.2667	8
Product ion mass	333.2075	340.251	7
		341.2573	8
	315.1971	322.2405	7
		323.2469	8
	271.2069	278.2508	7
	225.1135	231.1511	6
	207.1029	212.1342	5
	195.103	200.1343	5
	165.0924	169.1175	4
	163.1132	168.1443	5
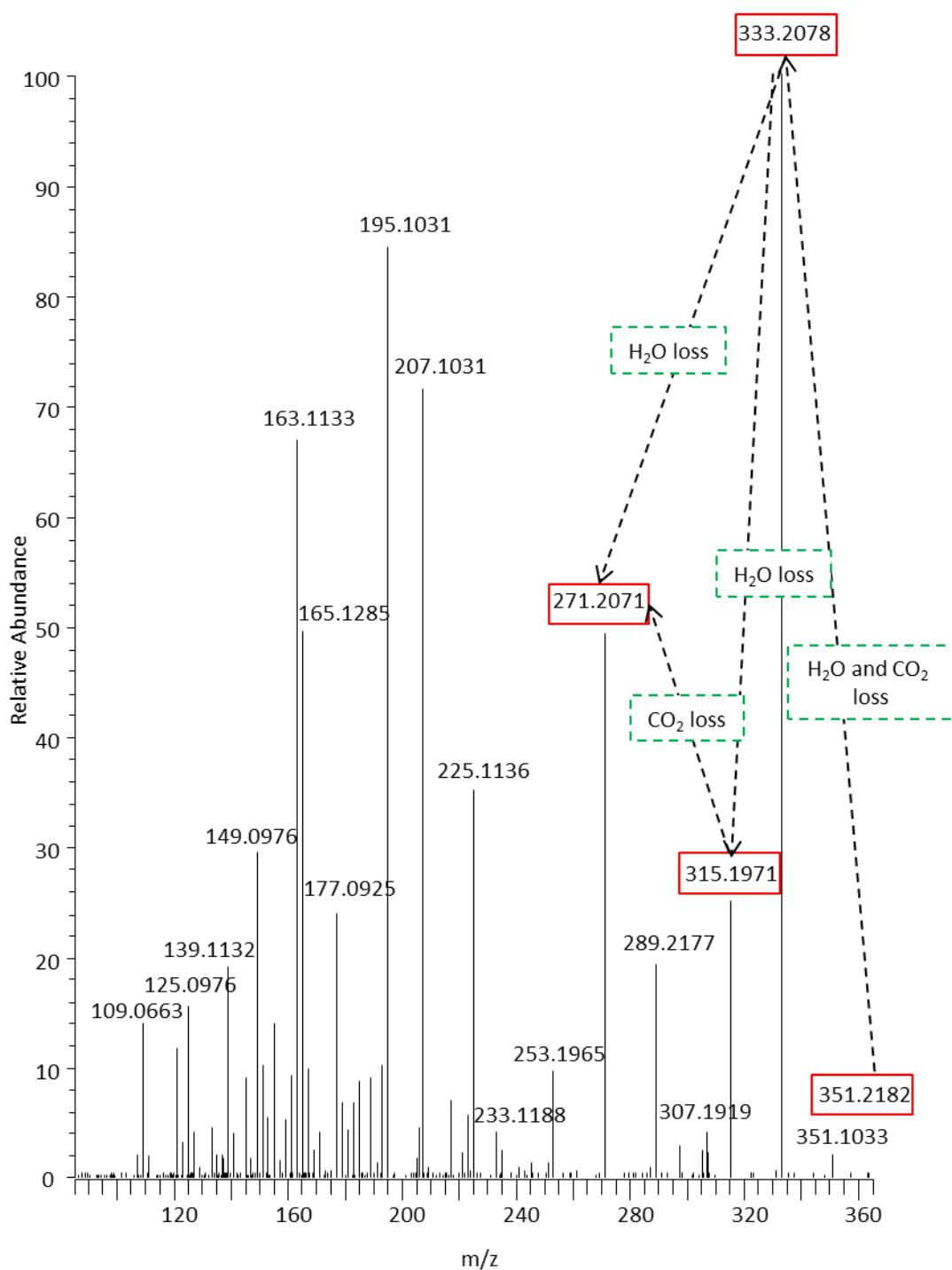
Figure 3.9. Fragmentation pathway of *m/z* 351.2182 to *m/z* 271.2071. LC/MS/MS spectrum of DXA$_3$ monitoring the fragmentation of *m/z* 351.2182 as described in 2.2.2 and 2.2.8. Data dependent MS^n experiments enabled the determination of the relationship between fragment ions marked in red.
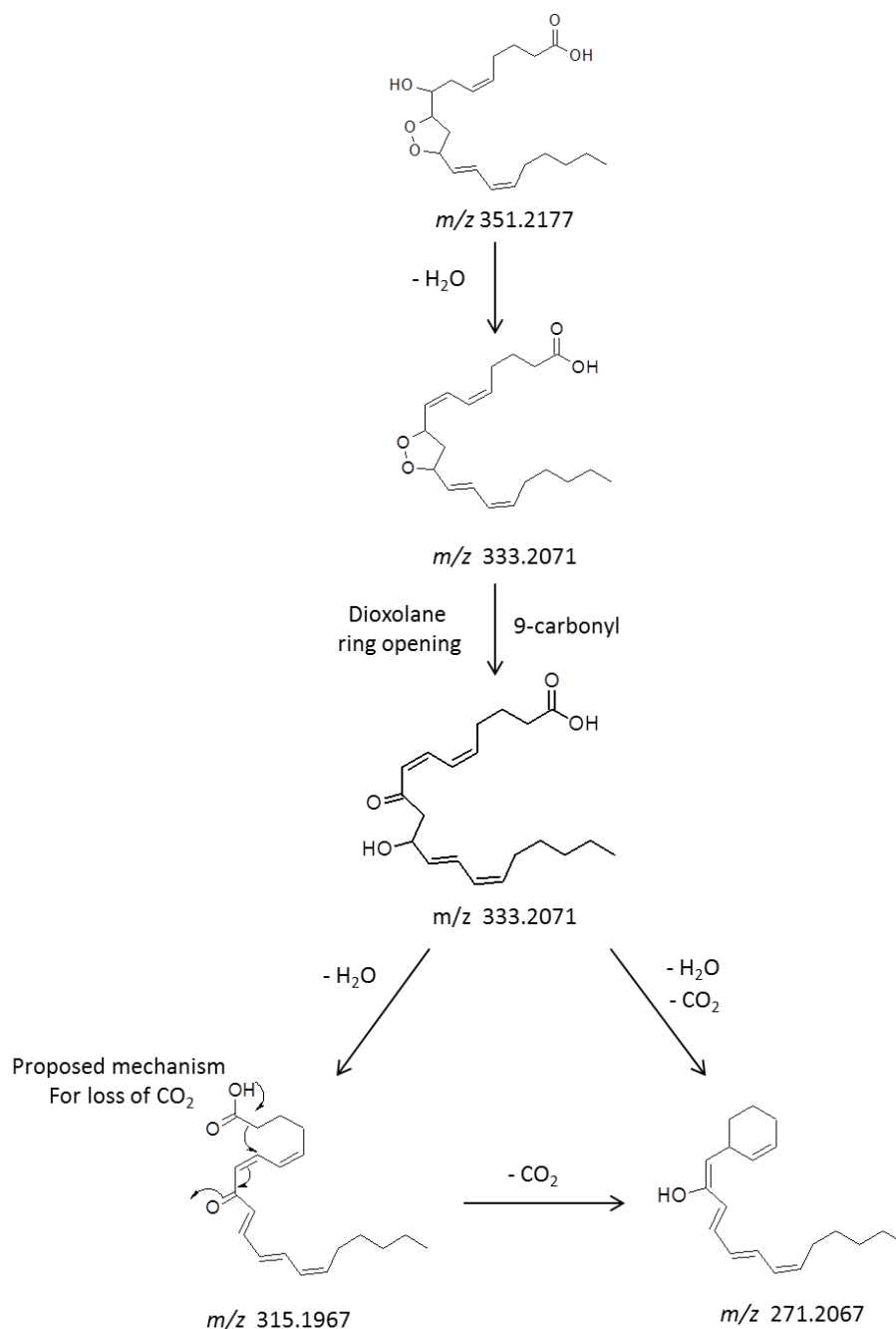
Figure 3.10. **Fragmentation pathway of DXA$_3$ from *m/z* 351.2177 to *m/z* 271.2067.** Fragmentation pathway based on MS^n data of DXA$_3$ performed on the Orbitrap Elite instrument as described in 2.2.8. The fragmentation of the parent ion *m/z* 351.2177 to *m/z* 271.2067 is shown. The pathway shows abstraction of both water and CO$_2$ alongside rearrangements of double bonds and neutral carbon atoms.
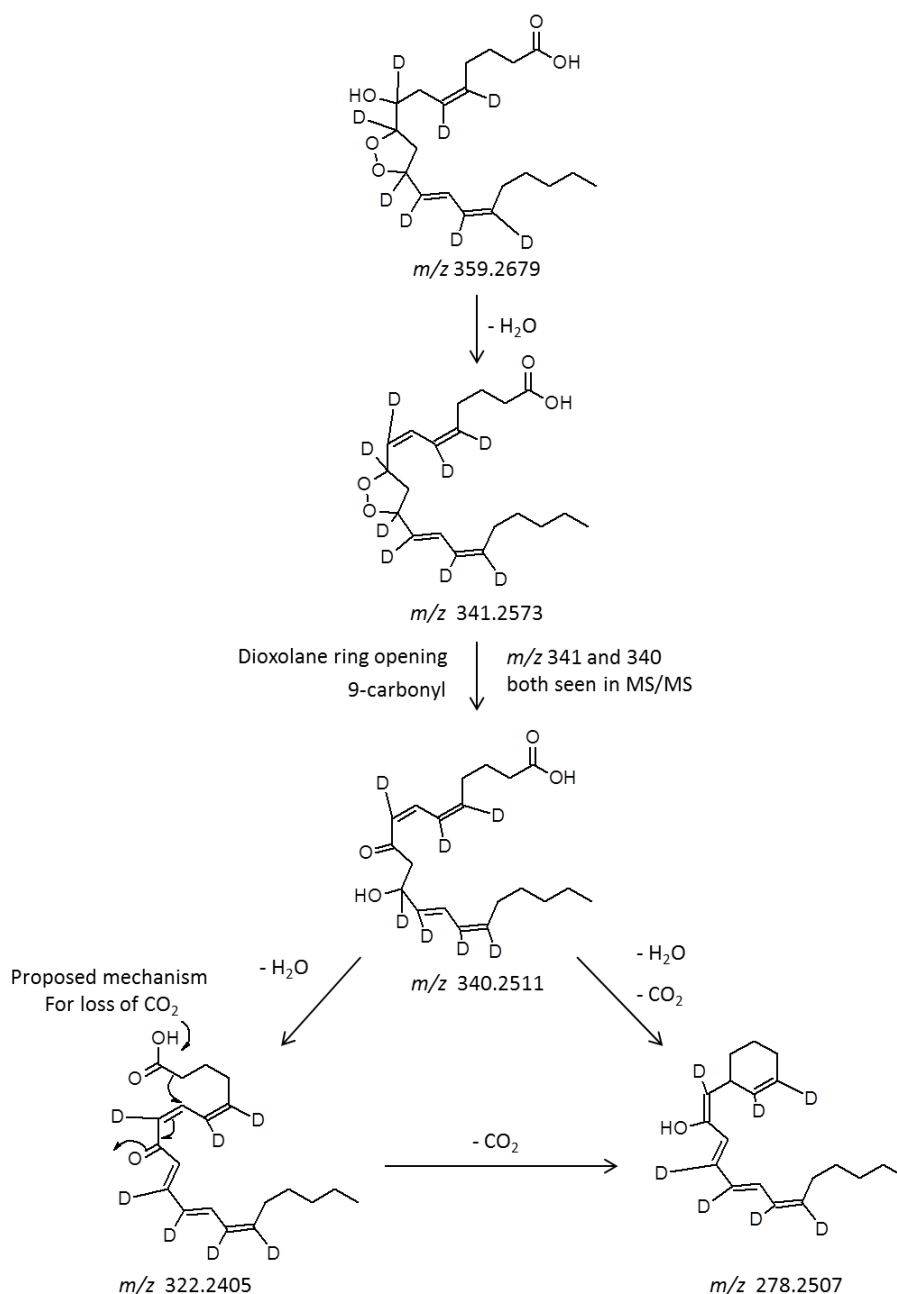
Figure 3.11. Fragmentation pathway of DXA₃-*d8* from *m/z* 359.2679 to *m/z* 278.2507. Fragmentation pathway based on MS^n data of DXA₃ performed on the Orbitrap Elite instrument as described in 2.2.8. The fragmentation of the parent ion *m/z* 359.2679 to *m/z* 278.2507 is shown. The pathway shows both abstraction of water and CO_2 alongside rearrangements of double bonds and neutral carbon atoms.

m/z 351.2177. Then, the dioxolane ring opens resulting in a carbonyl group at C9 leading to *m/z* 333.2071. The loss of both a water and a carbon dioxide molecule from this ion results in *m/z* 271.2067 via *m/z* 315.1967 (Figure 3.10). This proposed fragmentation pathway was supported by LC/MS^3 data of DXA$_3$-*d$_8$* as shown in Figure 3.11. In particular, examining both *m/z* 341.2573 and *m/z* 340.2511 in the LC/MS^n spectra of DXA$_3$-*d$_8$* led to the proposed ring opening as shown in Figure 3.11. As for DXA$_3$, DXA$_3$-d$_8$ fragmentation continues through loss of both a water and a carbon dioxide molecule leading to *m/z* 278.2507 via *m/z* 322.2405 (Figure 3.11).

3.2.4   FRAGMENTATION PATHWAY OF DXA$_3$ M/Z 351.2177 TO M/Z 163.1128

The second pathway of fragmentation of *m/z* 351.2177 to *m/z* 163.1132 is shown in the MS/MS spectrum (Figure 3.12). The structures of parent and fragment ions are depicted in Figure 3.13, Figure 3.14, and Figure 3.15. I propose that the dioxolane ring opening occurs first resulting in a carbonyl group at position C9 (Figure 3.13) or C11 (Figure 3.14). Sigmatrophic shifts and loss of one water molecule result in *m/z* 333.2071 and further loss of alkyl chains lead to *m/z* 225.1132. With the loss of a water molecule, *m/z* 207.1027 is generated, which then fragments to *m/z* 163.1128 due to loss of carbon dioxide and molecular rearrangement. This pathway is supported by fragmentation of DXA$_3$-*d8* (Figure 3.15).
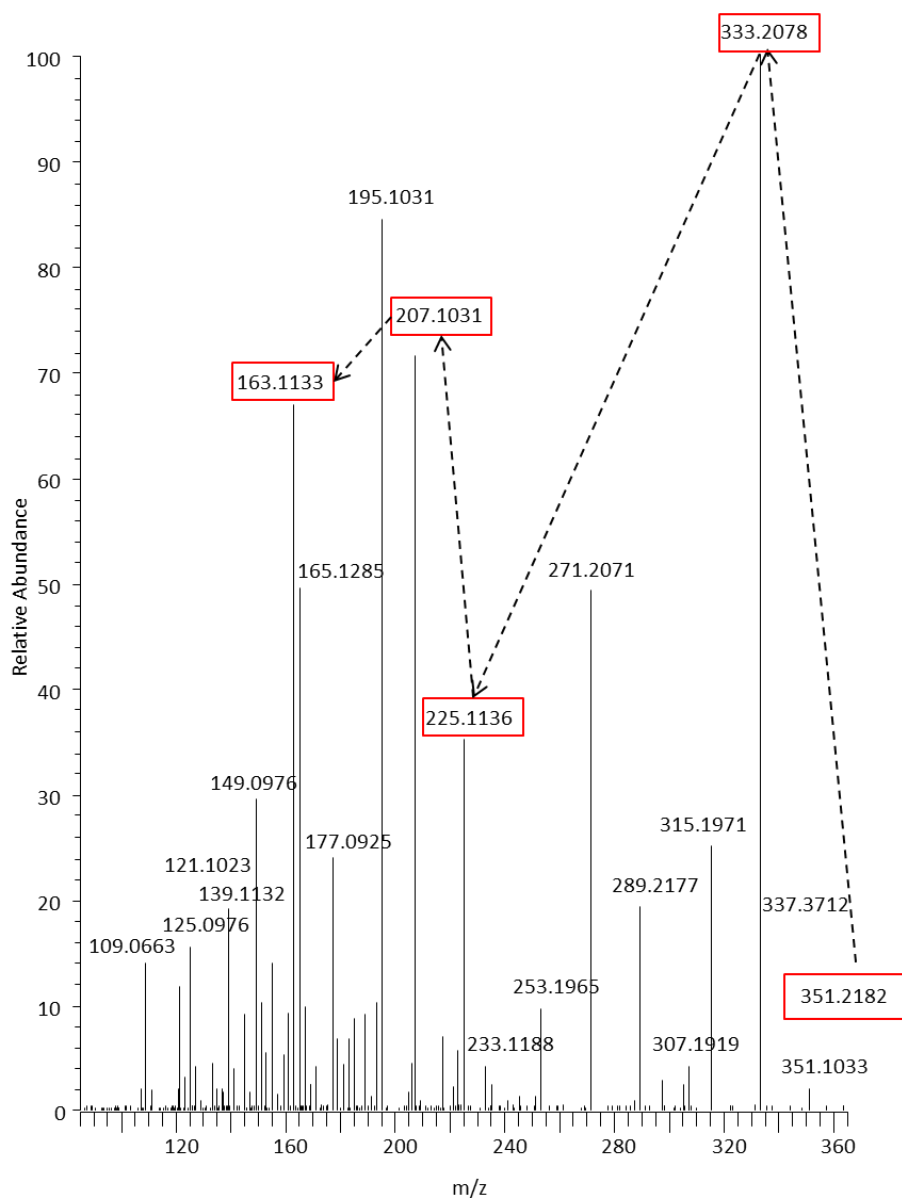
Figure 3.12. Pathway of fragmentation of DXA$_3$ from m/z 351.2182 to m/z 163.113. MS/MS spectrum of DXA$_3$ *m/z* 351.2182 as described in 2.2.7.6. Data dependent MS^n experiments enabled the determination of the relationship between all fragment ions marked in red.
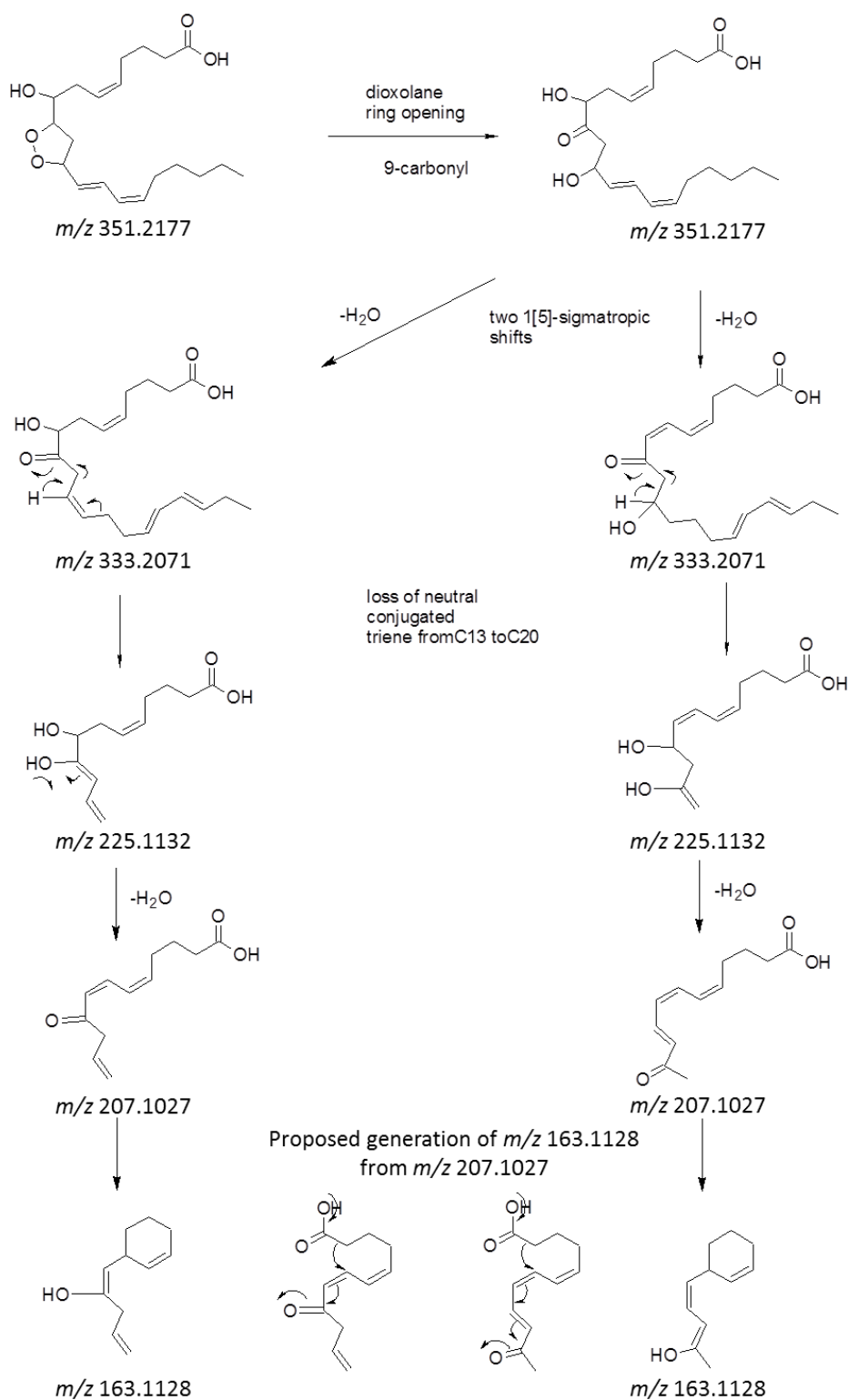
Figure 3.13. Fragmentation pathway of DXA$_3$ from *m/z* 351.2177 to *m/z* 163.1128 with dioxolane ring opening via 9-carbonyl. Fragmentation pathway based on MS^n data of DXA$_3$ performed on the Orbitrap Elite instrument as described in 2.2.2 and 2.2.8. The fragmentation of the parent ion *m/z* 351.2177 to *m/z* 163.1128 is shown. The pathway shows abstraction of both water and CO$_2$ and rearrangements of double bonds and neutral carbon atoms.
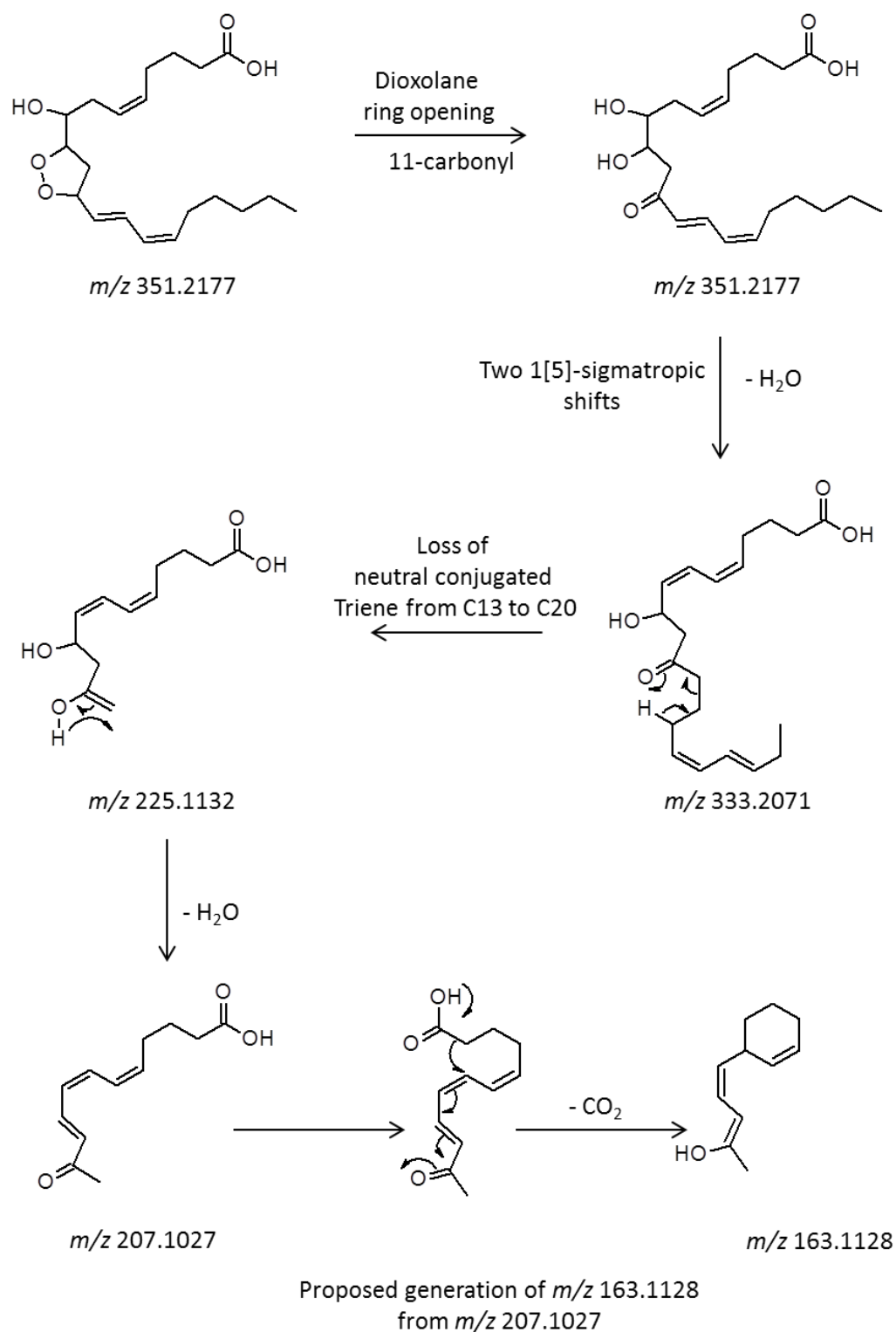
Figure 3.14. Fragmentation pathway of DXA₃ from *m/z* 351.2177 to *m/z* 163.1128 with dioxolane ring opening via 11-carbonyl. Fragmentation pathway based on MSⁿ data of DXA₃ performed on the Orbitrap Elite instrument as described in2.2.2 and 2.2.8. The fragmentation of the parent ion *m/z* 351.2177 to *m/z* 163.1128 is shown. The pathway shows abstraction of both a water and CO_2 molecule and rearrangements of double bonds and neutral carbon atoms.
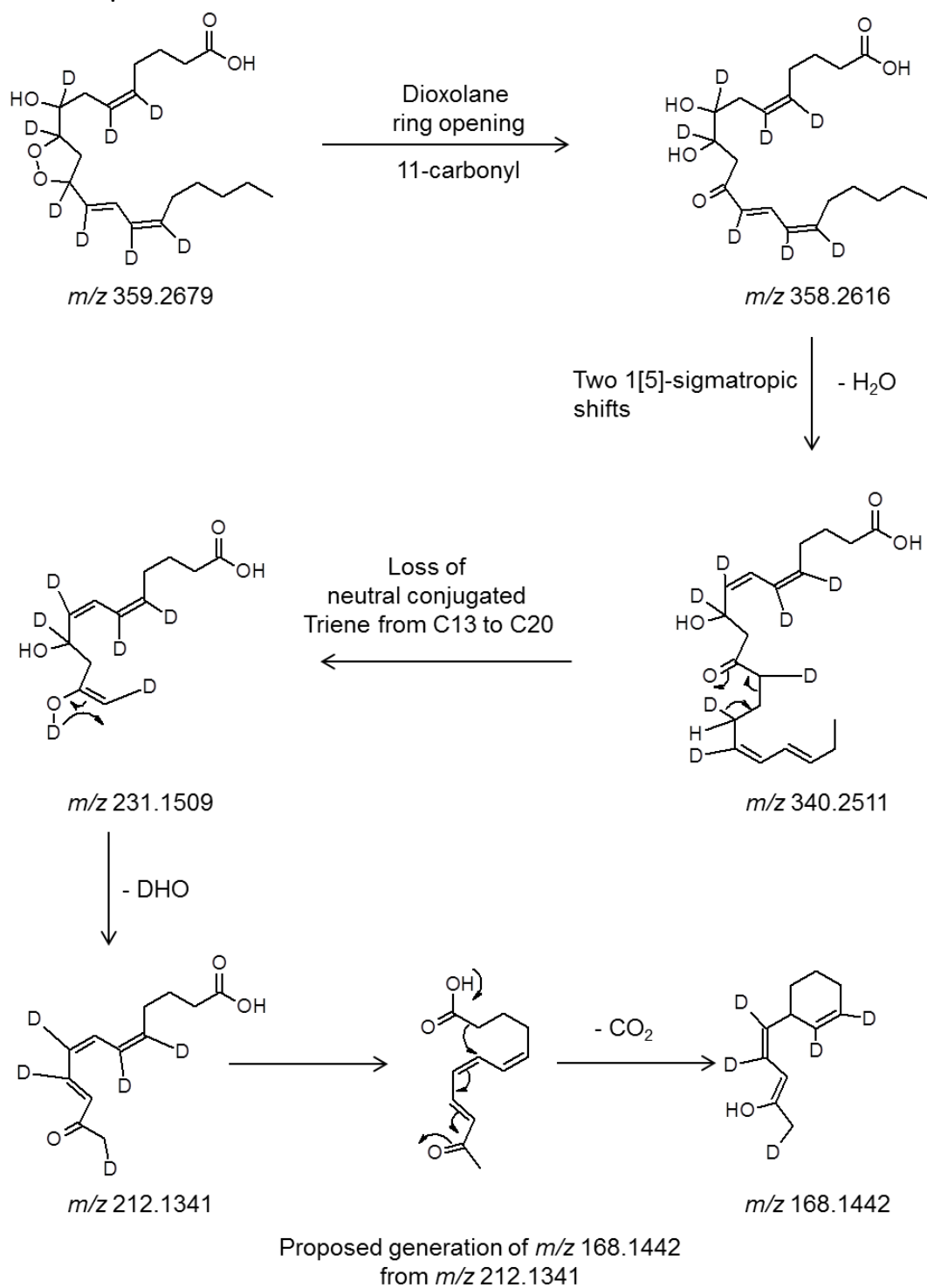
Figure 3.15. Pathway of fragmentation of DXA₃-*d8* from *m/z* 359.2679 to *m/z* 168.1442. Fragmentation pathway based on MS^n data of DXA₃ performed on the Orbitrap Elite instrument as described in 2.2.2 and 2.2.8. Depicted is the fragmentation of the parent ion *m/z* 359.2679 to *m/z* 168.1442. The pathway shows both abstraction of water and CO_2 and rearrangements of double bonds and neutral carbon atoms.

3.2.1 DXA₃ IS UV ACTIVE

DXA$_3$ was generated using COX-1 *in vitro* as described in 2.2.2. Lipid extract was analysed using LC/UV at 235 nm and fractions collected every 30 sec. MS analysis monitoring *m/z* 351.2 to 165.1 demonstrated that DXA$_3$ elutes at 47 min (Figure 3.16, Panel A). A lipid eluting at this retention time showed a UV spectrum (Figure 3.16, Panel B) similar to that for previous described dioxolanes, with a λmax at 238 nm (Figure 3.16, Panel C, Teder et al. 2015). Although this spectrum is weak, due to the low ng levels of DXA$_3$ present, it is strong evidence for the presence of the conjugated diene at C12-C15.

A Chromatogram of COX-1 lipid extract
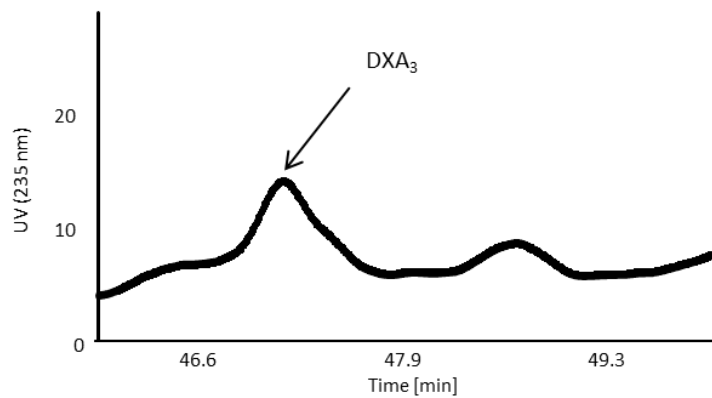
B UV spectrum of DXA$_3$
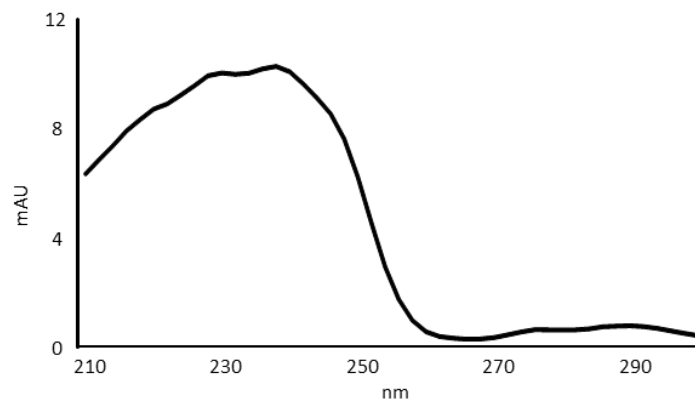
C UV spectrum, Teder et al. 2014
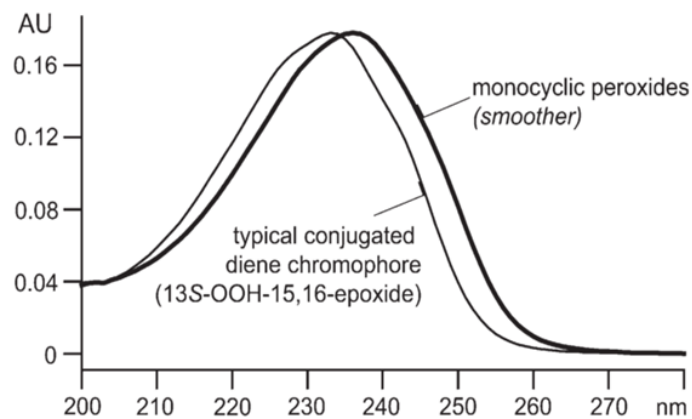
Figure 3.16. DXA$_3$ is UV active. DXA$_3$ was generated using COX-1 *in vitro* as described in 2.2.2. The lipid extract was analysed using LC-UV. DXA$_3$ was identified using MS (2.2.7.1). (A) DXA$_3$ elutes at 47 min in the UV chromatogram monitoring 235 nm. (B) UV spectrum of DXA$_3$. (C) UV spectrum of conjugated dienes and monocyclic peroxides (Teder et al. 2014).

3.3   DISCUSSION

In this chapter I further confirmed the proposed structure of DXA_3 to be 8-hydroxy, 9, 11-dioxolane eicosatrienoic acid using two different MS approaches; GC/MS and LC/MS^n.

GC/MS analysis represents a traditional analytical tool for structural characterisation of lipids (Murphy & Gaskell 2011). To confirm the proposed structure, DXA_3 was hydrogenated using Pd-C as shown for previously described dioxolanes (Roza & Francke 1978; Yin et al. 2004). However, due to the extremely small amounts available, analysis was challenging. For studies presented herein, DXA_3 derived from COX-1 *in vitro* was used. Although this approach yielded greater amounts of lipid than that generated by activated platelets derived from several donors (Chapter 7), additional isomers are formed during this reaction as shown in detail in Chapter 4. Therefore, the four peaks detected in the GC/MS chromatogram may be due to small amounts of contaminating isomers that were not separated during our chromatography. Additional ions observed in GC/MS spectra were detected throughout the entire chromatogram and are considered as background. The ions *m/z* 427, *m/z* 501 and *m/z* 517 appear with relative high abundance. As our synthetic protocol only yields low amounts of DXA_3, background ions appear with high abundance relative to the hydrogenated and derivatised DXA_3 *m/z* 575.

High resolution Orbitrap MS allow accurate mass analysis down to 1 ppm (O'Donnell et al. 2014; Perry et al. 2008). However, a mass range of 5 ppm is commonly used for ion identification, thus detecting DXA_3 at *m/z* 351.2177 ± 0.002 Da. In combination with LC, this enabled the separation of this lipid from other COX-1 -derived lipids and generation

of MS/MS spectra, without prior purification. This was crucial as a pure DXA$_3$ standard is not yet commercially available. Together with GC/MS analysis of hydrogenated DXA$_3$, the fragmentation patterns of DXA$_3$ and DXA$_3$-*d8* I developed from my high resolution dataset support the proposed lipid structure (Scheme 6). However, the stereochemistry of the three stereocentres (C8, C9 and C11) within DXA$_3$ and positions of double bonds are yet to be determined and require further investigation. Therefore, ongoing collaborations aim to synthesise larger amounts of pure DXA$_3$, which can then be used to further confirm our proposed structure. This will be further discussed in Chapter 9.1. The use of deuterated DXA$_3$ was essential for this analysis. However, some details of fragmentation still remain unclear. For example, for one of the pathways it could not be determined whether a carbonyl group forms at C9 or C11 since the masses of the resulting fragment ion masses are identical for both (Figure 3.13, Figure 3.14). Using a deuterated arachidonate analogue with fewer deuterium atoms at fixed positions could clarify this but this is not currently commercially available.

Herein, I showed that DXA$_3$ derived from COX-1 *in vitro* has a similar UV spectrum as that of a structurally related dioxolane (Teder et al 2014). This indicates the presence of a UV chromophore, and thus, further supports our proposed conjugated diene at C12-C15. In addition, the MS/MS spectrum of DXA$_3$ shows *m/z* 155.1 as low abundant ion consistent with the product ion spectrum of 8-HETE (LipidMaps). This eicosanoid contains a hydroxyl group at C8, identical to the proposed structure for DXA$_3$, and fragmentation between C8 and C9 results in generation of *m/z* 155.1. Therefore, this provides further evidence for our hypothesis that the hydroxyl group is located at C8.

DXA$_3$ represents a novel COX-1-derived lipid, which is structurally distinct to other COX products described previously and has never been shown to be generated by any cell

type to date. However, other studies have shown dioxolanes *in vitro*, variably identifying them as cyclic peroxides, monocyclic and serial cyclic dioxolanes, dioxolane isoprostanes or hydroxy-endoperoxides (Teder et al. 2014; Roza & Francke 1978; Havrilla et al. 2000; Yin et al. 2004). To date, no common nomenclature for this lipid class exists. Therefore, we proposed a name following the existing nomenclature system for prostaglandins described by Nelson (1974). The lipid stem name should be related to characteristic structural feature, e.g. dioxolane. As this lipid is the first described in its class it belongs to family A. Additionally, a numeric subscript was added indicating the number of double bonds resulting in dioxolane A_3, abbreviated to DXA_3.

In conclusion, data presented in this chapter fully support the proposed covalent structure of DXA_3. This is identical to a dioxolane previously shown to be generated *in vitro* through oxidation of 11-HpETE esterified to cholesterol (Havrilla et al., 2000). Therefore, in the next chapter I will investigate whether DXA_3 forms via this *in vitro* oxidation reaction, using the free acid, and will compare this to DXA_3 formed by human platelets and COX isoforms.

.

CHAPTER FOUR

GENERATION OF DXA$_3$ BY PLATELETS, COX-1 AND 11-

HpETE OXIDATION *IN VITRO*

4.1 INTRODUCTION

In Chapter 3, further evidence for the structure of a novel platelet COX product was obtained. This lipid is identical to the free fatty acid form of monocyclic oxidation products of cholesteryl -arachidonate esters, previously shown (Havrilla et al., 2000). However, to date no comparable data of both approaches exists. Havrilla et al. oxidised cholesteryl -arachidonate, purified the resulting cholesteryl -11-HpETE and oxidised this, leading to cholesteryl esters of mono and serial cyclic products (dioxolanes), and isoprostanes (Chapter 1, Scheme 1.3, Havrilla et al. 2000). For oxidation, a free radical initiator was used leading to an 11-hydroperoxyl radical (Scheme 1.). This indicates that the 11-hydroperoxyl radical is an essential intermediate in the resulting arachidonate derived dioxolane formation *in vitro*.

The 11-hydroperoxyl radical also forms as an intermediate of COX reactions (Marnett et al. 1984). Briefly, during the COX cycle, arachidonate is oxidized forming the 11-hydroperoxyl radical, which can either form PGG_2 or be released from the catalytic site and reduced to first 11(R)-HpETE, then 11(R)-HETE, a well-known and abundant side product of COX reactions (Hamberg & Samuelsson 1967; Harman et al. 2004).

In summary, the 11-hydroperoxyl radical is an intermediate of both, enzymatic and non-enzymatic arachidonate oxidation, either of which can lead to dioxolane formation (Havrilla et al. 2000; Marnett et al. 1984). Therefore, in this chapter I will investigate whether DXA_3 is formed during 11-HpETE oxidation *in vitro* and compare this data to that of DXA_3 derived from arachidonate oxidation by COX-1 *in vitro* and activated platelets. This will further our understanding of its enzymatic generation pathway in platelets.

4.1.1 AIMS

- Characterise DXA$_3$ generation by COX-1 *in vitro*

- Characterising DXA$_3$ formation by oxidation of 11-HpETE as shown by Havrilla et al., 2000

4.2   RESULTS

In this chapter, I used LC/MS/MS to compare MS/MS spectra from DXA_3 generated by platelets (4.2.1), purified COX-1 (4.2.2) and oxidation of 11-HpETE *in vitro* (4.2.3).

4.2.1   GENERATION OF DXA_3 BY THROMBIN ACTIVATED PLATELETS

Prior to my PhD, it was demonstrated that activated platelets generate DXA_3 (Aldrovandi, unpublished). Thus, platelet-derived lipid was compared with DXA_3 generated either by COX-1 or by 11-HpETE oxidation *in vitro*. For this, I isolated platelets from healthy human donors, activated them using 0.2 U/ml thrombin for 1 h followed by lipid extraction as described in 2.2.1.1, 2.2.1.3 and 2.2.5.1. LC/MS analysis demonstrated that four ions elute when monitoring the parent *m/z* of DXA_3 at 351.2 ([M-H]$^-$) (Figure 4.1, Panel A). PGE_2 elutes at 32.2 min. A single peak was observed eluting at 49.67 min when monitoring DXA_3 (Figure 4.1, Panel B). The product ion spectrum of this ion is shown in Figure 4.1, Panel C. Both retention time and spectra were used for identification of DXA_3 generated by COX-1 and 11-HpETE oxidation *in vitro*.

4.2.2   GENERATION OF DXA_3 USING COX-1 IN VITRO

To generate DXA_3 by COX-1, I incubated the purified or recombinant holo enzyme and arachidonate substrate for 3 min at 37 °C. This was followed by lipid extraction as described in 2.2.2 and 2.2.5.1.

A MS chromatogram *m/z* 351.2

B MS/MS chromatogram *m/z* 351.2 to 165.1

C MS/MS spectrum of DXA$_3$
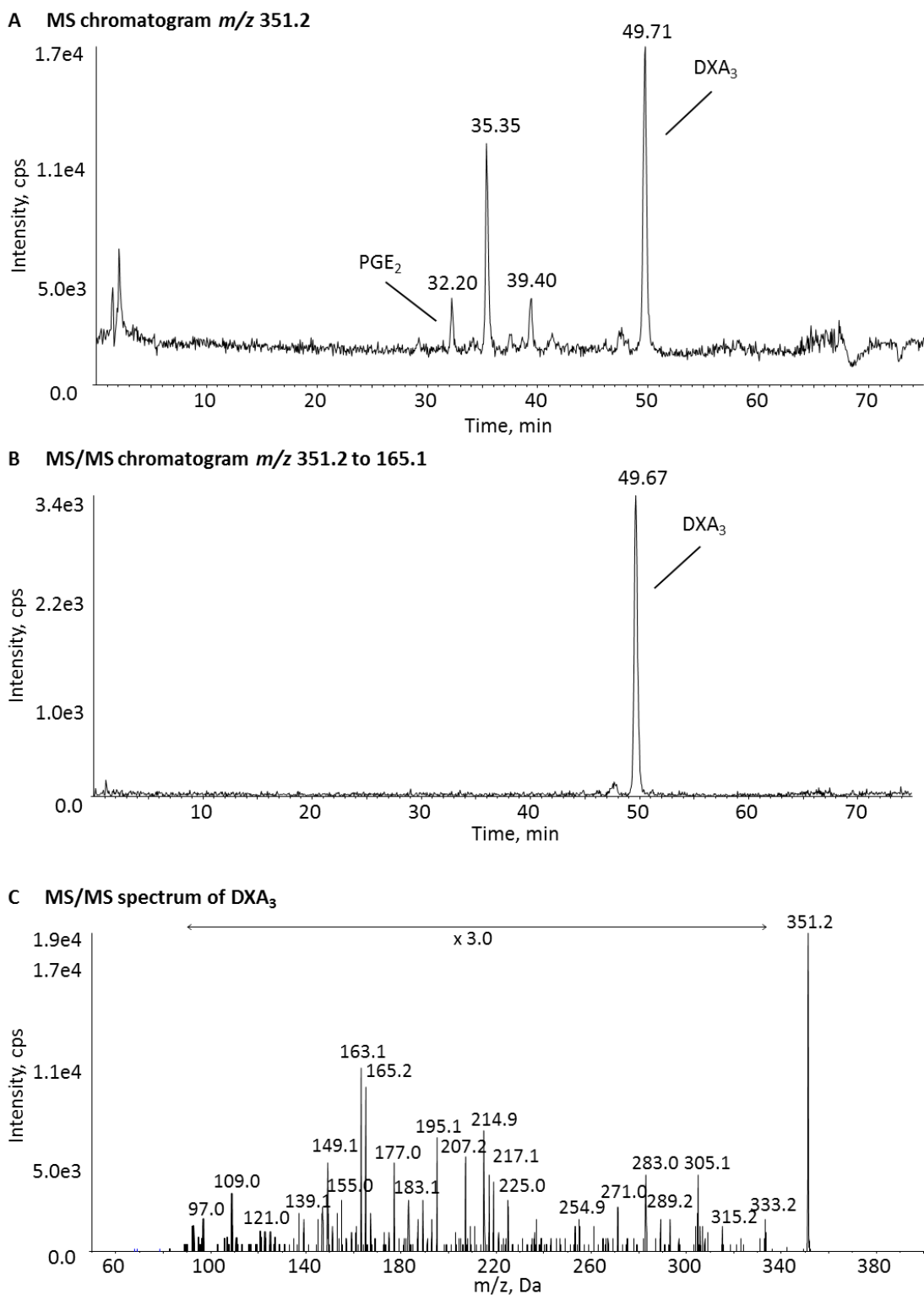
Figure 4.1. DXA$_3$ generated by thrombin activated platelets. LC/MS/MS analysis of a lipid extract derived from thrombin activated platelets as described in 2.2.1.1, 2.2.1.3, 2.2.5.1 and 2.2.7.3. (A) Chromatogram of lipids with a parent ion mass of *m/z* 351.2. PGE$_2$ elutes at 32.2 min and DXA$_3$ at 49.71 min. (B) Chromatogram of DXA$_3$ monitoring *m/z* 351.2 to 165.1. A single peak elutes at 49.67 min. (C) MS/MS spectrum of DXA$_3$ eluting at 49.67 min in (A).

121

Several peaks eluted in the chromatogram when monitoring the parent ion mass (Figure 4.2, Panel A). PGE_2 was identified eluting at 32.18 min and DXA_3 at 49.66 min (Figure 4.2, Panels B and C). However, when monitoring *m/z* 351.2 to 165.1 for DXA_3, two additional peaks were seen, eluting at 47.76 min and 51.18 min (Figure 4.2, Panels B and C). These will be discussed in 4.2.4.

4.2.3 *IN VITRO* OXIDATION OF 11-HpETE FORMS DXA_3

Havrilla et al. (2000) demonstrated that isoprostanes and mono and serial cyclic products are formed by a two-step oxidation of cholesteryl-arachidonate. To investigate whether DXA_3 forms during this reaction, arachidonate was oxidised using the free radical initiator NMBHA and MeOAMVN under oxygen atmosphere as described in 2.2.3. The resulting 11-HpETE was HPLC purified and oxidized again using the same approach (2.2.4). Unsaturated fatty acids such as arachidonate are likely to oxidise under oxygen as used in this reaction. However, to fasten this reaction, a free radical initiator was used. Therefore, a reaction blank without initiator was not monitored.

LC/MS/MS analysis demonstrated that several ions with similar abundance elute when monitoring the parent *m/z* of DXA_3 (Figure 4.3, Panel A). Based on retention time and MS/MS, DXA_3 was identified eluting at 49.56 min (Figure 4.3, Panels B and C). Two additional ions that elute at 47.70 min and 51.20 min were also detected (Figure 4.3, Panel B), identical to DXA_3 derived from COX-1 *in vitro* (Figure 4.2, Panel B). These will be described in 4.2.4.
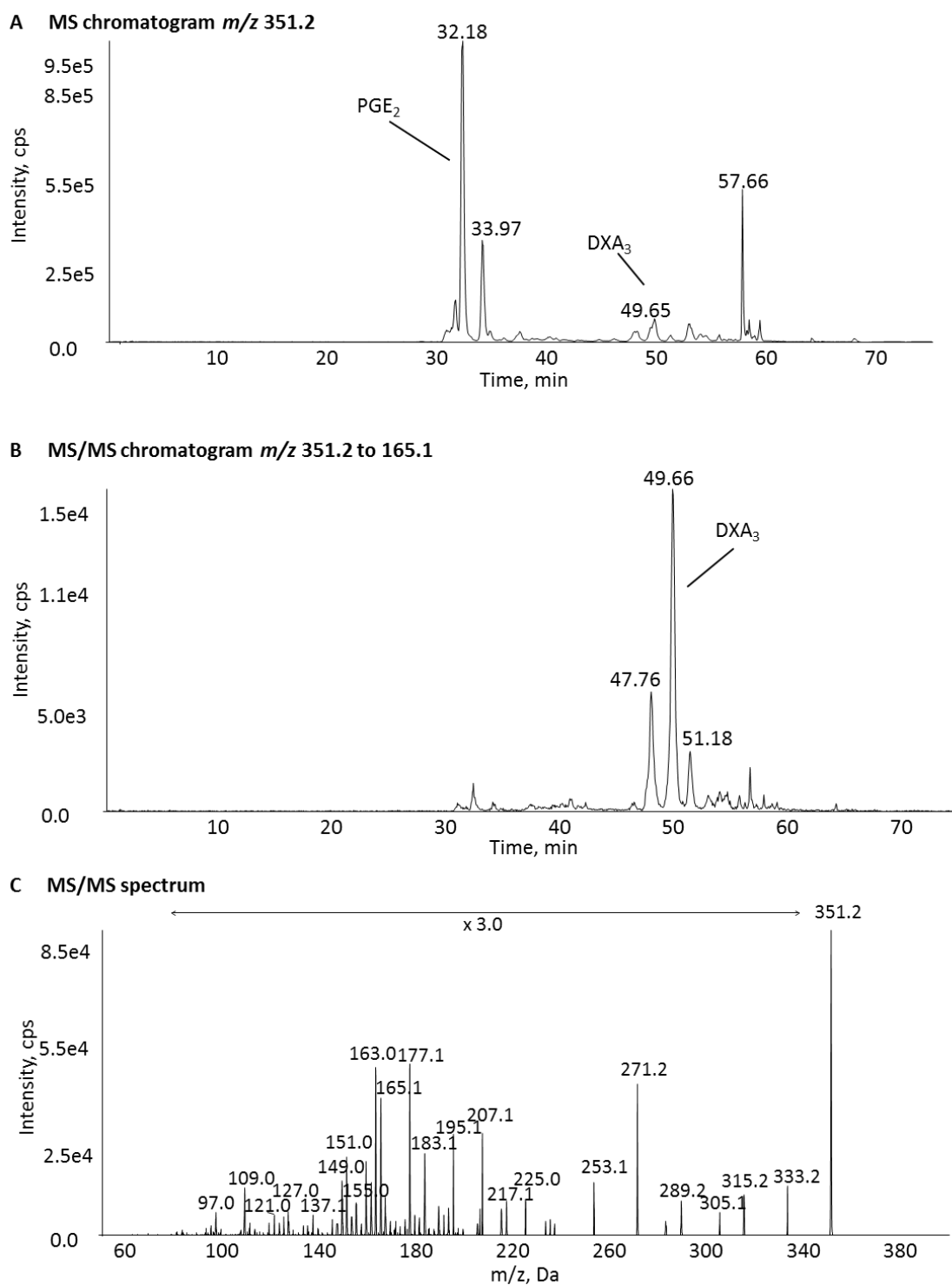
Figure 4.2. DXA₃ is generated using COX-1 *in vitro*. LC/MS/MS analysis of lipid extract of an *in vitro* COX-1 reaction as described in 2.2.2, 2.2.1.3, 2.2.5.1 and 2.2.7.3. (A) Chromatogram of lipids monitoring the parent mass of m/z 351.2. PGE_2 elutes at 32.18 min and DXA_3 at 49.65 min. (B) Chromatogram of DXA_3 monitoring m/z 351.2 to 165.1 showing three peaks eluting at 47.76 min, 49.66 min and 51.18 min. (C) MS/MS spectrum of peak eluting at 49.66 min in (panel B). LC/MS/MS analysis using an MRM experiment on the 4000 QTrap platform as described in 2.2.7.3.

A   MS chromatogram *m/z* 351.2

31.42

49.55

47.72

40.67

37.40

34.00

51.87

59.26

Intensity, cps

2.1e4

1.7e4

1.1e4

5.0e3

0.0

10   20   30   40   50   60   70

Time, min

B   MS/MS chromatogram *m/z* 351.2 to 165.1

49.56

DXA₃

47.70

51.20

Intensity, cps

4.2e3

3.4e3

2.2e3

1.0e3

0.0

10   20   30   40   50   60   70

Time, min

C   MS/MS spectrum of DXA₃

x 1.5

207.0

351.2

163.1

177.1

165.1   225.1

271.2

195.0 215.0

305.0

151.1

183.0

289.1

109.0   159.0   236.9   283.0   315.2 333.2

95.0   125.0 149.1

Intensity, cps

2.1e4

1.7e4

1.1e4

5.0e3

0.0

60   100   140   180   220   260   300   340   380

m/z, Da

Figure 4.3. DXA₃ is generated using an oxidation of arachidonate followed by oxidation of HPLC-purified 11-HpETE *in vitro*. LC/MS/MS analysis of lipid extract of *in vitro* arachidonate oxidation. (A) Chromatogram of lipids monitoring a parent mass of *m/z*351.2. (B) Chromatogram of DXA₃ monitoring *m/z* 351.2 to 165.1 displaying three peaks eluting at 47.70 min, 49.56 min and 51.20 min. (C) Spectrum of peak eluting at 49.56 min (panel B). LC/MS/MS using MRM experiment on the 4000QTrap platform as described in2.2.7.3

124

4.2.4 ISOMER FORMATION OF DXA$_3$ IN *IN VITRO* APPROACHES

DXA$_3$ was generated by platelets, COX-1 and oxidation of 11-HpETE *in vitro* (4.2.1, 4.2.2 and 4.2.3). However, two additional peaks, which elute close to DXA$_3$, are observed in both *in vitro* approaches (Figure 4.4). The spectra of these additional peaks are identical to DXA$_3$ and differ only in ion intensities (Figure 4.5, Figure 4.6). Identical spectra and close retention times indicate that these products are likely to be isomers, which are formed during the *in vitro* reactions. These are not seen in platelet lipid extracts.
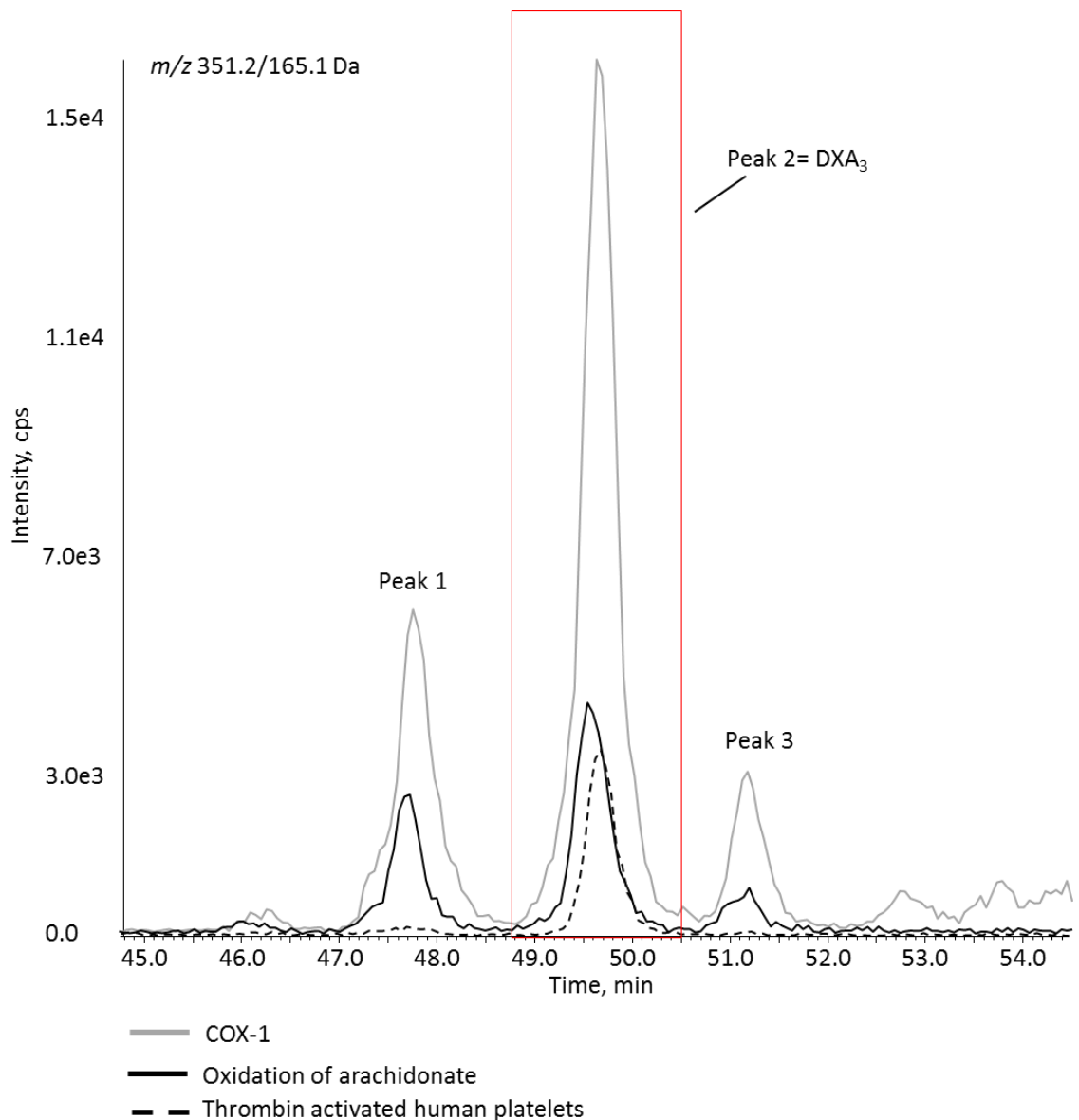
Figure 4.4. DXA₃ is generated by thrombin activated platelets, COX-1 and oxidation of arachidonate *in vitro*. Overlay of chromatograms monitoring *m/z* 351.2 to 165.1 shows only one peak eluting in lipid extract of thrombin activated platelets, Peak 2 (scattered line), whereas two additional peaks (Peak 1 and 3) elute in lipid extract of COX-1 (grey, solid line) and oxidation of arachidonate (black, solid line). Reversed phase LC/MS/MS analysis using MRM experiment on the 4000 QTrap platform as described in 2.2.7.3.
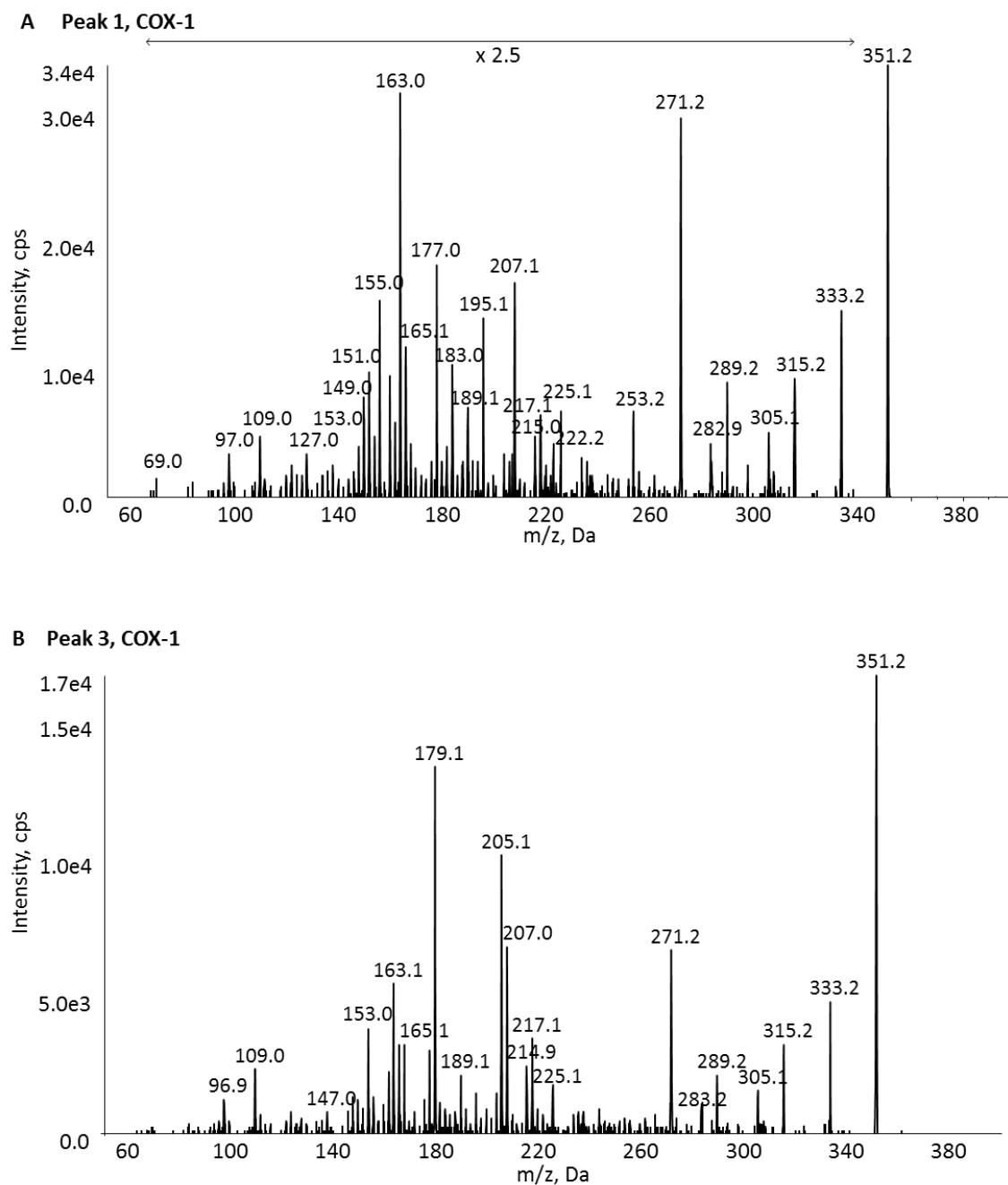
Figure 4.5. Two additional isoforms of DXA₃ are formed using COX-1 *in vitro*. Shown are LC/MS/MS spectra of Peak 1 and Peak 3 in Figure 4.2 derived from COX-1 *in vitro* as described in 2.2.2. (A) Spectrum of Peak 1 eluting at 47.76 min. (B) Spectrum of Peak 3 eluting at 51.18 min. Both spectra display identical product ions compared to DXA3 (Figure 4.2, Panel C). LC/MS/MS using the 4000 QTrap platform as described in 2.2.7.3.
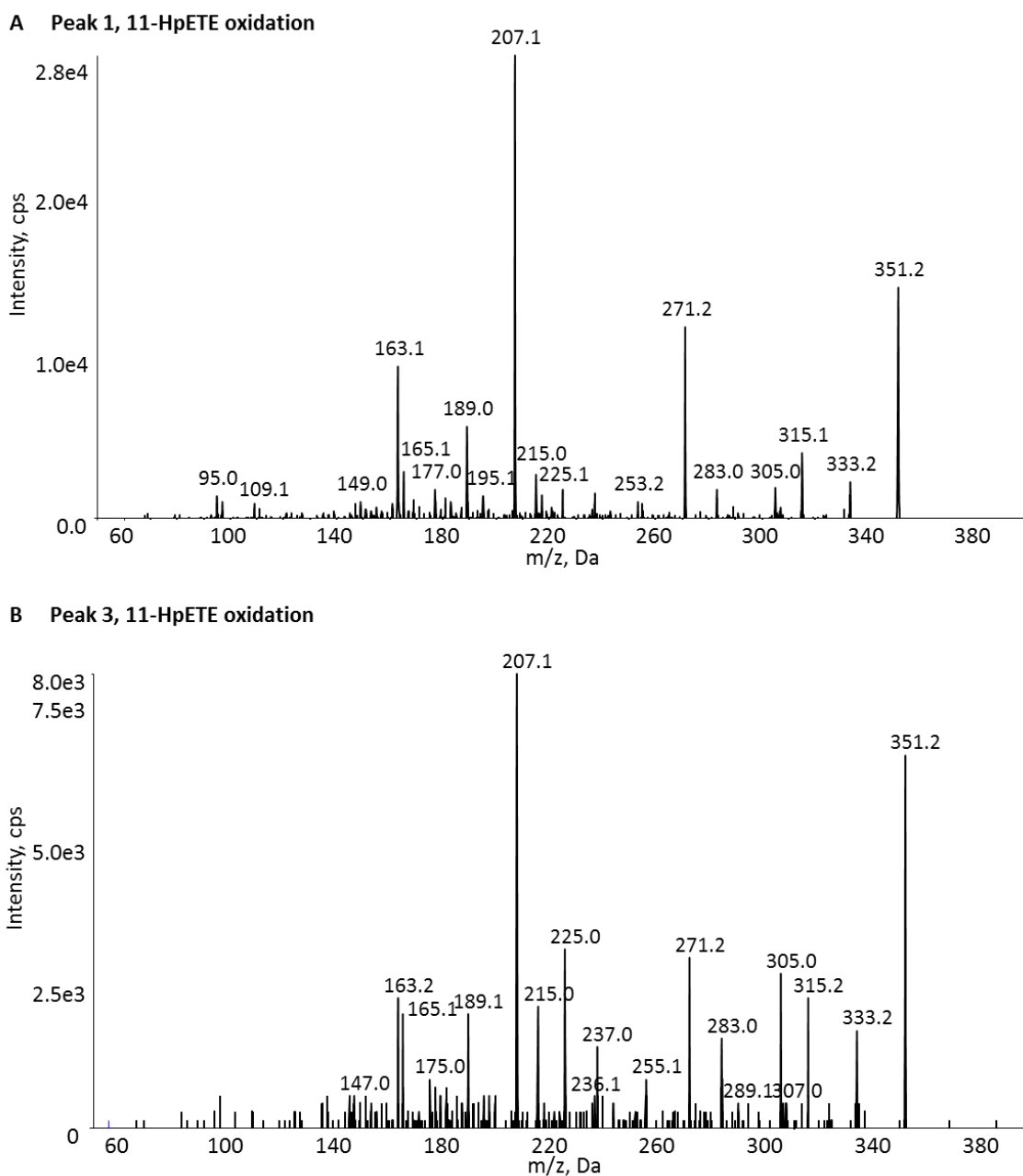
Figure 4.6. Two additional isomers of DXA₃ are formed during oxidation of 11-HpETE *in vitro*. LC/MS/MS spectra of Peak 1 and Peak 3 eluting in Figure 4.3. (A) Spectrum of Peak 1. (B) Spectrum of Peak 3. Both spectra display identical product ions compared to DXA₃ (Figure 4.3, Panel C). Sample preparation and LC/MS/MS analysis using the 4000 QTrap platform as described in 2.2.3, 2.2.4 and 2.2.7.3.

4.3   DISCUSSION

Studies presented herein demonstrate that DXA$_3$ can be formed using three approaches: by thrombin activated platelets, oxidation of arachidonate using COX-1 *in vitro* or 11-HpETE oxidation *in vitro*. Its formation via 11-HpETE oxidation indicates the 11- hydroperoxyl lipid radical is an essential intermediate. Thus, this lipid may also be an intermediate during COX-1 generation of DXA$_3$ in platelets or by purified enzyme. While a single isomer is generated in platelets, two additional isomers are formed *in vitro* by COX-1 and 11-HpETE oxidation. This suggests an uncontrolled reaction often observed during autoxidation processes, that is absent in cells. Indeed, Aldrovandi et al. (unpublished) demonstrated that small amounts of DXA$_3$-PEs are formed spontaneously *in vitro* using arachidonate and hematin but no enzyme suggesting an oxidative effect of hematin. This reagent was used for enzyme reconstitution in this study. Therefore, this might promote isomer formation during COX reactions.

Isomer formation has also been described by Havrilla et al. (2000) during the two step oxidation of cholesteryl-arachidonate. Their monocyclic product, which has the same structure as DXA$_3$, contains three stereocentres (Havrilla et al. 2000). These are shown in Scheme 4.1 for DXA$_3$.
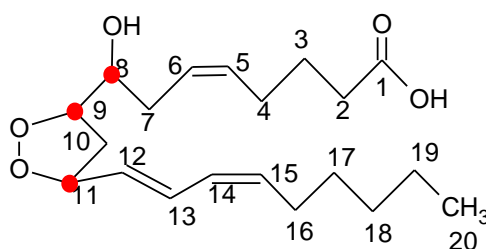
Scheme 4.1. Stereocentres in DXA$_3$.

These stereocentres can give rise to four possible pairs of enantiomers (eight stereoisomers: RRR, RRS, RSR, RSS, SSS, SSR, SRS and SRR) of DXA$_3$ (Havrilla et al. 2000). As enantiomers cannot be distinguished using our LC/MS/MS, four peaks would be expected in the chromatogram. In reality, however, only three peaks were detected following *in vitro* generation of DXA$_3$ (Figure 4.2, Figure 4.3). This observation may be explained if we consider the conformation of the stereocentres within the lipid which are present at positions C8, C9 and C11 with the dioxolane ring formed between C9 and C11 (Scheme 4.1). Applying the Cahn–Ingold–Prelog (CIP) sequence rules and considering the steric efficiency of dioxolane formation, the conformation of the stereocentres at C9 and C11 are likely to be the same (RRR, SSS, RSS, SRR) giving rise to two out of three peaks we observe in our chromatogram. In contrast, the less likely formed isomers (RRS, SSR, SRS, RSR) will appear with lower intensities or may not reach the limit of detection explaining why only three out of four pairs of enantiomers are detected. Alternatively, two pairs of enantiomers could coelute in our chromatography and appear as one peak, also potentially explaining the observation of three instead of four separate peaks. To investigate this further LC/MS/MS analysis in combination with a chiral HPLC-column could be used which enables differentiation between enantiomers. However, this methodology requires greater amounts of substrate than the LC/MS/MS techniques used herein. Therefore, this methodology may not be suitable for DXA$_3$ analysis as only small amounts of lipids are available.

As several products are formed in *in vitro* approaches which may coelute, a second transition in addition to *m/z* 351.2 to 165.1 could be added to the LC/MS/MS method allowing a more accurate identification when no MS/MS spectrum is monitored

alongside the MS/MS chromatogram. For example, *m/z* 351.2 to 271.1 as another very abundant fragment ion in the DXA$_3$ spectrum (Figure 4.2, Panel C) could be used.

In conclusion, my data suggests a 11-hydroperoxyl radical is an intermediate during DXA$_3$ formation and that its generation in platelets occurs in a controlled manner. Other prostanoids are generated from PGH$_2$ by specific synthases such as TxS downstream of COX (Haurand & Ullrich 1985; Shen & Tai 1986). To further investigate the enzymatic pathway by which DXA$_3$ is generated in platelets, the role of three enzymes upstream (cPLA$_2$) and downstream (TxS and peroxidase) of COX will be determined in the following chapter. Also, to further investigate whether 11-hydroperoxyl radical escape from the active site plays a role in enzymatic DXA$_3$ formation, I will study two recombinant COX-2 mutants, which were a kind gift of Dr Larry Marnett (Vanderbilt University, Nashville, USA). These allow greater escape of the 11-hydroperoxyl radical from the active site, and consequently generate more 11(R)-HETE but less PGH$_2$ than wildtype COX-2. Thus, I will use these enzymes to determine whether DXA$_3$ is generated as a result of 11-hydroperoxyl radical escape from the active site.

CHAPTER FIVE

ENZYMATIC PATHWAY OF DXA$_3$ FORMATION

5.1 INTRODUCTION

Prostanoid synthesis is regulated by the expression, tissue distribution and activity of PLA_2s, COXs, and additional specific synthases that act downstream of COXs. PLA_2s control the availability of arachidonate, which is hydrolysed from phospholipids of the intracellular membrane (Harizi et al. 2008; Makoto Murakami et al. 2011). In particular, $cPLA_2$ is the key player in eicosanoid generation since cells lacking this are unable to generate these lipids (Tramposch et al. 1994; Brooke et al. 2014; Riendeau et al. 1994; Bartoli et al. 1994). Inhibition of $cPLA_2$ *in vitro* using a pharmacological inhibitor leads to decreased eicosanoid levels including DXA_3 indicating that its generation depends on $cPLA_2$ (Aldrovandi, unpublished; Riendeau et al. 1994; Brooke et al. 2014). To further caracterise this, I utilised platelets derived from a $cPLA_2\alpha$ deficient patient and assessed their DXA_3 generation in response to thrombin stimulation. In this patient a homozygous 4 bp deletion (155574_77delGTAA) within the $cPLA_2\alpha$ gene suppresses expression of this enzyme. This abolishes TxA_2 synthesis and impairs platelet aggregation. The reduced eicosanoid levels are thought to cause further systemic complications including severe peptic and upper small-intestinal ulceration, extensive small-intestinal stricturing, fibrosis and fistulae, and multiple severe extraintestinal complications (Brooke et al. 2014).

Hydrolysed arachidonate can then be oxidised by COXs to generate PGH_2, which is subsequently utilised by synthases to form prostanoids including PGE_2 and TxA_2 (Marnett 2000). However, as described in 1.3.3.4, COXs also generate 11- and 15-HETEs as side products (Xiao et al. 1997; M Hamberg & Samuelsson 1974). These form when the 11- and 15-hydroperoxyl radicals escape from the COX active site,

instead of finishing the catalytic cycle. Mutations within the catalytic domain of COX lead to enhanced formation of PGG_2 and 15(S)-HETE (mutant V349L oPGHS-1) or 11(R)-HETE (mutant V349A/W387F) (Thuresson et al. 2000; Harman et al. 2004). In Chapter 4, I proposed that the 11-hydroperoxyl radical is an intermediate in DXA_3 formation. Furthermore, the structure of DXA_3 suggests that this lipid is unlikely to originate from PGH_2 itself. Consequently, we reasoned that DXA_3 formation occurs prior to PGH_2 release. To determine whether DXA_3 is formed from the escaping 11-hydroperoxyl radical (thus, whether the dioxolane ring forms before or after radical escape), I will investigate DXA_3 formation by wildtype (WT) COX-2 and the mutants V349A and W387F. If the 11-hydroperoxyl radical escapes and then becomes the dioxolane ring, then COX mutants predominantly generating 11(R)-HETE should yield greater DXA_3 amounts than WT enzyme.

Earlier, I showed that three DXA_3 isomers form during *in vitro* generation, but not in platelets (Chapter 4) suggesting additional regulation of formation in these cells. Indeed, the formation of other platelet COX-1 products requires additional enzymatic control. For example, TxA_2 (structure shown in Table 1.1), the most abundant COX product in platelets, is synthesised from PGH_2, which is released by COX-1, by thromboxane synthase (TxS). In this chapter I will investigate whether additional enzymes are involved in DXA_3 generation by targeting two enzymes in platelets that act downstream of COX-1 specifically peroxidases and TxS. Inhibition of peroxidases using iodoacetate decreases generation of 12-HHTrE (structure shown in Table 1.1), a product of COX-1 and TxS in platelets (Sutherland et al. 2001). This compound modifies cysteine residues preventing oxidation of SH side groups of glutathione and proteins. Consequently, it acts as a universal peroxidase inhibitor, likely through

removing reducing substrates. Separately, TxS will be inhibited by picotamide, a derivative of methoxy-isophtalic acid (Violi et al. 1988; Berrettini et al. 1990).

5.1.1 AIMS

- Examine DXA_3 generation in human platelets derived from a $cPLA_2\alpha$ deficient patient

- Determine the role of TxS in DXA_3 synthesis

- Investigate the role of peroxidases in DXA_3 generation

5.2   RESULTS

In this chapter I investigated DXA$_3$ formation by platelets, which were pharmacologically inhibited or showed a genetic deletion of cPLA$_2$α, and using WT and mutant COX-2s *in vitro*. Eicosanoid generation was compared using LC/MS/MS and the ratios of the integrated peak area of DXA$_3$, TxB$_2$, PGE$_2$, 11-HETE or 15-HETE compared to an IS.

5.2.1   CPLA$_2$A DEFICIENT HUMAN PLATELETS ARE UNABLE TO GENERATE DXA$_3$

Platelets from a cPLA$_2$α-deficient patient (Brooke et al. 2014) were isolated, activated using 0.2 U/ml thrombin and the lipids extracted and analysed using LC/MS/MS as described in 2.2.1.1, 2.2.1.3, 2.2.5.1 and 2.2.7.4. LC/MS/MS chromatograms of platelet lipid extracts indicate that DXA$_3$ is generated by healthy donors following activation (Figure 5.1, Panels A and C) but not by platelets derived from a cPLA$_2$α deficient patient (Figure 5.1, Panels B and D).

5.2.1   LESS DXA$_3$ IS GENERATED BY THE COX-2 MUTANTS V359A AND W387F

Arachidonate was oxidised using WT and mutant COX-2 isoforms *in vitro* as described in 2.2.2. Lipids were extracted (2.2.5.1) and eicosanoid levels monitored using LC/MS/MS (2.2.7.4). As expected, 11-HETE formation is significantly increased in V359A and W387F (Figure 5.2, Panel A). In contrast, generation of 15-HETE was not affected (Figure 5.2, Panel D). Both DXA$_3$ (Figure 5.2, Panel B) and PGE$_2$

A Healthy control
No thrombin

m/z 351.2 to 165.1

B c$PLA_2\alpha$ deficient patient
No thrombin

m/z 351.2 to 165.1

C Healthy control
30 min 0.2 U/ml thrombin

7.28

m/z 351.2 to 165.1

D c$PLA_2\alpha$ deficient patient
30 min 0.2 U/ml thrombin

m/z 351.2 to 165.1
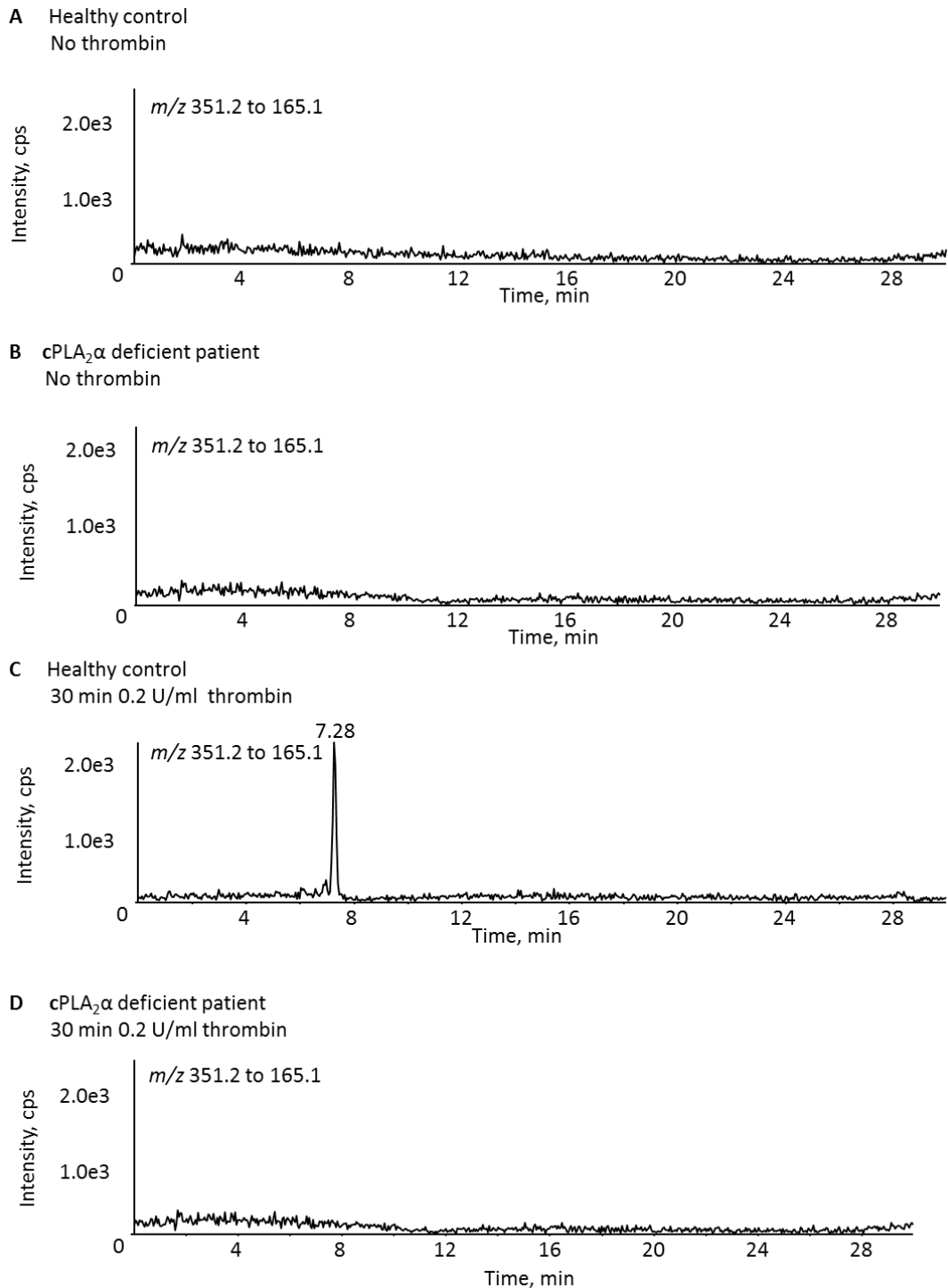
Figure 5.1. DXA$_3$ generation by human platelets is cPLA$_2\alpha$ dependent. Isolated human platelets (healthy donor and cPLA$_2\alpha$ deficient) were activated for 30 min at 37 ^{o}C using 0.2 U/ml thrombin as described in 2.2.1.1 and 2.2.1.3. Lipids were extracted and DXA$_3$ (*m/z* 351.2 to 165.1) as well as PGE$_2$-d$_4$ (*m/z* 355.2 to 271.2, data not shown) monitored using LC/MS/MS as described in 2.2.5.1 and 2.2.7.4.
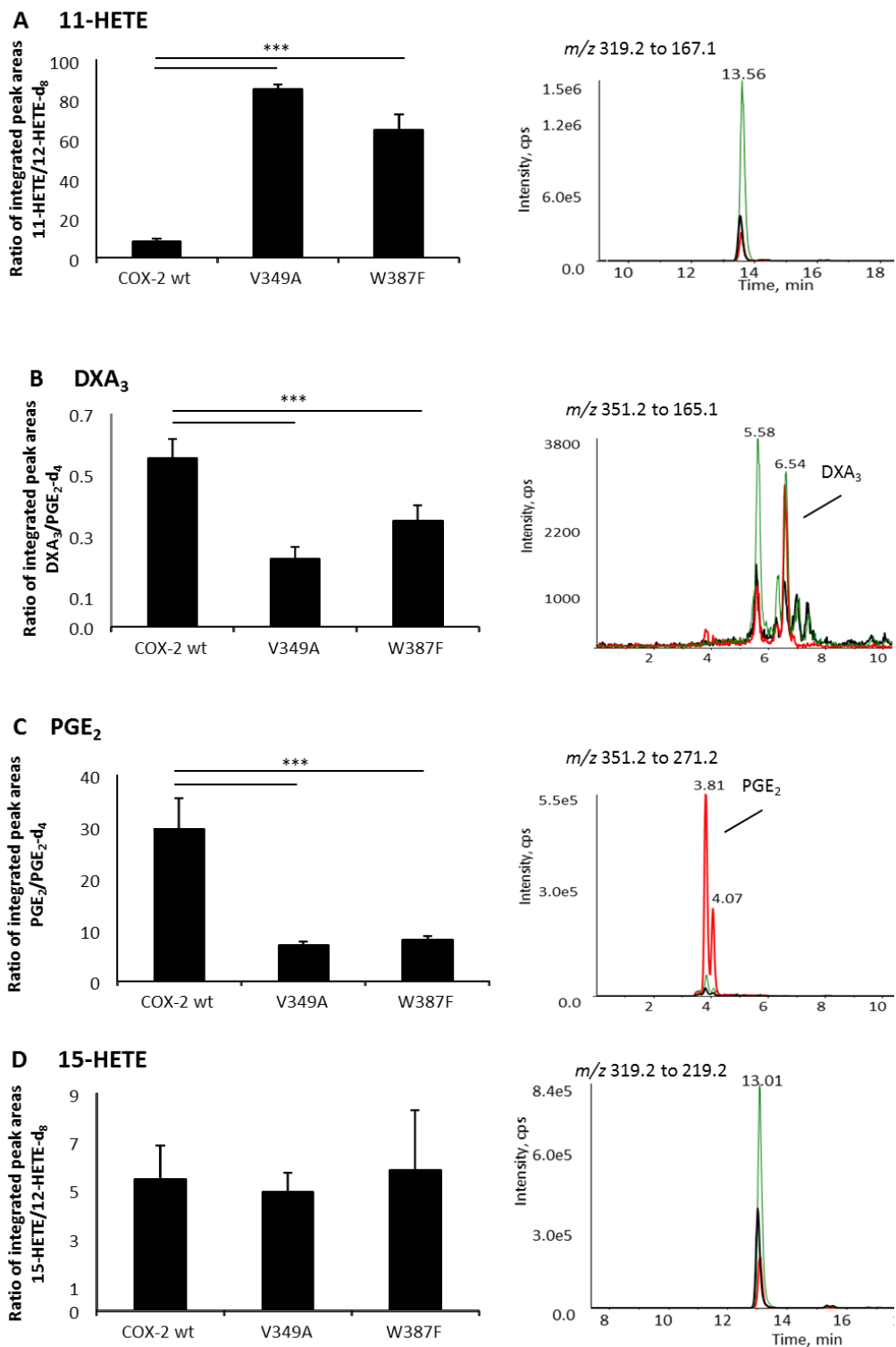
Figure 5.2. DXA₃ generation is decreased in COX-2 mutants that predominantly generate 11-HETE. Arachidonate was oxidised using WT COX-2 or COX-2 mutants (V349A, W387F) as described in 2.2.2. Eicosanoids were analysed utilizing LC/MS/MS (2.2.7.4). Ratios (analyte/IS) and representative chromatograms of (A) 11-HETE and (B) DXA₃, (C) PGE₂, and (D) 15-HETE. In chromatograms black is W387A, green is V349A, and red is wt. n=5-7 ± SEM, ***p ≤ 0.005, one way ANOVA followed by Bonferroni multiple comparisons test.

(Figure 5.2, Panel C) formation was significantly decreased in V359A and W387F compared to WT COX-2.

5.2.2 TxS inhibition does not affect DXA$_3$ Generation by platelets

To inhibit TxS, isolated platelets from three individual donors were treated with 50 µM of the TxS inhibitor picotamide prior to 0.2 U/ml thrombin (2.2.1.3). Extracted eicosanoids were analysed using LC/MS/MS (2.2.5.1, 2.2.7.4). DXA$_3$ generation was not affected by picotamide (Figure 5.3, Panel A). In contrast, PGE$_2$ formation was significantly increased and TxB$_2$ generation decreased by about 50% (Figure 5.3, Panels B and C).

5.2.3 Peroxidase inhibition decreases DXA$_3$ generation by platelet

Isolated platelets from three individual donors were treated with 1-10 mM iodoacetate prior to activation using 0.2 U/ml thrombin (2.2.1.3). TxB$_2$ levels were decreased at 1 mM inhibitor (Figure 5.4, Panel C). In contrast, DXA$_3$ and PGE$_2$ generation were decreased at higher inhibitor concentrations (Figure 5.4, Panels A and B).

5.2.3.1 An additional DXA$_3$ Isomers is formed Following peroxidase inhibition in platelets

LC/MS/MS demonstrates that a single DXA$_3$ isomer is formed by thrombin activated platelets (Figure 5.5, red). However, an additional isomer was seen to elute at 6.36 min in the chromatogram of iodoacetate-treated platelets (Figure 5.5, black).
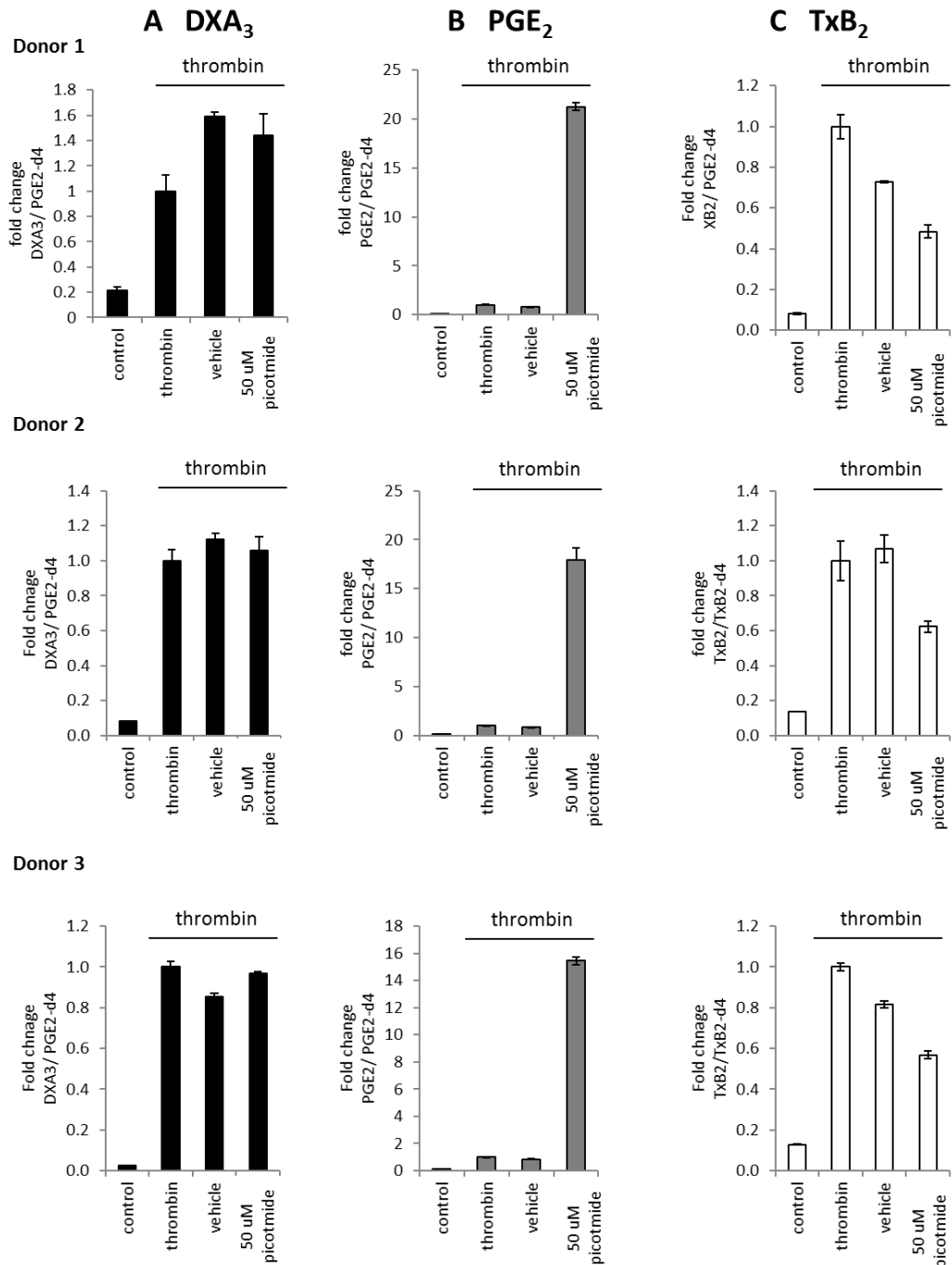
Figure 5.3. DXA₃ formation is not affected by TxS inhibition in platelets. Isolated human platelets were treated with 50 µM picotamide or ethanol (vehicle), then activated using 0.2 U/ml thrombin as described in 2.2.1.1 and 2.2.1.3. Control: untreated platelets. Eicosanoids were analysed using LC/MS/MS as described in 2.2.7.4. (A) DXA₃ (black), (B) PGE₂ (grey) and (C) TxB₂ (white). Thrombin activated platelets set as fold change 1. Triplicates of three donors ± SEM are shown.
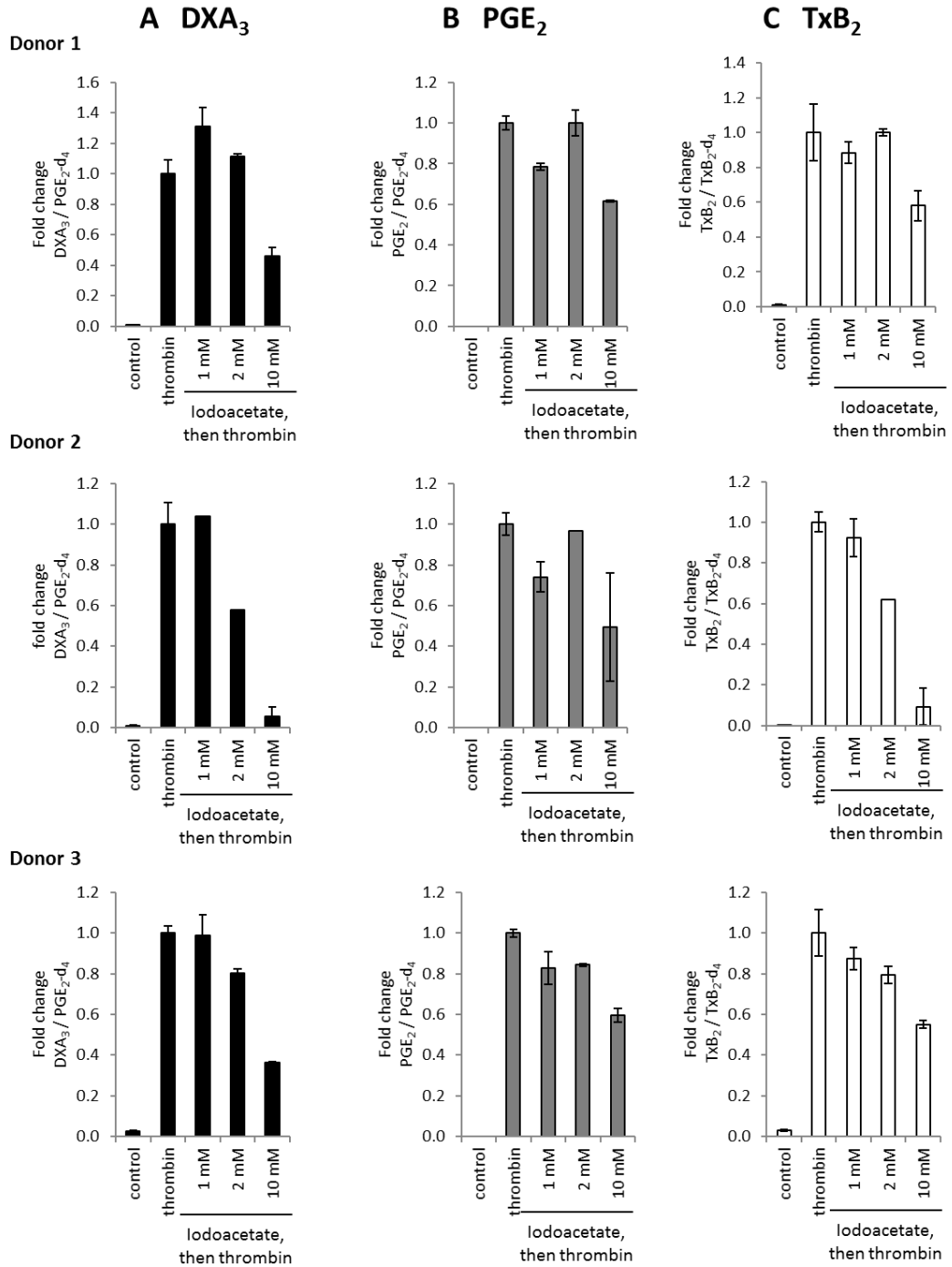
Figure 5.4. Peroxidase activity is required for DXA₃ formation. Isolated platelets were treated using 1-10 mM iodoacetate prior to activation using 0.2 U/ml thrombin (2.2.1.1, 2.2.1.3). LC/MS/MS was utilised to analyse eicosanoid levels as described in 2.2.7.4. (A) DXA₃ (black), (B) PGE₂ (grey) and (C) TxB₂ (white). Thrombin activated platelets set as fold change 1. Triplicates of three donors ± SEM are shown.
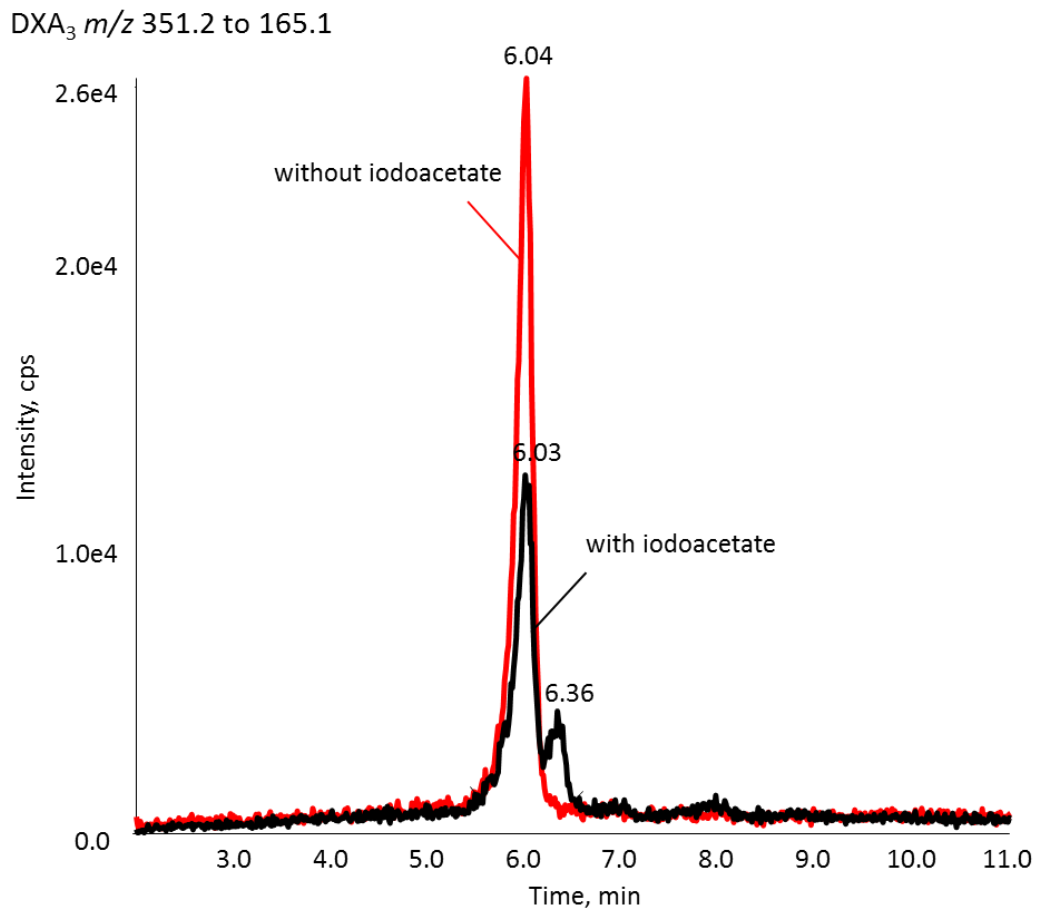
Figure 5.5. Isomers of DXA₃ are formed in platelets following peroxidase inhibition. To inhibit peroxidases, isolated platelets were treated using 2 mM iodoacetate 10 min prior to activation using 0.2 U/ml thrombin (2.2.1.1, 2.2.1.3). DXA₃ was monitored using LC/MS/MS as described in 2.2.7.4. LC/MS/MS chromatogram of DXA₃ with (black) and without (red) inhibition of peroxidases using 2 mM iodoacetate. One donor as representative of three genetically unrelated donors, repeated at least three times.

5.3   DISCUSSION

The rate-limiting step of eicosanoid synthesis is the hydrolysis of arachidonate from phospholipids by $cPLA_2$ as described in 1.3.3.1. The genetic deficiency of the gene encoding for $cPLA_2\alpha$ results in absence of the protein in the intestine causing inhibition of TxA_2 formation and decreased platelet aggregation (Brooke et al. 2014). My data showed that DXA_3 generation is blocked in platelets from a $cPLA_2\alpha$ deficient patient (5.2.1). This indicates that DXA_3 generation depends on $cPLA_2\alpha$ *in vivo* and confirms results using $cPLA_2$ inhibitors *in vitro* obtained prior to my PhD (Aldrovandi, unpublished). The major physiological importance of eicosanoids is demonstrated by the patients' medical conditions that include small bowel ulceration, stenosis of unknown aetiology (cryptogenic multifocal ulcerous stenosing enteritis (CMUSE)), and failures in immune responses indicated by repeated infections by Candida albicans, Campylobacter, Salmonella, and Staphylococcus (Brooke et al. 2014). Indeed, $cPLA_2\alpha$ is associated with efficient neutrophil-mediated bacterial killing and therefore, its deficiency may be responsible for these infections (Rubin et al. 2005). The biological function of DXA_3 is yet to be fully understood. However, in Chapter 8 I will demonstrate that this lipid increases integrin expression on neutrophils suggesting a role of DXA_3 in early immune responses and acute inflammation. Therefore, as DXA_3 represents a $cPLA_2\alpha$ dependent eicosanoid, its deficiency may play a role in the immune related medical conditions of the patient but this requires further investigation.

Prior to my PhD it was demonstrated that the signalling pathway upstream of COX that activates DXA_3 generation is the same as for other COX products (Aldrovandi,

unpublished). Thus, in this Chapter I investigated the enzymatic mechanism of COX that leads to the formation of this unique lipid, and the involvement of other enzymes that may act downstream of COX in platelets. My studies showed that, in comparison to other COX products, DXA_3 formation is affected differently by COX mutations and inhibition of either TxS or peroxidases in platelets. Inhibition of TxS will lead to an increase in its substrate, PGH_2. This could then non-enzymatic rearrange to PGE_2 explaining the increase in its levels following TxS inhibition (Figure 5.3, Figure 5.6, F). DXA_3 formation was not inhibited by picotamide, indicating that TxS or PGH_2 are not required for DXA_3 generation. Peroxidase inhibition decreased DXA_3 levels indicating that peroxidase function is required for its formation by platelets. In addition, I demonstrated that DXA_3 isomers were formed during peroxidase inhibition (Figure 5.6, I). Isomers also form during DXA_3 generation by COX-1 and 11-HpETE oxidation *in vitro* (4.2.4). Thus, the greater control of DXA_3 generation to form only one isomer in platelets may be facilitated by a peroxidase. As both oxidation and reduction is required to form DXA_3 following C8 radical escape, an enzyme exhibiting both functions may account for DXA_3 generation downstream of COX. Cytochrome P450s represent such enzymes and have been demonstrated to facilitate synthesis of certain prostanoids including TxA_2 and PGI_2 (Hecker & Ullrich 1989; Brash 2009). Furthermore, P450 -derived products such as 8, 9-epoxyeicosatrienoic acid (8,9-EET) and 14, 15-EET can be used by COX yielding epoxy-hydroxy products and by LOX forming dioxolanes *in vitro* (Zhang et al. 1992; Teder et al. 2014). Thus, P450 enzymes are potential candidates for DXA_3 synthase activity in platelets.
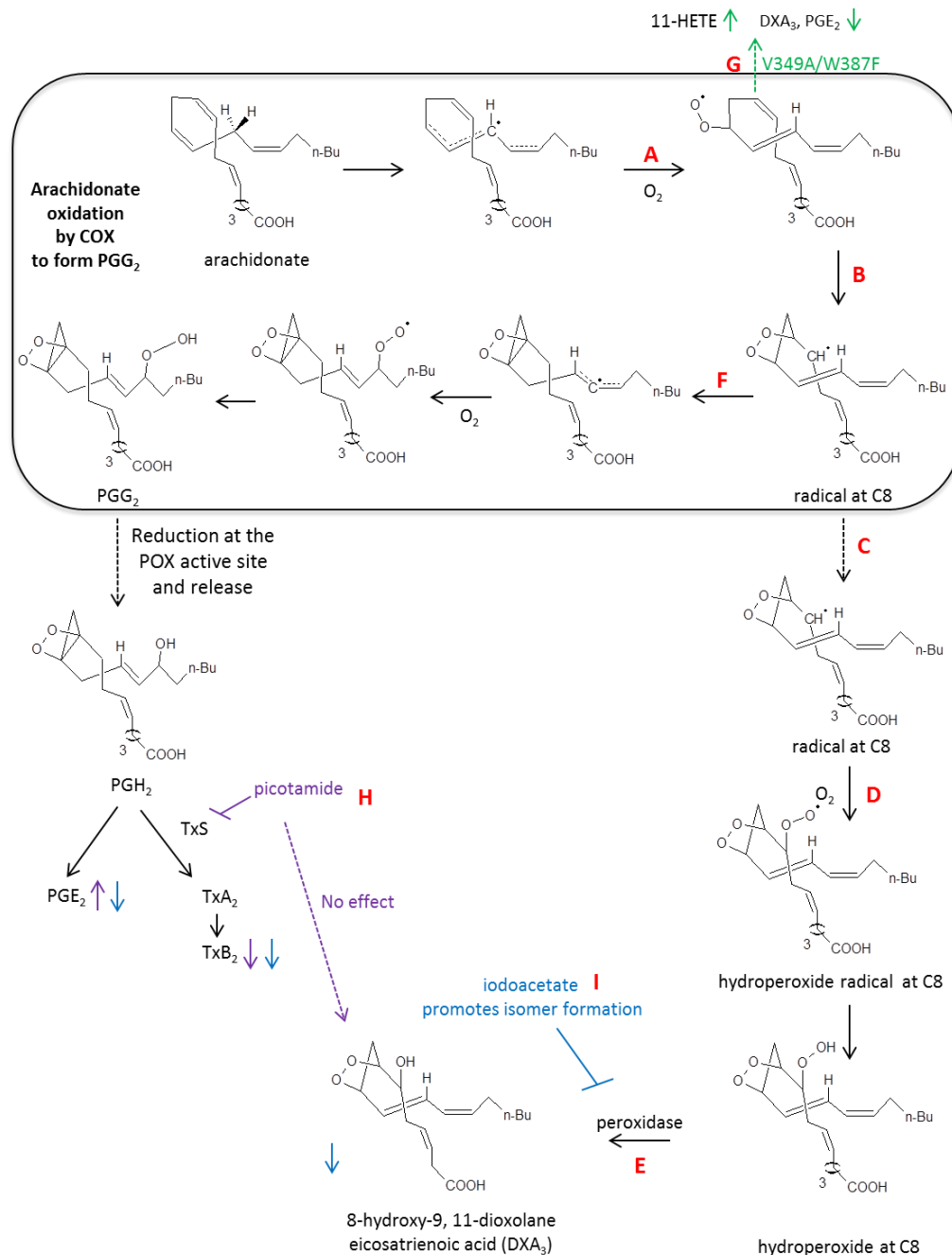
Figure 5.6. Proposed formation of DXA₃ by COXs. Oxidation of arachidonate by COX leads to PGH2 formation. Mutations within the COX active site result in decreased DXA₃ and PGE₂ levels, and increased 11(R)-HETE levels (G, green). TxS inhibition using picotamide does not affect DXA₃ levels (H, purple). Inhibition of peroxidases using iodoacetate leads to decreased DXA₃ levels and isomer formation (I, blue). A full description of this pathway is shown in 5.3.

Last, studies were undertaken to investigate DXA$_3$ generation by the COX-2 mutants V359A and W387F (Figure 5.2), which form greater levels of 11(R)-HETE than WT COX-2 as a result of increased 11-hydroperoxyl radical escape from the COX active site (Harman et al. 2004). My data showed that DXA$_3$ levels generated by these mutants are significantly decreased compared to WT enzyme (Figure 5.2, Figure 5.6, G). This indicates that DXA$_3$ formation does not involve the escape of the 11-hydroperoxyl radical. COXs are known to facilitate endoperoxide ring closure between C9 and C11 during catalysis (Marnett 2000). Therefore, I propose that the dioxolane ring of DXA$_3$ forms between C11 and C9 within the COX catalytic site, then the radical delocalises to C8 (Figure 5.6, B). As PGH$_2$ may not be an intermediate during DXA$_3$ generation (Figure 5.6, H), I suggest that this radical then escapes from the enzyme (Figure 5.6, C), rather than completing the COX catalytic cycle (Figure 5.6, F). Then, the C8 radical is further oxidised forming an 8-hydroperoxyl radical (Figure 5.6, D). Finally, this radical is reduced, possibly by a peroxidase, to a hydroxyl group (Figure 5.6, E) forming 8-hydroxyl-9, 11-dioxolane eicosatrienoic acid (DXA$_3$).

As the C11 of the escaping 11-HETE has an (R) configuration, DXA$_3$ would have the same stereochemistry at this position (Harman et al. 2004; Thuresson et al. 2000). Therefore, investigating the stereochemistry of DXA3 would further support my proposed structure.

My proposed mechanism includes the escape of a carbon centred radical at C8. Previously described enzymatic mechanisms of COX show that this radical is delocalised to C15 when continuing the COX cycle and then oxidised at this position in order to form PGH$_2$ (Marnett 2000). In addition, a carbon-carbon bond forms

between C8 and C12, which is not seen in my proposed DXA$_3$ structure (Figure 5.6, F). Consequently, it is unlikely that DXA$_3$ originates from an intermediate that is formed later than the C8 radical. As a novel mechanistic pathway proposed for COX, this requires further investigation that may include genetic mutations of the COX catalytic site aiming to increase escape of the C8 radical.

In conclusion, in this chapter I confirmed that DXA$_3$ generation requires cPLA$_2$. Its formation by and/or downstream of COX is distinct to that of other prostanoids and suggests the potential involvement of a specific synthase with peroxidase activity. Eicosanoids represent a large group of lipid mediators present in several cell types and tissues. Therefore, in the following chapter I will investigate whether DXA$_3$ is generated by leukocytes and detectable in human serum following clot induction *in vitro*.

CHAPTER SIX

DXA$_3$ IN HUMAN SERUM AND RAW246.7 CELLS

6.1 INTRODUCTION

Platelets are important mediators of haemostasis and play a role in early immune responses. Under healthy conditions, platelets circulate in a resting state in the blood. As described in 1.2.3.1, platelet activation subsequently leads to thrombus formation in prevention of bleeding. Apart from this physiological role, thrombi also form on the surface of atherosclerotic plaque and their rupture is a high risk factor for coronary artery diseases (CAD) that include stable and unstable angina, myocardial infarction and sudden coronary death (Badimon & Vilahur 2014; Libby 2005). At atherosclerotic lesions, activated platelets release bioactive mediators including growths factors and cytokines that lead to smooth-muscle proliferation and leukocyte recruitment promoting disease progression (Huo & Ley 2004). Furthermore, CAD and atherosclerosis are associated with elevated levels of activated platelets and eicosanoids including TxA_2 (Theken et al. 2012; Simon et al. 1989; Baker et al. 1999; Belton et al. 2000; Furman et al. 1998; Trip et al. 1990).

To determine whether DXA_3 could play a role in thrombus formation, I will investigate its generation during blood clot formation *in vitro*. To determine whether DXA_3 levels are altered in circulating platelets in atherosclerosis, its generation will be analysed in platelets of murine ApoE deficient mice, a murine strain that spontaneously develops this disease with age.

Eicosanoids are not only involved in cardiovascular events, but also play an important role during inflammation. In leukocytes these lipids are predominantly generated by macrophages expressing COX-1 and COX-2 (Harizi et al. 2008). Prior to this study, it was shown that DXA_3 is formed *in vitro* by both isoforms, COX-1

and COX-2 (Aldrovandi, unpublished). Therefore, in this chapter, I will investigate DXA$_3$ formation in the macrophage cell line RAW264.7, which expresses COX-2 upon LPS stimulation (Rouzer 2005).

6.1.1 Aims

- Determine the presence of DXA$_3$ in human serum and blood clots

- Examine DXA$_3$ generation by murine platelets and comparison of WT and ApoE deficient mice

- Determine DXA$_3$ formation in the macrophage cell line RAW264.7

6.2   Results

In this chapter I investigated whether DXA_3 can be detected in human serum and blood clots (6.2.1), murine platelets derived from WT and ApoE deficient mice (6.2.2), and stimulated RAW264.7 cells (6.2.3). These analyses were undertaken using LC/MS/MS and comparison of the obtained integrated peak areas ratios (lipid/IS).

6.2.1 DXA_3 is present in human serum during thrombus formation

During thrombus formation, platelets are activated leading to the release of bioactive mediators including eicosanoids. To determine whether DXA_3 is formed during clotting, whole blood was incubated for 15 min at 37 ^{o}C without anti-coagulant until a blood clot was formed. The serum was isolated and the lipids extracted from both, the blood clot and serum as described in 2.2.1.5 and 2.2.5.1. DXA_3 was detected using LC/MS/MS and compared to an activated platelet sample as positive control (Figure 6.1, Panel A; Figure 6.2, Panel A). DXA_3 was detected in serum (Figure 6.1, Panel C, E, G) and clot (Figure 6.2, Panel C) of three genetically unrelated donors.

6.2.2 DXA_3 levels are identical in thrombin activated platelets derived from wildtype and ApoE deficient mice

Platelets of wildtype and ApoE deficient mice were isolated and activated using 0.2 U/ml thrombin. Following lipid extraction DXA_3, PGE_2, TxB_2 and 12-HETE were monitored using LC/MS/MS as described in 2.2.1.2, 2.2.5.1 and 2.2.7.4.

151
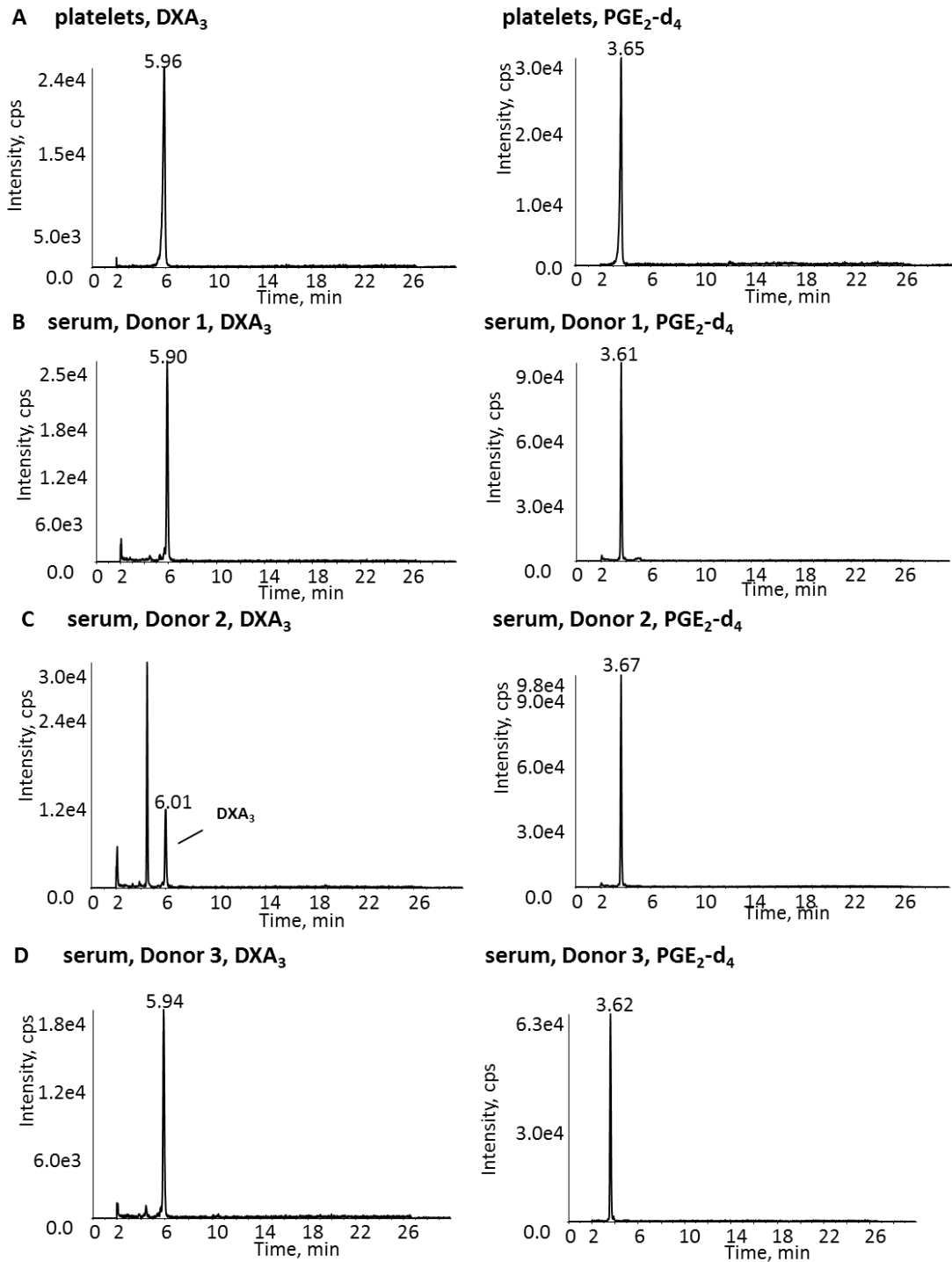
Figure 6.1. DXA₃ is detectable in human serum. Whole blood was incubated at 37 °C for 15 min until a blood clot was formed. Serum was isolated using centrifugation. Isolated platelets were activated using 0.2 U/ml thrombin. Lipids were extracted and analysed using LC/MS/MS as described in 2.2.1.5, 2.2.5.1 and 2.2.7.4. MS/MS chromatograms of DXA₃ and PGE₂-d₄ in platelet (A) and serum (B-D). Serum was obtained from three genetically unrelated donors.
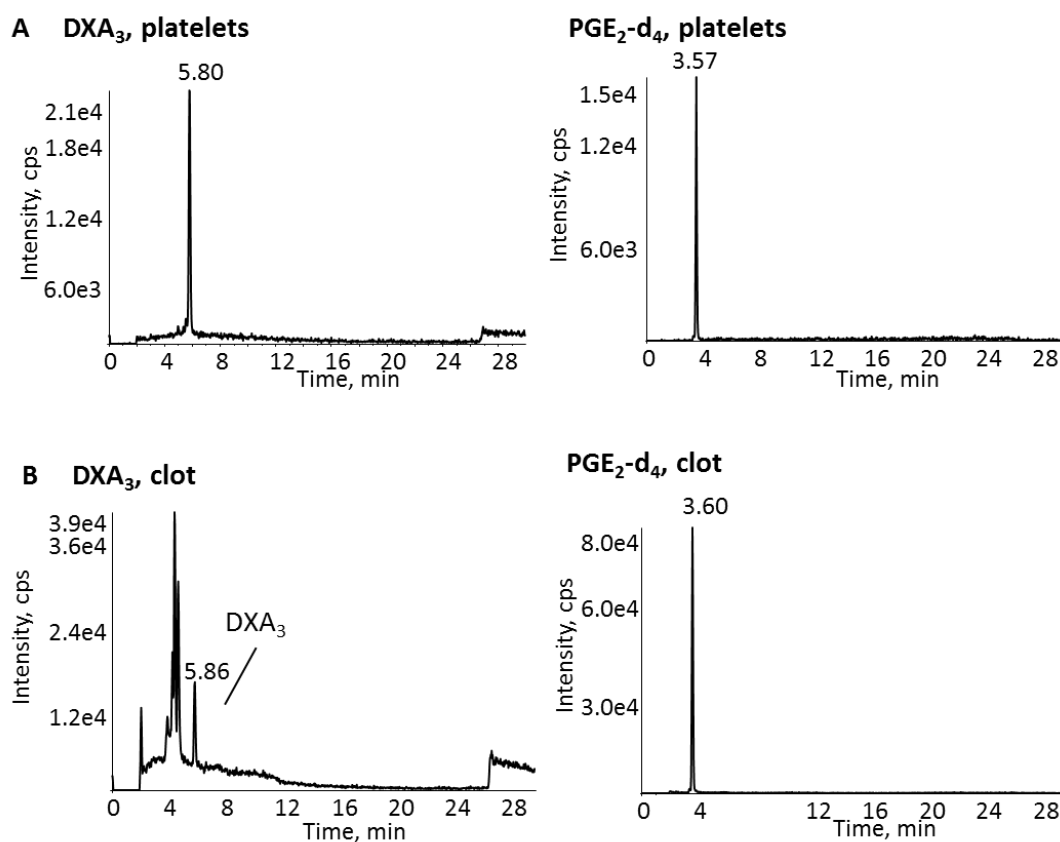
Figure 6.2. DXA₃ is detectable in human blood clot *in vitro*. Whole blood was incubated at 37 °C for 15 min until a blood clot was formed as described in 2.2.1.5. Isolated platelets were activated using 0.2 U/ml thrombin (2.2.1.1, 2.2.1.3). Lipids were analysed using LC/MS/MS as described in 2.2.5.1 and 2.2.7.4. MS/MS chromatograms of DXA₃ or PGE₂-d₄ derived from platelets (A) and blood clot (B). Shown is one donor as representative of three genetically unrelated donors.

DXA$_3$ was monitored in murine platelets (Figure 6.3). Its levels and that of PGE$_2$, 12-HETE and TxB$_2$ were increased following thrombin activation (Figure 6.3 A-D). They did not differ between WT (black) and Apo E deficient (grey) mice.

6.2.3 DXA$_3$ IS GENERATED BY THE MACROPHAGE CELL LINE RAW264.7

RAW264.7 cells were cultured to a confluence of 90% (2.2.1.8), activated with 200 ng/ml LPS and/or 1 μM calcium ionophore A23187 (2.2.1.9) and the lipids extracted and analysed using LC/MS/MS (2.2.5.1, 2.2.7.4).

Both PGE$_2$ and DXA$_3$ were absent in the culturing medium DMEM (Figure 6.4, Panel A). DXA$_3$ was detected at low levels in untreated (control) and LPS treated cells (Figure 6.4, Panels B and D). Ionophore activation increased DXA$_3$ (Figure 6.3, Panel D), but it was not further enhanced by LPS (Figure 6.4, D). In contrast, PGE$_2$ was generated on treatment with LPS but not A23187 (Figure 6.4, Panels B, C, and D). LPS and A23187 also increased PGE$_2$ compared to LPS alone (Figure 6.4, Panel E). PGD$_2$ is detected in the same MS/MS chromatogram eluting at 4.05 min under basal conditions (Figure 6.4, Panel B). It increased following treatment with A23187 but not LPS (Figure 6.4, Panels C, D, and E). These data demonstrate that DXA$_3$ formation requires A23187 but is unaffected by inflammatory stimulation. Therefore, generation of this lipid most likely to occurs via COX-1 but not COX-2 in RAW246.7 cells.
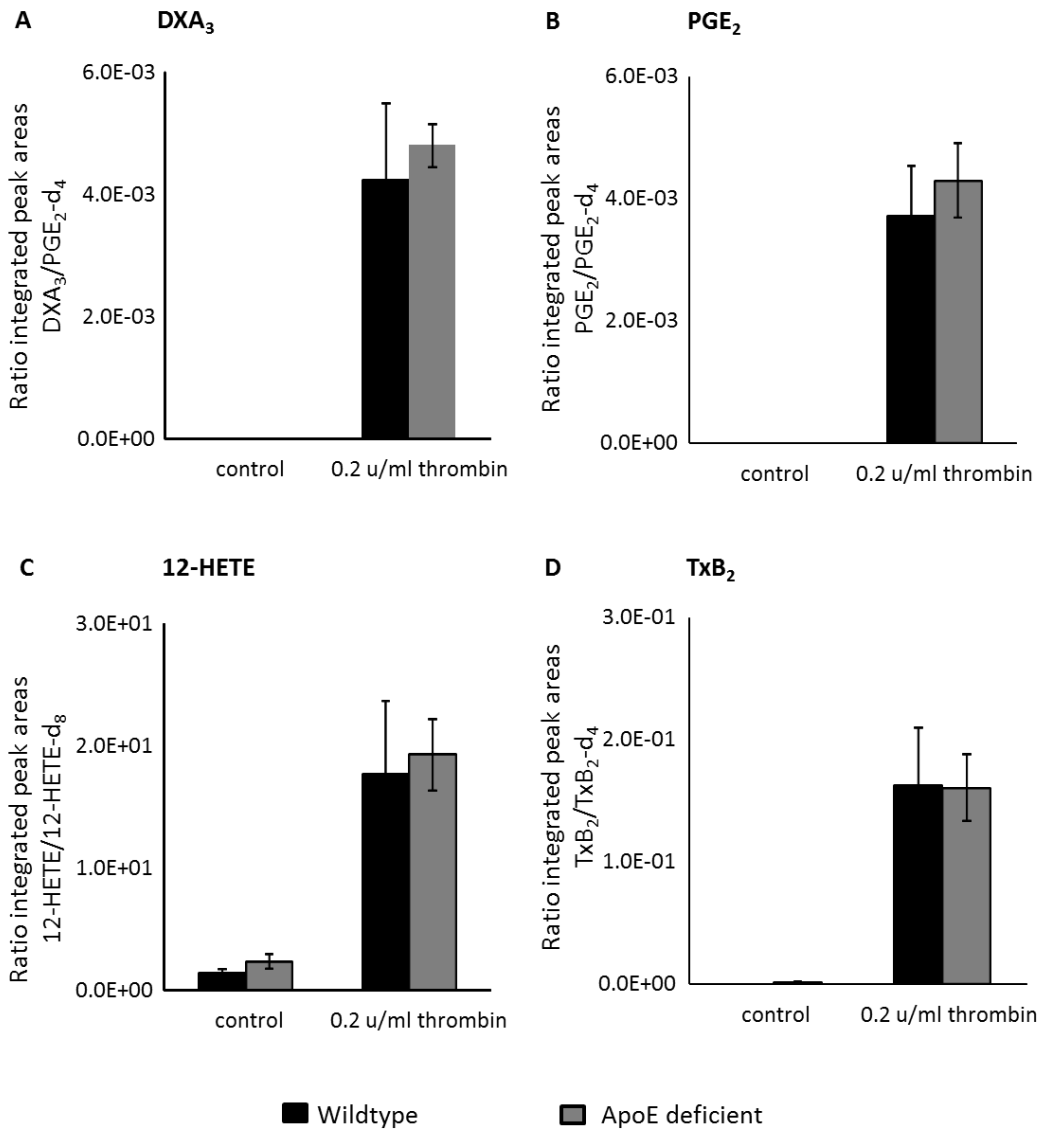
Figure 6.3. Eicosanoid levels do not differ in platelets from WT and ApoE deficient mice. Isolated platelets from either WT or ApoE deficient mice were activated using 0.2 U/ml thrombin, lipids extracted and analysed using LC/MS/MS as described in 2.2.1.2, 2.2.5.1 and 2.2.7.4. (A) DXA_3, (B) PGE_2, (C) 12-HETE and (D) TxB_2. Lipid levels are shown as ratios of integrated peak areas (lipids/IS).
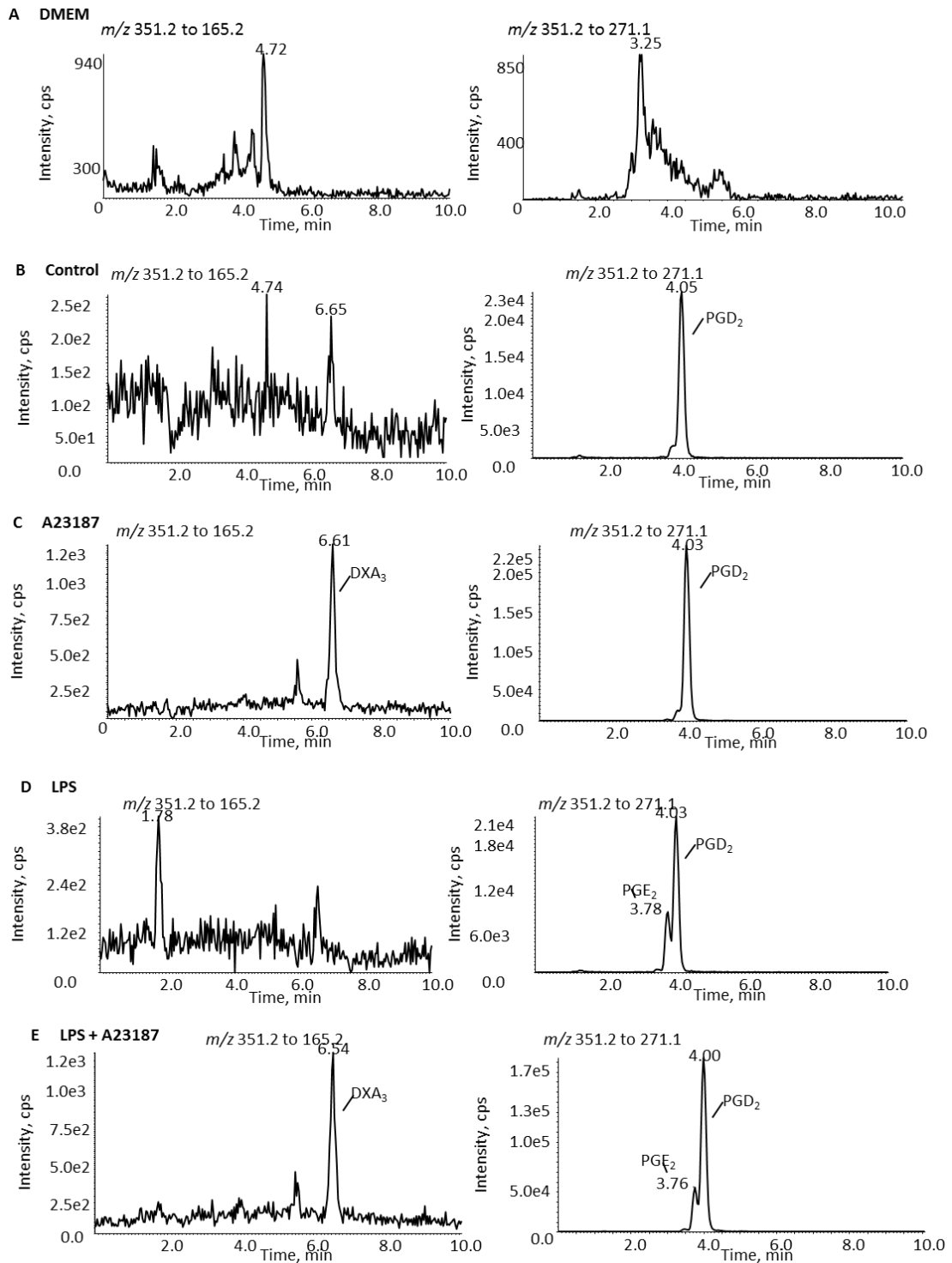
Figure 6.4. DXA₃ is generated by RAW264.7cells following calcium ionophore A23187 activation. RAW264.7 cells were activated using 10 µM calcium ionophore A23187 for 10 min at 37°C. In some experiments cells were stimulated using 200 ng/ml LPS for 24 h at 37°C prior to A23187 treatment. LC/MS/MS chromatograms of lipid extracts derived from RAW264.74 cells of DXA₃ (*m/z* 351.2 to 165.1) and PGE₂ (*m/z* 351.2 to 271.1) in (A) DMEM, (B) unstimulated cells, (C) A23187, (D) LPS and (E) both LPS and A23187 treated cells. Sample preparation and analysis as described in2.2.1.8, 2.2.1.9, 2.2.5.1 and 2.2.7.4.

156

6.3 Discussion

In this chapter I demonstrated that DXA_3 is detectable in human serum and blood clot during thrombus formation *in vitro*, in calcium ionophore A23187 activated RAW264.7 cells and in murine platelets following thrombin activation.

During thrombus formation circulating platelets rapidly adhere to the site of injury. Their interactions with exposed proteins such as von Willebrand factor (VWF) lead to activation. Adhesion induces intracellular signalling, which subsequently leads to synthesis and secretion of secondary platelet agonists such as TxA_2, which promotes platelet aggregation and together with fibrinogen results in blood clot formation (Nieswandt et al. 2011; Savage et al. 1998). Serum and blood clot samples tested in this study were obtained from whole blood without anti-coagulant, following spontaneous platelet activation and eicosanoid formation as indicated by TxB_2 detected in serum (not shown). In addition to this, DXA_3 (Figure 6.1) and PGE_2 (not shown) were detected in both serum and blood clots. During clot formation, TxA_2 contributes to further platelet activation and aggregation *in vivo* (Paul et al. 1999; Kroll & Schafer 1989). Therefore, DXA_3 may facilitate similar effects. However, this requires further investigation including determining the effect of DXA_3 on platelet activation as discussed later in 9.6.

Herein, I showed that DXA_3 generation is conserved among two species. I also investigated whether DXA_3 formation is altered in platelets derived from ApoE deficient compared to WT mice. Atherosclerotic lesions develop with age, and are larger and more advanced in female ApoE deficient mice than male (Caligiuri et al. 1999; Paigen et al. 1987). Levels of 12-HETE, DXA_3, TxB_2 and PGE_2 were not different in

activated platelets from WT and ApoE deficient mice (Figure 6.3) indicating similar eicosanoid generation and platelet reactivity *in vitro* in both strains. However, I have only investigated their generation *ex vivo*. *In vivo*, elevated TxB_2 (and its metabolite 2,3-dinor TxB_2) levels have been detected in serum (or urine) of ApoE deficient mice compared to WT. These levels were decreased following aspirin treatment (Praticò et al. 2000). Therefore, eicosanoid generation including that of DXA_3 may be different *in vivo* between both strains. To further investigate this, future studies may determine DXA_3 levels in serum of ApoE deficient and WT mice.

Data obtained prior to my PhD revealed that DXA_3 is generated by both COX-1 and COX-2 *in vitro* (Aldrovandi, unpublished). To investigate its cellular generation by COX-2, I analysed DXA_3 formation by RAW264.7 cells. These express COX-2 following a 24 hrs LPS stimulation (Rouzer 2005). COX-2 expression and its activation is coupled to increased PGE_2 generation (Giroux & Descoteaux 2000). Indeed, I found that LPS stimulation led to generation of PGE_2 indicating COX-2 upregulation. In contrast, DXA_3 was generated in A23187-activated RAW cells basally, and this was not elevated by LPS. This suggests a potential isoform-specific generation of this lipid in cells. To investigate this, future studies may investigate DXA_3 generation in RAW264.7 cells upon selective COX-1 and COX-2 inhibition.

In conclusion, my data suggests that DXA_3 generation is a local response to platelet activation during clot formation *in vitro*. The lipid is also generated by COX-1 in a macrophage cell line. Therefore, further investigation may determine whether DXA_3 generation is cell, COX isotype, and stimulus specific.

To determine whether a DXA_3 is likely to be biologically relevant, it is important to quantify its levels generated by human and murine platelets and compare them to the amounts of other platelet-derived eicosanoids. Therefore, in the next chapter I will develop a quantitative assay and quantify DXA_3 as both free fatty acid and esterified to PE in thrombin activated platelets.

CHAPTER SEVEN

QUANTIFICATION OF DXA$_3$ GENERATED BY PLATELETS

7.1 INTRODUCTION

DXA_3 represents a novel COX-1 product, thus no synthetic standard or other reagents to quantify this lipid are currently available. To determine DXA_3 levels generated by platelets and compare the amounts to other eicosanoids, I will develop a quantitative assay and assess the amounts of DXA_3, PGE_2, TxB_2 and 12-HETE in human and murine platelets.

Several methods are available for eicosanoid quantification including LC-UV, LC-MS, radioimmunoassay, and GC-MS (Schweer et al., 1985, Walenga et al., 1985, Kiyomiyaet al., 1986; Sweeney et al., 1987; Kurosawa et al., 1990, Miller and Weyker, 1990). However, synthetic standards are essential for all of these methods. In this study, I will generate a DXA_3 standard curve utilising radiolabelled [14C]-arachidonate and quantify DXA_3 in biological samples using LC/MS/MS (Bruins 1998; Deems et al. 2007; Margalit et al. 1996). Minor changes in extraction efficiencies and retention times of the LC/MS are corrected by adding an internal standard (IS) before lipid extraction. To allow accurate quantification, an IS should ideally be structurally and chemically identical to the lipid of interest (Ho et al. 2003). The simplest way to achieve this is by using stable isotope modified standards, e.g. PGE_2-d_4 for PGE_2 (Murphy et al. 2005). However, when an isotope standard is not available, lipids with similar structure can be employed as ISs in combination with a primary unlabelled standard identical to the molecule of interest (Ho et al. 2003). Therefore, I generated DXA_3 as primary standard, which was used to construct a standard curve with PGE_2-d_4 as IS as described in 7.2.3.

As DXA_3 can be esterified to four PE species (16:0p, 18:0p, 18:1p and 18:0a) following platelet activation, I will also quantify the esterified forms (Aldrovandi et al.,

unpublished). To achieve this, I will quantify free DXA$_3$ before and after hydrolysis of total platelet lipids as described in 7.2.4 and shown previously for PGE$_2$-PE (Aldrovandi et al. 2013).

7.1.1 Aims

- Establish a quantitative assay for DXA$_3$

- Determine the amounts of free and esterified DXA$_3$ generated by isolated human platelets

- Quantify the amount of free DXA$_3$ generated by isolated murine platelets

7.2   RESULTS

Currently, DXA$_3$ is not available as a commercial standard. Therefore, I generated [^{14}C]-DXA$_3$ by COX-1 oxidation of [^{14}C]-arachidonate *in vitro* as described in 2.2.2. A [^{14}C]-DXA$_3$ standard curve was generated and analysed using LC/MS/MS (7.2.2). This standard curve was then used to quantify unlabelled DXA$_3$ also generated by COX-1 oxidation, using LC/MS/MS. Finally, a standard curve was generated using unlabelled DXA$_3$, with PGE$_2$-d$_4$ as the IS (7.2.3), for quantification of the lipid in biological samples (7.2.4 and 7.2.5).

7.2.1   GENERATION OF A [^{14}C]-ARACHIDONATE STANDARD CURVE

In this approach the molar amounts of [^{14}C]-arachidonate and [^{14}C]-DXA$_3$ are directly comparable since one mol [^{14}C]-arachidonate is converted to one mol [^{14}C]-DXA$_3$:
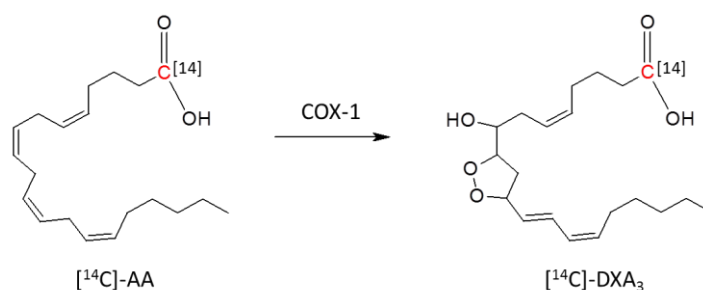
Therefore, [^{14}C]-DXA$_3$ can be quantified by radioactivity, using a [^{14}C]-arachidonate standard curve. This was generated within the limit of detection of the LC radiochemical detector, equivalent to a maximum of 30 Bq [^{14}C]-arachidonate. The integrated peak areas of varying [^{14}C]-arachidonate activity amounts (6 - 30 Bq) were calculated and the resulting standard curve used for [^{14}C]-DXA$_3$ quantification (Figure 7.1).

[14C]-arachidonate standard curve
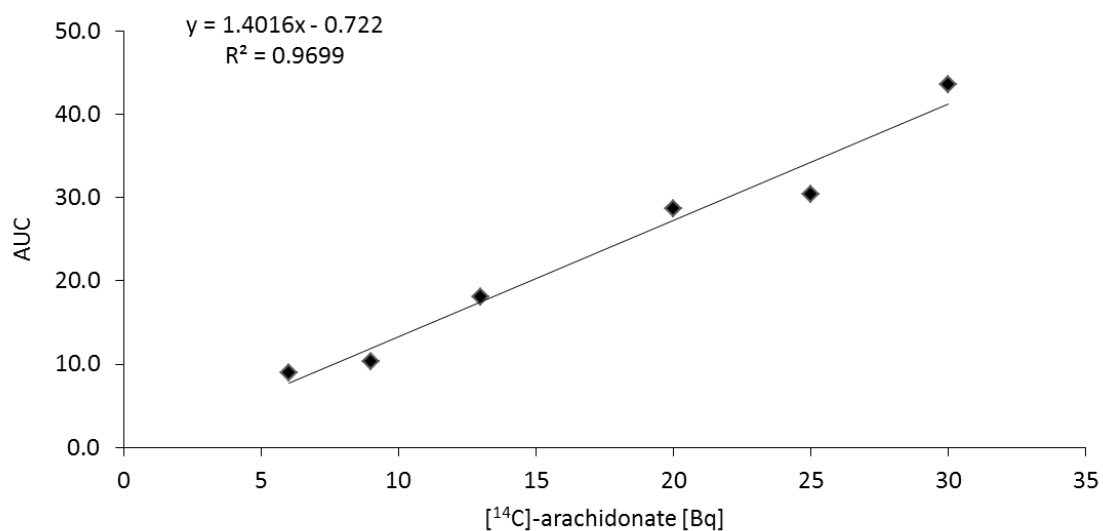
Figure 7.1. [14C]-arachidonate standard curve. A [14C]-arachidonate standard curve in the range of 6 - 30 Bq [14C] was monitored using a LC radioflow detector as described in 2.2.7.1. The integrated peak areas were calculated and plotted against the Bq values of [14C]-arachidonate.

7.2.2 Generation of a [^{14}C]-DXA$_3$ standard curve

[^{14}C]-DXA$_3$ was generated by oxidation of [^{14}C]-arachidonate by COX-1 *in vitro* as described in 2.2.2. Several peaks elute when monitoring [^{14}C] in the lipid extract of this enzyme reaction (Figure 7.2). Fractions were collected at 30 second intervals and [^{14}C]-DXA$_3$ identified using MS/MS monitoring *m/z* 353.2 to 165.1 eluting at 50.5 min on the LC-radiochemical system. Using the [^{14}C]-arachidonate standard curve (Figure 7.1), the radioactivity of the [^{14}C]-DXA$_3$ peak was determined to be 25.5 Bq [^{14}C]. As [^{14}C]-DXA$_3$ amounts are directly comparable to that of [^{14}C]-arachidonate, this equals 51.3 ng [^{14}C]-DXA$_3$.

A [^{14}C]-DXA$_3$ standard curve was generated (0.01 – 10 ng) and analysed utilizing LC/MS/MS as described in 2.2.7.3. The lipid elutes at 49.5 min on the Q-Trap platform (Figure 7.3, Panels A and B). As MS analysis (2.2.7.2) of the substrate, [^{14}C] arachidonate, revealed that only 66 % was radiolabelled (Figure 7.4), the [^{14}C]-DXA$_3$ levels were corrected by this percentage resulting in a specific [^{14}C]-DXA$_3$ standard curve in the range of 0.06 – 6.6 ng (Figure 7.3, Panel C). This standard curve was employed to quantify unlabelled DXA$_3$ also generated by COX-1 *in vitro* (7.2.3). Thus, the transition for [^{14}C]-DXA$_3$ at *m/z* 353.2 to 165.1 was directly compared for integrated area with that for cold DXA$_3$, at *m/z* 351.2 to 165.1.

7.2.3 Generation of a DXA$_3$ standard curve

Unlabelled DXA$_3$ was generated using COX-1 *in vitro* (2.2.2) and analysed using LC/MS/MS (2.2.7.3). The DXA$_3$ peak was integrated and quantified using the [^{14}C]-DXA$_3$ standard curve. Then, a second DXA$_3$ standard curve was generated with

Lipid extract of [^{14}C] arachidonate oxidation by COX-1 *in vitro*
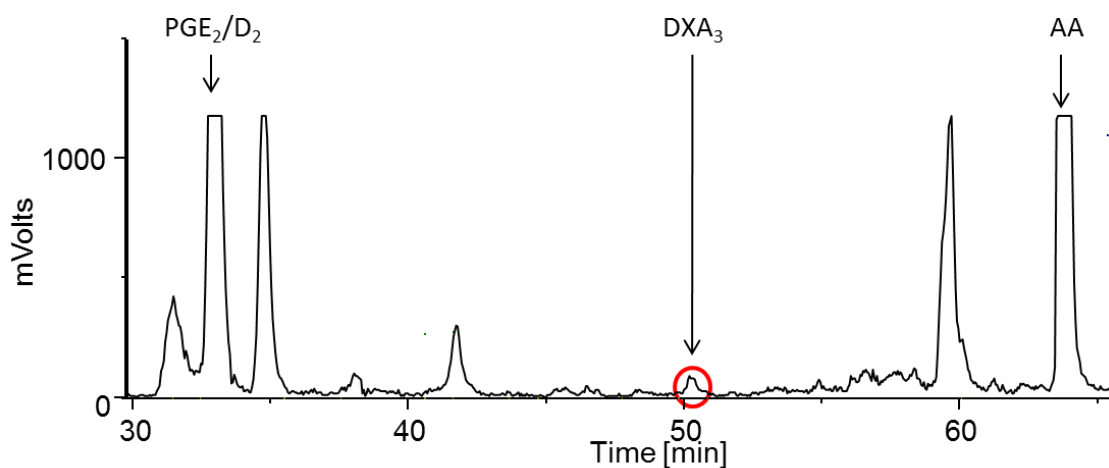
Figure 7.2. [^{14}C]-derived from COX-1 *in vitro* is detected when monitoring [^{14}C] labelled lipids on an LC radioflow detector. [^{14}C]-DXA$_3$ was generated using COX-1 *in vitro* and analysed using LC with radioflow detection as described in 2.2.2 and 2.2.7.1. A chromatogram derived from the [^{14}C] labelled lipid extract is shown. Fractions were collected every 30 sec and lipids identified using MS/MS on the 4000 QTrap as described in 2.2.7.3. The peak eluting at 50.5 min was identified as [^{14}C] - DXA$_3$.

A **[^{14}C] - DXA$_3$ generated by COX-1** *in vitro*
m/z 353.2 to 165.1

B **MS/MS spectrum of [^{14}C] – DXA$_3$**

C **[^{14}C] DXA$_3$ standard curve**

$y = 62652x + 2990.5$
$R^2 = 0.9997$
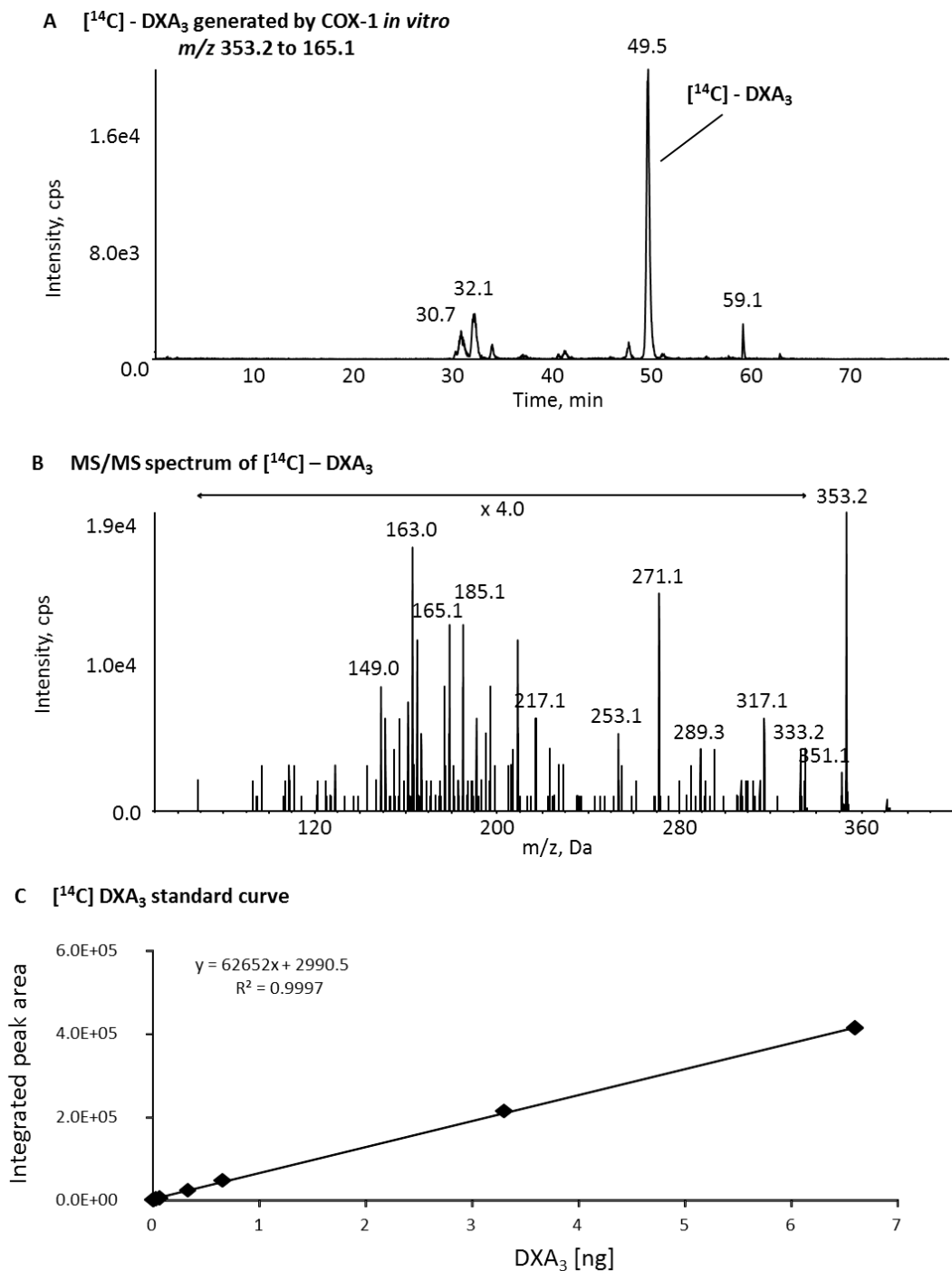
Figure 7.3. **LC/MS/MS analysis of the [^{14}C]-DXA$_3$ standard.** [^{14}C]-DXA$_3$ was generated using COX-1 *in vitro* as described in 2.2.2. [^{14}C]-DXA$_3$ was quantified by comparing the radiochemical response to [^{14}C]-arachidonate. (A) LC/MS/MS monitoring [^{14}C]-DXA$_3$ eluting at 49.5 min. (B) MS/MS spectrum of [^{14}C]-DXA$_3$. (C) [^{14}C]-DXA$_3$ standard curve. Integrated peaks area of [^{14}C]-DXA$_3$ vs. [^{14}C]-DXA$_3$ amounts [ng]. LC/MS/MS analysis on the 4000 QTrap instrument as described in 2.2.7.3.

167
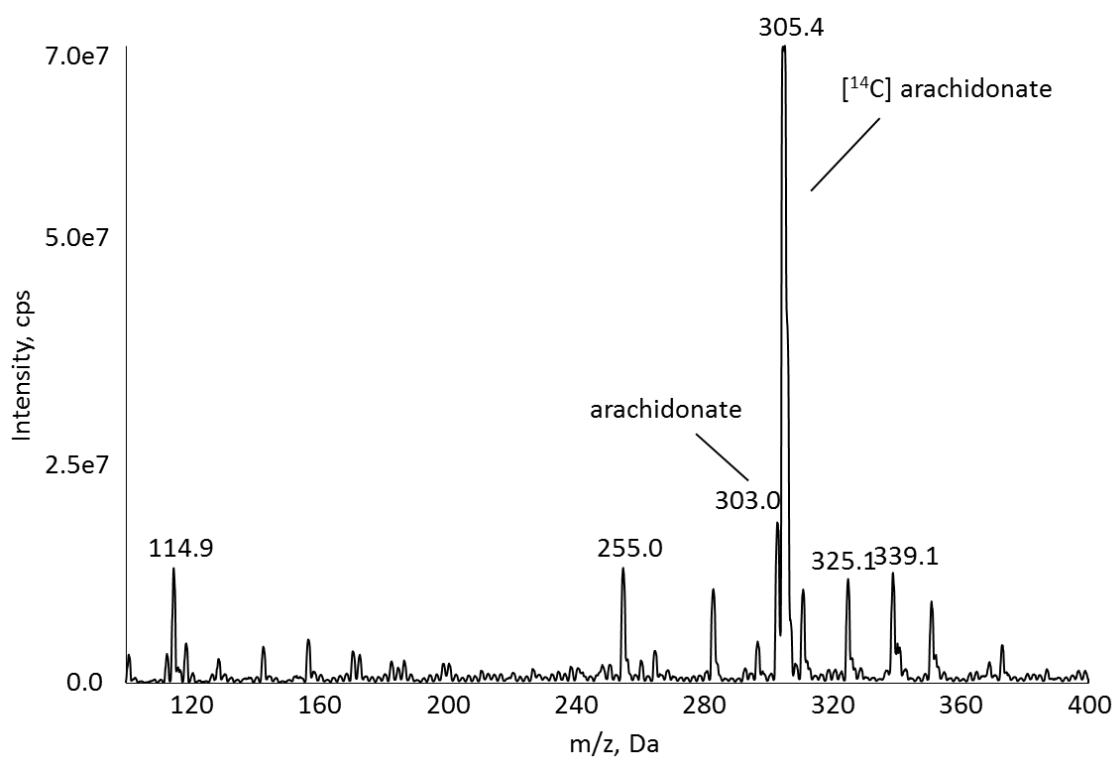
Figure 7.4. The majority of the [¹⁴C]-arachidonate standard is radiolabelled. To determine its radiolabelled content, the standard was analysed using a Q1 scan *m/z* 100 - 400 following direct injection (2.2.7.2).

varying amounts of unlabelled DXA$_3$ (0.01 - 10 ng) and constant PGE$_2$-d4 (100 pg) (Figure 7.5). To shorten analysis times a 30 min chromatography method was employed as described in 2.2.7.4.

7.2.4 HUMAN PLATELETS GENERATE NANOGRAM AMOUNTS OF FREE AND ESTERIFIED DXA$_3$ FOLLOWING THROMBIN ACTIVATION

Next, using the standard curve, I quantified free and esterified DXA$_3$ in human platelets. Free DXA$_3$ was undetectable basally until activation of platelets using thrombin. Following activation DXA$_3$ levels rise rapidly within 10 min of stimulation and increase steadily thereafter up to 2 hrs. This trend is also observed for TXB$_2$, 12-HETE and PGE$_2$ as shown for three representative donors in Figure 7.6. Eicosanoid synthesis was highly variable between genetically unrelated donors (Figure 7.7) with an average of 14.23 ± 3.33 ng DXA$_3$, 60.3 ± 35.57 ng TxB$_2$, 683.55 ± 147.85 ng 12-HETE, and 8.45 ± 2.26 ng PGE$_2$/2 x 10^8 platelets (n = 6 - 10, mean ± SEM) generated at 30 min post thrombin activation. For all donors DXA$_3$ levels generated were greater than those observed for PGE$_2$, but lower than 12-HETE. Interestingly, in two out of seven donors DXA$_3$ levels were greater than TxB$_2$ levels.

To quantify relative levels of esterified vs. free DXA$_3$, lipid extracts from thrombin activated platelets were analysed before and after hydrolysis using snake venom cPLA$_2$ as described in 2.2.1.2, 2.2.1.4 and 2.2.7.4. Simultaneously, the hydrolysis efficiency was calculated to be 83.8 % by monitoring the levels of all four DXA$_3$-PE species remaining after hydrolysis using LC/MS/MS (2.2.7.5).

DXA₃ standard curve
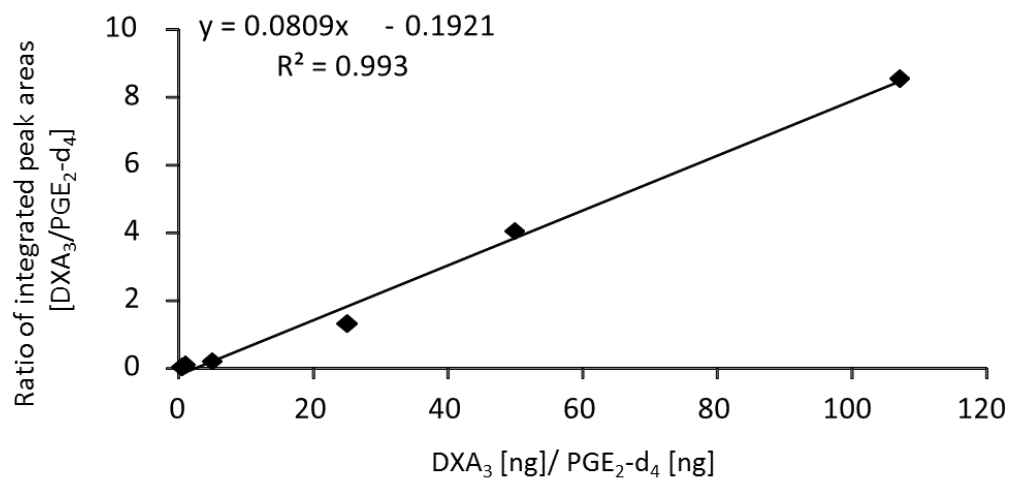
Figure 7.5. DXA₃ standard curve. A standard curve was generated with varying amounts of DXA₃ and integrated peak areas (DXA₃/PGE₂-d₄) plotted.
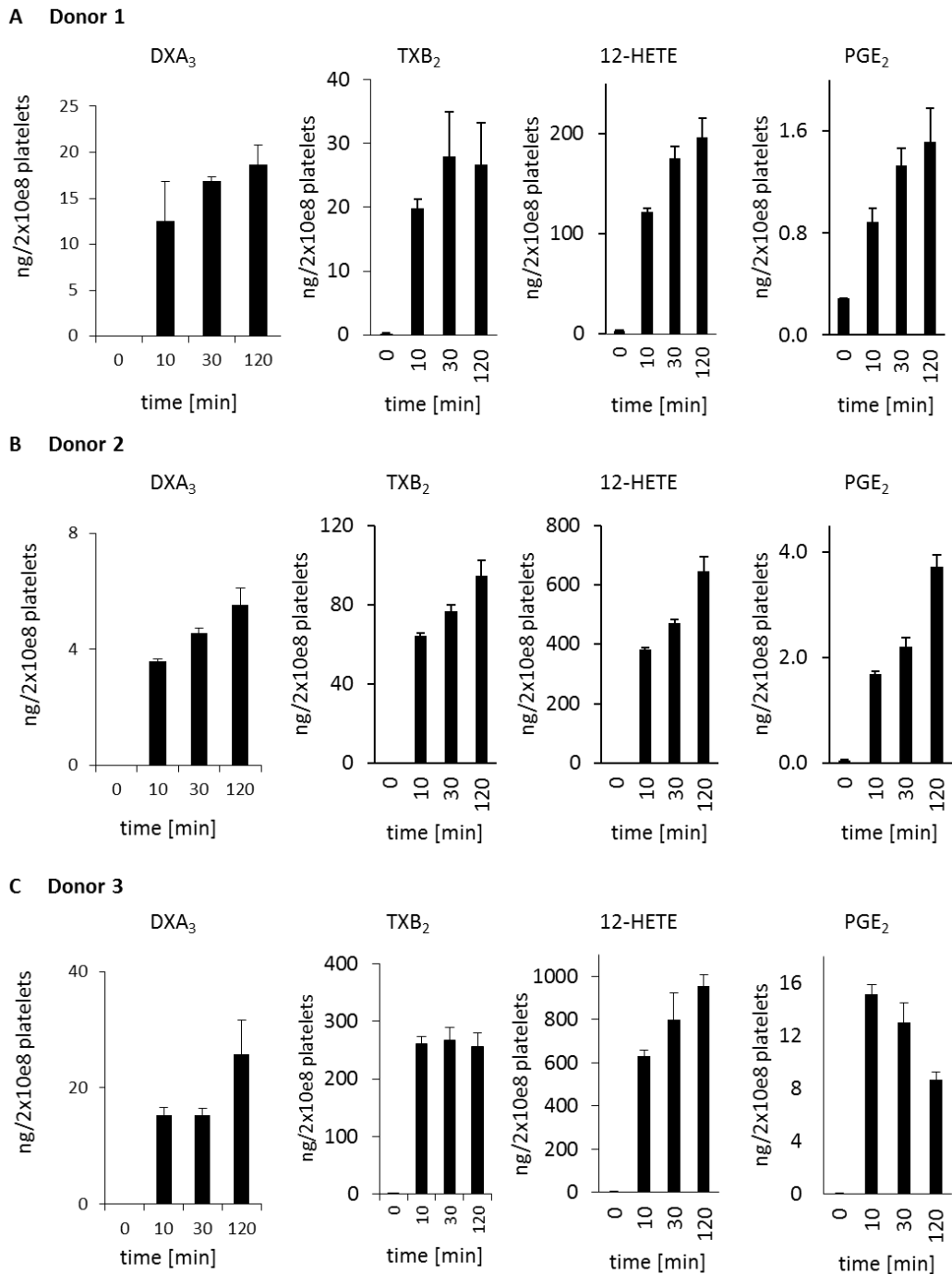
Figure 7.6. DXA₃ is generated in comparable amounts to other eicosanoids by human thrombin activated platelets. Isolated platelets were activated using 0.2 U/ml thrombin for 0, 10, 30 or 120 min and the lipids extracted as described in 2.2.1.1 and 2.2.1.3. DXA₃, TxB₂, 12-HETE and PGE₂ were quantified using LC/MS/MS (Panels A, B and C), (three genetically unrelated donors, triplicates ± SEM). Analysis was undertaken on the 4000 QTrap (ABSciex) using a biogenic DXA₃ standard curve as described in 2.2.7.4.
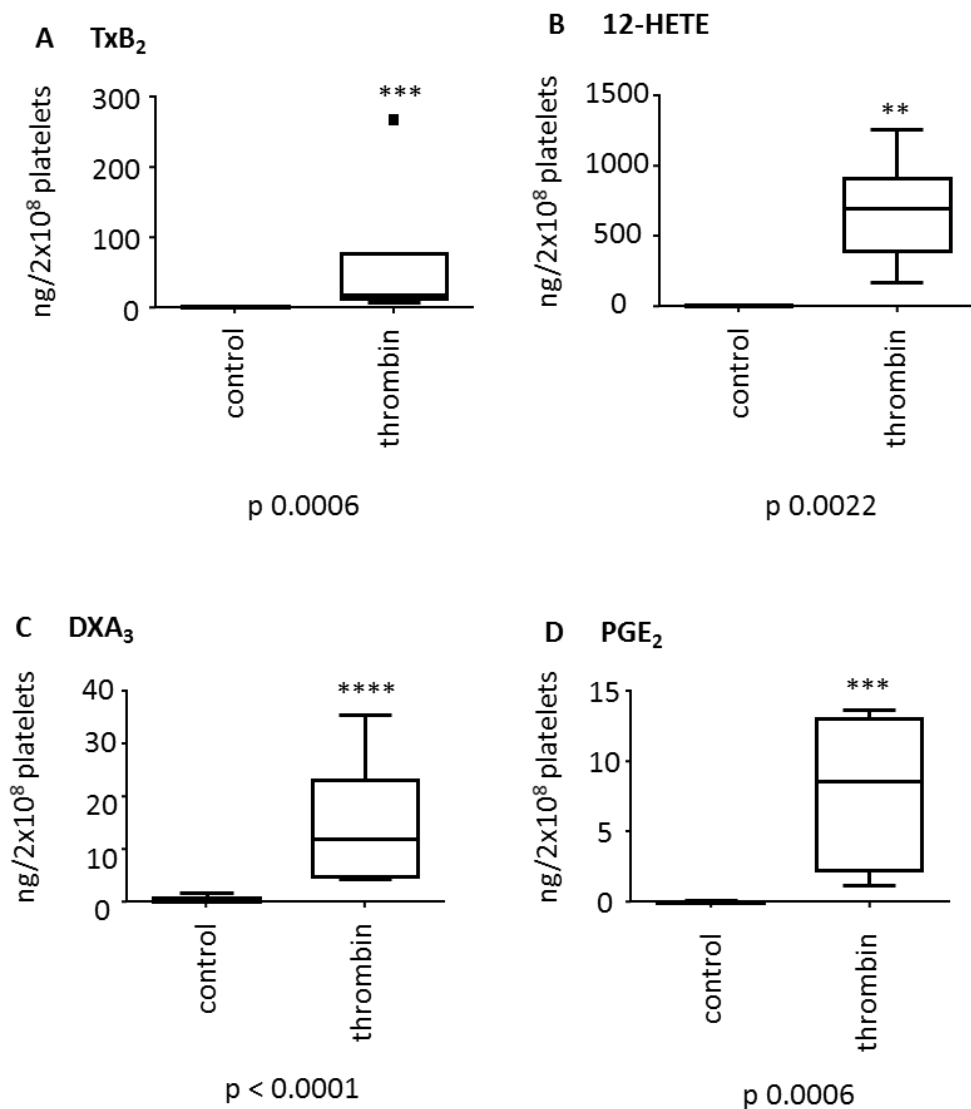
Figure 7.7. Eicosanoid generation by thrombin activated platelets varies between donors. Isolated platelets from healthy donors (n=6 – 10) were activated using 0.2 U/ml thrombin for 30 min and the lipids extracted as described in 2.2.1.1 and 2.2.1.3. (A) TxB$_2$, and (B) 12-HETE, (C) DXA$_3$ and (D) PGE$_2$ were quantified using LC/MS/MS. Genetically unrelated donors ± SEM. One way Anova with Bonferroni post hoc test, **** p≤0.0001, *** p≤0.001. Analysis was undertaken on the 4000 QTrap (ABSciex) using a biogenic DXA$_3$ standard curve as described in 2.2.7.4.

This was used to correct DXA_3 levels measured post-hydrolysis. Before hydrolysis 7.3 ± 2.2 ng DXA_3 / 2 x 10^8 platelets (n = 4, mean ± SEM) was detected. Following hydrolysis a total of 26.5 ± 6.8 ng DXA_3 / 2 x 10^8 platelets was found (Figure 7.8). Taking the hydrolysis efficiency into consideration, 31.6 ± 8.1 ng DXA_3 /2 x 10^8 platelets were calculated to be esterified to PE. This indicates that the majority (77 %) of DXA_3 is present in esterified form in activated human platelets.

7.2.5 MURINE PLATELETS GENERATE DXA_3 FOLLOWING THROMBIN ACTIVATION

Both platelet 12-LOX and COX-1 utilise arachidonate after it is hydrolysed from PL (Holinstat et al. 2011). Therefore, when LOX is inhibited, then more arachidonate could be available for COX turnover. To determine the effect of LOX inhibition on its synthesis by murine platelets, DXA_3, 12-HETE, PGE_2 and TxB_2 were quantified in murine C57BL/6J WT and 12-LOX deficient cells. Isolated murine platelets were activated using 0.2 U/ml thrombin and lipids extracted and analysed using LC/MS/MS as described in 2.2.1.2, 2.2.1.3 and 2.2.7.4. As for human platelets, WT platelets generated higher levels of DXA_3 than PGE_2, but the DXA_3 amounts were lower than that of TxB_2 or 12-HETE (Figure 7.9). 12-LOX deficient platelets generated higher levels of DXA_3, TxB_2 and PGE_2 compared to WT (Figure 7.9, Panels A, C and D). As expected the absence of 12-LOX results in undetectable 12-HETE in these platelets (Figure 7.9, Panel B).
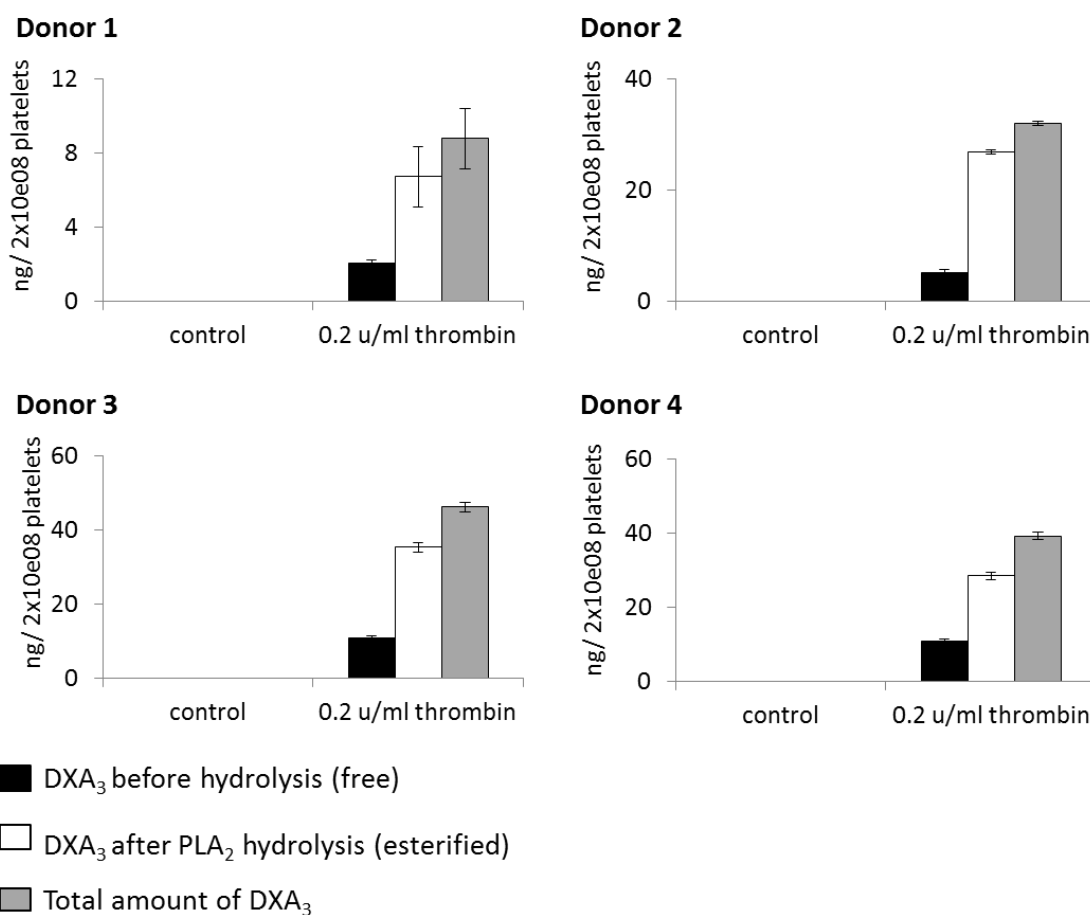
Figure 7.8. Two-thirds of DXA$_3$ are esterified to PE. DXA$_3$ and DXA$_3$-PE were generated by activation of platelets using 0.2 U/ml thrombin as described in 2.2.1.1 and 2.2.1.3. Quantification of free DXA$_3$ was undertaken using LC-MS/MS (2.2.7.4). Free DXA$_3$ generated by platelets was quantified. Following hydrolysis of PLs using snake venom PLA$_2$ (2.2.1.4), free DXA$_3$ was quantified again. Simultaneously, PE was analysed using LC-MS/MS (2.2.7.5) and PE/DMPE ratios used for calculation of hydrolysis efficiency. Shown is the amount of free (black), esterified (white) and total (grey) DXA$_3$ in ng / 2 x 10^8 platelets in four donors, for each donor triplicates, mean ± SEM.
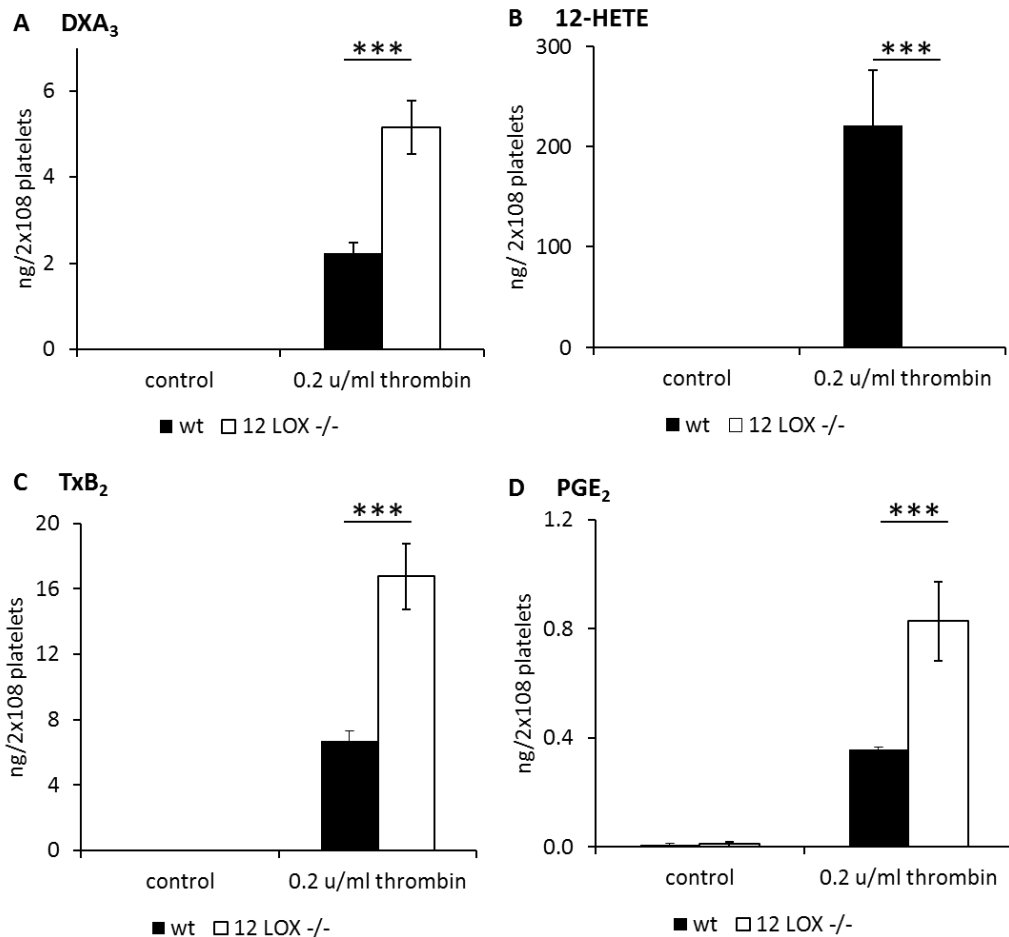
Figure 7.9. Murine platelets generate DXA₃. Isolated platelets from C57BL/6J WT (black) and 12-LOX deficient (white) mice were activated using 0.2 U/ml thrombin as described in. (A) DXA_3, (B) 12-HETE, (C) TxB_2 and (D) PGE_2 were quantified in unactivated (control) or following 30 min thrombin activation. Eicosanoid amounts are shown in ng / 2×10^8 platelets of three WT or 12-LOX deficient mice (n = 3, mean ± SEM), *** $p < 0.005$ using one way ANOVA followed by Bonferroni multiple comparisons test.

7.3 DISCUSSION

In this chapter, I generated DXA_3 standard using COX-1 *in vitro* and quantified free and esterified DXA_3 in human and murine platelets using a standard curve.

When an isotope standard is not available, lipids with similar structure can be employed as ISs, such as PGE_2-d_4 which is used as an IS for DXA_3 throughout this thesis (Ho et al. 2003). PGE_2-d_4 is structurally related to DXA_3, which is not commercially available, and elutes close to DXA_3 in our 30 min LC method. Therefore, my quantification method accounts for ionisation differences as DXA_3 was used as primary standard and possible retention time shifts. However, a disadvantage of this approach is that due to the structural differences that exist between PGE_2-d_4 and DXA_3, it cannot account for differences in extraction efficiency. Therefore, stable isotope labelled DXA_3 would be preferable for quantification, and generation of this will be a future goal.

My assay enabled quantification of DXA_3 in biological samples. The lipid was detected in ng amounts, and was higher than PGE_2 and lower then 12-HETE. Interestingly, greater DXA_3 levels than TxB_2 were observed in two out of seven donors 30 min post thrombin activation. TxB_2 is the stable metabolite of the pro-aggregatory TxA_2, one of the most abundant COX products in platelets (Hamberg et al. 1975). Donor variability in COX products generation by platelets is well known. For example, the generation of 12(S)-hydroxy-5-cis-8,10-trans-heptadecatrienoic acid (12-HHT) is also donor-dependent with levels greater than that of TxB_2 in some individuals (Matsunobu et al. 2013). This natural variation in eicosanoid generation may be due to different expression levels of COX, $cPLA_2$, TxS and also receptor-dependent

signalling proteins in platelets. Both 12-HHT and TxA_2 are physiologically important platelet lipids playing a role in haemostasis and immunity and signal at low nanomolar concentrations (Okuno et al. 2008; Hamberg et al. 1975). Although DXA_3 generation was as variable as that of 12-HHT, its concentration *in vivo*, target receptors and signalling pathways are yet to be identified. This will be further discussed in 8.3 and 9.5.

In 12-LOX deficient platelets the enzymatic pathway of LOX is genetically absent. In theory, this could lead to increased arachidonate levels that would then be available for COX resulting in a higher turnover rate of this enzyme. In agreement with this idea, increased levels of COX products including PGE_2, TxB_2 and DXA_3 were observed along with reduced 12-HETE as shown in Figure 7.8. This also indicates that DXA_3 generation is independent of 12-LOX function.

Our group recently discovered eicosanoid-esterified PLs including DXA_3-PE, PGE_2-PE, 12-HETE-PLs or 14-hydroxydocosahexaenoic acid (HDOHE)-PEs (Morgan et al. 2010; Thomas et al. 2010; Aldrovandi et al. 2013; Aldrovandi et al. unpublished). In contrast to DXA_3, the majority of 12-HETE is generated as a free fatty acid (40 - 60 ng / 2×10^7 platelets) rather than esterified to PLs (5 - 18 ng / 4×10^7 platelets) (Thomas et al. 2010). Similar trends were recently described for PGE_2 (3.8 ng / 2×10^8 platelet) and PGE_2-PE (28 pg / 2×10^8 platelet) (Aldrovandi et al. 2013, and unpublished data). In contrast, I found that 77 % of DXA_3 is formed esterified to PE following thrombin activation. A common characteristic of esterified eicosanoids including DXA_3-PE is their membrane association (Aldrovandi et al. 2013; Aldrovandi et al, unpublished;Thomas et al.2010, Aldrovandi et al. unpublished). Oxidised PLs contain polar groups and can protrude from the membrane surface into the aqueous space

as described for non-enzymatically generated analogues in the "Lipid Whisker Hypothesis" that proposes localisation of oxidised fatty acids attached to PL at the extracellular space (Greenberg et al. 2008). Our proposed DXA_3 structure (Chapter 3) suggests a high polarity of this lipid due its oxygenated functional groups. Thus, DXA_3-PE may protrude from the membrane surface, similar to other non-enzymatically-generated oxidised PL. This may promote interactions with external proteins such as coagulation factors or leukocyte adhesion receptors, which associate with negatively charged surfaces on activated platelet (Hemker et al. 1983).

In conclusion, data presented herein indicate that DXA_3 generation is donor dependent but levels are comparable between murine and human platelets. Together with previous findings, which showed that DXA_3 is generated using endogenous substrate and by platelet following activation with a physiological agonist, my data suggests that DXA_3 is biologically relevant (Aldrovandi, unpublished; Chapter 4, discussed in Chapter 9.5). Thus, to investigate the role of DXA_3 on leukocyte activation, in the next chapter I will determine the effect of this lipid on integrin expression by human neutrophils.

CHAPTER EIGHT

DXA$_3$ INCREASES AND PRIMES THE FMLP RESPONSE ON

MAC-1 EXPRESSION BY NEUTROPHILS

8.1 INTRODUCTION

Neutrophils are one of the first immune cells populations recruited to sites of infection and they play a key role in host defence in innate immunity. Basally, neutrophils patrol the circulation within blood vessels. During early infection they are recruited by activated, adherent platelets, which tether to circulating neutrophils via selectins (Scheme 8.1). This leads to neutrophil activation and integrin expression on their surface resulting in formation of platelet-neutrophil complexes (PNCs). These form via interactions of P-selectin and P-Selectin glycoprotein 1 (PGSL-1), glycoprotein Ibα (GPIbα) and Mac-1 (CD18/CD11b), as well as intracellular adhesion molecule-2 (ICAM-2) and LFA-1 (CD18/CD11a) (Scheme 8.1) (Weber & Springer 1997; Buttrum et al. 1993; Palabrica et al. 1992; Jungi et al. 1986; Hamburger & McEver 1990; Page & Pitchford 2013; Diacovo et al. 1996). In the presence of activated platelets, neutrophil adhesion to endothelial cells is increased *in vitro* and *in vivo* indicating a priming effect of PNCs on neutrophil chemotaxis and the requirement of platelets for firm neutrophil adhesion to the endothelium (Kirschenbaum et al. 2004; Mine et al. 2001; Sreeramkumar et al. 2014). This reveals a pro-inflammatory role of activated platelets. The activated neutrophils can then migrate to the site of infection where they contribute to host defence, for example by producing reactive oxygen species (ROS) to eliminate pathogens (Itoh et al. 2006; Nimeri et al. 2003). Neutrophil recruitment by platelets is mediated by chemokines and cytokines (Cox et al. 2011; Deuel et al. 1981; Deuel et al. 1982; Page & Pitchford 2013). Furthermore, eicosanoids such as 12-HETE, LTB_4 and PGE_2 decrease or increase neutrophil chemotaxis *in vitro* and *in vivo* either
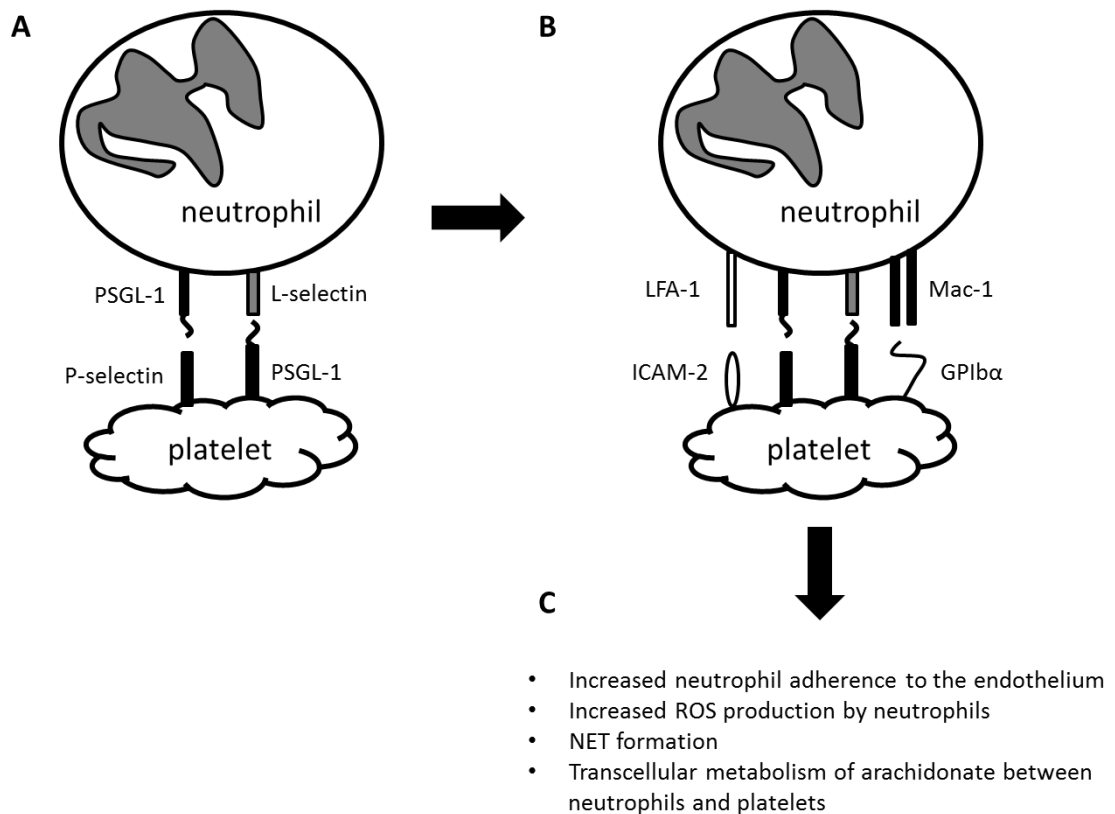
Scheme 8.1. Activated platelets bind to neutrophils forming platelet-neutrophil complexes. (A) Activated platelets tether to circulating neutrophils and bind via selectins. (B) This results in neutrophil activation and expression of integrins leading to the formation of platelet-neutrophil complexes. (C) These interactions enhance other neutrophil functions as shown. Modified from Page & Pitchford 2013.

directly via receptor binding or indirectly by altering the generation of chemoattractant cytokines (Armstrong 1995; Yu & Chadee 1998; Lemos et al. 2009; Gimbrone et al. 1984; Lindbom et al. 1982; Stenson & Parker 1980). However, a role for other COX-derived lipids on neutrophil chemotaxis is not known. Therefore, in this chapter I will investigate the ability of DXA_3 to activate neutrophils. Specifically, I will examine neutrophil Mac-1 expression in response to DXA_3 stimulation using flow cytometry. This integrin is expressed on activated neutrophils and required for firm adhesion to both platelets and endothelial cells, (Issekutz & Issekutz 1992; Osborn 1990; Evangelista et al. 1996; Evangelista et al. 1999).

8.1.1 AIM

- Investigate the ability of DXA_3 to activate human neutrophil Mac-1.

8.2   RESULTS

DXA$_3$ was generated using COX-1 *in vitro* as described in 2.2.2. Neutrophils were isolated from whole blood and treated with either DXA$_3$ alone or in combination with fMLP as described in 2.2.1.6. The cells were stained using an anti-CD11b antibody (2.2.1.7), which recognises the active form of CD11b (Mac-1).

8.2.1   GATING STRATEGY

The gating strategy for this experiment was designed using untreated neutrophils, as shown in Figure 8.1. Isolated neutrophils were stained using anti-human CD11b AlexaFluor647 antibody, and analysed utilizing the CyAn ADP (Beckman). The live neutrophil population was gated, representing 94.8 % of the total cells (Figure 8.1, Panel A). In order to exclude neutrophil aggregates from the analysis, a doublet exclusion gate was applied plotting the FSC-H against FSC-W and the singlets gated as shown (Figure 8.1, Panel B). Using doublet discrimination, 99.5 % of the cells within the neutrophil gate are single cells. The singlets were then plotted as histograms showing Mac-1 fluorescent cells in modal mode (Figure 8.1, Panel C), which scales all channels as a percentage of the maximum count. Gates within the histogram were set as Mac-1 negative (Mac-1 neg) and Mac-1 positive (Mac-1 pos).

.
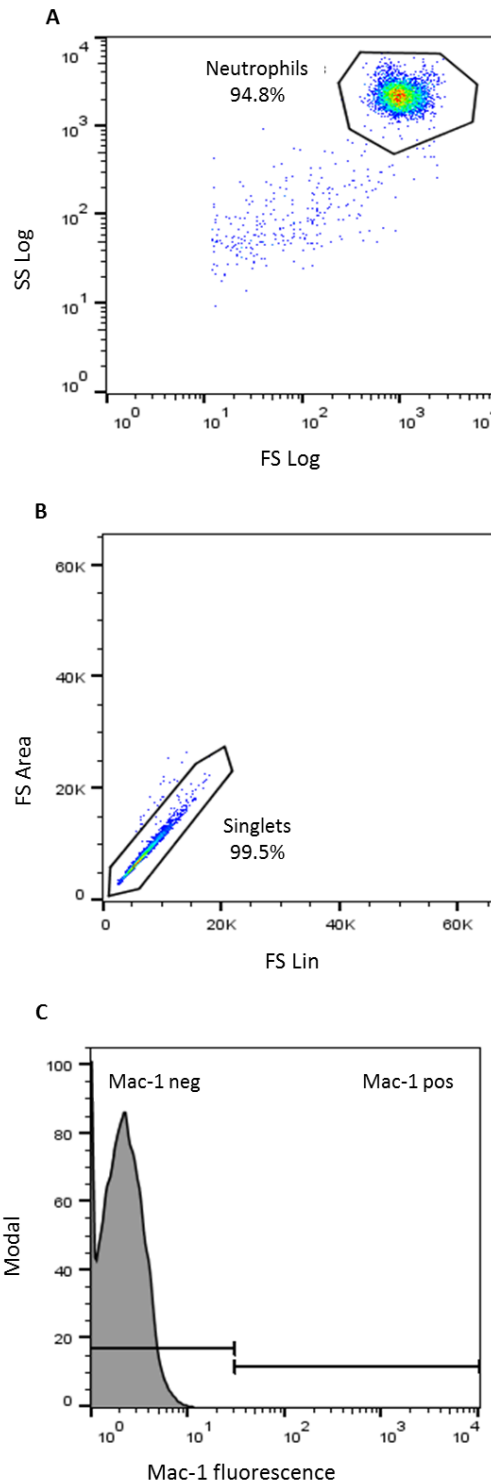
Figure 8.1. Gating strategy for isolated neutrophils. Human neutrophils were isolated from whole blood and stained using anti-human CD11b AlexaFlour647 antibody as described in 2.2.1.6 and 2.2.1.7. (A) Site scatter Log (SS Log) vs Forward Scatter Log (FS Log). 94.8 % of all cells are neutrophils. (B) Neutrophil singlets (99.5 %) were gated using FS Area vs. FS Lin. (C) Histogram of unstained neutrophils. Gates set as Mac-1 negative and positive. Flow cytometric analysis as described in 2.2.10.

8.2.2 DXA$_3$ INCREASES MAC-1 EXPRESSION BY NEUTROPHILS

Human neutrophils were incubated with 10 μM DXA$_3$ or vehicle control and / or 10 μM fMLP as described in 2.2.1.6 and 2.2.1.7.

Basally approximately 12 % of neutrophils were positive for Mac-1 (Figure 8.2, Panel E, untreated). This increased significantly to 35 % following fMLP (Figure 8.2, Panels A and E) and 25 % following DXA$_3$ treatment (Figure 8.2, Panels B and E). To investigate the effect of DXA$_3$ upon the fMLP response, neutrophils were incubated with vehicle or 10 nM DXA$_3$ 10 min prior to fMLP. Treatment with vehicle control also enhanced the proportion of Mac-1 positive neutrophils (Figure 8.2, Panels C and E). However, treatment of neutrophils with DXA$_3$ before fMLP significantly increased the proportion of Mac-1 positive neutrophils to 42 % compared to vehicle control (Figure 8.2, Panels C, D and E).

8.2.3 DXA$_3$ PRIMES NEUTROPHIL RESPONSES TO FMLP

To test whether DXA$_3$ has a priming effect, isolated neutrophils were treated with 1 - 10 nM DXA$_3$ alone or prior to fMLP as described in 2.2.1.6 and 2.2.1.7. These concentrations of DXA$_3$ alone did not increase Mac-1 expression (data not shown). When neutrophils were treated with 1 or 5 nM DXA$_3$ prior to fMLP no difference in Mac-1 expression was observed compared to vehicle control (Figure 8.3, Panels A and B). In contrast, 10 nM DXA$_3$ prior to fMLP increased Mac-1 expression demonstrating a priming effect upon the fMLP response (Figure 8.3).
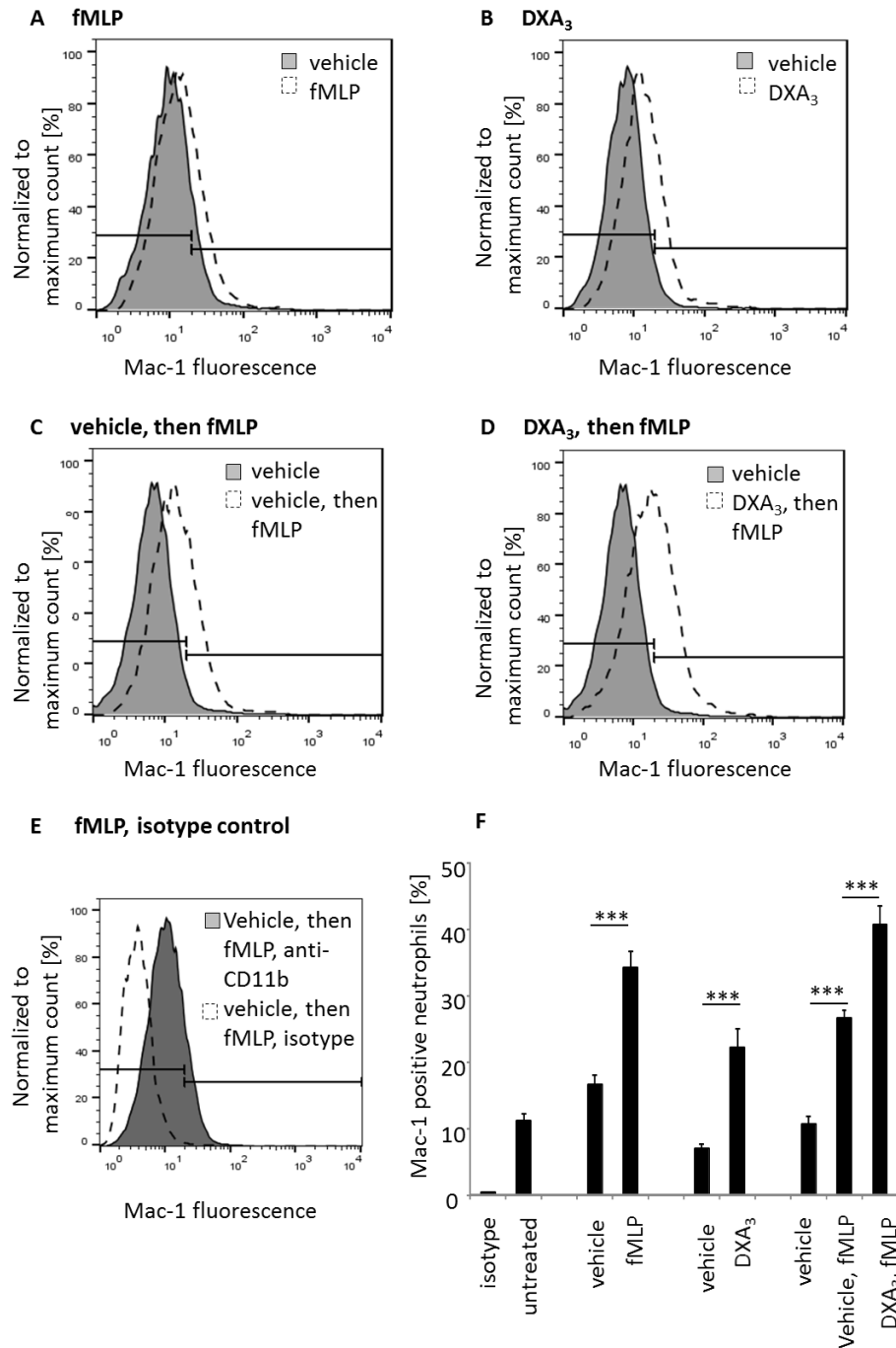
Figure 8.2. 10 μM DXA₃ increases Mac-1 expression by neutrophils. Isolated human neutrophils were treated with 10 μM DXA₃ and / or 10 μM fMLP as described in 2.2.1.6 and 2.2.1.7. Histograms of neutrophils following treatment with (A) 10 μM fMLP, (B) 10 μM DXA₃, (C) vehicle and 10 μM fMLP and (D) 10 μM DXA₃, then 10 μM fMLP. Treatments (scattered) compared to controls (grey). (E) Vehicle and 10 μM fMLP, isotype control (scattered) compared to anti-CD11b (grey). One donor shown as representative of three. Counts normalized to the maximum count. Gates set on the vehicle control. Flow cytometric analysis as described in 2.2.10. (F) Mac-1 positive neutrophils (%) following 10 μM fMLP, 10 μM DXA₃ or 10 μM DXA₃ prior to 10 μM fMLP. n = 3, three genetically unrelated donors (mean ± SEM). *** $p < 0.005$, using one way ANOVA followed by Bonferroni multiple comparisons test.
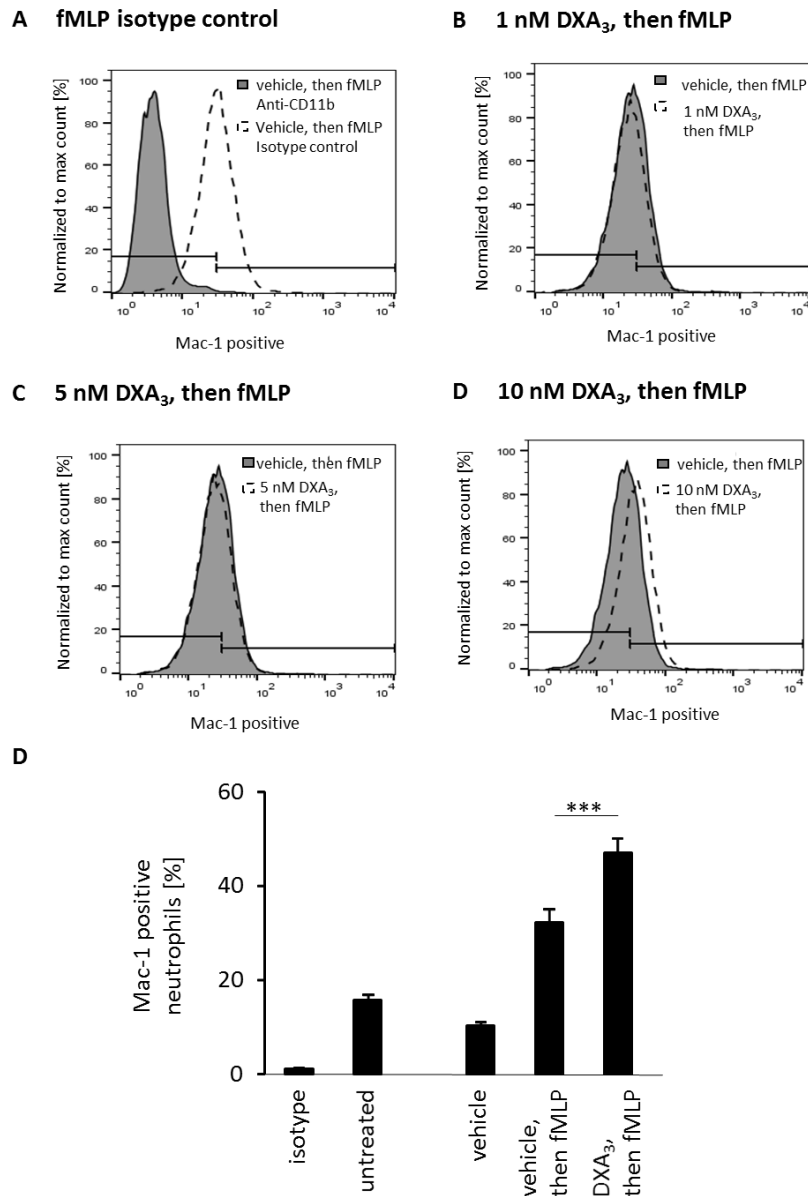
Figure 8.3. 10 nM DXA₃ primes fMLP activation of human neutrophils. Isolated neutrophils were incubated with varying concentrations of DXA_3 and 10 µM fMLP and analysed using flow cytometry as described in 2.2.1.6, 2.2.1.7 and 2.2.10 (A) Histogram of vehicle and fMLP treated neutrophils stained with either anti-CD11b antibody or isotype control. (C-D) Histograms showing Mac-1 positive human isolated neutrophils following treatment with 1 - 10 nM DXA_3 prior to 10 µM fMLP. For all panels vehicle control and fMLP (grey) vs. DXA_3 and fMLP (scattered). A representative donor is shown of three independent experiments. Histograms were normalized to the maximum count. Gates set on the vehicle control. Flow cytometric analysis as described in 2.2.10. (B) Percentage of Mac-1 positive neutrophils following treatment with vehicle or 10 nM DXA_3 prior to 10 µM fMLP. n = 3, genetically unrelated donors (mean ± SEM). *** p < 0.005, using one way ANOVA followed by Bonferroni multiple comparisons test.

8.3   DISCUSSION

In this chapter I demonstrated that DXA_3 promotes Mac-1 expression on human neutrophils. DXA_3 was generated using arachidonate oxidation by COX-1 *in vitro* yielding a total of 5 µg. Thus, functional studies were limited due to the very low DXA_3 amounts available.

Eicosanoids are known to exert diverse effects upon neutrophils. For example, LTB_4 or 5-oxo EET signal via BLT1, BLT2 or the OXO receptor mediating Mac-1 expression on neutrophils associated with neutrophil adhesion to the endothelium and therefore chemotaxis (Crooks & Stockley 1998; Tager & Luster 2003; Powell & Rokach, 2005; Grant et al. 2009; Futosi et al. 2013). PGE_2 affects several neutrophil functions via interactions with EP receptors expressed on the neutrophil surface such as inhibition of neutrophil chemotaxis via the EP2 receptor (Yamane et al. 2000; Armstrong 1995). It also mediates IL-23/IL-17-induced neutrophil migration by inhibiting IL-12 and IFNα generation in a murine model of rheumatoid arthritis suggesting distinct roles in health and disease (Lemos et al. 2009). In addition, PGE_2 inhibits superoxide generation, LTB_4 release, TNFα production, and fMLP-induced aggregation but enhances IL-6 generation by neutrophils (Wise & Jones 1994; Wise 1996; Wise 1998; Wheeldon & Vardey 1993; Talpain et al. 1995; Yamane et al. 2000). In this chapter, I demonstrated that DXA_3 increases Mac-1 expression suggesting that this lipid regulates neutrophil functions. Therefore, DXA_3 may mediate additional functions including ROS and NET formation, chemotaxis or chemokine production but this warrants further investigation. In addition, the signalling pathway and target receptor for DXA_3 leading to Mac-1 expression is currently unknown. In order to aid

determination of whether DXA_3 acts via receptor-dependent mechanisms, the concentration used herein can be compared to concentrations (Kd and EC50 or IC50 values) of other eicosanoids required to mediate similar bioactivities in neutrophils. For example, LTB_4 binds with high affinity to BLT1 (Kd = 0.39-1.5 nM) and low affinity to BLT2 (Kd = 22.7 nM) (Tager & Luster 2003). The latter is also a low affinity receptor for 12-HETE but and a high affinity one for 12-HHT (IC50 2.8 nM) (Okuno et al. 2008). Therefore, the DXA_3 concentration used herein (10 nM) is similar to that which is bioactive for other eicosanoids supporting the idea that it could regulate neutrophil function *in vivo*. It is possible that DXA_3 upregulates Mac-1 in neutrophils via a known receptor such as BLT1 or BLT2 (Futosi et al. 2013). This could be determined by pharmacological studies using receptor antagonists such as U-75302 (BLT-1) orLY255283 (BLT2) in combination with DXA_3.

Data presented herein demonstrated a priming effect of DXA_3 upon the fMLP response. This finding suggests that DXA_3 is an endogenous lipid mediator that alters the inflammatory response of neutrophils to exogenous stimuli.

In conclusion, DXA_3 increases Mac-1 expression at physiological concentrations, and thus, may promote the formation of PNCs and support neutrophil adhesion to the endothelium. However, further studies are necessary to identify target receptors, to understand the signalling pathway and to further investigate the effect of DXA_3 upon neutrophil function.

CHAPTER NINE

GENERAL DISCUSSION

In this thesis, I investigated the structure, enzymatic generation and biological actions of a novel COX product, which we termed DXA_3. Structural elucidation demonstrated a unique structure for this lipid (Chapter 3), which is generated by COX-1 in activated platelets via an enzymatic pathway proposed to be distinct from other prostanoids (Chapters 4, 5 and 6). To directly quantify DXA_3 generated by human and murine platelets in response to activation, a quantitative assay was developed which demonstrated that levels generated are comparable to other eicosanoids (Chapter 7). These lipids are important players in haemostasis and inflammation (Smith & Murphy 2002; Fahy 2005; Richardson et al. 2005; Semple et al. 2011; Giuliano & Warner 2002; Barrios-Rodiles et al. 1999; Caivano & Cohen 2000; Weller et al. 2007; Yu & Chadee 1998; Harris et al. 2002). Therefore, the ability of DXA_3 to activate neutrophils was determined and showed that this lipid increases integrin expression on human neutrophils. This suggests a potential role in promoting early innate immune responses (Chapter 8).

9.1   STRUCTURAL CHARACTERISATION

Mass spectrometry represents an essential analytical tool in lipid research. Whilst GC/MS enabled the discovery of the first volatile eicosanoids during the 1960's, the development of LC/MS during the 1980's revolutionised the field of lipid biology (Hamberg & Samulsson 1967; Hamberg et al. 1975; Hamberg & Samuelsson 1967). Today the greater mass accuracy and sensitivity that LC/MS provides and the constant evolution of MS techniques including ionisation and precursor scanning has allowed the identification and structural characterisation of hundreds of non-volatile

lipids, including phospholipid-esterified eicosanoids and related lipids such as protectins and resolvins (Hong et al. 2007; Masoodi et al. 2008; Serhan et al. 2002; Schwab et al. 2007; Thomas et al. 2010; Maskrey et al. 2007; Morgan et al. 2009; Aldrovandi et al. 2013; O'Donnell et al. 2014; Murphy & Gaskell 2011; Perry et al. 2008). Using extensive GC and LC/MS analysis, I proposed a covalent structure for DXA_3 as described in Chapter 3. However, as LC/MS is unable to distinguish between enantiomeric structures, other techniques such as NMR will be required to fully characterise the stereochemistry of DXA_3. Teder and colleagues recently used a similar multi-technique approach successfully for the structural elucidation of LOX-derived dioxolanes (Teder et al. 2014). Preliminary LC-UV spectral data demonstrates a λmax at 238 nm, indicating the presence of conjugated dienes. This is comparable to the UV spectrum of a structurally similar dioxolane generated by purified LOX, and further supports the proposed structure (Teder et al 2014). To further determine the stereochemistry of this lipid, NMR studies are in progress in collaboration with Dr. Andy Watson (Bristol University, UK). However, NMR analysis requires µg to mg amounts of lipids; therefore, full characterisation is extremely challenging due to the current limited availability of DXA_3.

Levels of DXA_3 generated by platelets are in the low ng range. Thus, in collaboration with Dr. Larry Marnett (Vanderbilt University, USA) I sought to establish an *in vitro* approach to generate greater quantities. Using ovine COX-1 isolated from seminal vesicles I was able to generate 5 µg of lipid. Whilst this was sufficient for the structural and functional data presented herein, to achieve full NMR analysis, high yield pure DXA_3 is required. In association with Cayman Chemicals (Ann Arbor) and Prof. Alan Brash (Vanderbilt University, TN, USA) we are attempting to produce DXA_3

enzymatically through the oxidation of 8, 9-EET by coral 8-LOX, which generates other dioxolanes from EETs (Teder et al. 2014). To maximize the likelihood of generating high-yield pure DXA$_3$ we are also setting up a total synthesis approach in collaboration with Dr. Andy Watson and Prof. Varinder Aggarwal (Bristol University). Whilst these studies are challenging, the efficient and reproducible generation of a pure DXA$_3$ standard would greatly enhance our ability to characterise its stereochemistry and biological functions.

9.2   DIOXOLANES AS NOVEL LIPID MEDIATORS

Arachidonate-derived dioxolanes were first discovered as products of cholesteryl arachidonate oxidation *in vitro* (Havrilla et al. 2000). However, to date no biological roles have been ascribed to these unusual lipids. A recent study by Teder et al. (2014) demonstrated that dioxolanes could be enzymatically generated via LOX *in vitro* but their formation in cells was not shown. Therefore, DXA$_3$ represents the first dioxolane reported to be generated by both enzymatic and non-enzymatic arachidonate oxidation *in vitro* and in cells. In contrast to COX-1 and 11-HpETE oxidation where three isomers were generated, DXA$_3$ is formed as a single isomer in platelets (4.2.4). In addition, the serial cyclic products observed by Havrilla et al. which contain more than one dioxolane ring, and are formed as additional oxidation products *in vitro* (Scheme 1.5), were not observed to be generated by platelets or COX *in vitro* (data not shown). This suggests a controlled generation of DXA$_3$ by agonist activated platelets, whereby it is formed enzymatically and is consistent with our idea that DXA$_3$ may play signaling physiological roles in innate immunity. Thus,

further studies are now required to investigate the generation and biological significance of this and other members of this lipid class during inflammation and innate immunity in cells and *in vivo* (Teder et al., 2014).

9.3 ENZYMOLOGY OF DXA$_3$ GENERATION

Oxidation of arachidonate by COXs yields predominantly PGH$_2$, whilst 11- and 15-HETE are generated as side products via radical escape from the catalytic site (Marnett 2000; Harman et al. 2004; Thuresson et al. 2000). My studies suggest that DXA$_3$ formation also includes a radical escape. However, my proposed mechanistic pathway is different to other COX products (5.2.2). I also demonstrated that DXA$_3$ generation requires peroxidase turnover (5.2.3). This may be mediated by a DXA$_3$ specific enzyme or by COX peroxidase itself. This is consistent with other prostanoids, which require specific synthases such as TxS downstream of COX, and requires further study to determine the enzymes that may be involved.

Herein, I proposed a mechanism for COX -mediated dioxolane formation (Chapter 5). Teder and colleagues (2014) also described dioxolane generation via a mechanism in which P450-derived EETs are oxidised by LOX. Together, these studies change our current understanding of enzymatic eicosanoid generation and will stimulate further investigations into the enzymatic mechanism of dioxolane synthesis both in cells and *in vitro*.

COX inhibition by NSAIDs is globally used to prevent cardiovascular events and dampen inflammation. Additionally, COX-1 selective NSAIDs plays an emerging role in the prevention of cancer metastasis (Rothwell et al. 2012; Algra & Rothwell 2012;

Rothwell et al. 2012). Therefore, determining both the enzymology of DXA_3 generation and its biological function could be of major future pharmacological interest.

9.4   Tissue distribution of DXA_3

Eicosanoids represent a large group of bioactive lipids generated by a variety of cells and tissues. Their synthesis is catalysed by several enzymes including PLA_2s, COXs, LOXs, as well as specific synthases such as TxS and PGIS (Smith & Murphy 2002; Hecker & Ullrich 1989; Naraba et al. 1998; Tramposch et al. 1994). Numerous studies have shown that eicosanoid generation is cell type dependent as it is regulated by the co-expression and (in)activation of their synthetising enzymes. Their synthesis is also controlled by the activating stimuli (Bos et al. 2004; Caughey et al. 2001; Ueno et al. 2001). For example, stimulation of rat peritoneal macrophages with A23187, a non-specific stimulant resulting in increased intracellular calcium levels, leads to preferential generation of TxB_2 vs. PGE_2. This is due to coupling of $cPLA_2$, COX-1, and TxS. In contrast, LPS stimulation, which increases COX-2 expression, of these cells predominantly results in PGE_2 synthesis via $cPLA_2$, COX-2, and PGES (Naraba et al. 1998; Matsumoto et al. 1997). Preliminary results showed that a mixed population of calcium ionophore A23187 activated leukocytes did not generate DXA_3 but PGE_2 (data not shown) suggesting that its synthesis could be similarly controlled. To further determine this, future studies could investigate its synthesis by individual leukocyte populations following treatment using a series of reagents such as cytokines or TLR agonists. A stimulus specific synthesis of DXA_3 would provide

insights into the signalling pathway that leads to generation of this lipid. As levels of certain eicosanoids are elevated during biological events, such as PGE_2 during inflammation and TxA_2 during haemostasis, identifying cells that synthesise DXA_3 and stimuli that activate its generation would help to determine when its synthesis may be biologically relevant (Kurland & Bockman 1978; Yu & Heinen et al. 1986; Chadee 1998; Nakayama et al. 2006; Wang & Lau 2006; Hamberg et al. 1975).

9.5 DXA_3 QUANTIFICATION

In order to determine whether sufficient levels of DXA_3 are generated to trigger receptor-dependent signaling, the lipid needs to be quantified and compared to other known lipid mediators. Different approaches can be used for this, including either calculated estimation or direct lipid quantification. Calculated estimation is based either on the amount of initial substrate used or on the detection of the total products generated (Podrez et al. 2002). However, this approach is less precise than direct quantification. Fatty acids can be directly quantified either as esterified methyl esters (FAME) using GC/MS or as free fatty acids using UV or LC/MS/MS (Dodds et al. 2005; Le Faouder et al. 2013; Guarrasi et al. 2010; Carvalho et al. 2012). However, the limitation of these approaches is that they require pure lipid standards, which are not yet commercially available for DXA_3. Alternatively, radiolabeled standards can be utilised which are synthesised *de novo* (Dreon et al. 2002; Nare et al. 1999; Rapoport 2005; Ho et al. 2016). Based on this approach I developed a quantification assay using $[^{14}C]$-DXA_3 derived from oxidation of $[^{14}C]$-arachidonate by COX-1 (Chapter 7). Although this enabled the quantification of DXA_3 in biological samples,

it has minor limitations in its accuracy due to PGE_2-d_4 being used as an IS. Therefore, once DXA_3 and its stable isotope analogue are synthetised, a new standard curve will be generated allowing a greater accuracy of quantification.

Herein, I demonstrated that agonist activated platelets generate 14.23 ± 3.33 ng DXA_3 / 2×10^8 platelets (n = 10 $\pm$ SEM, Chapter 7). As this is the average cell number per ml blood, it would in theory equal to 0.04 nmol DXA_3/ml blood, if all the platelets were activated, and is equivalent to an approximate concentration of 40.4 nM (Thon et al. 2012). Although this concentration remains theoretical, it allows comparison with concentrations of other eicosanoids known to be required for receptor signaling. TxA_2 mimetics and 12-HETE mediate their signaling functions, such as platelet activation and neutrophil chemotaxis with receptor dependent affinities (ranging between low-high nanomolar concentrations) (Hamberg et al. 1975; Ko et al. 1995; Burch et al. 1985; Dorn et al. 1997; Armstrong et al. 1993; Paul et al. 1999; Ohkubo et al. 1996; Goetzl et al. 1980; Reynaud & Pace-Asciak 1997; Guo et al. 2011; Herbertsson et al. 1999). In addition, 12-HHT activates the leukotriene receptor BLT2, expressed by neutrophils, at an IC50 of 2.8 nM (Okuno et al. 2008; Matsunobu et al. 2013). This suggests that DXA_3 will be generated at sufficient concentrations to mediate receptor-dependent signaling *in vivo*.

Eicosanoid esterified PLs can be indirectly quantified using LC/MS/MS (Morgan et al. 2009; Aldrovandi et al. 2013; Maskrey et al. 2007; A. H. Morgan et al. 2010). For this, the fatty acid, which is esterified to the PL, is hydrolysed from the lipid and subsequently quantified (Morgan et al. 2009; Aldrovandi et al. 2013; Maskrey et al. 2007). For example, PGE_2-PE levels generated by activated platelets were determined by quantification of PGE_2 before and after lipid hydrolysis using snake

venom cPLA$_2$ (Aldrovandi et al. 2013). An identical approach was used herein to quantify DXA$_3$-PE. To increase accuracy, future experiments could include *de novo* synthesis of deuterated DXA$_3$-PE as a standard. This may be generated via esterification of deuterated DXA$_3$ into lyso-PE using rat liver microsomes, which contain a set of enzymes involved in fatty acid metabolism including long chain fatty acyl-CoA synthetase (LC-FACS) and lysophospholipid acytransferase (LPAT), as shown for arachidonate-*d8* esterified to PE (Shindou et al. 2013; Suzuki et al. 1990; Aldrovandi, PhD thesis, 2013). However, as a pure deuterated DXA$_3$ standard is yet to be synthesised, this would be part of further studies.

9.6 NEUTROPHIL ACTIVATION

Prostanoids play important roles in inflammation and haemostasis (Smith & Murphy 2002; Fahy 2005; Richardson et al. 2005; Semple et al. 2011; Giuliano & Warner 2002; Barrios-Rodiles et al. 1999; Caivano & Cohen 2000; Weller et al. 2007; Yu & Chadee 1998; Harris et al. 2002). To investigate their biological effects, pure lipid standards are required. These enable functional assays to be undertaken, either on isolated cells and tissues *in vitro* or *in vivo*. Although arachidonate oxidation by COX-1 *in vitro* was used to yield higher amounts of DXA$_3$ than generated by platelets, the overall quantity synthesised was too low to enable a full functional characterisation of the role of the lipid *in vivo.*

Herein, I investigated the effect of DXA$_3$ on leukocyte activation by determining the ability of DXA$_3$ to upregulate integrin expression by neutrophils (Chapter 8). This is a major event in response to activation of leukocytes and is required for the formation

of PNCs and neutrophil adhesion to the endothelium (Page & Pitchford 2013). Specifically, upon activation, neutrophils express the intergrin Mac-1 (CD11b/CD18), which is responsible for their binding to both platelet and endothelial cells (Pitchford et al. 2005; Kirton & Nash 2000; Konstantopoulos et al. 1998; Evangelista et al. 1996). In my studies, I found that DXA$_3$ stimulates and primes Mac-1 expression by neutrophils *in vitro* (8.2.2 and 8.2.3). Further studies are warranted to determine whether DXA$_3$ only increases Mac-1 expression, or if it mediates a similar effect upon other integrin family members such as PSGL-1 (Moore et al. 1995; Xiao et al. 2006; Schmidtke & Diamond 2000).

DXA$_3$ was found to be generated by activated platelets (Aldrovandi, unpublished; Chapter 4). These can recruit and activate neutrophils at a site of injury leading to increases in neutrophil adhesion to the endothelium, transendothelial migration, NET formation and ROS production (Dole et al. 2012; Singbartl et al. 2001; Miedzobrodzki et al. 2008; Suzuki et al. 2001; Caudrillier et al. 2012; Clark et al. 2007; Lam et al. 2011; Carestia et al. 2016). The aforementioned studies identified that platelet surface receptors such as TLR4 or P-selectin play a role in these activities. However, the involvement of eicosanoids in platelet-neutrophil interactions remains poorly understood. NET formation and ROS production are activated by free and esterified 5-HETE (Clark et al. 2011). However, effects of COX products on neutrophil functions are unknown. Since DXA$_3$ activates integrin expression, it may also mediate further neutrophil functions, which could be investigated in future studies. For example, the ability of DXA$_3$ to modulate neutrophil migration could be examined by determining the expression of adhesion molecules such as JAM-A and PECAM-1 (Woodfin et al. 2007; Ostermann et al. 2002).

The formation of PNCs is thought to be a key event in inflammation, with platelets promoting neutrophil adhesion and migration. These interactions also have been observed in atherosclerosis, asthma, various bacterial infections, sepsis and sickle cell disease (Ott et al. 1996; Pamuk et al. 2006; Asaduzzaman et al. 2009; Pitchford et al. 2003; Zarbock et al. 2006; Gawaz et al. 1995; Polanowska-Grabowska et al. 2010; Langer et al. 2012; Setianto et al. 2010; Johansson et al. 2011, Sreeramkumar et al. 2014, Lievens et al. 2010). Thus, determining the role that DXA_3 may play in chronic diseases warrants further study. This could include *in vivo* studies to examine the effect of DXA_3 on leukocyte recruitment in murine models of inflammatory disease such as atherosclerosis and infection.

In pilot studies not presented herein, I examined the ability of DXA_3 to activate platelets. Preliminary data suggested that it can increase P-selectin expression (data not shown). However, due to the low amounts of DXA_3 available, these studies could not be repeated. Consequently, once synthetic DXA_3 is available, future work will include investigating the role of DXA_3 in platelet activation and aggregation.

It is important to investigate both the effects of DXA_3 on receptor expression and its signalling via target receptors. Therefore, once sufficient lipid is available, pharmacological studies will investigate whether DXA_3 signals via known eicosanoid receptors such as for BLT2, which is known to be activated by eicosanoids including LTB_4, 12- and 15-HETE, 12-HpETE, and 12-HHT (Tager & Luster 2003; Yokomizo et al. 2001; Toshiaki Okuno et al. 2008; Okuno et al. 2015; Matsunobu et al. 2013).

9.7   Summary

To summarise, I have demonstrated that DXA_3 is a new COX-derived lipid of likely physiological importance. Due to its activation of integrin expression on neutrophils,

I propose that DXA_3 potentially facilitates pro-inflammatory signaling *in vivo*. This will be followed up in future studies on its generation and role in inflammatory vascular disorders such as atherosclerosis. In particular, if DXA_3 is a pro-inflammatory eicosanoid, then it could represent a potential therapeutic target for chronic inflammatory disease.

CHAPTER TEN

BIBLIOGRAPHY

Abramovitz, M., Boie, Y., Nguyen, T., Rushmore, T.H., Bayne, M. a., Metters, K.M., Slipetz, D.M. & Grygorczyk, R., 1994. Cloning and expression of a cDNA for the human prostanoid FP receptor. *Journal of Biological Chemistry*, 269(4), pp.2632–2636.

Aldrovandi, M., Hammond, V.J., Podmore, H., Hornshaw, M., Clark, S.R., Marnett, L.J., Slatter, D. a, Murphy, R.C., Collins, P.W. & O'Donnell, V.B., 2013. Human platelets generate phospholipid-esterified prostaglandins via cyclooxygenase-1 that are inhibited by low dose aspirin supplementation. *Journal of lipid research*, 54(11), pp.3085–97.

Algra, A.M. & Rothwell, P.M., 2012. Effects of regular aspirin on long-term cancer incidence and metastasis: a systematic comparison of evidence from observational studies versus randomised trials. *The Lancet Oncology*, 13(5), pp.518–527.

Andonegui, G., Kerfoot, S., McNagny, K., Ebbert, K., Patel, K. & Kubes, P., 2005. Platelets express functional toll-like receptor-4 (TLR4). *Blood*, 106(7), pp.2417–2423.

Antithrombotic Trialists' (ATT) Collaboration, 2009. Aspirin in the primary and secondary prevention of vascular disease: collaborative meta-analysis of individual participant data from randomised trials. *The Lancet*, 373(9678), pp.1849–1860.

Armstrong, R. a, 1995. Investigation of the inhibitory effects of PGE2 and selective EP agonists on chemotaxis of human neutrophils. *British journal of pharmacology*, 116(7), pp.2903–2908.

Armstrong, R.A., Humphrey, P.P. & Lumley, P., 1993. Characteristics of the binding of [3H]-GR32191 to the thromboxane (TP-) receptor of human platelets. *Br J Pharmacol*, 110(2), pp.539–47.

Asaduzzaman, M., Lavasani, S., Rahman, M., Zhang, S., Braun, O.O., Jeppsson, B. & Thorlacius, H., 2009. Platelets support pulmonary recruitment of neutrophils in abdominal sepsis. *Critical care medicine*, 37(4), pp.1389–1396.

Aslam, R., Speck, E.R., Kim, M., Crow, A.R., Bang, K.W., Nestel, F.P., Ni, H., Lazarus, A.H., Freedman, J. & Semple, J.W., 2006. Platelet Toll-like receptor expression modulates lipopolysaccharide-induced thrombocytopenia and tumor necrosis factor-alpha production in vivo. *Blood*, 107(2), pp.637–641.

Awtry, E. & Loscalzo, J., 2000. Cardiovascular drugs. Aspirin. *Circulation*, 101, pp.1206–1218.

Badimon, L. & Vilahur, G., 2014. Thrombosis formation on atherosclerotic lesions and plaque rupture. *Journal of Internal Medicine*, 276(6), pp.618–632.

Baker, C.S., Hall, R.J., Evans, T.J., Pomerance, A., Maclouf, J., Creminon, C., Yacoub, M.H. &

Polak, J.M., 1999. Cyclooxygenase-2 is widely expressed in atherosclerotic lesions affecting native and transplanted human coronary arteries and colocalizes with inducible nitric oxide synthase and nitrotyrosine particularly in macrophages. *Arteriosclerosis, thrombosis, and vascular biology*, 19(3), pp.646–55.

Balsinde, J., Balboa, M.A. & Dennis, E.A., 1998. Functional coupling between secretory phospholipase A2 and cyclooxygenase-2 and its regulation by cytosolic group IV phospholipase A2. *Proceedings of the National Academy of Sciences of the United States of America*, 95(14), pp.7951–6.

Balsinde, J. & Dennis, E., 1996. Distinct Roles in Signal Transduction for Each of the Phospholipase A Enzymes Present in P388D Macrophages. *Journal of Biological Chemistry*, 271(12), pp.6758–6765.

Barrios-Rodiles, M., Tiraloche, G. & Chadee, K., 1999. Lipopolysaccharide Modulates Cyclooxygenase-2 Transcriptionally and Posttranscriptionally in Human Macrophages Independently from Endogenous IL-1 β and TNF- α. *The Journal of Immunology*, 163, pp.963–969.

Bartley, T.D., Bogenberger, J., Hunt, P., Li, Y.S., Lu, H.S., Martin, F., Chang, M.S., Samal, B., Nichol, J.L. & Swift, S., 1994. Identification and cloning of a megakaryocyte growth and development factor that is a ligand for the cytokine receptor Mpl. *Cell*, 77(7), pp.1117–1124.

Bartoli, F., Lin, H.-K., GhomashchiP, F., GelbPnll, M.H., Jain, M.K. & Apitz-Castro, R., 1994. Tight Binding Inhibitors of 85-kDa Phospholipase A, but Not 14-kDa Phospholipase A, Inhibit Release of Free Arachidonate in Thrombin-stimulated Human Platelets. *The Journal of biological chemistry*, 269(22), pp.15625–15630.

Belton, O., Byrne, D., Kearney, D., Leahy, A. & Fitzgerald, D.J., 2000. Cyclooxygenase-1 and -2 Dependent Prostacyclin Formation in Patients With Atherosclerosis. *Circulation*, (102), pp.840–845.

Bergstroem, S., Danielsson, H. & Samuelsson, B., 1964. The enzymatic formation of prostaglandin E2 from arachidonic acid Prostaglandin$ and related factors 32. *Biochimica et biophysica acta*, 90, pp.204–207.

Bergstroem, S., Ryhage, R., Samuelsson, B. & Sjoevall, J., 1963. Prostaglandins and related factors. *The Journal of biological chemistry*, 238(11), pp.3555–3564.

Bergstroem, S. & Sjoevall, J., 1960. The isolation of prostaglandin E from sheep prostate

glands. *Acte Chemica Scandinavia*, 14, pp.1701–1705.

Bergström, S. & Samuelsson, B., 1962. Isolation of prostaglandin E1 from human seminal plasma. *Journal of Biological Chemistry*, 237(9), pp.3005–3006.

Berrettini, M., Cunto, M.D., Parise, R., Grasselli, S. & Nenci, G.G., 1990. "In vitro" and "ex vivo" effects of picotamide, a combined thromboxane A2-synthase inhibitor and -receptor antagonist , on human platelets. *European Journal of Clinical Pharmacology*, (39), pp.495–500.

Borgeat, P., Hamberg, M. & Samuelsson, B., 1976. Transformation of Arachidonic Acid and Homo-Gamma-Linolenic Acid by Rabbit Polymorphonuclear Leukocytes. Monohydroxy acids from Novel Lipoxygenases. *Journal of Biological Chemistry*, 251(24), pp.7816–7820.

Bos, C.L., Richel, D.J., Ritsema, T., Peppelenbosch, M.P. & Versteeg, H.H., 2004. Prostanoids and prostanoid receptors in signal transduction. *The international journal of biochemistry & cell biology*, 36(7), pp.1187–205.

Botting, R., 2003. COX-1 and COX-3 inhibitors. *Thrombosis Research*, 110(5-6), pp.269–272.

Brancaleone, V., Gobbetti, T., Cenac, N., Le Faouder, P., Colom, B., Flower, R.J., Vergnolle, N., Nourshargh, S. & Perretti, M., 2013. A vasculo-protective circuit centered on lipoxin A4 and aspirin-triggered 15-epi-lipoxin A4 operative in murine microcirculation. *Blood*, 122(4), pp.608–617.

Brandt, E., Petersen, F., Ludwig, A., Ehlert, J.E., Bock, L. & Flad, H.D., 2000. The beta-thromboglobulins and platelet factor 4: blood platelet-derived CXC chemokines with divergent roles in early neutrophil regulation. *Journal of leukocyte biology*, 67(April), pp.471–478.

Brash, A.R., 2009. Mechanistic aspects of CYP74 allene oxide synthases and related cytochrome P450 enzymes. *Phytochemistry*, 70(13-14), pp.1522–1531.

Bray, M.A., Ford-Hutchinson, A.W. & Smith, M.J.H., 1981. LEUKOTRIENE B 4 : AN INFLAMMATORY MEDIATOR IN VIVO. *Prostaglandins*, 22(2), pp.213–222.

Brooke, M. a, Longhurst, H.J., Plagnol, V., Kirkby, N.S., Mitchell, J. a, Rüschendorf, F., Warner, T.D., Kelsell, D.P. & MacDonald, T.T., 2014. Cryptogenic multifocal ulcerating stenosing enteritis associated with homozygous deletion mutations in cytosolic phospholipase A2-α. *Gut*, 63, pp.96–104.

Bruins, A.P., 1998. Mechanistic aspects of electrospray ionization. *Journal of Chromatography A*, 794(1-2), pp.345–357.

Bryant, R.W., Bailey, J.M., Schewe, T. & Rapoport, S.M., 1982. Positional specificity of a reticulocyte lipoxygenase. Conversion of arachidonic acid to 15-S-hydroperoxy-eicosatetraenoic acid. *J Biol Chem*, 257(11), pp.6050–6055.

Burch, R.M., Mais, D.E., Saussy, D.L. & Halushka, P. V, 1985. Solubilization of a thromboxane A2 / prostaglandin H2 antagonist binding site from human platelets. *Proc Natl Acad Sci U S A*, 82(November), pp.7434–7438.

Burke, J.E. & Dennis, E.A., 2009. Phospholipase A2 biochemistry. *Cardiovasc Drugs Ther*, 23(1), pp.49–59.

Buttrum, S.M., Hatton, R. & Nash, G.B., 1993. Selectin-mediated rolling of neutrophils on immobilized platelets. *Blood*, 82(4), pp.1165–74.

Bylund, J., Ericsson, J. & Oliw, E.H., 1998. Analysis of Cytochrome P450 Metabolites of Arachidonic and Linoleic Acids by Liquid Chromatography–Mass Spectrometry with Ion Trap MS2. *Analytical Biochemistry*, 265(1), pp.55–68.

Caivano, M. & Cohen, P., 2000. Role of mitogen-activated protein kinase cascades in mediating lipopolysaccharide-stimulated induction of cyclooxygenase-2 and IL-1 beta in RAW264 macrophages. *Journal of Immunology*, 164, pp.3018–3025.

Caligiuri, G., Nicoletti, a, Zhou, X., Törnberg, I. & Hansson, G.K., 1999. Effects of sex and age on atherosclerosis and autoimmunity in apoE-deficient mice. *Atherosclerosis*, 145(2), pp.301–8.

Cao, C., Matsumura, K., Yamagata, K. & Watanabe, Y., 1997. Involvement of cyclooxygenase-2 in LPS-induced fever and regulation of its mRNA by LPS in the rat brain. *The American journal of physiology*, 272(6 Pt 2), pp.R1712–25.

Capdevila, J.H., Falck, J.R. & Harris, R.C., 2000. Cytochrome P450 and arachidonic acid bioactivation. Molecular and functional properties of the arachidonate monooxygenase. *Journal of lipid research*, 41, pp.163–181.

Carvalho, M.S., Mendon??a, M.A., Pinho, D.M.M., Resck, I.S. & Suarez, P.A.Z., 2012. Chromatographic analyses of fatty acid methyl esters by HPLC-UV and GC-FID. *Journal of the Brazilian Chemical Society*, 23(4), pp.763–769.

Caudrillier, A., Kessenbrock, K., Gilliss, B.M., Nguyen, J.X., Marques, M.B., Monestier, M., Toy, P., Werb, Z. & Looney, M.R., 2012. Platelets induce neutrophil extracellular traps in transfusion-related acute lung injury. *J. Clin. Invest.*, 122(7), pp.2661–2671.

Caughey, G.E., Cleland, L.G., Penglis, P.S., Gamble, J.R. & James, M.J., 2001. Roles of

Cyclooxygenase (COX)-1 and COX-2 in Prostanoid Production by Human Endothelial Cells: Selective Up-Regulation of Prostacyclin Synthesis by COX-2. *The Journal of Immunology*, 167(5), pp.2831–2838.

Chan, A.T., Arber, N., Burn, J., Chia, W.K., Elwood, P., Hull, M. a., Logan, R.F., Rothwell, P.M., Schrör, K. & Baron, J. a., 2012. Aspirin in the chemoprevention of colorectal neoplasia: An overview. *Cancer Prevention Research*, 5(2), pp.164–178.

Chandrasekharan, N. & Simmons, D.L., 2004. The cyclooxygenases. *Genome biology*, 5(9), p.241.

Chandrasekharan, N. V, Dai, H., Roos, K.L.T., Evanson, N.K., Tomsik, J., Elton, T.S. & Simmons, D.L., 2002. COX-3, a cyclooxygenase-1 variant inhibited by acetaminophen and other analgesic/antipyretic drugs: cloning, structure, and expression. *Proceedings of the National Academy of Sciences of the United States of America*, 99(21), pp.13926–31.

Chen, C., 2010. COX-2's new role in inflammation. *Nature chemical biology*, 6(6), pp.401–402.

Chen, J., Capdevila, J.H., Zeldin, D.C. & Rosenberg, R.L., 1999. Inhibition of cardiac L-type calcium channels by epoxyeicosatrienoic acids. *Molecular pharmacology*, 55, pp.288–295.

Chen, Q.R., Miyaura, C., Higashi, S., Murakami, M., Kudo, I., Saito, S., Hiraide, T., Shibasaki, Y. & Suda, T., 1997. Activation of cytosolic phospholipase A2 by platelet-derived growth factor is essential for cyclooxygenase-2-dependent prostaglandin E2 synthesis in mouse osteoblasts cultured with interleukin-1. *The Journal of biological chemistry*, 272(9), pp.5952–8.

Chiyotani, A., Tamaoki, J., Sakai, N., Isono, K., Kondo, M. & Konno, K., 1992. THROMBOXAWE A2 MIMETIC U46619 STIMULATES CILIARY MOTILITY OF RABBIT TRACHEAL EPITHELIAL CELLS. *Prostaglandins*, 43(2), pp.111–120.

Clark, J.D., Lin, L.L., Kriz, R.W., Ramesha, C.S., Sultzman, L.A., Lin, A.Y., Milona, N. & Knopf, J.L., 1991. A novel arachidonic acid-selective cytosolic PLA2 contains a Ca(2+)-dependent translocation domain with homology to PKC and GAP. *Cell*, 65(6), pp.1043–1051.

Clark, S.R., Guy, C.J., Scurr, M.J., Taylor, P.R., Kift-Morgan, A.P., Hammond, V.J., Thomas, C.P., Coles, B., Roberts, G.W., Eberl, M., Jones, S. a, Topley, N., Kotecha, S. & O'Donnell, V.B., 2011. Esterified eicosanoids are acutely generated by 5-lipoxygenase in primary human neutrophils and in human and murine infection. *Blood*, 117(6), pp.2033–43.

Clark, S.R., Ma, A.C., Tavener, S.A., McDonald, B., Goodarzi, Z., Kelly, M.M., Patel, K.D.,

Chakrabarti, S., McAvoy, E., Sinclair, G.D., Keys, E.M., Allen-Vercoe, E., DeVinney, R., Doig, C.J., Green, F.H.Y. & Kubes, P., 2007. Platelet TLR4 activates neutrophil extracellular traps to ensnare bacteria in septic blood. *Nature Medicine*, 13(4), pp.463–469.

Clark, S.R., Thomas, C.P., Hammond, V.J., Aldrovandi, M., Wilkinson, G.W., Hart, K.W., Murphy, R.C., Collins, P.W. & O'Donnell, V.B., 2013. Characterization of platelet aminophospholipid externalization reveals fatty acids as molecular determinants that regulate coagulation. *Proceedings of the National Academy of Sciences of the United States of America*, 110(15), pp.5875–80.

Cognasse, F., Hamzeh, H., Chavarin, P., Acquart, S., Genin, C. & Garraud, O., 2005. Evidence of Toll-like receptor molecules on human platelets. *Immunology and Cell Biology*, 83(2), pp.196–198.

Cook, N.R., Lee, I., Zhang, S.M., Moorthy, M.V. & Buring, J.E., 2013. Alternative-day, Low-Dose Aspirin and Cancer Risk: Long-Term Observational Follow-up of a Randomized Trial. *Annals of Internal Medicine*, 159, pp.77–85.

Coppinger, J.A., Cagney, G., Toomey, S., Kislinger, T., Belton, O., McRedmond, J.P., Cahill, D.J., Emili, A., Fitzgerald, D.J. & Maguire, P.B., 2004. Characterization of the proteins released from activated platelets leads to localization of novel platelet proteins in human atherosclerotic lesions. *Blood*, 103(6), pp.2096–104.

Corken, A., Russell, S., Dent, J., Post, S.R. & Ware, J., 2014. Platelet Glycoprotein Ib-IX as a Regulator of Systemic Inflammation. *Arteriosclerosis, Thrombosis, and Vascular Biology*, 34(5), pp.996–1001.

Coughlin, S.R., 2000. Thrombin signalling and protease-activated receptors. *Nature*, 407(6801), pp.258–264.

Cox, D., Kerrigan, S.W. & Watson, S.P., 2011. Platelets and the innate immune system: Mechanisms of bacterial-induced platelet activation. *Journal of Thrombosis and Haemostasis*, 9(6), pp.1097–1107.

Cuzick, J., Otto, F., Baron, J.A., Brown, P.H., Burn, J., Greenwald, P., Jankowski, J., La Vecchia, C., Meyskens, F., Senn, H.J. & Thun, M., 2009. Aspirin and non-steroidal anti-inflammatory drugs for cancer prevention: an international consensus statement. *The Lancet Oncology*, 10(5), pp.501–507.

Cyrus, T., Witztum, J.L., Rader, D.J., Tangirala, R., Fazio, S., Linton, M.F. & Funk, C.D., 1999. Disruption of the 12/15-lipoxygenase gene diminishes atherosclerosis in apo E-deficient

mice. *J Clin Invest*, 103(11), pp.1597–1604.

Daikh, B.E., Lasker, J.M., Raucy, J.L. & Koop, D.R., 1994. Reglo- and Stereoselective Cytochromes Epoxidation of Arachidonic 2C8 and 2C91 Acid by. *The Journal of Pharmacology and Experimental Theropeutics*, 271(3), pp.1427–1433.

Danese, S., de la Motte, C., Reyes, B.M., Sans, M., Levine, A.D. & Fiocchi, C., 2004. Cutting edge: T cells trigger CD40-dependent platelet activation and granular RANTES release: a novel pathway for immune response amplification. *Journal of Immunology*, 172(4), pp.2011–2015.

Deems, R., Buczynski, M.W., Bowers-Gentry, R., Harkewicz, R. & Dennis, E.A., 2007. Detection and Quantitation of Eicosanoids via High Performance Liquid Chromatography-Electrospray Ionization-Mass Spectrometry. *Methods in Enzymology*, 432, pp.59–82.

Deuel, T.F., Senior, R.M., Chang, D., Griffin, G.L., Heinrikson, R.L. & Kaiser, E.T., 1981. Platelet factor 4 is chemotactic for neutrophils and monocytes. *Proceedings of the National Academy of Sciences of the United States of America*, 78(7), pp.4584–4587.

Deuel, T.F., Senior, R.M., Huang, J.S. & Griffin, G.L., 1982. Chemotaxis of monocytes and neutrophils to platelet-derived growth factor. *J Clin Invest*, 69(4), pp.1046–1049.

DeWitt, D.L., 1999. Cox-2-selective inhibitors: the new super aspirins. *Molecular pharmacology*, 55(4), pp.625–631.

DeWitt, D.L., El-Harith, E.A., Kraemer, S.A., Andrews, M.J., Yao, E.F., Armstrong, R.L. & Smith, W.L., 1990. The aspirin and heme-binding sites of ovine and murine prostaglandin endoperoxide synthases. *Journal of Biological Chemistry*, 265(9), pp.5192–5198.

DeWitt, D.L. & Smith, W.L., 1988. Primary structure of prostaglandin G/H synthase from sheep vesicular gland determined from the complementary DNA sequence. *Proceedings of the National Academy of Sciences of the United States of America*, 85(5), pp.1412–6.

Diacovo, T.G., Roth, S.J., Buccola, J.M., Bainton, D.F. & Springer, T. a, 1996. Neutrophil rolling, arrest, and transmigration across activated, surface-adherent platelets via sequential action of P-selectin and the beta 2-integrin CD11b/CD18. *Blood*, 88(1), pp.146–157.

Dodds, E.D., McCoy, M.R., Rea, L.D. & Kennish, J.M., 2005. Gas chromatographic quantification of fatty acid methyl esters: Flame ionization detection vs. electron impact mass spectrometry. *Lipids*, 40(4), pp.419–428.

Dole, V.S., Bergmeier, W., Mitchell, H.A., Eichenberger, S.C., Denisa, D., Dc, W. & Wagner, D.D., 2012. Activated platelets induce Weibel-Palade – body secretion and leukocyte

rolling in vivo : role of P-selectin Activated platelets induce Weibel-Palade – body secretion and leukocyte rolling in vivo : role of P-selectin. , 106(7), pp.2334–2339.

Dorn, G.W. 2nd & Becker, M.W., 1993. Thromboxane A2 stimulated signal transduction in vascular smooth muscle. *The Journal of pharmacology and experimental therapeutics*, 265(1), pp.447–456.

Dorn, G.W., Davis, M.G. & Angelo, D.D.D., 1997. Structural Determinants for Agonist Binding Affinity to Thromboxane / Prostaglandin Endoperoxide (TP) Receptors. *The Journal of biological chemistry*, 272(19), pp.12399–12405.

van Dorp, D.A., Beerthuis, R.K., Nugteren, D.. & Vonkeman, H., 1964. The biosynthesis of prostaglandins. *Biochimica et biophysica acta*, 90, pp.204–207.

Dreon, M., Lavarias, S., Garin, C.F., Heras, H. & Pollero, R.J., 2002. Synthesis, distribution, and levels of an egg lipoprotein from the apple snail Pomacea canaliculata (mollusca: Gastropoda). *Journal of Experimental Zoology*, 292(3), pp.323–330.

Ebbeling, L., Robertson, C., McNicol, a & Gerrard, J.M., 1992. Rapid ultrastructural changes in the dense tubular system following platelet activation. *Blood*, 80(3), pp.718–723.

Elneihoum, A., 1997. Leukocyte activation in atherosclerosis: correlation with risk factors. *Atherosclerosis*, 131(1), pp.79–84.

Euler, U.S. von, 1936. On the specific vaso-dilating and plain muscle stimulating substances from accessory genital glands in man and certain animals (prostaglandin and veriglandin. *The Journal of Physiology*, pp.213–233.

Evangelista, B.V., Manarini, S., Sideri, R., Rotondo, S., Martelli, N., Piccoli, A., Totani, L., Piccardoni, P., Vestweber, D., Gaetano, G. De & Cerletti, C., 1999. Platelet/Polymorphonuclear Leukocyte Interaction: P-Selectin Triggers Protein-Tyrosine Phosphorylation–Dependent CD11b/CD18 Adhesion: Role of PSGL-1 as a Signaling Molecule. *Blood*, 93(3), pp.876–885.

Evangelista, V., Manarini, S., Rotondo, S., Martelli, N., Polischuk, R., Mcgregor, J.L., de Gaetano, G., Cerletti, C., Cdllbicd, I., Evangelista, B.V. & Gaetano, G. De, 1996. Platelet/polymorphonuclear leukocyte interaction in dynamic conditions: evidence of adhesion cascade and cross talk between P-selectin and the beta 2 integrin CD11b/CD18. *Blood*, 88(11), pp.4183–94.

Evans, J.H., Spencer, D.M., Zweifach, A. & Leslie, C.C., 2001. Intracellular calcium signals regulating cytosolic phospholipase A2 translocation to internal membranes. *The Journal*

of biological chemistry, 276(32), pp.30150–60.

Fahy, E., 2005. A comprehensive classification system for lipids. *The Journal of Lipid Research*, 46(5), pp.839–862.

Le Faouder, P., Baillif, V., Spreadbury, I., Motta, J.P., Rousset, P., Chêne, G., Guigné, C., Tercé, F., Vanner, S., Vergnolle, N., Bertrand-Michel, J., Dubourdeau, M. & Cenac, N., 2013. LC-MS/MS method for rapid and concomitant quantification of pro-inflammatory and pro-resolving polyunsaturated fatty acid metabolites. *Journal of Chromatography B: Analytical Technologies in the Biomedical and Life Sciences*, 932, pp.123–133.

Feder, R., Banton, V., Sayre, D., Costa, J., Baldini, M. & Kim, B., 1985. Direct imaging of Live Human Platelets by Flash X-Ray Microscopy. *Science*, 227(4682), pp.63–64.

Fonteh, A.N., Bass, D.A., Marshall, L.A., Seeds, M., Samet, J.M. & Chilton, F.H., 1994. Evidence that secretory phospholipase A2 plays a role in arachidonic acid release and eicosanoid biosynthesis by mast cells. *J Immunol*, 152(11), pp.5438–5446.

François, B., Trimoreau, F., Vignon, P., Fixe, P., Praloran, V. & Gastinne, H., 1997. Thrombocytopenia in the sepsis syndrome: role of hemophagocytosis and macrophage colony-stimulating factor. *The American journal of medicine*, 103(2), pp.114–20.

Furman, M.I., Benoit, S.E., Barnard, M.R., Valeri, C.R., Borbone, M.L., Becker, R.C., Hechtman, H.B. & Michelson, a D., 1998. Increased platelet reactivity and circulating monocyte-platelet aggregates in patients with stable coronary artery disease. *Journal of the American College of Cardiology*, 31(2), pp.352–358.

Futosi, K., Fodor, S. & Mócsai, A., 2013. Neutrophil cell surface receptors and their intracellular signal transduction pathways. *International Immunopharmacology*, 17(3), pp.638–650.

Gawaz, M., Fateh-Moghadam, S., Pilz, G., Gurland, H.J. & Werdan, K., 1995. Platelet activation and interaction with leucocytes in patients with sepsis or multiple organ failure. *European journal of clinical investigation*, 25(11), pp.843–851.

George, J.N., 2000. Platelets. *The Lancet*, 355(April), pp.1531–1539.

Gierse, J.K., McDonald, J.J., Hauser, S.D., Rangwala, S.H., Koboldt, C.M. & Seibert, K., 1996. A single amino acid difference between cyclooxygenase-1 (COX-1) and -2 (COX-2) reverses the selectivity of COX-2 specific inhibitors. *Journal of Biological Chemistry*, 271(26), pp.15810–15814.

Gimbrone, M. a, Brock, a F. & Schafer, a I., 1984. Leukotriene B4 stimulates

polymorphonuclear leukocyte adhesion to cultured vascular endothelial cells. *The Journal of clinical investigation*, 74(4), pp.1552–1555.

Giroux, M. & Descoteaux, A., 2000. Cyclooxygenase-2 expression in macrophages: modulation by protein kinase C-alpha. *The Journal of Immunology*, 165(7), pp.3985–3991.

Giuliano, F. & Warner, T.D., 2002. Origins of Prostaglandin E 2 : Involvements of Cyclooxygenase (COX) -1 and COX-2 in Human and Rat Systems. , 303(3), pp.1001–1006.

Gladding, P. a., Webster, M.W.I., Farrell, H.B., Zeng, I.S.L., Park, R. & Ruijne, N., 2008. The Antiplatelet Effect of Six Non-Steroidal Anti-Inflammatory Drugs and Their Pharmacodynamic Interaction With Aspirin in Healthy Volunteers. *American Journal of Cardiology*, 101(7), pp.1060–1063.

Gleissner, C., von Hundelshausen, P. & Ley, K., 2008. Platelet chemokines in vascular disease. *Arterisclerosis, Thrombosis and Vascular Biology*, 28(11), pp.1920–1927.

Goetzl, E.J., Brash, A.R., Tauber, A.I., Oates, J.A. & Hubbard, W.C., 1980. Modulation of human neutrophil function by monohydroxy-eicosatetraenoic acids. *Immunology*, 39(4), pp.491–501.

Goetzl, E.J. & Sun, F.F., 1979. GENERATION OF UNIQUE MONO-HYDROXY-EICOSATETRAENOIC ACIDS FROM ARACHIDONIC ACID BY HUMAN NEUTROPHILS. *Journal of Experimental Medicine*, 150, pp.406–411.

Goetzl, E.J., Weller, P.F. & Sun, F.F., 1980. The regulation of human eosinophil function by endogenous mono-hydroxy-eicosatetraenoic acids (HETEs). *Journal of immunology (Baltimore, Md. : 1950)*, 124(2), pp.926–33.

Gormand, F., Chabannes, B., Moliere, P., Perrin-Fayolle, M., Lagarde, M. & Pacheco, Y., 1996. Uptake of 12-HETE by human bronchial epithelial cells (HBEC): effects on HBEC cytokine production. *Prostaglandins*, 51(4), pp.263–73.

Grant, G.E., Rokach, J. & Powell, W.S., 2009. 5-Oxo-ETE and the OXE receptor. *Prostaglandins and Other Lipid Mediators*, 89(3-4), pp.98–104.

Greenberg, M.E., Li, X.M., Gugiu, B.G., Gu, X., Qin, J., Salomon, R.G. & Hazen, S.L., 2008. The lipid whisker model of the structure of oxidized cell membranes. *Journal of Biological Chemistry*, 283(4), pp.2385–2396.

Greene, E.R., Huang, S., Serhan, C.N. & Panigrahy, D., 2011. Regulation of inflammation in cancer by eicosanoids. *Prostaglandins & Other Lipid Mediators*, 96(1-4), pp.27–36.

Gross, G.J., Falck, J.R., Gross, E.R., Isbell, M., Moore, J. & Nithipatikom, K., 2005. Cytochrome

P450 and arachidonic acid metabolites: role in myocardial ischemia/reperfusion injury revisited. *Cardiovascular research*, 68(1), pp.18–25.

Guarrasi, V., Mangione, M.R., Sanfratello, V., Martorana, V. & Bulone, D., 2010. Quantification of underivatized fatty acids from vegetable oils by HPLC with UV detection. *Journal of chromatographic science*, 48(September), pp.663–668.

Gudbrandsdottir, S., Hasselbalch, H.C. & Nielsen, C.H., 2013. Activated platelets enhance IL-10 secretion and reduce TNF-α secretion by monocytes. *Journal of immunology (Baltimore, Md. : 1950)*, 191(8), pp.4059–67.

Guo, Y., Zhang, W., Giroux, C., Cai, Y., Ekambaram, P., Dilly, A.-K., Hsu, A., Zhou, S., Maddipati, K.R., Liu, J., Joshi, S., Tucker, S.C., Lee, M.-J. & Honn, K. V, 2011. Identification of the orphan G protein-coupled receptor GPR31 as a receptor for 12-(S)-hydroxyeicosatetraenoic acid. *The Journal of biological chemistry*, 286(39), pp.33832–40.

Hamberg, M. & Samuelsson, B., 1973. Detection and isolation of an endoperoxide intermediate in prostaglandin biosynthesis. *Proceedings of the National Academy of Sciences of the United States of America*, 70(3), pp.899–903.

Hamberg, M. & Samuelsson, B., 1967. Oxygenation of Unsaturated Fatty Acids by the Vesicular Gland of Sheep. *The Journal of biological chemistry*, 242, pp.5344–5354.

Hamberg, M. & Samuelsson, B., 1974. Prostagland Endoperoxides . Novel Transformations of Arachidonic Acid in Human Platelets *. *Proceedings of the National Academy of Sciences of the United States of America*, 71(9), pp.3400–3404.

Hamberg, M. & Samuelsson, B., 1974. Prostaglandin endoperoxides. Novel transformations of arachidonic acid in human platelets. *Proceedings of the National Academy of Sciences of the United States of America*, 71(9), pp.3400–3404.

Hamberg, M. & Samulsson, B., 1967. On the mechanism of the biosynthesis of prostaglandins E1 and F1α. *J. Biol. Chem.*, 242(22), pp.5336–5343.

Hamberg, M., Svensson, J. & Samuelsson, B., 1975. Thromboxanes: a new group of biologically active compounds derived from prostaglandin endoperoxides. *Proceedings of the National Academy of Sciences of the United States of America*, 72(8), pp.2994–2998.

Hamburger, S.A. & McEver, R.P., 1990. GMP-140 mediates adhesion of stimulated platelets to neutrophils. *Blood*, 75(3), pp.550–4.

Hammond, V.J. & O'Donnell, V.B., 2012. Esterified eicosanoids: Generation, characterization

and function. *Biochimica et Biophysica Acta - Biomembranes*, 1818(10), pp.2403–2412.

Hanahan, D., 1986. Platelet Activating Factor : A Biologically Active Phosphoglyceride. *Annual Review of Biochemistry*, (55), pp.483–509.

Harizi, H., Corcuff, J.B. & Gualde, N., 2008. Arachidonic-acid-derived eicosanoids: roles in biology and immunopathology. *Trends in Molecular Medicine*, 14(September), pp.461–469.

Harman, C. a., Rieke, C.J., Garavito, R.M. & Smith, W.L., 2004a. Crystal structure of arachidonic acid bound to a mutant of prostaglandin endoperoxide H synthase-1 that forms predominantly 11- hydroperoxyeicosatetraenoic acid. *Journal of Biological Chemistry*, 279(41), pp.42929–42935.

Harman, C. a., Rieke, C.J., Garavito, R.M. & Smith, W.L., 2004b. Crystal structure of arachidonic acid bound to a mutant of prostaglandin endoperoxide H synthase-1 that forms predominantly 11- hydroperoxyeicosatetraenoic acid. *Journal of Biological Chemistry*, 279, pp.42929–42935.

Harris, S.G., Padilla, J., Koumas, L., Ray, D. & Phipps, R.P., 2002. Prostaglandins as modulators of immunity. *Trends in Immunology*, 23(3), pp.144–150.

Hartwig, J.H., 1992. Mechanisms of actin rearrangements mediating platelet activation. *Journal of Cell Biology*, 118(6), pp.1421–1441.

Hata, A.N. & Breyer, R.M., 2004. Pharmacology and signaling of prostaglandin receptors: multiple roles in inflammation and immune modulation. *Pharmacology & therapeutics*, 103(2), pp.147–66.

Haurand, M. & Ullrich, V., 1985. Isolation and characterization of thromboxane synthase from human platelets as a cytochrome P-450 enzyme. *The Journal of biological chemistry*, 260(28), pp.15059–15067.

Havrilla, C.M., Hachey, D.L. & Porter, N. a, 2000. Coordination (Ag+) Ion Spray–Mass Spectrometry of Peroxidation Products of Cholesterol Linoleate and Cholesterol Arachidonate: High-Performance Liquid Chromatography–Mass Spectrometry Analysis of Peroxide Products from Polyunsaturated Lipid Autoxidation. *Journal of the American Chemical Society*, 122(33), pp.8042–8055.

Hecker, M. & Ullrich, V., 1989. On the mechanism of prostacyclin and thromboxane A2 biosynthesis. *Journal of Biological Chemistry*, 264, pp.141–150.

Hecker, M., Ullrich, V., Fischer, C. & Meese, C.O., 1987. Identification of novel arachidonic acid

metabolites formed by prostaglandin H synthase. *European journal of biochemistry / FEBS*, 169(1), pp.113–23.

Hemker, H.C., van Rijn, J.L., Rosing, J., van Dieijen, G., Bevers, E.M. & Zwaal, R.F., 1983. Platelet membrane involvement in blood coagulation. *Blood cells*, 9(2), pp.303–317.

Hemler, W., Lands, W. & Smith, W.L., 1976. Purification of the Cyclooxygenase That Forms Prostaglandins. *The Journal of biological chemistry*, 251(18), pp.5575–5579.

Henn, V., Slupsky, J.R., Gr a fe, M., Anagnostopoulos, I., F o rster, R., M u ller-Berghaus, G. & Kroczek, R.A., 1998. CD40 ligand on activated platelets triggers an inflammatory reaction of endothelial cells. *Nature*, 391(6667), pp.591–594.

Henn, V., Steinbach, S., Büchner, K., Presek, P. & Kroczek, R. a., 2001. The inflammatory action of CD40 ligand (CD154) expressed on activated human platelets is temporally limited by coexpressed CD40. *Blood*, 98(4), pp.1047–1054.

Henriksen, R.A. & Hanks, V.K., 2002. PAR-4 agonist AYPGKF stimulates thromboxane production by human platelets. *Arterioscler.Thromb.Vasc.Biol.*, 22(5), pp.861–866.

Herbertsson, H., Kühme, T. & Hammarström, S., 1999. The 650-kDa 12(S)-hydroxyeicosatetraenoic acid binding complex: occurrence in human platelets, identification of hsp90 as a constituent, and binding properties of its 50-kDa subunit. *Archives of biochemistry and biophysics*, 367(1), pp.33–8.

Van Hinsbergh, V.W.M., 2012. Endothelium - Role in regulation of coagulation and inflammation. *Seminars in Immunopathology*, 34(1), pp.93–106.

Hinz, C., Aldrovandi, M., Uhlson, C., Podmore, H., Marnett, L.J., Longhurst, H.J., Warner, T.D., Alam, S., Slatter, D.A., Lauder, S.N., Allen-redpath, K., Collins, P.W., Robert, C., Thomas, C.P. & Donnell, V.B.O., Lipidomic Identification of Dioxolane A 3 , a Neutrophil-Activating Eicosanoid Formed. *Manuscript*.

Hirata, M., Kakizuka, A., Aizawa, M., Ushikubi, F. & Narumiya, S., 1994. Molecular characterization of a mouse prostaglandin D receptor and functional expression of the cloned gene. *Proceedings of the National Academy of Sciences*, 91(23), pp.11192–11196.

Hirata, T. & Narumiya, S., 2011. Prostanoid receptors. *Chemical reviews*, 111, pp.6209–6230.

Ho, C.S., Lam, C.W.K., Chan, M.H.M., Cheung, R.C.K., Law, L.K., Lit, L.C.W., Ng, K.F., Suen, M.W.M. & Tai, H.L., 2003. Electrospray ionisation mass spectrometry: principles and clinical applications. *The Clinical biochemist*, 24(1), pp.3–12.

Holinstat, M., 2006. PAR4, but Not PAR1, Signals Human Platelet Aggregation via Ca2+

Mobilization and Synergistic P2Y12 Receptor Activation. *Journal of Biological Chemistry*, 281(36), pp.26665–26674.

Holinstat, M., Boutaud, O., Apopa, V., Bala, M., Oates, J. & Hamm, H., 2011. Protease-Activated Receptor Signaling in Platelets Activates Cytosolic Phospholipase A2_ Differently for Cyclooxygenase-1 and 12-Lipoxygenase Catalysis. *Arteriosclerosis, Thrombosis, and Vascular Biology*, 31(2), pp.435–442.

Hong, S., Lu, Y., Yang, R., Gotlinger, K.H., Petasis, N. a. & Serhan, C.N., 2007. Resolvin D1, Protectin D1, and Related Docosahexaenoic Acid-Derived Products: Analysis via Electrospray/Low Energy Tandem Mass Spectrometry Based on Spectra and Fragmentation Mechanisms. *Journal of the American Society for Mass Spectrometry*, 18(1), pp.128–144.

Htun, P., Fateh-Moghadam, S., Tomandl, B., Handschu, R., Klinger, K., Stellos, K., Garlichs, C., Daniel, W. & Gawaz, M., 2006. Course of platelet activation and platelet-leukocyte interaction in cerebrovascular ischemia. *Stroke; a journal of cerebral circulation*, 37(9), pp.2283–7.

Huo, Y. & Ley, K.F., 2004. Role of Platelets in the Development of Atherosclerosis. *Trends in Cardiovascular Medicine*, 14(1), pp.18–22.

Issekutz, A.C. & Issekutz, T.B., 1992. The contribution of LFA-1 (CD11a/CD18) and MAC-1 (CD11b/CD18) to the in vivo migration of polymorphonuclear leucocytes to inflammatory reactions in the rat. *Immunology*, 76(4), pp.655–61.

Itoh, S., Susuki, C. & Tsuji, T., 2006. Platelet activation through interaction with hemodialysis membranes induces neutrophils to produce reactive oxygen species. *Journal of Biomedical Materials Research - Part A*, 77(2), pp.294–303.

Jackson, L.M., Wu, K.C., Mahida, Y.R., Jenkins, D. & Hawkey, C.J., 2000. Cyclooxygenase (COX) 1 and 2 in normal, inflamed, and ulcerated human gastric mucosa. *Gut*, 47(6), pp.762–770.

Jaffar, Z., Ferrini, M.E., Shaw, P.K., FitzGerald, G. a & Roberts, K., 2011. Prostaglandin I$_2$promotes the development of IL-17-producing γδ T cells that associate with the epithelium during allergic lung inflammation. *Journal of immunology*, 187(10), pp.5380–91.

Jakschik, B.A., Sams, A.R., Sprecher, H. & Needleman, P., 1980. FATTY ACID STRUCTURAL

REQUIREMENTS FOR LEUKOTRIENE BIOSYNTHESIS. *Prostaglandins*, 20(2), pp.401–410.

Jimenez, A.H., Stubbs, M.E., Tofler, G.H., Winther, K., Williams, G.H. & Muller, J.E., 1992. Rapidity and duration of platelet suppression by enteric-coated aspirin in healthy young men. *The American journal of cardiology*, 69(3), pp.258–62.

Johansson, D., Shannon, O. & Rasmussen, M., 2011. Platelet and neutrophil responses to Gram positive pathogens in patients with bacteremic infection. *PLoS ONE*, 6(11).

Jonasson, L., Holm, J., Skalli, O., Bondjers, G. & Hansson, G.K., 1985. Regional accumulations of T cells, macrophages, and smooth muscle cells in the human atherosclerotic plaque. *Arteriosclerosis (Dallas, Tex.)*, 6(2), pp.131–138.

Jungi, T.W., Spycher, U.E., Nydegger, U.E. & Barandun, S., 1986. Platelet-Leukocyte Interaction: Selective Binding of Thrombin-Stimulated Platelets to Human Monocytes, Polymorphonuclear Leukocytes, and related Cell Lines. *Blood*, 67(3), pp.629–636.

Kamath, S., 2001. Platelet activation: assessment and quantification. *European Heart Journal*, 22(17), pp.1561–1571.

Kaushansky, K., 2005. The molecular mechanisms that control thrombopoiesis. *Journal of Clinical Investigation*, 115(12), pp.3339–3347.

Kaushansky, K., Lok, S., Holly, R.D., Broudy, V.C., Lin, N., Bailey, M.C., Forstrom, J.W., Buddle, M.M., Oort, P.J. & Hagen, F.S., 1994. Promotion of megakaryocyte progenitor expansion and differentiation by the c-Mpl ligand thrombopoietin. *Nature*, 369, pp.568–571.

Kempen, E.C., Yang, P., Felix, E., Madden, T. & Newman, R.A., 2001. Simultaneous quantification of arachidonic acid metabolites in cultured tumor cells using high-performance liquid chromatography/electrospray ionization tandem mass spectrometry. *Analytical biochemistry*, 297(2), pp.183–90.

Kennedy, I., Coleman, R. a, Humphrey, P.P., Levy, G.P. & Lumley, P., 1982. Studies on the characterisation of prostanoid receptors: a proposed classification. *Prostaglandins*, 24(5), pp.667–689.

Kirschenbaum, L.A., McKevitt, D., Rullan, M., Reisbeck, B., Fujii, T. & Astiz, M.E., 2004. Importance of platelets and fibrinogen in neutrophil-endothelial cell interactions in septic shock. *Critical care medicine*, 32(9), pp.1904–9.

Kirton, C.M. & Nash, G.B., 2000. Activated platelets adherent to an intact endothelial cell monolayer bind flowing neutrophils and enable them to transfer to the endothelial surface. *Journal of Laboratory and Clinical Medicine*, 136(4), pp.303–313.

Kita, Y., Takahashi, T., Uozumi, N. & Shimizu, T., 2005. A multiplex quantitation method for eicosanoids and platelet-activating factor using column-switching reversed-phase liquid chromatography-tandem mass spectrometry. *Analytical Biochemistry*, 342(1), pp.134–143.

Ko, F.N., Yu, S.M., Kang, Y.F. & Teng, C.M., 1995. Characterization of the thromboxane (TP-) receptor subtype involved in proliferation in cultured vascular smooth muscle cells of rat. *British journal of pharmacology*, 116(2), pp.1801–1808.

Konstantopoulos, K., Neelamegham, S., Burns, a. R., Hentzen, E., Kansas, G.S., Snapp, K.R., Berg, E.L., Hellums, J.D., Smith, C.W., McIntire, L. V. & Simon, S.I., 1998. Venous levels of shear support neutrophil-platelet adhesion and neutrophil aggregation in blood via P-selectin and beta2-integrin. *Circulation*, 98(9), pp.873–82.

de Korte, C.L., 2002. Identification of Atherosclerotic Plaque Components With Intravascular Ultrasound Elastography In Vivo: A Yucatan Pig Study. *Circulation*, 105(14), pp.1627–1630.

Koshkin, V. & Dunford, H.B., 1999. Coupling of the peroxidase and cyclooxygenase reactions of prostaglandin H synthase. *Biochimica et Biophysica Acta - Protein Structure and Molecular Enzymology*, 1430(2), pp.341–348.

Kozak, K.R., Rowlinson, S.W. & Marnett, L.J., 2000. Oxygenation of the endocannabinoid, 2-arachidonylglycerol, to glyceryl prostaglandins by cyclooxygenase-2. *The Journal of biological chemistry*, 275(43), pp.33744–9.

Kroll, M. & Schafer, A., 1989. Biochemical Mechanism of Platelet Activation. *Blood*, 74(4), pp.1181–1195.

Kühn, H. & O'Donnell, V.B., 2006. Inflammation and immune regulation by 12/15-lipoxygenases. *Progress in Lipid Research*, 45(4), pp.334–356.

Kulkarni, S., Woollard, K.J., Thomas, S., Oxley, D. & Jackson, S.P., 2007. Conversion of platelets from a proaggregatory to a proinflammatory adhesive phenotype: role of PAF in spatially regulating neutrophil adhesion and spreading. *Blood*, 110(6), pp.1879–86.

Kulmacz, R. & Wang, L., 1995. Comparison of hydroperoxide initiator requirements for the cyclooxygenase activities of prostaglandin H synthase-1 and -2. *J Biol Chem*, 270(41), pp.24019–23.

Kulmacz, R.J., 1998. Cellular regulation of prostaglandin H synthase catalysis. *FEBS letters*, 430(3), pp.154–7.

Kunikata, T., Yamane, H., Segi, E., Matsuoka, T., Sugimoto, Y., Tanaka, S., Tanaka, H., Nagai, H., Ichikawa, A. & Narumiya, S., 2005. Suppression of allergic inflammation by the prostaglandin E receptor subtype EP3. *Nature Immunology*, 6(5), pp.524–531.

Kurland, J. & Bockman, R., 1978. Prostaglandin E Production By Human Blood Monocytes And Mouse Peritoneal Macrophages. *The Journal of Experimental Medicine*, 147, pp.952–957.

Lam, F.W., Burns, A.R., Smith, C.W. & Rumbaut, R.E., 2011. Platelets enhance neutrophil transendothelial migration via P-selectin glycoprotein ligand-1. *American journal of physiology. Heart and circulatory physiology*, 300(2), pp.H468–H475.

Lambeir, A.M., Markey, C.M., Dunford, H.B. & Marnett, L.J., 1985. Spectral properties of the higher oxidation states of prostaglandin H synthase. *J. Biol. Chem.*, 260(28), pp.14894–14896.

Laneuville, O., Breuer, D., Xu, N., Huang, Z., Gage, D., Watson, J., Lagarde, M., DeWitt, D.L. & Smith, W.L., 1995. Fatty Acid Substrate Specificities of Human Prostaglandin-endoperoxide H Synthase-1 and -2. *The Journal of biological chemistry*, 270(33), pp.19330–19336.

Langer, H.F. et al., 2012. Platelets contribute to the pathogenesis of experimental autoimmune encephalomyelitis. *Circulation Research*, 110(9), pp.1202–1210.

Langer, H.F. et al., 2007. Platelets Recruit Human Dendritic Cells Via Mac-1 / JAM-C Interaction and Modulate Dendritic Cell Function In Vitro. *Arteriosclerosis & Thrombosis Vasc Biol.*, 27, pp.1463–1470.

Lassmann, G., Odenwaller, R., Curtis, J.F., DeGray, J.A., Mason, R.P., Marnett, L.J. & Eling, T.E., 1991. Electron spin resonance investigation of tyrosyl radicals of prostaglandin H synthase. Relation to enzyme catalysis. *J. Biol. Chem.*, 266(30), pp.20045–20055.

Lecomte, M., Laneuville, O., Ji, C., DeWitt, D.L. & Smith, W.L., 1994. Acetylation of human prostaglandin endoperoxide synthase-2 (cyclooxygenase-2) by aspirin. *Journal of Biological Chemistry*, 269(18), pp.13207–13215.

Lemos, H.P., Grespan, R., Vieira, S.M., Cunha, T.M., Verri, W.A., Fernandes, K.S.S., Souto, F.O., McInnes, I.B., Ferreira, S.H., Liew, F.Y. & Cunha, F.Q., 2009. Prostaglandin mediates IL-23/IL-17-induced neutrophil migration in inflammation by inhibiting IL-12 and IFNgamma production. *Proceedings of the National Academy of Sciences of the United States of America*, 106(14), pp.5954–9.

Lesault, P.F., Boyer, L., Pelle, G., Covali-Noroc, A., Rideau, D., Akakpo, S., Teiger, E., Dubois-Rande, J.L. & Adnot, S., 2011. Daily administration of the TP receptor antagonist terutroban improved endothelial function in high-cardiovascular-risk patients with atherosclerosis. *Br.J Clin.Pharmacol.*, 71(6), pp.844–851.

Levin, G., Duffin, K.L., Obukowicz, M.G., Hummert, S.L., Fujiwara, H., Needleman, P. & Raz, A., 2002. Differential metabolism of dihomo-gamma-linolenic acid and arachidonic acid by cyclo-oxygenase-1 and cyclo-oxygenase-2: implications for cellular synthesis of prostaglandin E1 and prostaglandin E2. *Biochemical Journal*, 365(Pt 2), pp.489–496.

Levy, G.N., 1997. Prostaglandin H synthases, nonsteroidal anti-inflammatory drugs, and colon cancer. *The FASEB journal : official publication of the Federation of American Societies for Experimental Biology*, 11, pp.234–247.

Libby, P., 2005. Pathophysiology of Coronary Artery Disease. *Circulation*, 111(25), pp.3481–3488.

Lindbom, L., Hedqvist, P., Dahle, S.E., Lindgren, J.A. & Arfors, K.E., 1982. Leukotriene B4 induces extravasation and migration of polymorphonuclear leukocytes in vivo. *Medicine, Experimental*, 4(116), pp.105–108.

Lindgren, J.A., 1981. Formation of novel hydroxylated eicosatetraenoic acids in preparations of human polymorphonuclear leukocytes. , 128(2), pp.329–335.

Liu, M., Saeki, K., Matsunobu, T., Okuno, T., Koga, T., Sugimoto, Y., Yokoyama, C., Nakamizo, S., Kabashima, K., Narumiya, S., Shimizu, T. & Yokomizo, T., 2014. 12-Hydroxyheptadecatrienoic acid promotes epidermal wound healing by accelerating keratinocyte migration via the BLT2 receptor. *The Journal of experimental medicine*, 211(6), pp.1063–78.

Loll, P.J., Picot, D. & Garavito, R.M., 1995. The structural basis of aspirin activity inferred from the crystal structure of inactivated prostaglandin H2 synthase. *Nature structural biology*, 2(8), pp.637–643.

Machlus, K.R. & Italiano, J.E., 2013. The incredible journey: From megakaryocyte development to platelet formation. *The Journal of Cell Biology*, 201(6), pp.785–796.

Malkowski, M.G., Ginell, S.L., Smith, W.L. & Garavito, R.M., 2000. The productive conformation of arachidonic acid bound to prostaglandin synthase. *Science (New York, N.Y.)*, 289(5486), pp.1933–1937.

Mancini, J. a, O'Neill, G.P., Bayly, C. & Vickers, P.J., 1994. Mutation of serine-516 in human

prostaglandin G/H synthase-2 to methionine or aspirin acetylation of this residue stimulates 15-R-HETE synthesis. *FEBS letters*, 342(1), pp.33–7.

Manev, H., Chen, H., Dzitoyeva, S. & Manev, R., 2011. Cyclooxygenases and 5-lipoxygenase in Alzheimer's disease. *Progress in neuro-psychopharmacology & biological psychiatry*, 35(2), pp.315–9.

Marcus, a J., Zucker-Franklin, D., Safier, L.B. & Ullman, H.L., 1966. Studies on human platelet granules and membranes. *The Journal of clinical investigation*, 45(1), pp.14–28.

Margalit, a, Duffin, K.L. & Isakson, P.C., 1996. Rapid quantitation of a large scope of eicosanoids in two models of inflammation: development of an electrospray and tandem mass spectrometry method and application to biological studies. *Analytical biochemistry*, 235(1), pp.73–81.

Marnett, L.J., 2000. Cyclooxygenase mechanisms. *Current opinion in chemical biology*, 4(5), pp.545–52.

Marnett, L.J., Rowlinson, S.W., Goodwin, D.C., Amit, S.K. & Lanzo, C. a., 1999. Arachidonic Acid Oxygenation by COX-1 and COX-2. MECHANISMS OF CATALYSIS AND INHIBITION. *Journal of Biological Chemistry*, 274(33), pp.22903–22906.

Marnett, L.J., Siedlik, P.H., Ochs, R.C., Pagels, W.R., Das, M., Honn, K. V, Warnock, R.H., Tainer, B.E. & Eling, T.E., 1984. Mechanism of the stimulation of prostaglandin H synthase and prostacyclin synthase by the antithrombotic and antimetastatic agent, nafazatrom. *Molecular pharmacology*, 26, pp.328–335.

Martin, J.H., Carson, F.L. & Race, G.J., 1974. Calcium-Containing Platelet Granules. *The Journal of Cell Biology*, 60(3), pp.775–777.

Maskrey, B.H., Bermúdez-Fajardo, A., Morgan, A.H., Stewart-Jones, E., Dioszeghy, V., Taylor, G.W., Baker, P.R.S., Coles, B., Coffey, M.J., Kühn, H. & O'Donnell, V.B., 2007. Activated platelets and monocytes generate four hydroxyphosphatidylethanolamines via lipoxygenase. *The Journal of biological chemistry*, 282(28), pp.20151–63.

Mason, K.D., Carpinelli, M.R., Fletcher, J.I., Collinge, J.E., Hilton, A.A., Ellis, S., Kelly, P.N., Ekert, P.G., Metcalf, D., Roberts, A.W., Huang, D.C.S. & Kile, B.T., 2007. Programmed Anuclear Cell Death Delimits Platelet Life Span. *Cell*, 128(6), pp.1173–1186.

Mason, R.P., Kalyanaraman, B., Tainer, B.E. & Eling, T.E., 1980. A carbon-centered free radical intermediate in the prostaglandin synthetase oxidation of arachidonic acid. Spin trapping and oxygen uptake studies. *Journal of Biological Chemistry*, 255(11), pp.5019–5022.

Masoodi, M., Mir, A.A., Petasis, N.A. & Serhan, C.N., 2008. Simultaneous lipidomic analysis of three families of bioactive lipid mediators leukotrienes , resolvins , protectins and related hydroxy- fatty acids by liquid chromatography / electrospray tandem mass spectrometry. *Rapid communications in mass spectrometry*, 22(2), pp.75–83.

Matsumoto, H., Naraba, H., Murakami, M., Kudo, I., Yamaki, K., Ueno, a & Oh-ishi, S., 1997. Concordant induction of prostaglandin E2 synthase with cyclooxygenase-2 leads to preferred production of prostaglandin E2 over thromboxane and prostaglandin D2 in lipopolysaccharide-stimulated rat peritoneal macrophages. *Biochemical and biophysical research communications*, 230(1), pp.110–4.

Matsunobu, T., Okuno, T., Yokoyama, C. & Yokomizo, T., 2013. Thromboxane A synthase-independent production of 12-hydroxyheptadecatrienoic acid, a BLT2 ligand. *Journal of lipid research*, 54(11), pp.2979–87.

May, G., Eberlein, K., Furberg, C., Passamani, E. & DeMets, D., 1982. Secondary prevention after myocardial infarction: a review of long-term trials. *Progress in Cardiovascular Disease*, 24(4), pp.331–352.

McGeer, P.L. & McGeer, E.G., 1999. Inflammation of the brain in Alzheimer's disease: implications for therapy. *Journal of Leukocyte Biology*, 65(April), pp.409–415.

Merlie, J., Fagan, D., Mudd, J. & Needleman, P., 1988. Isolation and Characterization of the Complementary DNA for Sheep Seminal Vesicle Prostaglandin Endoperoxide Synthase (Cyclooxygenase). *The Journal of biological chemistry*, 263(8), pp.3550–3553.

Michael Garavito, R., Malkowski, M.G. & DeWitt, D.L., 2002. The structures of prostaglandin endoperoxide H synthases-1 and -2. *Prostaglandins and Other Lipid Mediators*, 68-69, pp.129–152.

Michelson, A.D., Barnard, M.R., Krueger, L.A., Valeri, C.R. & Furman, M.I., 2001. Circulating Monocyte-Platelet Aggregates Are a More Sensitive Marker of In Vivo Platelet Activation Than Platelet Surface P-Selectin. *Circulation*, 104, pp.1533–1537.

Mickelson, J., Lakkis, N., Villarreal-Levy, G., Hughes, B. & Smith, C., 1996. Leukocyte Activation With Platelet Adhesion After Coronary Angioplasty : A Mechanism for Recurrent Disease ? *Journal of the American College of Cardiology*, 28(2), pp.345–353.

Miedzobrodzki, J., Panz, T., Płonka, P.M., Zając, K., Dracz, J., Pytel, K., Mateuszuk, Ł. & Chłopicki, S., 2008. Platelets augment respiratory burst in neutrophils activated by selected species of gram-positive or gram-negative bacteria. *Folia Histochemica et*

Cytobiologica, 46(3), pp.383–388.

Miedzobrodzki, J.M.I., Lach, G., Jaworek, R. & Panz, T., 2010. Drug Biochemistry Effect of Nicotinamide and Its Two Derivatives on the Generation of Reactive Oxygen Species in Human Monocytes Cooperating With Platelets. *Acta Poloniae Pharmaceutica*, 67(5), pp.487–494.

Mine, S., Fujisaki, T., Suematsu, M. & Tanaka, Y., 2001. Activated platelets and endothelial cell interaction with neutrophils under flow conditions. *Internal Medicine*, 40(11), pp.1085–1092.

Miyamoto, T., Ogino, N., Yamamoto, S. & Hayaishi, O., 1976. Purification of Prostaglandin Endoperoxide Synthetase from Bovine Vesicular Gland Microsomes. *The Journal of biological chemistry*, 251(9), pp.2629–2636.

Montuschi, P., Barnes, P.J. & Roberts, L.J., 2004. Isoprostanes: markers and mediators of oxidative stress. *The FASEB journal : official publication of the Federation of American Societies for Experimental Biology*, 18(15), pp.1791–1800.

Moore, K.L., Patel, K.D., Bruehl, R.E., Li, F., Johnson, D.A., Lichenstein, H.S., Cummings, R.D., Bainton, D.F. & McEver, R.P., 1995. P-selectin glycoprotein ligand-1 mediates rolling of human neutrophils on P-selectin. *The Journal of Cell Biology*, 128(4), pp.661–671.

Morgan, A.H., Dioszeghy, V., Maskrey, B.H., Thomas, C.P., Clark, S.R., Mathie, S. a, Lloyd, C.M., Kühn, H., Topley, N., Coles, B.C., Taylor, P.R., Jones, S. a & O'Donnell, V.B., 2009. Phosphatidylethanolamine-esterified eicosanoids in the mouse: tissue localization and inflammation-dependent formation in Th-2 disease. *The Journal of biological chemistry*, 284(32), pp.21185–91.

Morgan, A.H., Hammond, V.J., Morgan, L., Thomas, C.P., Tallman, K. a, Garcia-Diaz, Y.R., McGuigan, C., Serpi, M., Porter, N. a, Murphy, R.C. & O'Donnell, V.B., 2010. Quantitative assays for esterified oxylipins generated by immune cells. *Nature protocols*, 5(12), pp.1919–31.

Morgan, L.T., Thomas, C.P., Kühn, H. & O'Donnell, V.B., 2010. Thrombin-activated human platelets acutely generate oxidized docosahexaenoic-acid-containing phospholipids via 12-lipoxygenase. *The Biochemical journal*, 431(1), pp.141–8.

Moriuchi, H., Koda, N., Okuda-Ashitaka, E., Daiyasu, H., Ogasawara, K., Toh, H., Ito, S., Woodward, D. & Watanabe, K., 2008. Molecular Characterization of a Novel Type of Prostamide/Prostaglandin F Synthase, Belonging to the Thioredoxin-like Superfamily. *J.*

Biol. Chem, 283(2), pp.792–801.

Murakami, M., Koduri, R.S., Enomoto, A., Shimbara, S., Seki, M., Yoshihara, K., Singer, A., Valentin, E., Ghomashchi, F., Lambeau, G., Gelb, M.H. & Kudo, I., 2001. Distinct arachidonate-releasing functions of mammalian secreted phospholipase A2s in human embryonic kidney 293 and rat mastocytoma RBL-2H3 cells through heparan sulfate shuttling and external plasma membrane mechanisms. *Journal of Biological Chemistry*, 276(13), pp.10083–10096.

Murakami, M., Taketomi, Y., Girard, C., Yamamoto, K. & Lambeau, G., 2010. Emerging roles of secreted phospholipase A2 enzymes: Lessons from transgenic and knockout mice. *Biochimie*, 92(6), pp.561–582.

Murakami, M., Taketomi, Y., Miki, Y., Sato, H., Hirabayashi, T. & Yamamoto, K., 2011. Recent progress in phospholipase A2 research: From cells to animals to humans. *Progress in Lipid Research*, 50(2), pp.152–192.

Murakami, M., Taketomi, Y., Sato, H. & Yamamoto, K., 2011. Secreted phospholipase A2 revisited. *Journal of Biochemistry*, 150(3), pp.233–255.

Murphy, R.C., Barkley, R.M., Berry, K.Z., Hankin, J., Harrison, K., Johnson, C., Krank, J., McAnoy, A., Uhlson, C. & Zarini, S., 2005. Electrospray ionization and tandem mass spectrometry of eicosanoids. *Analytical Biochemistry*, 346(1), pp.1–42.

Murphy, R.C. & Gaskell, S.J., 2011. New applications of mass spectrometry in lipid analysis. *Journal of Biological Chemistry*, 286(29), pp.25427–25433.

Murphy, R.C., Hammarström, S. & Samuelsson, B., 1979. Leukotriene C: a slow-reacting substance from murine mastocytoma cells. *Proceedings of the National Academy of Sciences of the United States of America*, 76(9), pp.4275–9.

Mustard, J.F., Rowsell, H.C. & Murphy, E. a, 1966. Platelet economy (platelet survival and turnover). *British journal of haematology*, 12(1), pp.1–24.

Nagao, K., Tanaka, H., Komai, M., Masuda, T., Narumiya, S. & Nagai, H., 2003. Role of prostaglandin I2 in airway remodeling induced by repeated allergen challenge in mice. *American Journal of Respiratory Cell and Molecular Biology*, 29(3 I), pp.314–320.

Nakagawa, O., Tanaka, I., Usui, T., Harada, M., Sasaki, Y., Itoh, H., Yoshimasa, T., Namba, T., Narumiya, S. & Nakao, K., 1994. Molecular cloning of human prostacyclin receptor cDNA and its gene expression in the cardiovascular system. *Circulation*, 90(4), pp.1643–7.

Nakayama, T., Mutsuga, N., Yao, L. & Tosato, G., 2006. Prostaglandin E 2 promotes degranulation-independent release of MCP-1 from mast cells Abstract : Mast cells (MCs) are common compo- proangiogenic factors . Inflammation is often ac-. *J leukoc Biol*, 79(January), pp.95–104.

Nakeff, A. & Floeh, D., 1976. Separation of Megakaryocytes From Mouse Bone Marrow by density Gradient Centrifugation. *Blood*, 48(1), pp.133–138.

Nannizzi-Alaimo, L., Alves, V.L. & Phillips, D.R., 2003. Inhibitory effects of glycoprotein IIb/IIIa antagonists and aspirin on the release of soluble CD40 ligand during platelet stimulation. *Circulation*, 107(8), pp.1123–1128.

Naraba, H., Murakami, M., Matsumoto, H., Shimbara, S., Ueno, A., Kudo, I. & Oh-ishi, S., 1998. Segregated coupling of phospholipases A2, cyclooxygenases, and terminal prostanoid synthases in different phases of prostanoid biosynthesis in rat peritoneal macrophages. *J.Immunol.*, 160(6), pp.2974–2982.

Nare, B., Allocco, J.J., Kuningas, R., Galuska, S., Myers, R.W., Bednarek, M. a & Schmatz, D.M., 1999. Development of a scintillation proximity assay for histone deacetylase using a biotinylated peptide derived from histone-H4. *Analytical biochemistry*, 267(1999), pp.390–396.

Nayak, M.K., Kulkarni, P.P. & Dash, D., 2013. Regulatory role of proteasome in determination of platelet life span. *Journal of Biological Chemistry*, 288(10), pp.6826–6834.

Nelson, N. a, 1974. Prostaglandin nomenclature. *Journal of medicinal chemistry*, 17(9), pp.911–8.

Nieswandt, B., Pleines, I. & Bender, M., 2011. Platelet adhesion and activation mechanisms in arterial thrombosis and ischaemic stroke. *Journal of Thrombosis and Haemostasis*, 9(1 S), pp.92–104.

Nimeri, G., Majeed, M., Elwing, H., Öhman, L., Wetterö, J. & Bengtsson, T., 2003. Oxygen radical production in neutrophils interacting with platelets and surface-immobilized plasma proteins: role of tyrosine phosphorylation. *Journal of biomedical materials research. Part A*, 67(2), pp.439–447.

Nithipatikom, K., Grall, A.J., Holmes, B.B., Harder, D.R., Falck, J.R. & Campbell, W.B., 2001. Liquid Chromatographic – Electrospray Ionization – Mass Spectrometric Analysis of Cytochrome P450 Metabolites of Arachidonic Acid. *Analytical Biochemistry*, 336, pp.327–336.

Node, K., Huo, Y., Ruan, X., Yang, B., Spiecker, M., Ley, K., Zeldin, D.C. & Liao, J.K., 1999. Anti-inflammatory Properties of Cytochrom P450 Epoxygenase- Derived Eicosanoids. *Science*, 285, pp.1276–1280.

Nussbaum, a K., Dick, T.P., Keilholz, W., Schirle, M., Stevanović, S., Dietz, K., Heinemeyer, W., Groll, M., Wolf, D.H., Huber, R., Rammensee, H.G. & Schild, H., 1998. Cleavage motifs of the yeast 20S proteasome beta subunits deduced from digests of enolase 1. *Proceedings of the National Academy of Sciences of the United States of America*, 95(21), pp.12504–12509.

O'Donnell, V.B. & Murphy, R.C., 2012. New families of bioactive oxidized phospholipids generated by immune cells: Identification and signaling actions. *Blood*, 120(10), pp.1985–1992.

O'Donnell, V.B., Murphy, R.C. & Watson, S.P., 2014. Platelet lipidomics: Modern day perspective on lipid discovery and characterization in platelets. *Circulation Research*, 114, pp.1185–1203.

O'Neill, G., Mancini, J. & Kargman, S., 1994. Overexpression of human prostaglandin G/H synthase-1 and-2 by recombinant vaccinia virus: inhibition by nonsteroidal anti-inflammatory drugs and biosynthesis of. *Molecular ….*

Ohkubo, S., Nakahata, N. & Ohizumi, Y., 1996. Thromboxane A2-mediated shape change: independent of Gq-phospholipase C--Ca2+ pathway in rabbit platelets. *British journal of pharmacology*, 117(6), pp.1095–1104.

Okuno, T., Iizuka, Y., Okazaki, H., Yokomizo, T., Taguchi, R. & Shimizu, T., 2008. 12(S)-hydroxyheptadeca-5Z, 8E, 10E-trienoic acid is a natural ligand for leukotriene B4 receptor 2. *Journal of Experimental Medicine*, 205(4), pp.759–766.

Okuno, T., Iizuka, Y., Okazaki, H., Yokomizo, T., Taguchi, R. & Shimizu, T., 2008. 12(S)-Hydroxyheptadeca-5Z, 8E, 10E-trienoic acid is a natural ligand for leukotriene B4 receptor 2. *The Journal of experimental medicine*, 205(4), pp.759–766.

Okuno, T., Ishitani, T. & Yokomizo, T., 2015. Biochemical characterization of three BLT receptors in zebrafish. *PLoS ONE*, 10(3), pp.1–19.

Osborn, L., 1990. Leukocyte adhesion to endothelium in inflammation. *Cell*, 62(1), pp.3–6.

Ostermann, G., Weber, K.S.C., Zernecke, A., Schröder, A. & Weber, C., 2002. JAM-1 is a ligand of the beta(2) integrin LFA-1 involved in transendothelial migration of leukocytes. *Nature immunology*, 3(2), pp.151–158.

van der Ouderaa, F., Buytenhek, M., Nugeteren, D. & van Dorp, D., 1977. Purification and characterisation of prostaglandin endoperoxide synthase from sheep vesiclular glands. *Biochimica et biophysica acta*, 487(1), pp.315–331.

Page, C. & Pitchford, S., 2013. Neutrophil and platelet complexes and their relevance to neutrophil recruitment and activation. *International Immunopharmacology*, 17(4), pp.1176–1184.

Paigen, B., Morrow, A., Holmes, P.A., Mitchell, D. & Williams, R.A., 1987. Quantitative assessment of atherosclerotic lesions in mice. *Atherosclerosis*, 68(3), pp.231–240.

Palabrica, T., Lobb, R., Furie, B.C., Aronovitz, M., Benjamin, C., Hsu, Y.M., Sajer, S. a & Furie, B., 1992. Leukocyte accumulation promoting fibrin deposition is mediated in vivo by P-selectin on adherent platelets. *Nature*, 359(6398), pp.848–851.

Pamuk, G., Varul, O., Turgut, B., Demir, M., Uemit, H. & Tezel, A., 2006. Increased Circulating Platelet–Neutrophil, Platelet–Monocyte Complexes, and Platelet Activation in Patients With Ulcerative Colitis: A Comparative Study. *American journal of hematology*, 8, pp.753–759.

Passacquale, G., Vamadevan, P., Pereira, L., Hamid, C., Corrigall, V. & Ferro, A., 2011. Monocyte-platelet interaction induces a pro-inflammatory phenotype in circulating monocytes. *PloS one*, 6(10), pp.1–12.

Patrignani, P., Filabozzi, P. & Patrono, C., 1982. Selective cumulative inhibition of platelet thromboxane production by low-dose aspirin in healthy subjects. *Journal of Clinical Investigation*, 69(6), pp.1366–1372.

Patrignani, P. & Patrono, C., 2015. Cyclooxygenase inhibitors: From pharmacology to clinical read-outs. *Biochimica et Biophysica Acta (BBA) - Molecular and Cell Biology of Lipids*, 1851(4), pp.422–432.

Patrono, C., 2004. Expert Consensus Document on the Use of Antiplatelet Agents The Task Force on the Use of Antiplatelet Agents in Patients with Atherosclerotic Cardiovascular Disease of the European Society of Cardiology. *European Heart Journal*, 25(2), pp.166–181.

Patrono, C. & Baigent, C., 2009. Low-dose aspirin, coxibs, and other NSAIDS: a clinical mosaic emerges. *Molecular interventions*, 9(1), pp.31–39.

Paul, B.Z.S., Jin, J. & Kunapuli, S.P., 1999. Molecular Mechanism of Thromboxane A2-induced Platelet Aggregation. *Journal of Biological Chemistry*, 274(41), pp.29108–29114.

Pease, D., 1956. An Electron Microscopic Study of Red Bone Marrow. *Blood*, 11(6), pp.501–526.

Penz, S., 2005. Human atheromatous plaques stimulate thrombus formation by activating platelet glycoprotein VI. *The FASEB Journal*, 19(8), pp.898–909.

Perry, R.H., Cooks, R.G. & Noll, R.J., 2008. ORBITRAP MASS SPECTROMETRY : INSTRUMENTATION , ION MOTION AND APPLICATIONS. *Mass spectrometry reviews*, (27), pp.661–699.

Picot, D., Loll, P.J. & Garavito, R.M., 1994. The X-ray crystal structure of the membrane protein prostaglandin H2 synthase-1. *Nature*, 367(6460), pp.243–249.

Pitchford, S.C., Momi, S., Giannini, S., Casali, L., Spina, D., Page, C.P. & Gresele, P., 2005. Platelet P-selectin is required for pulmonary eosinophil and lymphocyte recruitment in a murine model of allergic inflammation. *Blood*, 105(5), pp.2074–2081.

Pitchford, S.C., Yano, H., Lever, R., Riffo-Vasquez, Y., Ciferri, S., Rose, M.J., Giannini, S., Momi, S., Spina, D., O'Connor, B., Gresele, P. & Page, C.P., 2003. Platelets are essential for leukocyte recruitment in allergic inflammation. *Journal of Allergy and Clinical Immunology*, 112(1), pp.109–118.

Podrez, E. a, Poliakov, E., Shen, Z., Zhang, R., Deng, Y., Sun, M., Finton, P.J., Shan, L., Febbraio, M., Hajjar, D.P., Silverstein, R.L., Hoff, H.F., Salomon, R.G. & Hazen, S.L., 2002. A novel family of atherogenic oxidized phospholipids promotes macrophage foam cell formation via the scavenger receptor CD36 and is enriched in atherosclerotic lesions. *The Journal of biological chemistry*, 277(41), pp.38517–23.

Polanowska-Grabowska, R., Wallace, K., Field, J.J., Chen, L., Marshall, M.A., Figler, R., Gear, A.R.L. & Linden, J., 2010. P-selectin-mediated platelet-neutrophil aggregate formation activates neutrophils in mouse and human sickle cell disease. *Arteriosclerosis, Thrombosis, and Vascular Biology*, 30(12), pp.2392–2399.

Praticò, D., Cyrus, T., Li, H. & FitzGerald, G. a, 2000. Endogenous biosynthesis of thromboxane and prostacyclin in 2 distinct murine models of atherosclerosis. *Blood*, 96(12), pp.3823–3826.

Pratt, P.F., Rosolowsky, M. & Campbell, W.B., 2002. Effects of epoxyeicosatrienoic acids on polymorphonuclear leukocyte function. *Life Sciences*, 70(21), pp.2521–2533.

Prescott, S., Zimmerman, G., Stafforini, D. & McIntyre, T., 2000. Platelet-Activating Factor and Related Lipid Mediators. *Annual Review of Biochemistry*, 69, pp.419–445.

Pulfer, M. & Murphy, R.C., 2003. Electrospray mass spectrometry of phospholipids. *Mass Spectrometry Reviews*, 22(5), pp.332–364.

Rabinovitch, H., Durand, J., Rigaud, M. & Mendy, F., 1981. Transformation of arachidonic acid into monohydroxy-eicosatetraenoic acids by mouse peritoneal macrophages. *Lipids*, (7), pp.518–524.

Rådmark, O., 2002. Arachidonate 5-lipoxygenase. , 69, pp.211–234.

Rapoport, S.I., 2005. In vivo approaches and rationale for quantifying kinetics and imaging brain lipid metabolic pathways. *Prostaglandins and Other Lipid Mediators*, 77(1-4 SPEC. ISS.), pp.185–196.

Raychowdhury, M.K., Yukawa, M., Collins, L.J., McGrail, S.H., Kent, K.C. & Ware, J.A., 1994. Alternative splicing produces a divergent cytoplasmic tail in the human endothelial thromboxane A2 receptor. *Journal of Biological …*, 269(30), pp.19256–19261.

Reddy, S.T. & Herschman, H.R., 1997. Prostaglandin synthase-1 and prostaglandin synthase-2 are coupled to distinct phospholipases for the generation of prostaglandin D2 in activated mast cells. *The Journal of biological chemistry*, 272(6), pp.3231–7.

Regan, J.W., Bailey, T.J., Pepperl, D.J., Pierce, K.L., Bogardus, a M., Donello, J.E., Fairbairn, C.E., Kedzie, K.M., Woodward, D.F. & Gil, D.W., 1994. Cloning of a novel human prostaglandin receptor with characteristics of the pharmacologically defined EP2 subtype. *Molecular pharmacology*, 46(2), pp.213–220.

Reynaud, D. & Pace-Asciak, C.R., 1997. 12-HETE and 12-HPETE potently stimulate intracellular release of calcium in intact human neutrophils. *Prostaglandins, leukotrienes, and essential fatty acids*, 56(1), pp.9–12.

Richardson, J.L., Shivdasani, R.A., Boers, C., Hartwig, J.H. & Italiano, J.E., 2005. Mechanisms of organelle transport and capture along proplatelets during platelet production. *Blood*, 106(13), pp.4066–4075.

Riendeau, D., Guay, J., Weech, P.K., Laliberté, F., Yergey, J., Li, C., Desmarais, S., Perrier, H., Liu, S. & Nicoll-Griffith, D., 1994. Arachidonyl trifluoromethyl ketone, a potent inhibitor of 85-kDa phospholipase A2, blocks production of arachidonate and 12-hydroxyeicosatetraenoic acid by calcium ionophore-challenged platelets. *The Journal of biological chemistry*, 269(22), pp.15619–15624.

Rinder, H.M., Bonan, J.L., Rinder, C.S., Ault, K. a & Smith, B.R., 1991. Dynamics of leukocyte-platelet adhesion in whole blood. *Blood*, 78(7), pp.1730–1737.

RM, K., EF, R., Hyslop, P., Utterback, B., Hui, K. & Jakubowski, J., 1995. Differential Activation of Cytosolic Phospholipase A2 (cPLA2) by Thrombin and Thrombin Receptor Agonist Peptide in Human Platelets. *The Journal of biological chemistry*, 270(16), pp.14816 – 14823.

Rodriguez, L., Hernandes-Diaz, S. & de Abajo, F., 2001. Association between aspirin and upper gastrointestinal complications : Systematic review of epidemiologic studies. *British Journal of Clinical Pharmacology*, 52, pp.563–571.

Rosolowsky, M. & Campbell, W.B., 1993. Role of PGI2 and epoxyeicosatrienoic acids in relaxation of bovine coronary arteries to arachidonic acid. *The American journal of physiology*, 264(2 Pt 2), pp.H327–35.

Rosolowsky, M. & Campbell, W.B., 1996. Synthesis of hydroxyeicosatetraenoic (HETEs) and epoxyeicosatrienoic acids (EETs) by cultured bovine coronary artery endothelial cells. *Biochimica et biophysica acta*, 1290, pp.267–277.

Rothwell, P.M., Price, J.F., Fowkes, F.G.R., Zanchetti, A., Roncaglioni, M.C., Tognoni, G., Lee, R., Belch, J.F., Wilson, M., Mehta, Z. & Meade, T.W., 2012. Short-term effects of daily aspirin on cancer incidence, mortality, and non-vascular death: analysis of the time course of risks and benefits in 51 randomised controlled trials. *The Lancet*, 379(9826), pp.1602–1612.

Rothwell, P.M., Wilson, M., Price, J.F., Belch, J.F.F., Meade, T.W. & Mehta, Z., 2012. Effect of daily aspirin on risk of cancer metastasis: A study of incident cancers during randomised controlled trials. *The Lancet*, 379(9826), pp.1591–1601.

Rouzer, C. a. & Marnett, L.J., 2003. Mechanism of free radical oxygenation of polyunsaturated fatty acids by cyclooxygenases. *Chemical Reviews*, 103(6), pp.2239–2304.

Rouzer, C.A., 2005. RAW264.7 cells lack prostaglandin-dependent autoregulation of tumor necrosis factor- secretion. *The Journal of Lipid Research*, 46(5), pp.1027–1037.

Rowlinson, S.W., Crews, B.C., Lanzo, C. a. & Marnett, L.J., 1999. The binding of arachidonic acid in the cyclooxygenase active site of mouse prostaglandin endoperoxide synthase-2 (COX-2). A putative L-shaped binding conformation utilizing the top channel region. *Journal of Biological Chemistry*, 274(33), pp.23305–23310.

Roza, M. & Francke, A., 1978. CYCLIC PEROXIDES FROM A SOYA LIPOXYGENASE-CATALYSED OXYGENATION OF METHYL LINOLENATE. *Biochimica et Biophysics Acta,*, 528, pp.119–126.

Rubin, B. et al., 2005. Cytosolic Phospholipase A2 -α Is Necessary for Platelet-activating Factor Biosynthesis, Efficient Neutrophil-mediated Bacterial Killing, and the Innate Immune Response to Pulmonary Infection: cPLA2-α DOES NOT REGULATE NEUTROPHIL NADPH OXIDASE ACTIVITY. *The Journal of biological chemistry*, 280(9), pp.7519–7529.

Samuelsson, B., 1963. Isolation and Identification of Prostaglandins from Human Seminal Plasma. *J. Biol. Chem.*, 238(10), pp.3229–3234.

Samuelsson, B., 1983. Leukotrienes: mediators of immediate hypersensitivity reactions and inflammation. *Science (New York, N.Y.)*, 220(4597), pp.568–575.

Samuelsson, B. & Hamberg, M., 1978. Nomenclature of Thromboxanes. *Prostaglandins*, 16(6), pp.857–860.

Santilli, F., Davì, G., Consoli, A., Cipollone, F., Mezzetti, A., Falco, A., Taraborelli, T., Devangelio, E., Ciabattoni, G., Basili, S. & Patrono, C., 2006. Thromboxane-dependent CD40 ligand release in type 2 diabetes mellitus. *Journal of the American College of Cardiology*, 47(2), pp.391–7.

de Sauvage, F.J., Hass, P.E., Spencer, S.D., Malloy, B.E., Gurney, a L., Spencer, S. a, Darbonne, W.C., Henzel, W.J., Wong, S.C. & Kuang, W.J., 1994. Stimulation of megakaryocytopoiesis and thrombopoiesis by the c-Mpl ligand. *Nature*, 369, pp.533–538.

Savage, B., Almus-Jacobs, F. & Ruggeri, Z.M., 1998. Specific synergy of multiple substrate-receptor interactions in platelet thrombus formation under flow. *Cell*, 94(5), pp.657–666.

Schmidtke, D.W. & Diamond, S.L., 2000. Direct Obsevation of Membrane Tethers Formed during Neutrophil Attachement to Platelets or P-selectin under Physiologigal Flow. *J. Cell Biol.*, 149(3), pp.719–729.

Schrottmaier, W.C., Kral, J.B., Badrnya, S. & Assinger, A., 2015. Aspirin and P2Y 12 Inhibitors in platelet-mediated activation of neutrophils and monocytes. *Thrombosis and Haemostasis*, 1(9), pp.1–12.

Schwab, J.M., Chiang, N., Arita, M. & Serhan, C.N., 2007. Resolvin E1 and protectin D1 activate inflammation-resolution programmes. *Nature*, 447(7146), pp.869–74.

Seibert, K., Zhang, Y., Leahy, K., Hauser, S., Masferrer, J., Perkins, W., Lee, L. & Isakson, P., 1994. Pharmacological and biochemical demonstration of the role of cyclooxygenase 2 in inflammation and pain. *Proceedings of the National Academy of Sciences of the United States of America*, 91(25), pp.12013–7.

Semple, J.W., Italiano, J.E. & Freedman, J., 2011. Platelets and the immune continuum. *Nature Reviews Immunology*, 11(4), pp.264–274.

Serhan, C.N., Hong, S., Gronert, K., Colgan, S.P., Devchand, P.R., Mirick, G. & Moussignac, R.-L., 2002. Resolvins: A Family of Bioactive Products of Omega-3 Fatty Acid Transformation Circuits Initiated by Aspirin Treatment that Counter Proinflammation Signals. *Journal of Experimental Medicine*, 196(8), pp.1025–1037.

Serhan, C.N., Nicolaou, K.C., Webber, S.E., Veale, C.A., Dahlén, S.E., Puustinen, T.J. & Samuelsson, B., 1986. Lipoxin A. Stereochemistry and biosynthesis. *J Biol Chem*, 261(35), pp.16340–16345.

Setianto, B.Y., Hartopo, A.B., Gharini, P.P.R., Anggrahini, D.W. & Irawan, B., 2010. Circulating soluble CD40 ligand mediates the interaction between neutrophils and platelets in acute coronary syndrome. *Heart and Vessels*, 25(4), pp.282–287.

Shankarraman, V., Davis-Gorman, G., McDonagh, P.F. & Caplan, M.R., 2012. Intracellular signaling controls endothelial cell prostacyclin secretion and regulation of blood clotting time. *Journal of Biomedical Materials Research - Part A*, 100 A(12), pp.3374–3383.

Shashkin, P.N., Brown, G.T., Ghosh, A., Marathe, G.K. & McIntyre, T.M., 2008. Lipopolysaccharide is a direct agonist for platelet RNA splicing. *Journal of immunology (Baltimore, Md. : 1950)*, 181(5), pp.3495–3502.

Shen, R.F. & Tai, H.H., 1986. Immunoaffinity purification and characterization of thromboxane synthase from porcine lung. *Journal of Biological Chemistry*, 261(25), pp.11592–11599.

Sheng, H., Shao, J., Kirkland, S.C., Isakson, P., Coffey, R.J., Morrow, J., Beauchamp, R.D. & DuBois, R.N., 1997. Inhibition of human colon cancer cell growth by selective inhibition of cyclooxygenase-2. *The Journal of clinical investigation*, 99(9), pp.2254–9.

Shimokawa, T. & Smith, W.L., 1992. Prostaglandin endoperoxide synthase. The aspirin acetylation region. *J Biol Chem*, 267(17), pp.12387–12392.

Shindou, H., Hishikawa, D., Harayama, T., Eto, M. & Shimizu, T., 2013. Generation of membrane diversity by lysophospholipid acyltransferases. *Journal of Biochemistry*, 154(1), pp.21–28.

Shinohara, H., Balboa, M.A., Johnson, C.A., Balsinde, J. & Dennis, E.A., 1999. Regulation of Delayed Prostaglandin Production in Activated P388D1 Macrophages by Group IV Cytosolic and Group V Secretory Phospholipase A2s. *The Journal of biological chemistry*, 274(18), pp.12263–12268.

Shiraki, R., Inoue, N., Kawasaki, S., Takei, A., Kadotani, M., Ohnishi, Y., Ejiri, J., Kobayashi, S., Hirata, K.I., Kawashima, S. & Yokoyama, M., 2004. Expression of Toll-like receptors on human platelets. *Thrombosis Research*, 113(6), pp.379–385.

Shridas, P., Webb, N.R. & Ky, L., 2014. Diverse Functions of Secretory Phospholipases A 2. , 2014(859), pp.1–22.

Simmons, D.L., Botting, R.M. & Hla, T., 2004. Cyclooxygenase isozymes: the biology of prostaglandin synthesis and inhibition. *Pharmacological reviews*, 56(3), pp.387–437.

Simon, T.C., Makheja, A.N. & Bailey, J.M., 1989. Formation of 15-hydroxyeicosatetraenoic acid (15-HETE) as the predominant eicosanoid in aortas from Watanabe heritable hyperlipidemic and cholesterol-fed rabbits. *Atherosclerosis*, 75, pp.31–38.

Singbartl, K., Forlow, S.B. & Ley, K., 2001. Platelet, but not endothelial, P-selectin is critical for neutrophil-mediated acute postischemic renal failure. *FASEB journal : official publication of the Federation of American Societies for Experimental Biology*, 15(13), pp.2337–44.

Six, D.A. & Dennis, E.A., 2000. The expanding superfamily of phospholipase A 2 enzymes : classi ¢ cation and characterization. *Biochimica et biophysica acta*, 1488, pp.1–19.

Smith, D.L., Willis, A.L. & Mahmud, I., 1984. EICOSANOID EFFECTS ON CELL PROLIFERATION IN VITRO : RELEVANCE TO ATHEROSCLEROSIS. *Prostaglandins Leukotrienes and Medicine*, (16), pp.1–10.

Smith, W.L., 1989. The eicosanoids and their biochemical mechanisms of action. *The Biochemical journal*, 259(2), pp.315–24.

Smith, W.L., DeWitt, D.L. & Garavito, R.M., 2000. C YCLOOXYGENASES : Structural, Cellular, and Molecular Biology. *Annual Review of Biochemistry*, 69(1), pp.145–182.

Smith, W.L. & Murphy, R.C., 2002. The eicosanoids: cyclooxygenase, lipoxygenase, and epoxygenase pathways. *Biochemistry of Lipids, Lipoproteins and Membranes*, (4), pp.341–371.

Song, I., Ball, T.M. & Smith, W.L., 2001. Different suicide inactivation processes for the peroxidase and cyclooxygenase activities of prostaglandin endoperoxide H synthase-1. *Biochemical and biophysical research communications*, 289(4), pp.869–75.

Spurney, R.F., Onorato, J.J., Albers, F.J., Coffman, M., Onorato, J.J. & Coffman, M., 1993. Thromboxane binding and signal transduction in rat glomerular mesangial cells. *American Journal of Physiology*, 264, pp.F292–F299.

Sreeramkumar, V., Adrover, J.M., Ballesteros, I., Cuartero, M.I., Rossaint, J., Bilbao, I., Nacher,

M., Pitaval, C., Radovanovic, I., Fukui, Y., McEver, R.P., Filippi, M.D., Lizasoain, I., Ruiz-Cabello, J., Zarbock, A., Moro, M.A. & Hidalgo, A., 2014. Neutrophils scan for activated platelets to initiate inflammation. *Science*, 344(1969), pp.8–13.

Sreeramkumar, V., Adrover, J.M., Ballesteros, I., Cuartero, M.I., Rossaint, J., Bilbao, I., Nácher, M., Pitaval, C., Radovanovic, I., Fukui, Y., McEver, R.P., Filippi, M.D., Lizasoain, I., Ruiz-Cabello, J., Zarbock, A., Moro, M.A. & Hidalgo, A., 2014. Neutrophils scan for activated platelets to initiate inflammation. *Science*, 346(6194), pp.1234–1237.

Stenson, W.F. & Parker, C.W., 1980. Monohydroxyeicosatetraenoic acids (HETEs) induce degranulation of human neutrophils. *Journal of immunology (Baltimore, Md. : 1950)*, 124(5), pp.2100–4.

Sutherland, M., Shankaranarayanan, P., Schewe, T. & Nigam, S., 2001. Evidence for the presence of phospholipid hydroperoxide glutathione peroxidase in human platelets: implications for its involvement in the regulatory network of the 12-lipoxygenase pathway of arachidonic acid metabolism. *The Biochemical journal*, 353, pp.91–100.

Sugimoto, Y., Yamasaki, A., Segi, E., Tsuboi, K., Aze, Y., Nishimura, T., Oida, H., Yoshida, N., Tanaka, T., Katsuyama, M., Hasumoto, K., Murata, T., Hirata, M., Ushikubi, F., Negishi, M., Ichikawa, A. & Narumiya, S., 1997. Failure of parturition in mice lacking the prostaglandin F receptor. *Science*, 277(5326), pp.681–683.

Suzuki, H., Kawarabayasi, Y., Kondo, J., Abe, T., Nishikawa, K., Kimura, S., Hashimoto, T. & Yamamoto, T., 1990. Structure and regulation of rat long-chain acyl-CoA synthetase. *The Journal of biological chemistry*, 265(15), pp.8681–8685.

Suzuki, K., Sugimura, K., Hasegawa, K., Yoshida, K., Suzuki, A., Ishizuka, K., Ohtsuka, K., Honma, T., Narisawa, R. & Asakura, H., 2001. Activated platelets in ulcerative colitis enhance the production of reactive oxygen species by polymorphonuclear leukocytes. *Scand J Gastroenterol.*, 36, pp.1301–1306.

Swirski, F.K. & Nahrendorf, M., 2013. Leukocyte Behavior in Atherosclerosis, Myocardial Infarction, and Heart Failure. *Science*, 339, pp.161–166.

Tager, A.M. & Luster, A.D., 2003. BLT1 and BLT2: The leukotriene B4 receptors. *Prostaglandins Leukotrienes and Essential Fatty Acids*, 69, pp.123–134.

Takahashi, Y., Tokuoka, S., Masuda, T., Hirano, Y., Nagao, M., Tanaka, H., Inagaki, N., Narumiya, S. & Nagai, H., 2002. Augmentation of allergic inflammation in prostanoid IP

receptor deficient mice. *British journal of pharmacology*, 137(3), pp.315–22.

Talpain, E., Armstrong, R.A., Coleman, A. & Vardey, J., 1995. Characterization of the PGE receptor subtype mediating inhibition of superoxide production in human neutrophils. , pp.1459–1465.

Teder, T., Boeglin, W.E. & Brash, A.R., 2014. Lipoxygenase-catalyzed transformation of epoxy fatty acids to hydroxy-endoperoxides : a potential P450 and lipoxygenase interaction. *Journal of lipid research*, 55, pp.2587–2596.

Theken, K.N., Schuck, R.N., Edin, M.L., Tran, B., Ellis, K., Bass, A., Lih, F.B., Tomer, K.B., Poloyac, S.M., Wu, M.C., Hinderliter, A.L., Zeldin, D.C., Stouffer, G. a. & Lee, C.R., 2012a. Evaluation of cytochrome P450-derived eicosanoids in humans with stable atherosclerotic cardiovascular disease. *Atherosclerosis*, 222(2), pp.530–536.

Theken, K.N., Schuck, R.N., Edin, M.L., Tran, B., Ellis, K., Bass, A., Lih, F.B., Tomer, K.B., Poloyac, S.M., Wu, M.C., Hinderliter, A.L., Zeldin, D.C., Stouffer, G. a. & Lee, C.R., 2012b. Evaluation of cytochrome P450-derived eicosanoids in humans with stable atherosclerotic cardiovascular disease. *Atherosclerosis*, 222(2), pp.530–536.

Thomas, C.P., Morgan, L.T., Maskrey, B.H., Murphy, R.C., Kühn, H., Hazen, S.L., Goodall, A.H., Hamali, H. a., Collins, P.W. & O'Donnell, V.B., 2010. Phospholipid-esterified eicosanoids are generated in agonist-activated human platelets and enhance tissue factor-dependent thrombin generation. *The Journal of biological chemistry*, 285(10), pp.6891–903.

Thon, J.N., Devine, M.T., Begonja, A.J., Tibbitts, J. & Italiano, J.E., 2012. High-content live-cell imaging assay used to establish mechanism of trastuzumab emtansine (T-DM1)-mediated inhibition of platelet production. *Blood*, 120(10), pp.1975–1984.

Thon, J.N., Montalvo, A., Patel-Hett, S., Devine, M.T., Richardson, J.L., Ehrlicher, A., Larson, M.K., Hoffmeister, K., Hartwig, J.H. & Italiano, J.E., 2010. Cytoskeletal mechanics of proplatelet maturation and platelet release. *The Journal of Cell Biology*, 191(4), pp.861–874.

Thuresson, E.D., Lakkides, K.M., Rieke, C.J., Sun, Y., Wingerd, B. a, Micielli, R., Mulichak, A.M., Malkowski, M.G., Garavito, R.M. & Smith, W.L., 2001. Prostaglandin endoperoxide H synthase-1: The functions of cyclooxygenase active site residues in the binding, positioning, and oxygenation of arachidonic acid. *Journal of Biological Chemistry*,

276(13), pp.10347–10357.

Thuresson, E.D., Lakkides, K.M., Rieke, C.J., Sun, Y., Wingerd, B. a., Micielli, R., Mulichak, A.M., Malkowski, M.G., Garavito, R.M. & Smith, W.L., 2001. Prostaglandin endoperoxide H synthase-1: The functions of cyclooxygenase active site residues in the binding, positioning, and oxygenation of arachidonic acid. *Journal of Biological Chemistry*, 276, pp.10347–10357.

Thuresson, E.D., Lakkides, K.M. & Smith, W.L., 2000. Different catalytically competent arrangements of arachidonic acid within the cyclooxygenase active site of prostaglandin endoperoxide H synthase-1 lead to the formation of different oxygenated products. *Journal of Biological Chemistry*, 275(12), pp.8501–8507.

Thuresson, E.D., Lakkides, K.M. & Smith, W.L., 2000. Different catalytically competent arrangements of arachidonic acid within the cyclooxygenase active site of prostaglandin endoperoxide H synthase-1 lead to the formation of different oxygenated products. *The Journal of biological chemistry*, 275(12), pp.8501–8507.

Tohgi, H., Konno, S., Tamura, K., Kimura, B. & Kawano, K., 1992. Effects of low-to-high doses of aspirin on platelet aggregability and metabolites of thromboxane A2 and prostacyclin. *Stroke; a journal of cerebral circulation*, 23(10), pp.1400–1403.

Tramposch, K.M., Chilton, F.H., Stanley, P.L., Franson, R.C., Havens, M.B., Nettleton, D.O., Davern, L.B., Darling, I.M. & Bonney, R.J., 1994. Inhibitor of phospholipase A2 blocks eicosanoid and platelet activating factor biosynthesis and has topical anti-inflammatory activity. *The Journal of pharmacology and experimental therapeutics*, 271(2), pp.852–859.

Trip, M.D., Manger Cats, V., van Capelle, F.J.L. & Vreeken, J., 1990. Platelet Hyperreactivity And Prognosis In Survivors Of Myocardial Infarction. *The New England Journal of Medicine*, 322(22), pp.1549–1554.

Tsai, A.L. & Kulmacz, R.J., 2010. Prostaglandin H synthase: Resolved and unresolved mechanistic issues. *Archives of Biochemistry and Biophysics*, 493(1), pp.103–124.

Ueno, N., Murakami, M., Tanioka, T., Fujimori, K., Tanabe, T., Urade, Y. & Kudo, I., 2001. Coupling between cyclooxygenase, terminal prostanoid synthase, and phospholipase A2. *The Journal of biological chemistry*, 276(37), pp.34918–27.

Ushikubi, F., Nakajima, M., Hirata, M., Okuma, M., Fujiwara, M. & Narumiya, S., 1989. Purification of the thromboxane A2/prostaglandin H2 receptor from human blood

platelets. *The Journal of biological chemistry*, 264(28), pp.16496–501.

Ushikubi, F., Segi, E., Sugimoto, Y., Murata, T., Matsuoka, T., Kobayashi, T., Hizaki, H., Tuboi, K., Katsuyama, M., Ichikawa, a, Tanaka, T., Yoshida, N. & Narumiya, S., 1998. Impaired febrile response in mice lacking the prostaglandin E receptor subtype EP3. *Nature*, 395(6699), pp.281–284.

Vane, J.R., Bakhle, Y.S. & Botting, R.M., 1998. Cyclooxygenases 1 and 2. , pp.97–120.

Vane, J.R. & Botting, R.M., 2003. The mechanism of action of aspirin. *Thrombosis Research*, 110(5-6), pp.255–258.

Viles-Gonzalez, J.F., Fuster, V., Corti, R., Valdiviezo, C., Hutter, R., Corda, S., Anand, S.X. & Badimon, J.J., 2005. Atherosclerosis regression and TP receptor inhibition: effect of S18886 on plaque size and composition--a magnetic resonance imaging study. *European heart journal*, 26(15), pp.1557–1561.

Violi, F., Ghiselli, a., Iuliano, L., Praticò, D., Alessandri, C. & Balsano, F., 1988. Inhibition by picotamide of thromboxane production in vitro and ex vivo. *European Journal of Clinical Pharmacology*, 33(6), pp.599–602.

Wang, X.S. & Lau, H.Y.A., 2006. Prostaglandin E2 potentiates the immunologically stimulated histamine release from human peripheral blood-derived mast cells through EP1/EP3 receptors. *Allergy: European Journal of Allergy and Clinical Immunology*, 61(4), pp.503–506.

Warner, T.D., Nylander, S. & Whatling, C., 2011. Anti-platelet therapy: cyclo-oxygenase inhibition and the use of aspirin with particular regard to dual anti-platelet therapy. *British Journal of Clinical Pharmacology*, 72(4), pp.619–633.

Weber, C. & Springer, T. a., 1997. Neutrophil accumulation on activated, surface-adherent platelets in flow is mediated by interaction of Mac-1 with fibrinogen bound to αIIbβ3 and stimulated by platelet-activating factor. *Journal of Clinical Investigation*, 100(8), pp.2085–2093.

Weller, C.L., Collington, S.J., Hartnell, A., Conroy, D.M., Kaise, T., Barker, J.E., Wilson, M.S., Taylor, G.W., Jose, P.J. & Williams, T.J., 2007. Chemotactic action of prostaglandin E 2 on mouse mast cells acting via the PGE 2 receptor 3. *Proceedings of the National Academy of Sciences*, 104(28), pp.11712–11717.

Weyrich, A. & Zimmerman, G., 2004. Platelets: signaling cells in the immune continuum. *Trends in immunology*.

Wheeldon, A. & Vardey, C.J., 1993. Characterization of the inhibitory prostanoid receptors on human neutrophils. *British Journal of Pharmacology*, 108, pp.1051–1054.

White, J.G., 1972. Interaction of Membrane Systems in Blood-Platelets. *American Journal of Pathology*, 66(2), pp.295–314.

Whiteheart, S.W., 2011. Platelet granules: Surprise packages. *Blood*, 118(5), pp.1190–1191.

Willis, A.L., Smith, D.L. & Vigo, C., 1986. Suppression of Principle Atherosclerotic Mechanisms By Prostacyclins and Other Eicosanoids. *Progress in Lipid Research*, 25, pp.645–666.

Wise, H., 1998. Activation of the prostaglandin EP4-receptor subtype is highly coupled to inhibition of N-formyl-methionyl-leucyl-phenylalanine-stimulated rat neutrophil aggregation. *Prostaglandins Leukotrienes and Essential Fatty Acids*, 58(1), pp.77–84.

Wise, H., 1996. The inhibitory effect of prostaglandin E2 on rat neutrophil aggregation. *Journal of Leukocyte Biology*, 60, pp.480–486.

Wise, H. & Jones, R.L., 1994. Characterization of prostanoid receptors on rat neutrophils. *British journal of pharmacology*, 113(2), pp.581–7.

Wolfe, L.S., 1982. Eicosanoids: prostaglandins, thromboxanes, leukotrienes, and other derivatives of carbon-20 unsaturated fatty acids. *Journal of neurochemistry*, 38(1), pp.1–14.

Woodfin, A., Reichel, C.A., Khandoga, A., Corada, M., Voisin, M.B., Scheiermann, C., Haskard, D.O., Dejana, E., Krombach, F. & Nourshargh, S., 2007. JAM-A mediates neutrophil transmigration in a stimulus-specific manner in vivo: Evidence for sequential roles for JAM-A and PECAM-1 in neutrophil transmigration. *Blood*, 110(6), pp.1848–1856.

Wu, G., Kulmacz, R.J. & Tsai, A.-L., 2003. Cyclooxygenase inactivation kinetics during reaction of prostaglandin H synthase-1 with peroxide. *Biochemistry*, 42(46), pp.13772–7.

Wu, G., Lü, J.-M., van der Donk, W.A., Kulmacz, R.J. & Tsai, A., 2011. Cyclooxygenase reaction mechanism of prostaglandin H synthase from deuterium kinetic isotope effects. *Journal of Inorganic Biochemistry*, 105(3), pp.382–390.

Wu, G., Wei, C., Kulmacz, R.J., Osawa, Y. & Tsai, a L., 1999. A mechanistic study of self-inactivation of the peroxidase activity in prostaglandin H synthase-1. *The Journal of biological chemistry*, 274(14), pp.9231–7.

Xiao, G., Tsai, A.L., Palmer, G., Boyar, W.C., Marshall, P.J. & Kulmacz, R.J., 1997. Analysis of hydroperoxide-induced tyrosyl radicals and lipoxygenase activity in aspirin-treated human prostaglandin H synthase-2. *Biochemistry*, 36(7), pp.1836–1845.

Xiao, Z., Goldsmith, H.L., McIntosh, F. a, Shankaran, H. & Neelamegham, S., 2006. Biomechanics of P-Selectin PSGL-1 Bonds: Shear Threshold and Integrin-Independent Cell Adhesion. *Biophysical Journal*, 90(6), pp.2221–2234.

Yamane, H., Sugimoto, Y., Tanaka, S. & Ichikawa, a, 2000. Prostaglandin E(2) receptors, EP2 and EP4, differentially modulate TNF-alpha and IL-6 production induced by lipopolysaccharide in mouse peritoneal neutrophils. *Biochemical and biophysical research communications*, 278(1), pp.224–228.

Yamashita, M. & Fenn, J.B., 1984. Electrospray ion source. Another variation on the free-jet theme. *J Phys.Chem.*, 88(20), pp.4451–4459.

Yang, K. & Han, X., 2011. Accurate Quantification of Lipid Species by Electrospray Ionization Mass Spectrometry — Meets a Key Challenge in Lipidomics. *Metabolites*, 1, pp.21–40.

Yin, H., Morrow, J.D. & Porter, N. a, 2004. Identification of a Novel Class of Endoperoxides from Arachidonate Autoxidation. *Journal of Biological Chemistry*, 279(5), pp.3766–3776.

Yokomizo, T., Kato, K., Hagiya, H., Izumi, T. & Shimizu, T., 2001. Hydroxyeicosanoids Bind to and Activate the Low Affinity Leukotriene B 4 Receptor, BLT2. *Journal of Biological Chemistry*, 276(15), pp.12454–12459.

Yu, Y. & Chadee, K., 1998. Prostaglandin E 2 stimulates IL-8 gene expression in human colonic epithelial cells by a posttranscriptional mechanism. *Journal of Immunology*, 161(7), pp.3746–3752.

Yuhki, K.I., Kojima, F., Kashiwagi, H., Kawabe, J.I., Fujino, T., Narumiya, S. & Ushikubi, F., 2011. Roles of prostanoids in the pathogenesis of cardiovascular diseases: Novel insights from knockout mouse studies. *Pharmacology and Therapeutics*, 129(2), pp.195–205.

Zaman, A.., Helft, G., Worthley, S.. & Badimon, J.., 2000. The role of plaque rupture and thrombosis in coronary artery disease. *Atherosclerosis*, 149(2), pp.251–266.

Zarbock, A., Polanowska-Grabowska, R.K. & Ley, K., 2007. Platelet-neutrophil-interactions: Linking hemostasis and inflammation. *Blood Reviews*, 21, pp.99–111.

Zarbock, A., Singbartl, K. & Ley, K., 2006. Complete reversal of acid-induced acute lung injury by blocking of platelet-neutrophil aggregation. *The Journal of clinical investigation*, 116, pp.3211–3219.

Zeldin, D.C., 2001. Epoxygenase Pathways of Arachidonic Acid Metabolism. *Journal of Biological Chemistry*, 276(39), pp.36059–36062.

Zeldin, D.C., Moomaw, C.R., Jesse, N., Tomer, K.B., Beetham, J., Hammock, B.D. & Wu, S., 1996. Biochemical characterization of the human liver cytochrome P450 arachidonic acid epoxygenase pathway. *Archives of biochemistry and biophysics*, 330(1), pp.87–96.

Zhang, J., Prakash, C., Yamashita, K. & Blair, I., 1992. Regiospecific and Enantioselective Metabolism of 8,9-Epoxyeicosatrienoic Acid by Cyclooxygenase. *Biochemical and biophysical research communications*, 183(1), pp.138–143.

Zhang, L. et al., 2012. A novel role of sphingosine 1-phosphate receptor S1pr1 in mouse thrombopoiesis. *Journal of Experimental Medicine*, 209(12), pp.2165–2181.